frontiers | Research Topics

Ecology, environment, and human microbiome interaction with infection

Edited by
Fumito Maruyama and Yukiko Koizumi

Published in
Frontiers in Public Health
Frontiers in Microbiology
Frontiers in Immunology
Frontiers in Microbiomes

ISSN 1664-8714
ISBN 978-2-8325-5088-5
DOI 10.3389/978-2-8325-5088-5

About Frontiers

Frontiers is more than just an open access publisher of scholarly articles: it is a pioneering approach to the world of academia, radically improving the way scholarly research is managed. The grand vision of Frontiers is a world where all people have an equal opportunity to seek, share and generate knowledge. Frontiers provides immediate and permanent online open access to all its publications, but this alone is not enough to realize our grand goals.

Frontiers journal series

The Frontiers journal series is a multi-tier and interdisciplinary set of open-access, online journals, promising a paradigm shift from the current review, selection and dissemination processes in academic publishing. All Frontiers journals are driven by researchers for researchers; therefore, they constitute a service to the scholarly community. At the same time, the *Frontiers journal series* operates on a revolutionary invention, the tiered publishing system, initially addressing specific communities of scholars, and gradually climbing up to broader public understanding, thus serving the interests of the lay society, too.

Dedication to quality

Each Frontiers article is a landmark of the highest quality, thanks to genuinely collaborative interactions between authors and review editors, who include some of the world's best academicians. Research must be certified by peers before entering a stream of knowledge that may eventually reach the public - and shape society; therefore, Frontiers only applies the most rigorous and unbiased reviews. Frontiers revolutionizes research publishing by freely delivering the most outstanding research, evaluated with no bias from both the academic and social point of view. By applying the most advanced information technologies, Frontiers is catapulting scholarly publishing into a new generation.

What are Frontiers Research Topics?

Frontiers Research Topics are very popular trademarks of the *Frontiers journals series*: they are collections of at least ten articles, all centered on a particular subject. With their unique mix of varied contributions from Original Research to Review Articles, Frontiers Research Topics unify the most influential researchers, the latest key findings and historical advances in a hot research area.

Find out more on how to host your own Frontiers Research Topic or contribute to one as an author by contacting the Frontiers editorial office: frontiersin.org/about/contact

Ecology, environment, and human microbiome interaction with infection

Topic editors

Fumito Maruyama — Hiroshima University, Japan

Yukiko Koizumi — American Dental Association, United States

Citation

Maruyama, F., Koizumi, Y., eds. (2024). *Ecology, environment, and human microbiome interaction with infection*. Lausanne: Frontiers Media SA.

doi: 10.3389/978-2-8325-5088-5

Table of contents

frontiers | Frontiers in Public Health

TYPE Editorial
PUBLISHED 23 May 2023
DOI 10.3389/fpubh.2023.1217927

OPEN ACCESS

EDITED AND REVIEWED BY
Marc Jean Struelens,
Université libre de Bruxelles, Belgium

*CORRESPONDENCE
Fumito Maruyama
✉ fumito@hiroshima-u.ac.jp
Yukiko Koizumi
✉ koizumiy@ada.org

†These authors have contributed equally to this work

RECEIVED 06 May 2023
ACCEPTED 12 May 2023
PUBLISHED 23 May 2023

CITATION
Koizumi Y and Maruyama F (2023) Editorial: Ecology, environment, and human microbiome interaction with infection.
Front. Public Health 11:1217927.
doi: 10.3389/fpubh.2023.1217927

Editorial: Ecology, environment, and human microbiome interaction with infection

Yukiko Koizumi[1*†] and Fumito Maruyama[2,3*†]

[1]Applied Research, American Dental Association Science and Research Institute, Chicago, IL, United States, [2]Microbial Genomics and Ecology, Center for the Planetary Health and Innovation Science, The IDEC Institute, Hiroshima University, Higashihiroshima, Japan, [3]Project Research Center for Holobiome and Built Environment (CHOBE), Hiroshima University, Higashihiroshima, Japan

KEYWORDS

eco epidemiology, human microbiome, biotic-abiotic interaction with infection pathobiont, dysbiosis, One Health

Editorial on the Research Topic
Ecology, environment, and human microbiome interaction with infection

One Health paradigm, conceived in the early years of the 21st century, encapsulates a global initiative endorsing interdisciplinary collaborations and knowledge dissemination across all dimensions of health sciences. This framework accentuates the intricate interdependencies amongst humans, animals, vegetation, and their shared environment. Ground-breaking advancements in DNA sequencing methodologies and computational biology have significantly transformed the domain of microbiome studies. Analyses of previously uncultured microorganisms deliver exhaustive insights into the associations between animals, the environment, and human microbiota, including various disease implications. Within the context of this investigative topic, we are interested in examining the impact of environmental stressors on bacterial populations and the implications these shifts have for human health.

Environmental fluctuations, inclusive of meteorological variations, influence the propagation of infectious diseases. Liao et al. delineated the correlation between climatic factors and the emergence of scrub typhus. The authors discovered lagging associations between specific meteorological parameters (rainfall, relative humidity, and ambient temperature) and incidents of scrub typhus that exhibited inverse-U trajectories. The research was oriented toward the development of a preliminary warning system for scrub typhus by harnessing the lagging graphs and associations with meteorological data. Pathogens can be directly transmitted via airborne particles or fomites (e.g., influenza) or indirectly through food, water (e.g., cholera), or a vector (e.g., malaria, dengue), and may involve non-human reservoir species (zoonotic pathogens, e.g., hantavirus). Nagy et al. identified rooks as carriers of extended-spectrum beta-lactamase (ESBL)-producing *Escherichia coli* in a university clinic vicinity. The authors characterized the ESBL gene and established a zoonotic connection between humans and rooks. This study underscored rooks as a long-distance vector that conveys antibiotic resistance to the hospital setting. Antibiotic resistance is universally acknowledged as a pressing One Health concern.

Healthcare-associated infections (HAIs) pose a significant challenge, particularly within hospital environments. These are primarily transmitted via medical equipment, facilities, and healthcare professionals and are often attributable to antibiotic-resistant bacteria. Vancomycin-resistant *Enterococci* and *Clostridium difficile* are the most prominent

examples; these tend to originate from environmental sources and subsequently infect the human body. Traditionally, it was presumed that *C. difficile* was primarily hospital-acquired; however, whole-genome sequencing results suggest that the majority of hospital *C. difficile* infection cases originate from external sources/reservoirs that play a vital role in transmission. Tozzo et al. elucidated the localization, transmission, and prevention of ESKAPE species (*Enterococcus faecium*, *Staphylococcus aureus*, *Klebsiella pneumoniae*, *Acinetobacter baumannii*, *Pseudomonas aeruginosa*, and *Enterobacter species*) and *C. difficile*, the most common pathogens causing HAIs. Tozzo et al.'s review highlighted the fact that microorganisms survive on surfaces for extended periods and that specific cleaning procedures can inadvertently increase the prevalence of pathogenic strains over benign ones. Consequently, treatments that augment populations of beneficial microorganisms, as opposed to those that incompletely clean surfaces, could offer a superior solution to the problem of HAIs.

Patients in ICUs are often prescribed antibiotics, which can annihilate commensal microbiota and therefore escalate the risk of HAIs. Consequently, it is crucial to understand the alterations in commensal microbiota induced by antibiotics and medication profiles in patients. Gage et al. reported that diisopropylfluorophosphate induces a significant reduction in alpha diversity after 48 h, but not 7 days or 5 weeks, in gut microbiota. This study illuminated the relationship between medication, commensal microbiota alterations, and the timing of these occurrences. Scheuring et al. presented a robust system utilizing the Salmoid model to comprehend adaptively significant host–microbe and microbe–microbe interactions. The authors posited that the restoration of healthy microbiota is crucial to averting pathogenic infections. To consolidate our knowledge of healthy microbiota, the identification of pathobionts is integral. Sun et al. discussed the role of human microbiota in the initiation and progression of lung cancer, which is apparent in its induction of inflammatory responses and participation in immune regulation. Furthermore, Yamazaki et al. investigated how the oral pathobionts *Prevotella intermedia* and *Porphyromonas gingivalis*, but not the oral symbionts *Actinomyces. naeslundii* and *Veillonella. rogosae*, exacerbated High-fat diet induced NAFLD, with *P. gingivalis* demonstrating higher pathogenicity. These authors identified potential pathobionts and established their connection with systemic diseases.

To reestablish healthy microbiota, fecal microbiota transplantation has emerged as a more accessible treatment option for those suffering from HAIs and gut dysbiosis, such as inflammatory bowel disease and ulcerative colitis. The dominance of *Candida albicans* in immunocompromised hosts is widely recognized. Munoz et al. developed a probiotic approach utilizing a *Lactobacillus johnsonii* strain (MT4) from the oral cavity of mice and characterized its effect on *C. albicans* growth in planktonic and biofilm states. The authors identified the key genetic and phenotypic traits associated with growth inhibition activity against *C. albicans*. Munoz et al. and Scheuring et al. provided examples of how healthy microbiota can combat nosocomial pathogens.

A microbiota comprises structured multi-kingdom microorganisms, including fungi, archaea, viruses, and bacteria. Current technological advancements facilitate our understanding of inter-kingdom relationships in diseases. Tadmor et al. argued that elucidating the ecology of human-associated phages may have a significant impact on human health because of the potential ability of phages to modulate the abundances and phenotypes of commensal bacteria. They discovered that, despite the great interpersonal diversity observed among human viromes, humans harbor distinct phage families characterized by shared conserved hallmark genes known as large terminase subunit genes. Interestingly, certain phage families were found to be highly correlated with pathogenic, carriage, and disease-related isolates and may serve as novel biomarkers for disease.

In this research area, authors have delineated how environmental shifts precipitate the emergence of infectious diseases. They have further underscored the potential of animals, such as rooks, to carry antibiotic-resistant bacteria to hospitals. Such exogenous resistomes and pathogens contribute to HAIs, which are a global concern. Given that HAIs are not entirely preventable via the cleaning of medical equipment, this topic emphasizes the importance of restoring commensal flora and adopting a probiotic approach to combating nosocomial pathogens, including the identification of pathobionts. The authors have introduced the relationships between animals, the environment, and human microbiota, including various disease correlations.

Author contributions

Both authors listed have made a substantial, direct, and intellectual contribution to the work and approved it for publication.

Acknowledgments

We thank Suzanne Leech, Ph.D., from Edanz (https://jp.edanz.com/ac) for editing a draft of this manuscript.

Conflict of interest

The authors declare that the research was conducted in the absence of any commercial or financial relationships that could be construed as a potential conflict of interest.

Publisher's note

frontiers in Immunology

ORIGINAL RESEARCH
published: 11 October 2021
doi: 10.3389/fimmu.2021.766170

Oral Pathobiont-Induced Changes in Gut Microbiota Aggravate the Pathology of Nonalcoholic Fatty Liver Disease in Mice

*Kyoko Yamazaki[1,2], Tamotsu Kato[3], Yuuri Tsuboi[4], Eiji Miyauchi[3], Wataru Suda[5], Keisuke Sato[1,2], Mayuka Nakajima[2], Mai Yokoji-Takeuchi[1,2], Miki Yamada-Hara[1,2], Takahiro Tsuzuno[1,2], Aoi Matsugishi[1,2], Naoki Takahashi[2], Koichi Tabeta[2], Nobuaki Miura[6], Shujiro Okuda[6,7], Jun Kikuchi[4], Hiroshi Ohno[3,8] and Kazuhisa Yamazaki[1,3]**

[1] Research Unit for Oral-Systemic Connection, Division of Oral Science for Health Promotion, Niigata University Graduate School of Medical and Dental Sciences, Niigata, Japan, [2] Division of Periodontology, Niigata University Graduate School of Medical and Dental Sciences, Niigata, Japan, [3] Laboratory for Intestinal Ecosystem, RIKEN Centre for Integrative Medical Sciences (IMS), Yokohama, Japan, [4] RIKEN Center for Sustainable Resource Science, Yokohama, Japan, [5] Laboratory for Microbiome Sciences, RIKEN Center for Integrative Medical Sciences, Yokohama, Japan, [6] Division of Bioinformatics, Niigata University Graduate School of Medical and Dental Sciences, Niigata, Japan, [7] Medical AI Center, Niigata University School of Medicine, Niigata, Japan, [8] Intestinal Microbiota Project, Kanagawa Institute of Industrial Science and Technology, Kawasaki, Japan

Background & Aims: Periodontitis increases the risk of nonalcoholic fatty liver disease (NAFLD); however, the underlying mechanisms are unclear. Here, we show that gut dysbiosis induced by oral administration of *Porphyromonas gingivalis*, a representative periodontopathic bacterium, is involved in the aggravation of NAFLD pathology.

Methods: C57BL/6N mice were administered either vehicle, *P. gingivalis*, or *Prevotella intermedia*, another periodontopathic bacterium with weaker periodontal pathogenicity, followed by feeding on a choline-deficient, l-amino acid-defined, high-fat diet with 60 kcal % fat and 0.1% methionine (CDAHFD60). The gut microbial communities were analyzed by pyrosequencing the 16S ribosomal RNA genes. Metagenomic analysis was used to determine the relative abundance of the Kyoto Encyclopedia of Genes and Genomes pathways encoded in the gut microbiota. Serum metabolites were analyzed using nuclear magnetic resonance-based metabolomics coupled with multivariate statistical analyses. Hepatic gene expression profiles were analyzed *via* DNA microarray and quantitative polymerase chain reaction.

Results: CDAHFD60 feeding induced hepatic steatosis, and in combination with bacterial administration, it further aggravated NAFLD pathology, thereby increasing fibrosis. Gene expression analysis of liver samples revealed that genes involved in NAFLD pathology were perturbed, and the two bacteria induced distinct expression profiles. This might be due to quantitative and qualitative differences in the influx of bacterial products in the gut because the serum endotoxin levels, compositions of the gut microbiota, and serum metabolite profiles induced by the ingested *P. intermedia* and *P. gingivalis* were different.

OPEN ACCESS

Edited by:
Markus M. Heimesaat,
Charité – Universitätsmedizin Berlin, Germany

Reviewed by:
Azita Hekmatdoost,
National Nutrition and Food Technology Research Institute, Iran
Yu-Syuan Luo,
National Taiwan University, Taiwan

***Correspondence:**
Kazuhisa Yamazaki
kaz@dent.niigata-u.ac.jp;
kazuhisa.yamazaki@riken.jp

Specialty section:
This article was submitted to Microbial Immunology, a section of the journal Frontiers in Immunology

Received: 28 August 2021
Accepted: 28 September 2021
Published: 11 October 2021

Citation:
Yamazaki K, Kato T, Tsuboi Y, Miyauchi E, Suda W, Sato K, Nakajima M, Yokoji-Takeuchi M, Yamada-Hara M, Tsuzuno T, Matsugishi A, Takahashi N, Tabeta K, Miura N, Okuda S, Kikuchi J, Ohno H and Yamazaki K (2021) Oral Pathobiont-Induced Changes in Gut Microbiota Aggravate the Pathology of Nonalcoholic Fatty Liver Disease in Mice. Front. Immunol. 12:766170. doi: 10.3389/fimmu.2021.766170

Conclusions: Swallowed periodontopathic bacteria aggravate NAFLD pathology, likely due to dysregulation of gene expression by inducing gut dysbiosis and subsequent influx of gut bacteria and/or bacterial products.

Keywords: metabolome, metagenomic analysis, NAFLD, periodontopathic bacteria, oral–gut connection, periodontitis, *Porphyromonas gingivalis*

INTRODUCTION

Nonalcoholic fatty liver disease (NAFLD), a hepatic manifestation of metabolic syndrome and obesity, affects 20%–30% of the general Western population, and the associated morbidity is continuously increasing (1). NAFLD constitutes a spectrum ranging from simple steatosis and nonalcoholic steatohepatitis (NASH) to fibrosis, cirrhosis, and hepatocellular carcinoma. NAFLD is now considered to be a multifactorial disease involving multiple intracellular signaling pathways (2), dietary factors (3, 4), gut barrier dysfunction, endoplasmic reticulum (ER) stress, microbiota, and genetic factors (5).

Periodontal disease is a chronic inflammatory disease caused by a complex interaction between oral pathobionts and host defense mechanisms (6) that affects tooth-supporting structures, leading to tooth loss if left untreated. Accumulating evidence strongly suggests that periodontal disease not only destroys the periodontium, but also increases the risk of various non-oral diseases including metabolic disorders such as NAFLD (7). Epidemiological studies have demonstrated a significant association between clinical and/or microbial periodontal parameters and NAFLD (8–10). In addition, animal studies employing infection with periodontopathic bacteria such as *Porphyromonas gingivalis*, a representative periodontopathic bacterium with various unique virulence factors (11), or ligature-induced periodontitis have shown that these experimental conditions aggravate the clinical manifestations of NAFLD (10, 12, 13).

The possible mechanisms by which periodontal disease exacerbates NAFLD conditions have been considered to include endotoxemia and diffusion of inflammatory mediators from the periodontal tissue to the systemic circulation. These notions are based on studies showing that periodontal bacterial DNA is present in the various locations, such as the atheroma tissue, and that elevated serum levels of proinflammatory cytokines and high-sensitivity C-reactive protein are elevated in periodontitis patients (7). Although dental procedures, especially scaling and root planing, facilitate the entry of bacteria residing in periodontal pockets into the bloodstream (14), spontaneous bacteremia in patients with periodontal disease is rarely seen without such intervention (15). In addition, oral bacteria other than periodontopathic bacteria and enterobacteria can be detected in the vascular lesions of patients with cardiovascular disease and periodontitis, with a prevalence notably higher than that of periodontopathic bacteria (16). Therefore, there may be another causal mechanism responsible for the link between periodontal disease and NAFLD.

Recent observations strongly suggest that the gut microbiota plays a substantial role in the development of NAFLD in humans (17–19), as well as in animal models (20, 21). In this regard, we have demonstrated that orally administered *P. gingivalis* induces alterations in the composition of gut microbiota (22–25). The dysbiosis induced by periodontopathic bacteria is closely associated with decreased expression of tight junction proteins, endotoxemia, and the inflammatory phenotype of various tissues, including liver tissue and adipose tissue. These inflammatory changes are also associated with NAFLD, suggesting that changes in the gut microbiota caused by orally administered *P. gingivalis* may be involved in the pathogenesis and progression of NAFLD. Although *P. gingivalis* is the most well-known and extensively investigated periodontopathic bacterium, the effect of other bacteria, such *Prevotella intermedia* [which was reported to have minor effects on gut microbiota in a collagen-induced arthritis model (24)], are not known. Therefore, the present study was designed to investigate the underlying causal mechanisms through which periodontal disease increases the risk of NAFLD leveraging the oral–gut connection.

MATERIALS AND METHODS

Ethics Statement

This study was approved by the Institutional Animal Care and Use Committee of Niigata University (permit number; SA00328). All experiments were performed in accordance with the Regulations and Guidelines on Scientific and Ethical Care and Use of Laboratory Animals of the Science Council of Japan, enforced on June 1, 2006.

All authors had access to the study data and had reviewed and approved the final manuscript.

Bacterial Cultures

P. gingivalis strain W83 and *P. intermedia* ATCC25611 maintained in our laboratory were cultured in modified Gifu anaerobic medium broth (Nissui, Tokyo, Japan). *Veillonella rogosae* JCM 15642^T and *Actinomyces naeslundii* ATCC19039 obtained from Dr. Mashima at Aichi-Gakuin University, Nagoya Japan and maintained in our laboratory, respectively were cultured in brain–heart infusion broth. *P. gingivalis* and *P. intermedia* were used as periodontopathic bacteria whereas *A. naeslundii* and *V. rogosae* were used as commensal controls.

Dietary Treatment and Bacterial Administration

Six-week-old male C57BL/6N mice were obtained from Japan SLC (Shizuoka, Japan). After acclimatization under specific pathogen-free conditions and feeding regular chow and sterile water for 1 week, the mice were orally administered with any one

of the following: vehicle (PBS with 2% carboxymethyl cellulose; Sigma-Aldrich, St. Louis, MO), or a total of 1×10^9 colony-forming units of each bacterial species suspended in vehicle through a feeding needle five times a week for 3 weeks. The number of administered bacteria was determined by considering the body weight and the number of bacteria in the saliva of periodontitis patients (26–28). At 1 week after the commencement of infection, the diet was changed to CDAHFD60 (#A06071302, Research Diets Inc., New Brunswick, NJ), except for the negative control group that was only administered the vehicle only until the end of the experiment. To analyze the effect of bacteria alone, an experimental group without diet change was also set (**Figure 1**).

Liver Histology and Biochemical Analyses

Part of the left and medial lobes were fixed in neutral-buffered formalin. After deparaffinization and rehydration, paraffin-embedded sections (5 µm in thickness) were stained with hematoxylin and eosin (H&E) or were subjected to Masson's trichrome staining to visualize collagen fibrils.

Liver triglycerides were determined using a Triglyceride Quantification Colorimetric kit (BioVision Inc., Milpitas, CA, USA). Triglyceride levels were expressed as the concentration of triglycerides divided by the total protein concentration. The hepatic hydroxyproline level was photometrically measured using a commercially available kit (Quickzyme Bioscience, Leiden, Netherlands), according to the manufacturer's instructions.

Sequencing of 16S rRNA and Analysis of the Gut Microbiota

Feces were collected and stored at −80°C until ready for use. Fecal DNA extraction was performed as described previously (29, 30). DNA was extracted from fecal samples by using lysozyme (Wako Pure Chemical Industries, Osaka, Japan), achromopeptidase (Wako Pure Chemical Industries), and proteinase K (Merck & Co., Inc., Kenilworth, NJ).

Bacterial DNA from fecal samples was amplified by PCR, as described previously (25). Primers (515F and 806R) with the adaptor sequencing for the Illumina MiSeq platform (Illumina, San Diego, CA, USA) were used. PCR amplification using Ex Taq Hot Start Version (Takara Bio, Shiga, Japan) was performed for 25 cycles. Amplicons were purified with AMPure XP (Beckman Coulter, Brea, CA, USA) and sequenced using the Illumina MiSeq platform.

Metagenomic Sequencing and Analysis

Metagenome shotgun libraries (insert size of 500 bp) were prepared using the TruSeq Nano DNA kit (Illumina) and sequenced on the Illumina NovaSeq platform. After quality filtering, reads mapped to the reference human genome (HG19), and the phiX bacteriophage genome were removed. For each individual, filter-passed NovaSeq reads were assembled using MEGAHIT (v1.2.4). Contigs with a length <500 bp were removed. Gene prediction was performed using the Prodigal software (31). The nucleotide sequences of the predicted genes were clustered using CD-HIT-est v.4.6, with ≥95% sequence identity and ≥90% coverage. The clustered gene sequences were translated into proteins. Functional annotation of the predicted proteins against the KEGG database (release 63) was performed using DIAMOND v0.8, with an E-value of 1e−5. A total of 1 million high-quality reads were mapped onto the nonredundant gene set using bowtie2 to quantify the functional composition of each sample.

Serum Markers

Serum levels of ALT and AST were analyzed using commercially available kits (BioVision, Inc., Milpitas, CA, USA), according to the manufacturer's instructions.

Endotoxin Assay

Serum endotoxin levels were determined using a Limulus Amoebocyte Lysate Test (Toxicolor™ LS50M, Seikagaku Co., Tokyo, Japan), according to the manufacturer's instructions. Serum samples were 1:4 diluted for the assay. Optical densities were measured using an enzyme-linked immunosorbent assay (ELISA) plate reader (Emax Plus, Molecular Devices, San Jose, CA, USA) at 545 nm.

DNA Microarray Analysis

Total RNA from the tissue samples was extracted using the TRIzol reagent (Molecular Research Center) 24 h after the final bacterial or sham administration, and quantified using a NanoDrop 2000 (Thermo Scientific, Wilmington, DE, USA).

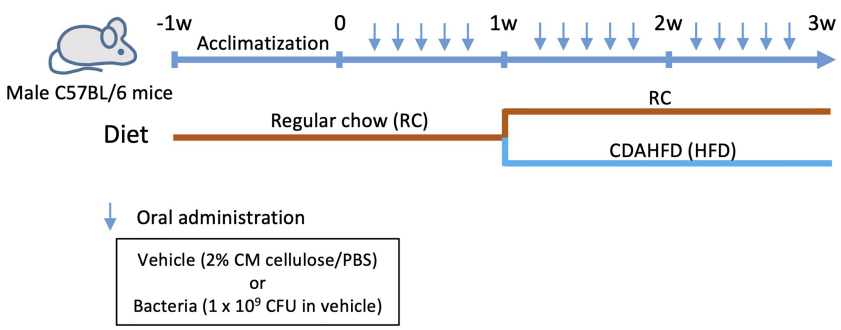

FIGURE 1 | Flowchart depicting the experimental workflow.

The total RNA was labeled and then hybridized to an Agilent SurePrint G3 Mouse Gene Expression 8 x 60K mRNA microarray chip (Agilent Technologies). All microarray experiments were conducted in Macrogen, Japan (Kyoto, Japan).

Microarray results were extracted using the Agilent Feature Extraction software v11.0 (Agilent Technologies). Hierarchical cluster analysis was performed using complete linkage and Euclidean distance as a measure of similarity. Gene enrichment and functional annotation analysis for the significant probe list was performed using the GO resource (www.geneontology.org/). All data analyses and visualization of differentially expressed genes were conducted using R 3.3.2 (www.r-project.org).

Gene Set Enrichment Analysis

Hierarchical cluster analysis was carried out using Ward's linkage (ward.D2) with Euclidean distance (32), and transcriptomic data were clustered into 21 groups. Among the 21 clusters, we selected seven characteristic clusters with up- or downregulated genes in *Pg* mice. Enrichment analyses were performed to obtain more information about the biological functions and pathways significantly enriched in up- and downregulated genes by focusing on the GO term biological process and KEGG pathways using the DAVID enrichment analysis system (33). P-values were corrected for multiple testing using the Benjamini–Hochberg method implemented in DAVID (34).

Quantitative Analysis of Gene Expression in the Liver and Intestines

cDNA was synthesized using the Transcriptor Universal cDNA Master (Roche Molecular Systems, Pleasanton, CA, USA). Primers and probes for real-time PCR were purchased from Life Technologies (Waltham, MA, USA). Reactions were carried out in a LightCycler 96 System (Roche) using TaqMan Gene Expression Assays (Life Technologies) as described previously (24). The LightCycler 96 software (Roche) was used to analyze the standards and perform quantification. The relative quantity of each mRNA was normalized to that of glyceraldehyde-3-phosphate dehydrogenase mRNA.

Quantitation of Serum and Liver Metabolites

Serum samples diluted to one-sixth of their original concentration in 100 mmol/L potassium phosphate buffer (in deuterium oxide containing 1 mmol/L sodium 2,2-dimethyl-2-silapentane-5-sulfonate, pH = 7) were quantified using an Nuclear Magnetic Resonance (NMR) spectrometer (Bruker AVANCE II 700, Bruker Biospin, Rheinstetten, Germany) as described previously (25, 35). Intact liver samples were placed in zirconia 4 mm diameter zirconia rotors and analyzed by ^{1}H high-resolution magic angle spinning (hr-MAS) NMR spectroscopy at 500.132 MHz, with a spin rate of 4000 Hz (36). To annotate the signals detected in the ^{1}H NMR spectra, two-dimensional *J*-resolved (*J*-res) NMR measurements (Bruker standard pulse program "jresgpprqf") and hetero-nuclear single quantum coherence (HSQC) measurements (Bruker standard pulse program "hsqcetgpsisp2.2" were performed as described previously (37–39). The detected signals were annotated using the SpinCouple program (40) (http://dmar.riken.jp/spincouple/), and InterAnalysis program (41) (http://dmar.riken.jp/interanalysis/) based on HSQC and *J*-res cross peaks.

Immunofluorescence Staining

Tissue sections above mentioned were deparaffinized with xylene, and rehydrated. This was followed by heat-induced antigen retrieval in BD Retrievagen A (pH 6.0, BD Biosciences, San Diego CA, USA). After blocking in fetal bovine serum (FBS), tissues were incubated with fluorescence-labeled anti-E-cadherin antibody (Alexa FluorTM 594 anti-mouse/human CD324, Biolegend, San Diego, CA, USA). After mounting with VECTASHIELD HardSet Mounting Medium with DAPI (Vector Laboratories, ABurlingame CA, USA), the stained sections were visualized by fluorescence microscopy (Biozero BZ-X710; Keyence Corporation, Osaka, Japan).

Cell Culture

HepG2 cells were obtained from the American Type Culture Collection (Manassas, VA) and maintained in Dulbecco's modified Eagle's medium (DMEM) supplemented with 1% penicillin/streptomycin and 10% FBS in an atmosphere of 5% CO_2 at 37°C. The cells were seeded in a 48-well plate at 3×10^5 cells/well and cultivated for 24 h. Thereafter, the medium was changed to DMEM without FBS and the cells were cultured overnight. The cells were treated with a free fatty acid solution (final concentrations: 0.5 mM oleic acid and 0.25 mM palmitic acid) and fat-free bovine serum albumin for 24 h. The cells were then stimulated with LPS (1 μg/mL *P. gingivalis* or *P. intermedia* LPS, and 1 ng/mL *E. coli* LPS) for 4 h. Total RNA was extracted from the cells as described above and used for quantitative PCR.

Bioinformatics and Statistical Analyses

Taxonomic assignments and estimation of relative abundance from sequencing data were performed using the analysis pipeline of the QIIME2 version 2020.6.0 (42). Amplicon sequence variants (ASVs) were inferred from the denoised reads using DADA2 (43) implemented in QIIME2. The ASV taxonomy was assigned based on a comparison with the SILVA version 138 (44). β-Diversity was calculated using weighted UniFrac distances based on the operational taxonomic unit distribution across samples and visualized by principal coordinate analysis (PCoA).

From the results of metagenomic analysis at TP2 and TP3, KEGG orthologies (KOs) with significant differences determined by the t-tests, which were carried out by using R, between two groups, except for RC mice, were extracted under the condition of $P < 0.01$. The KOs were mapped to the reference pathway in the KEGG database. Significant pathways were enriched with Fisher's exact probability tests using the number of KOs mapped in each pathway. The p-values were adjusted by using the Benjamini–Hochberg method, which are used as q-values in the **Figure 6**. The quantified metabolome data were normalized using an autoscaling method and statistically analyzed using PCA.

Statistical analyses were performed using the GraphPad Prism version 9 (GraphPad Software, Inc., La Jolla, CA, USA)

and R (version 4.0.4.). Randomization or blinding was not performed in the present study. All data are expressed as the mean ± standard error of the mean. Statistical analyses were performed using one-way analysis of variance with Tukey's correction. Analysis of similarity was performed to identify differences in bacterial community compositions and PERMANOVA (PERmutational Multivariant Analysis Of Variance) was used for comparison of microbes between groups. Statistical significance was set at $P < 0.05$.

RESULTS

Oral Pathobionts, But Not Symbionts, Worsen NAFLD Pathology

Oral administration of bacteria did not affect body weight until commencement of the diet change, and no difference was observed among the vehicle-, *Actinomyces naeslundii*-, *Veillonella rogosae*-, *P. gingivalis*- and *P. intermedia*-administered mice (hereafter referred to as Sham, *An*, *Vr*, *Pg*, and *Pi* mice, respectively). After changing the diet from regular chow (RC) to choline-deficient, l-amino acid-defined, high-fat diet with 60 kcal% fat and 0.1% methionine (CDAHFD60) (CDAHFD60; HFD), a gain in body weight was suppressed in all experimental groups in comparison with RC-fed mice. In contrast, the liver-to-body weight ratio was significantly increased in Sham, *An*, and *Pg* mice compared with that in RC-fed mice (**Figure 2A**). HFD feeding promoted hepatic steatosis in all experimental groups, and the degree of steatosis was greater with *P. intermedia* administration, and it was further aggravated by *P. gingivalis* administration (**Figure 2B**). Similarly, the degree of fibrosis was progressively exacerbated with increasing bacterial burden (sham < *P. intermedia* < *P. gingivalis*) (**Figure 2C**). In contrast, no additional histological changes were observed with *A. naeslundii* and *V. rogosae* administration compared with those in Sham mice. Bacterial administration induced minimal histological changes in the liver of RC-fed mice except for *Pg* mice, in which slight steatosis was observed (**Supplementary Figure 1**). Therefore, further analyses were focused on *Pg* and *Pi* mice.

Under these conditions, the content of hepatic hydroxyproline increased with the increasing bacterial burden (**Figure 2D**). Although triglyceride content and aspartate transaminase (AST) and alanine transaminase (ALT) activities were significantly higher in HFD-fed groups, bacterial administration had no effect on them (**Supplementary Figure 2**).

Effect of Bacterial Administration on Gut Barrier Function

Dysregulation of gut barrier function and subsequent endotoxemia are major contributors to NAFLD. Therefore, we analyzed whether the barrier function was altered in *Pg* mice, and if the barrier function was disorganized, whether endotoxemia was induced. As shown in **Figure 3A**, the expression of *Tjp1*, encoding tight junction protein, tended to be lower in *Pg* mice compared with other groups. Moreover, a decrease in the expression of E-cadherin was observed in the colon of *Pg* mice (**Figure 3B**). Additionally, the serum endotoxin level was increased with the increasing bacterial burden. The level was significantly higher in *Pi* mice compared with that in RC-fed and Sham mice, and it was further elevated in *Pg* mice (**Figure 3C**).

Administration of Oral Bacteria Affects the Gut Microbial Composition and the Expression Profile of Genes in the Intestine

The global differences among experimental groups were evident from baseline (time point 1; TP1) to TP2, after 1 week of bacterial administration, as well as after additional HFD-feeding (TP3), according to the analyses of α- (**Figure 4A**) and β-diversities (**Figure 4B**).

At TP2, the proportion of the phylum Firmicutes was significantly lower in *Pg* mice than that in Sham mice (**Figure 5A**). However, the proportion of phylum Bacteridota (previously known as Bacteroidetes) did not differ among the experimental groups. At the genus level, the proportion of *Eubacterium fissicatena* group was significantly higher in *Pg* mice than in Sham mice. In contrast, the proportion of *Lactobacillus* was significantly lower and tended to be lower in *Pg* mice compared to RC-fed and Sham mice, respectively (**Figure 5B**).

HFD feeding had a strong effect on the gut microbiota composition. Despite the considerable effect of diet, bacterial administration induced a substantial change in the gut microbiota composition. Although no difference was observed in the phylum Firmicutes, HFD feeding significantly decreased the proportion of the phylum Bacteridota (**Figure 5C**). At the genus level, significantly elevated proportions of *Atopostipes* and *Colidextribacter* were observed in *Pg* mice compared with those in RC and Sham mice. The proportions of *Lactobacillus* and *Muribaculaceae* were significantly lower in HFD-fed mice and there was no effect of bacterial administration (**Figure 5D**). Although HFD feeding increased the abundance of many genera, there were some notable patterns of relative abundance among the different experimental groups. While *P. intermedia* administration further increased the relative abundance of some genera, it suppressed the effect of HFD feeding in some genera (**Supplementary Figure 3**).

Thus, hepatic pathology observed in *Pg* mice appeared to be directly related to gut dysbiosis. Consistent with these findings, the expression profile of genes in the intestine showed distinct patterns when compared between any two experimental groups (**Supplementary Figure 4**), suggesting that diet as well as the administered bacteria have a characteristic effect on gene expression, possibly through changes in the gut microbiota composition.

Effect of Oral Pathobiont Administration on Metabolic Pathways in the Gut

Enrichment analysis was applied to the relative abundance of Kyoto Encyclopedia of Genes and Genomes (KEGG) pathways *via* metagenomic analysis to study the function of gut microbiota in different groups at different time points. At TP2, in *Pg* and *Pi* mice, the enriched KEGG pathways overlapped with elevated amino acid

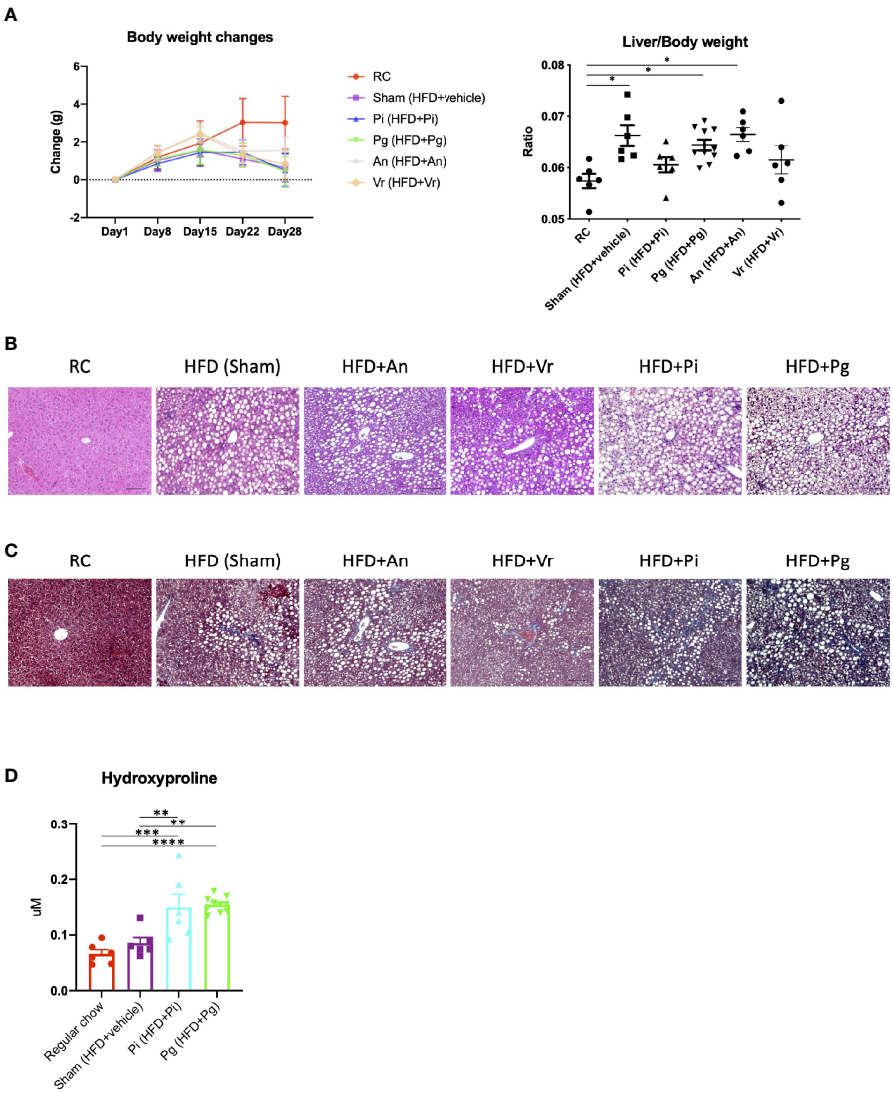

FIGURE 2 | Bacterial administration exacerbates high fat diet-induced liver pathology. **(A)** Changes in body weight and liver/body weight ratios of mice in each group during the experimental period. *Pi* mice had a significantly lower body weight compared with RC mice at day 28 (n=6-10/group). **(B)** Hematoxylin and eosin staining of liver (scale bars, 100 μm). **(C)** Masson's trichrome staining of the liver. **(D)** Hepatic contents of hydroxyproline (n=6-10/group). RC: C57BL/6N mice fed regular chow; Sham: Mice fed CDAHFD60 plus sham administration; *Pi*: Mice fed CDAHFD60 plus *P. intermedia* administration; *Pg*: Mice fed CDAHFD60 plus *P. gingivalis* administration, *An*: Mice fed CDAHFD60 plus *A naeslundii* administration, *Vr*: Mice fed CDAHFD60 plus *V. rogosae* administration. Data are expressed as the mean ± standard error of the mean (SEM). *P* values were calculated using one-way ANOVA with Tukey's multiple comparisons test. $^{*}P < 0.05$, $^{**}P < 0.005$, $^{***}P < 0.001$, $^{****}P < 0.0001$.

metabolism, particularly, with respect to phenylalanine, tyrosine, and tryptophan biosynthesis. In *Pi* mice, the lipopolysaccharide biosynthesis pathway was also notably overrepresented. A total of eight enriched KEGG pathways, including the NOD-like receptor signaling pathway, were observed in *Pg* mice relative to the pathways observed in *Pi* mice (**Figure 6A**). Although the effect of bacterial administration on the gut metabolic pathways was diminished after HFD feeding (the number of pathways enriched at TP2 decreased compared to that at TP2), the difference between *Pg* mice and *Pi* mice was even more pronounced. Similar to TP2, amino acid metabolic pathways were the characteristic pathways when the two groups were compared. In addition, the pathways for fatty acid degradation and the two-component system were enriched in *Pg* mice relative to those in *Pi* mice (**Figure 6B**).

Metabolic Profiles Are Affected by Bacterial Administration

We further analyzed liver tissue and serum samples to assess whether the murine metabolome was perturbed by bacterial administration, in addition to being affected by diet. We performed an untargeted analysis of all the data acquired to examine a wider pool of metabolites. Principal component analysis (PCA) was conducted using nuclear magnetic resonance (NMR)-derived data to obtain an overview of the differences among

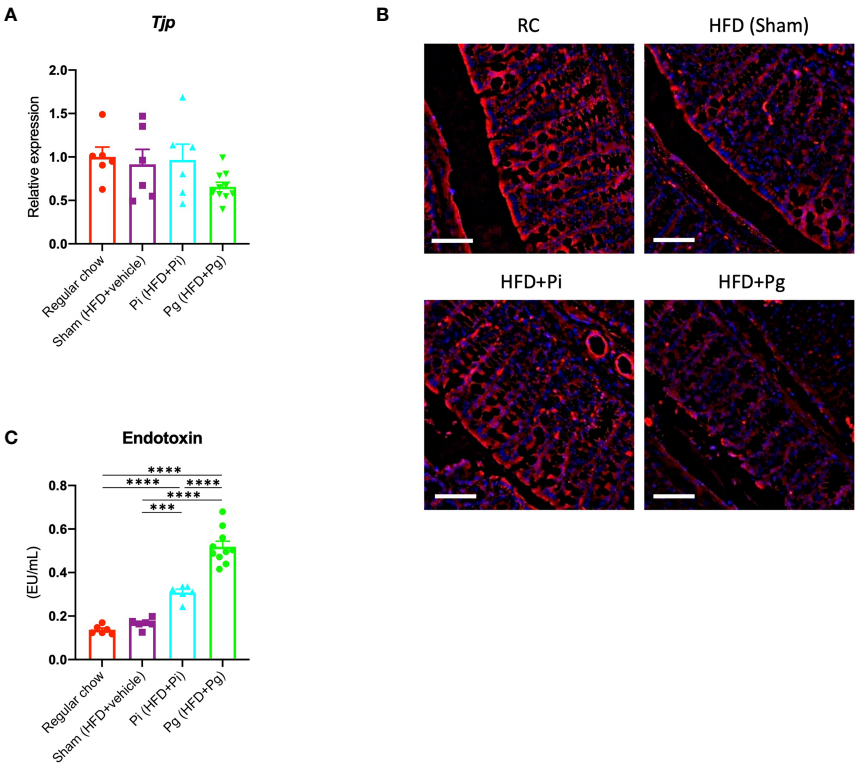

FIGURE 3 | *P. gingivalis* administration induces gut barrier dysfunction. **(A)** Expression of *Tjp1* in the small intestines. cDNA was amplified with primers specific for *Tjp1* (n=6-10/group). The relative quantity of mRNA was normalized to that of glyceraldehyde-3-phosphate dehydrogenase mRNA. **(B)** Immunofluorescence analysis of E-cadherin in large intestines from each group. Red: E-cadherin, blue: DAPI, scale bars: 50 μm. **(C)** Serum endotoxin levels in the various groups (n=6-10/group). Data are expressed as the mean ± standard error of the mean (SEM). *P* values were calculated using one-way ANOVA with Tukey's multiple comparisons test. $^{***}P < 0.001$, $^{****}P < 0.0001$.

the groups. This analysis not only differentiated HFD-fed mice from RC-fed mice, but also highlighted the effect of *P. gingivalis* administration among HFD-fed mice in the liver tissue and serum metabolites (**Supplementary Figure 5A** and **Figure 7A**), which was consistent with the histological findings. Furthermore, the machine-learning model allowed a discrete classification within the four groups in both tissue and serum metabolites; maltose, choline, a fatty acid (FA.CH3.n.3), choline metabolite (CHONCH3), and methionine were among the characteristic metabolites in the tissue (**Supplementary Figure 5B**), whereas metabolites such as ROI.38 [which has been suggested to be a sugar-phosphate (sugar-P)], tyrosine, and choline were revealed to be important in the serum (**Figure 7B**). The tissue profile of short-chain fatty acids (SCFAs) showed no difference among the groups (**Supplementary Figure 6A**). In contrast, the levels of acetate and citrate were significantly higher in HFD-fed mice compared with those in RC-fed mice and tended to increase with an increasing bacterial burden, with the highest level in the serum of *Pg* mice. However, there was no difference in the level of the other SCFAs (**Supplementary Figure 7A**). With respect to the amino acid levels in the tissue, the level of lysine was significantly decreased in HFD-fed mice, with a further decrease in *Pg* mice compared with Sham mice. A similar trend was observed for threonine (**Supplementary Figure 6B**). The level of ChoNCH3, a choline metabolite, showed a pattern similar to that of choline (**Supplementary Figure 5C**). The levels of lipid metabolites were increased in HFD-fed mice; however, bacterial administration had a minimal effect on these levels (**Supplementary Figure 5C**). In the sera, HFD feeding significantly elevated the serum levels of the annotated signals, except for isoleucine, glutamine, and phenylalanine (**Supplementary Figure 7B**). Notably, tyrosine levels were significantly elevated in *Pg* mice compared with those in Sham mice. Similarly, sugar-P levels were significantly higher in *Pg* mice compared with those in the other groups. The choline levels were drastically lower in *Pg* mice compared with those in the other groups (**Figure 7C**). The levels of other annotated molecules were also elevated in HFD-fed mice, except those of allantoin, which increased with increasing nutrition and bacterial burden, and there was a significant difference in these levels between RC-fed and *Pg* mice (**Supplementary Figure 7C**).

Oral Administration of Periodontopathic Bacteria Modulates the Hepatic Expression of Genes Implicated in NAFLD Pathology

Although the effect of HFD feeding on the liver was robust, it was evident that the administration of both bacteria induced additional and substantial changes in the expression profile of

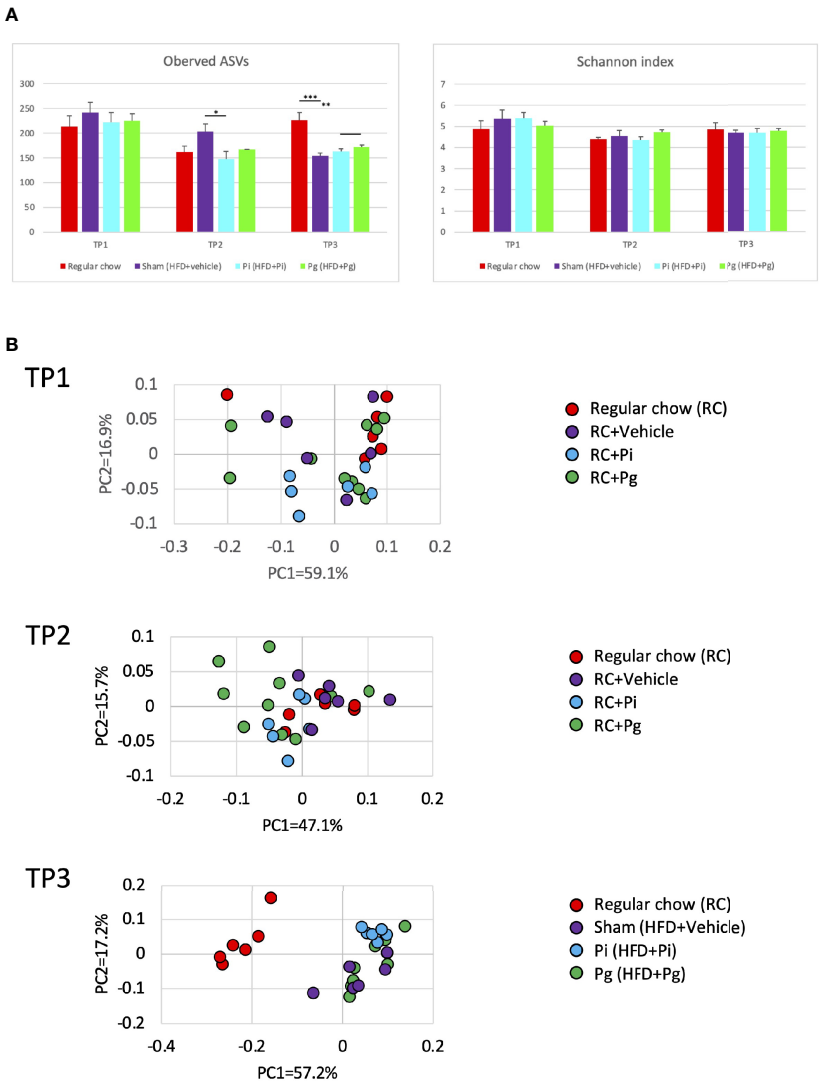

FIGURE 4 | Effect of CDAHFD60 feeding and subsequent bacterial administration on the gut microbiota composition (n=6-10/group). Fecal samples from mice in various treatment groups were subjected to 16S rRNA sequencing. **(A)** Alpha diversity of each experimental group at different time points. ASV, Amplicon sequence variant. **(B)** Principal coordinate analysis score plot of the gut microbiota profiles of each experimental group at different time points using weighted UniFrac distance. Data are expressed as the mean ± standard error of the mean (SEM). *P* values were calculated using one-way ANOVA with Tukey's multiple comparisons test. $^{*}P < 0.05$, $^{**}P < 0.005$, $^{***}P < 0.001$.

genes. Moreover, the expression profile of genes in the liver was clearly distinct between *Pi* and *Pg* mice (**Supplementary Figure 8**). Therefore, we evaluated the expression of genes in the liver using functional enrichment analysis.

Based on hierarchical clustering, we extracted seven clusters in which genes in clusters 1–3 were downregulated, whereas those in clusters 4–6 were upregulated in *Pg* mice compared with the other groups. Cluster 7 included genes, the expression levels of which were higher in *Pg* mice than those in RC-fed mice, but lower compared with those in Sham and *Pi* mice (**Supplementary Figure 9**). The genes in these clusters are listed in **Supplementary Table 1**.

In cluster 1, significantly downregulated genes were mostly annotated as those involved in the biosynthesis and metabolic processes of lipids, organic acids, oxoacids, steroids, and fatty acids. No gene ontology (GO) terms were enriched in clusters 2 and 3. In cluster 4, genes involved in the cell cycle, cell death, nuclear division, DNA replication, responses to oxidative and ER stress, and regulation of intrinsic apoptosis were upregulated. In cluster 5, genes involved in the inflammatory response, such as in the regulation of leukocyte migration, response to lipopolysaccharide (LPS), cellular response to inflammatory cytokines, and nuclear factor-κB (NF-κB) pathways, were significantly enriched. In cluster 7, genes involved in the biological processes for circadian regulation of gene expression were significantly enriched (**Supplementary Table 2**).

The significantly enriched KEGG pathways in clusters 1, 2, and 4 are shown in **Supplementary Table 3**. These included

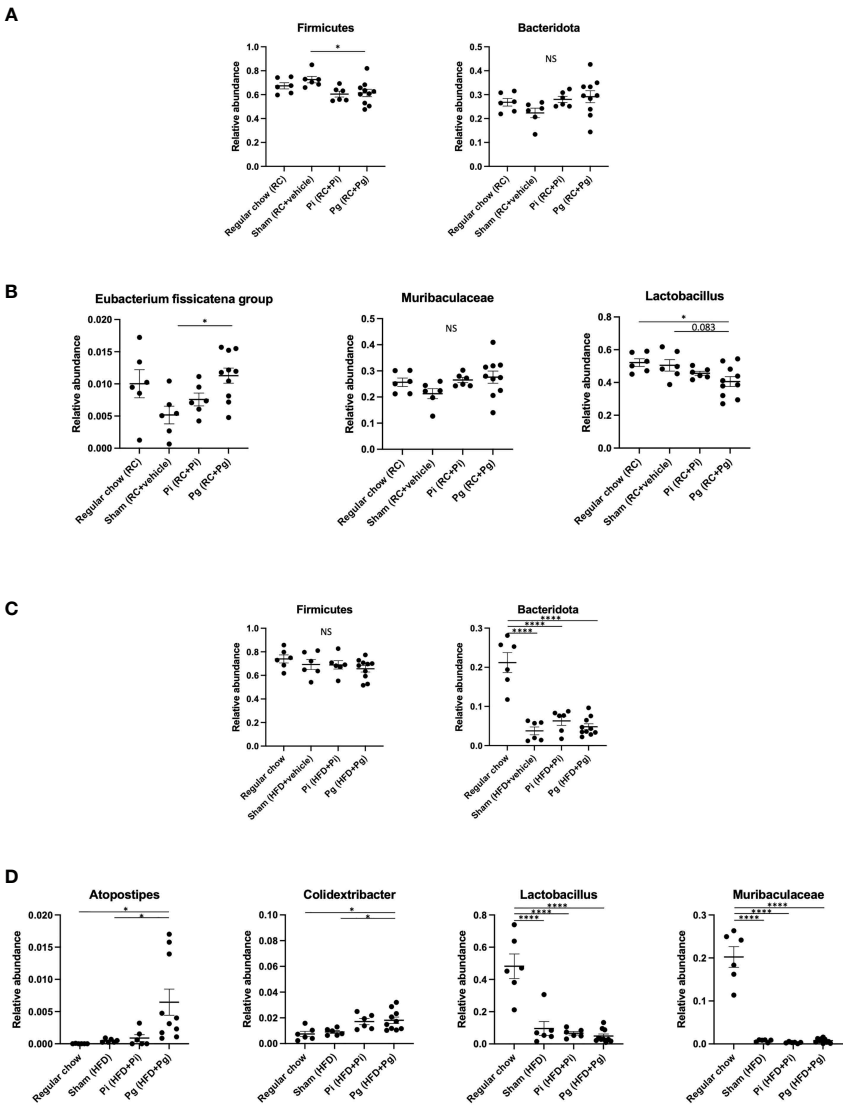

FIGURE 5 | Effect of bacterial administration (TP2) and additional diet change (TP3) on the gut microbiota composition (n=6-10/group). Fecal samples from mice that received the various treatments were subjected to 16S rRNA sequencing. **(A)** Relative abundance of phyla Firmicutes and Bacteridota at TP2. **(B)** Relative abundances of characteristic genera in each experimental group at TP2. **(C)** Relative abundance of phyla Firmicutes and Bacteridota at TP3. **(D)** Relative abundances of characteristic genera in each experimental group at TP3. Data are expressed as the mean ± standard error of the mean (SEM). *P* values were calculated using one-way ANOVA with Tukey's multiple comparisons test. $^{*}P < 0.05$, $^{****}P < 0.0001$. NS, not significant.

various pathways for steroid hormones, retinol, primary bile acids, arachidonic acid, amino sugars, and nucleotide sugars. Some metabolic pathways were consistent with the enriched Gene Ontology (GO) terms in cluster 1. The top 15 significant GO terms and the complete list of enriched KEGG pathways in each cluster are shown in **Figure 8**.

Progression from simple steatosis to steatohepatitis, fibrosis, and hepatocellular carcinoma is believed to be mediated by multiple parallel factors, including inflammation, ER stress, lipotoxicity, and altered circadian rhythms. The GO terms and KEGG pathways implicated in these events were found to be significantly enriched in the clusters (**Supplementary Tables 2, 3**). To confirm the data of DNA microarray analysis, quantitative real-time PCR was conducted for representative genes involved in the pathological mechanisms of NAFLD. Genes involved in the inflammatory responses were upregulated by HFD feeding, irrespective of the bacterial administration. The expression of *Tsc22d3*, which mediates the anti-inflammatory response, was only elevated in *Pg* mice, reflecting a weaker elevation of inflammatory genes in this group (**Supplementary Figure 10A**).

Fibrosis- and ER stress-related genes were enriched and classified in cluster 4. Whereas *Col1a1* and *Timp1* were upregulated by HFD feeding, *Ctgf* was upregulated specifically by *P. gingivalis* administration (**Supplementary Figure 10B**).

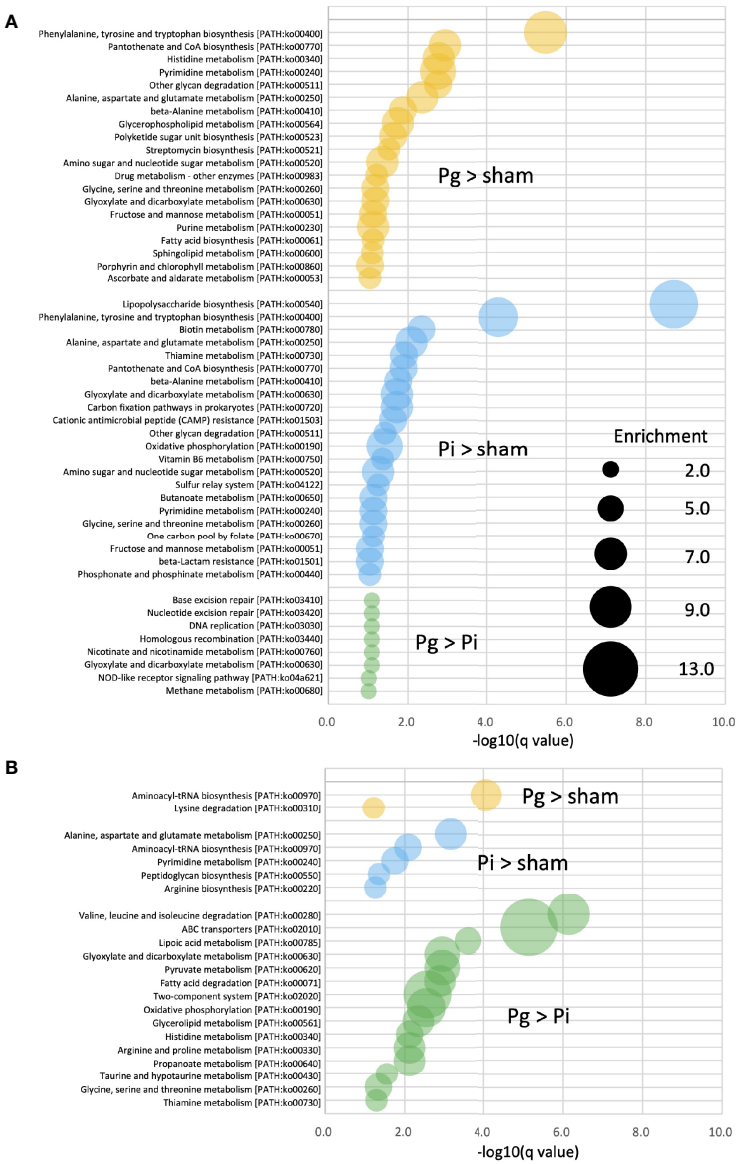

FIGURE 6 | KEGG biomarkers from the metagenomic analysis of gut microbiota. Pathway analysis of differentially enriched genes between two groups. Enriched KEGG pathways ($q < 0.1$) at TP2 **(A)** and TP3 **(B)** are shown. The bubble size indicates the number of KOs enriched in each pathway. Expressions containing inequality signs (e.g., "*Pg* > Sham") indicate that the results of enrichment analysis with Kos, in which the abundant of KOs for the left category (*Pg* mice) are significantly more abundant than those in the right category (Sham mice).

ER stress-related genes *Chop*/*Ddit3* and *Ddit4* were also elevated by *P. gingivalis*. Consistent with these findings, *Fgf21* and *Trib3*, both of which are induced by ER stress and have been reported to be elevated in NAFLD, were significantly upregulated in *Pg* mice, but not in *Pi* mice (**Supplementary Figure 10C**).

The GO terms associated with the cell cycle process, which are potentially implicated in carcinogenesis and end-stage NAFLD, were also enriched in cluster 4. The expression of *Hnf6* and *Hhex* was upregulated in *Pi* mice, but not in *Pg* mice (**Supplementary Figure 10D**). The expression of *Hnf6* in hepatocellular carcinoma (HCC) cells is negatively associated with their malignancy. Delivery of *Hhex* into a hepatoma cell line has been reported to decrease the expression of several proto-oncogenes and to increases the expression of some tumor suppressor genes (45).

In cluster 7, GO terms associated with controlling the circadian rhythm were enriched. Fluctuations in the circadian rhythm affect metabolism and alter the expression of liver clock genes in NAFLD pathology. In this connection, the clock gene, *Per1*, was significantly elevated in *Pg* mice. *Pg* and *Pi* mice demonstrated contrasting expression patterns of *Bmal1* and *Dbp*. (**Supplementary Figure 10E**).

These distinctive expression profiles of hepatic genes in RC-fed, *Pi*, and *Pg* mice may not be due to the direct effect of administered

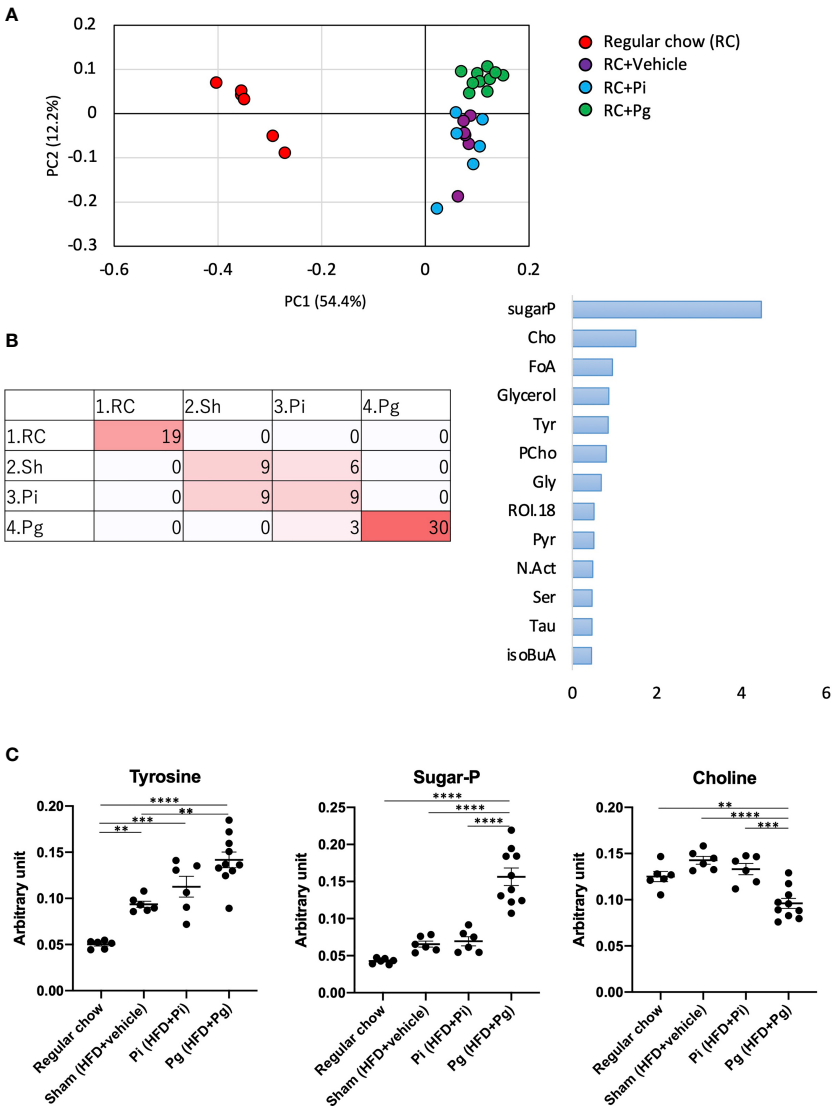

FIGURE 7 | Effect of CDAHFD60 feeding and subsequent bacterial administration on serum metabolites. **(A)** PCA of serum metabolites in each group. **(B)** Machine learning (random forest) classification of each group. Left: confusion matrix (RC, regular chow; Sham, HFD + vehicle; Pi, HFD + Pi; Pg, HFD + Pg). Right: important variables (metabolites) contributing to four classifications. Tyr, tyrosine; CHO, choline; FoA, formate; Gly, glycine; CiA, citrate; GPC, glycerophosphocholine; Ac, acetate; ROI, region of interest. **(C)** Compounds that differed in abundance among groups (n=6-10/group). Data are expressed as the mean ± standard error of the mean (SEM). *P* values were calculated using one-way ANOVA with Tukey's multiple comparisons test. $^{**}P < 0.005$, $^{***}P < 0.001$, $^{****}P < 0.0001$.

bacteria, but rather due to differences in the gut microbiota compositions triggered bacterial administration. In support of this assumption, the gene expression of ER stress-related genes in HepG2 cells stimulated with LPS from *P. intermedia*, *P. gingivalis*, and *E. coli* was different from that in the liver of each experimental group (**Supplementary Figure 11**).

DISCUSSION

Recent indisputable evidence suggests that gut dysbiosis is a driver of NAFLD progression. An association between gut dysbiosis and NAFLD pathology has been described in the context of increased gut permeability, exposure of the liver to bacteria and bacterial products, and altered metabolites produced by the gut microbiota (46). Oral dysbiosis is a characteristic feature of periodontitis patients, and these patients continuously and unconsciously swallow pathobionts present in the saliva. Therefore, the concept that swallowed pathogenic oral microbiota induces gut dysbiosis is likely to be another possible causal mechanism linking periodontitis and NAFLD. In fact, in this study, the oral pathobionts *P. intermedia* and *P. gingivalis*, but not the oral symbionts *A. naeslundii* and *V. rogosae*, worsened HFD-induced NAFLD, with *P. gingivalis*

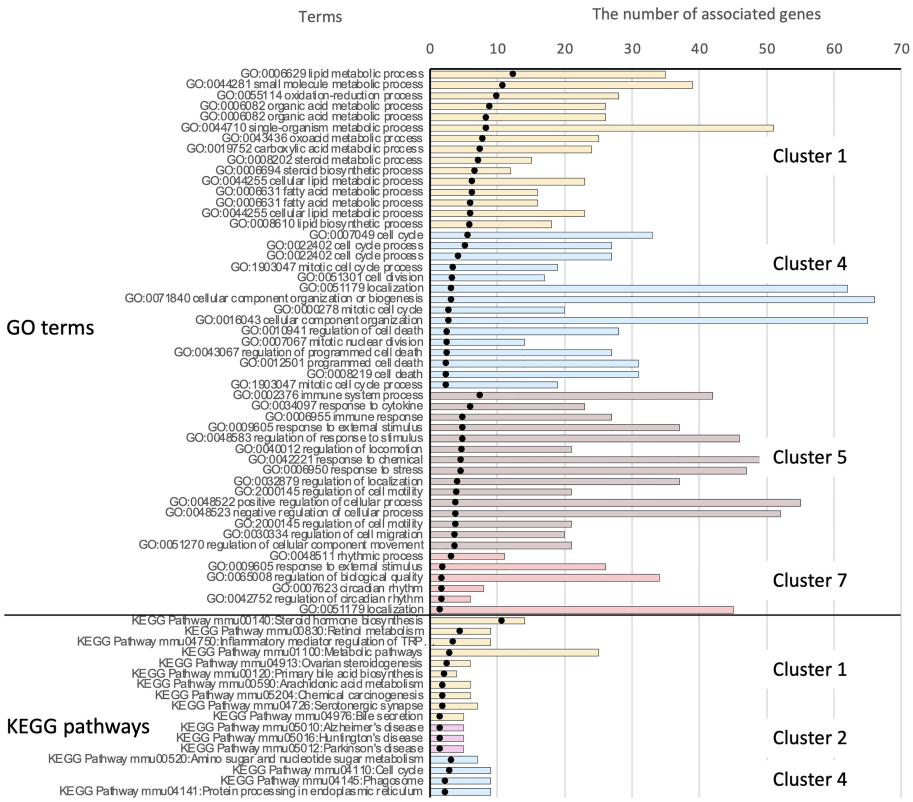

FIGURE 8 | Results of functional enrichment analysis. Owing to the large number of significant GO terms (corrected $p < 0.05$), only the top 15 significant terms from each cluster are shown. For results of KEGG pathway analysis, all significant pathways are presented. Black dots indicate the –log10 of Benjamini-Hochberg-corrected p-values. The top 51 bars show the results of GO enrichment, and the bottom 17 bars show enriched KEGG pathways. Bars showing the associated clusters are indicated.

showing higher pathogenicity. These pathological changes coincided with the reduction in the gut barrier function and serum levels of endotoxin, which is a gut dysbiosis-related risk factor for NAFLD.

Consistent with the results of our previous study and those of others, gavage of oral pathobionts induced changes in the gut microbiota composition (**Figure 4**). Despite the pronounced effect of diet change on the gut microbiota composition, the effect of oral pathobionts remained obvious. Furthermore, a significant difference in the microbiota composition was observed between *Pi* and *Pg* mice. Because the effect of *P. gingivalis* was not distinctive compared to that of *P. intermedia* at TP2, ingestion for a longer time and consumption of HFD may synergistically affect the gut microbiota composition.

P. gingivalis, but not *P. intermedia*, induced a significant reduction in the proportion of bacteria belonging to the phylum Firmicutes (**Figure 5**). Among the bacteria in the phylum Firmicutes, the proportion of *Lactobacillus* was significantly decreased in *Pg* mice, supporting the findings of the protective role of *Lactobacillus* against NAFLD (47, 48). In addition, significant changes in the *Eubacterium fissicatena* group were observed at TP2. Although some species of *Eubacterium* have been reported to be contribute to NAFLD pathogenesis (49), the role of these bacteria remains to be determined.

Additionally, the fundamental effect of *P. gingivalis* on the gut microbiota was evident after the change in diet (TP3 in **Figure 4B**). Although the role of these bacteria in liver pathology has not been clarified, *Colidextribacter* has recently been reported to be positively correlated with serum levels of oxidative markers (50) and hyperlipidemia-related parameters (51). In addition, functional enrichment analysis of the expression profiles of genes in the liver demonstrated that the genes involved in the response to oxidative stress were enriched (Cluster 4) in *Pg* mice.

Metagenomics analysis demonstrated the accumulation of genes implicated in the different KEGG pathways characteristic of each experimental group, suggesting a functional alteration of the gut microbiota by different pathobionts (**Figure 6**). At TP2, phenylalanine, tyrosine, and tryptophan biosynthesis pathways (ko00400) and alanine, aspartate, and glutamate metabolism pathways (ko00250) were significantly enriched in *Pg* and *Pi* mice compared with Sham mice. Alanine, aspartate, and glutamate metabolism pathways have recently received attention as risk factors in the development of NAFLD. Dysregulated glutamine metabolism has also been implicated in NAFLD pathology (52).

Despite the significant effect of HFD on gut microbiota, the effect of oral pathobionts was still obvious, given the enriched amino acid metabolism at TP3. In addition, fatty acid metabolism and the two-component system were enriched in *Pg* mice, as compared with *Pi* mice. The former (ko00071) is related to increased levels of L-palmitoyl-carnitine, which has been reported to be associated with ischemic heart disease (53), and the latter (ko02020) is known to regulate various virulence genes (54), suggesting a pathogenic role of oral pathobionts against the gut microbiota.

A change in the gut microbiota composition can affect NAFLD pathology *via* various pathways and involved metabolites that are the products of gut microbial metabolism. Such bioactive metabolites are absorbed from the intestinal tract into the systemic circulation *via* the portal vein; therefore, serum metabolomic data can partially reflect the level of gut microbial metabolites. Although a significant effect of diet on the serum metabolomic profile was anticipated at TP3, it is noteworthy that the profile of *Pg* mice was clearly distinct from that of RC-fed and *Pi* mice (**Figure 7A**). Among several metabolites that were found to be differentially abundant in each group, tyrosine was of particular interest. The serum levels of tyrosine were significantly elevated in HFD-fed mice and were further increased in *Pg* mice. Recently, serum levels of amino acids have been shown to be associated with metabolic diseases. Aromatic amino acids have been shown to be associated with the risk of developing not only diabetes (55) and cardiovascular disease (56) but also NAFLD (57, 58). Another molecule of note is choline. Choline deficiency contributes to the development of fatty liver disease through multiple mechanisms, which are fundamental to the animal model used in this study. The level of choline, as a component of lard, was low in the HFD, not meeting the level necessary for optimal health (59). Therefore, the change from RC to the HFD induced NAFLD. Although the HFD was equally fed to Sham, *Pi*, and *Pg* mice, *P. gingivalis* administration further lowered the serum choline levels (**Figure 7C**). In addition to low dietary choline intake, the estrogen status, single nucleotide polymorphisms (60), and gut microbiota are important modulators of choline bioavailability (61), suggesting that the low level of choline in *Pg* mice was highly attributable to the change in gut microbiota. Recently, eight strains of bacteria in the human gut, mostly belonging to the order Clostridiales, were identified to produce trimethylamine from choline (62). This metabolic pathway is highly relevant, with respect to an increased risk of atherosclerosis *via* elevation of trimethylamine-N-oxide levels (63). However, the relative abundance of bacteria belonging to the order Clostridiales was not different among the experimental groups. Therefore, it is assumed that other bacteria may be associated with low levels of serum choline in *Pg* mice. In addition, sugar phosphate was characterized as a metabolite in *Pg* mice. Although the reason for this finding is not known, this may indicate cell damage because phosphorylated sugars are usually localized in cells.

Interplay between the gut microbiota, including the production of byproducts, is the primary mechanism underlying the pathogenesis of NAFLD. DNA microarray and subsequent qPCR analyses of the liver tissue provided insights into the pathological mechanisms induced by different periodontopathic bacteria. Altered expression of genes in the liver caused by administration of either *P. gingivalis*- or *P. intermedia* became evident as a driving force for a more severe disease phenotype by influencing various aspects of disease mechanisms (**Supplementary Figure 10**). Functional enrichment analysis revealed the activation of multiple pathological pathways in the liver by oral pathobionts, particularly *P. gingivalis*. These include genes associated with the NF-κB pathway, ER stress, circadian rhythm, fibrosis-, and tumorigenesis. Among these, the modulation of the expression of ER stress-related genes is of particular interest.

Recently, the importance of ER stress in various aspects of NAFLD has been highlighted (64). Excessive calorie intake and the resulting accumulation of lipids in hepatocytes evoke cellular stress pathways. This type of cellular stress originates from the accumulation of unfolded or misfolded proteins in the ER and usually triggers an adaptive response to resolve the ER stress, namely the unfolded protein response (UPR).

Chop/*Ddit3* is involved in the activation of NF-κB signaling (65) and the promotion of apoptosis in hepatocyte (66), mediating inflammation and fibrosis, and the progression from steatosis to NASH, respectively. Furthermore, another gene, *Trib3*, which has a deleterious effect on insulin signaling in hepatocytes under the control of Chop (67) was significantly upregulated by *P. gingivalis* administration. Similarly, the levels of *Ddit4*, another ER stress-related gene, the expression of which is also mediated through the Perk, IRE1α, and ATF6-dependent cascade (68), were elevated. Considering that the expression of both *Chop* and *Ddit4* in Sham mice was comparable with that in RC-fed mice, the effect of HFD feeding itself might have been well controlled by the UPR, but the additional effect of *P. gingivalis* administration was beyond the well-controlled UPR.

Another notable finding was the disruption of the molecular clock by bacterial administration (**Supplementary Table 3** and **Supplementary Figure 10E**). Factors affecting NAFLD pathology, such as liver metabolic pathways, bile acid synthesis, and immune/inflammatory processes, show circadian patterns driven by the biological clock. Therefore, disruption of the circadian clock leads to various diseases, including NAFLD (69). Although it has been demonstrated that diet-induced dysbiosis disturbs the balance between microbes and host circadian networks, which affects metabolism and obesity (70), orally administered bacteria further modulate the expression of clock genes with distinct patterns induced by different bacteria, suggesting another causal relationship between periodontitis and NAFLD.

The end-stage of NAFLD is HCC. Although histological changes and distinct expression of oncogenes were not observed, carcinogenesis-related genes were enriched in cluster 4 (upregulated in *Pg* mice compared with the other groups; **Supplementary Table 2**), in addition to cellular stress- and inflammation-related genes that are indirectly associated with carcinogenesis. The expression of tumor suppressor genes was significantly elevated in *Pi* mice (**Supplementary Figure 10D**).

In addition, these results suggest that many of the differentially expressed genes in the liver of *Pg* mice were directly or indirectly involved in increased production of secondary bile acid, cytokine responses, and cellular responses to LPS, which are considered to be consequences of impaired gut barrier function.

In the present study, using a nutrient-deficient NAFLD model, orally administered periodontopathic bacteria (especially *P. gingivalis*) induced a change in the gut microbiota composition and serum metabolome, resulting in alteration of the liver transcriptome toward aggravation of the pathology in NAFLD. These results provide new insights into the mechanisms by which periodontitis contributes to NAFLD pathology.

Although our mouse model can be considered to be a reliable physiological model that is clinically relevant to the human disease, it does not fully reflect pathology in humans. For example, it lacks the development of significant obesity and glucose intolerance (71). Moreover, administration of a single species of periodontopathic bacteria does not completely replicate the condition of periodontitis patients, although the number of bacteria required to do so is not excessive, considering the number of bacteria in saliva of periodontitis patients (26–28). Furthermore, we were unable to identify the pathogenic gut bacteria involved in aggravation of NAFLD. Therefore, further studies are needed to identify the bacteria responsible for the exacerbation of NAFLD caused by *P. gingivalis* administration.

DATA AVAILABILITY STATEMENT

The datasets presented in this study can be found in online repositories. The names of the repository/repositories and accession number(s) can be found below: https://www.ncbi.nlm.nih.gov/, GSE136937.

ETHICS STATEMENT

The animal study was reviewed and approved by The Institutional Animal Care and Use Committee of Niigata University (permit number; SA00328).

AUTHOR CONTRIBUTIONS

KyY generated data and wrote the manuscript. TK, YT, KS, MN, MY-T, MY-H, TT, and AM generated data. TK, NM, EM, WS, JK, and SO analyzed the data. NT, KT, JK, and HO contributed to the discussion. KaY planned the study and wrote the manuscript. All authors had access to the study data and reviewed and approved the final manuscript.

FUNDING

This work was supported by JSPS KAKENHI [JP15H02578 and JP18H04067 (to KaY), and JP16H05207 to HO)], the Japan Agency for Medical Research and Development-Core Research for Evolutional Science and Technology (JP18gm0710009 to HO) and Sunstar Inc. (to KaY).

ACKNOWLEDGMENTS

We would like to thank Editage (www.editage.com) for English language editing.

SUPPLEMENTARY MATERIAL

The Supplementary Material for this article can be found online at: https://www.frontiersin.org/articles/10.3389/fimmu.2021.766170/full#supplementary-material

REFERENCES

1. Angulo P. Nonalcoholic Fatty Liver Disease. *N Engl J Med* (2002) 346 (16):1221–31. doi: 10.1056/NEJMra011775346/16/1221
2. Tilg H, Moschen AR. Evolution of Inflammation in Nonalcoholic Fatty Liver Disease: The Multiple Parallel Hits Hypothesis. *Hepatology* (2010) 52 (5):1836–46. doi: 10.1002/hep.24001
3. Mouzaki M, Allard JP. The Role of Nutrients in the Development, Progression, and Treatment of Nonalcoholic Fatty Liver Disease. *J Clin Gastroenterol* (2012) 46(6):457–67. doi: 10.1097/MCG.0b013e31824cf51e
4. Williams CD, Stengel J, Asike MI, Torres DM, Shaw J, Contreras M, et al. Prevalence of Nonalcoholic Fatty Liver Disease and Nonalcoholic Steatohepatitis Among a Largely Middle-Aged Population Utilizing Ultrasound and Liver Biopsy: A Prospective Study. *Gastroenterology* (2011) 140(1):124–31. doi: 10.1053/j.gastro.2010.09.038S0016-5085(10)01416-2
5. Buzzetti E, Pinzani M, Tsochatzis EA. The Multiple-Hit Pathogenesis of Non-Alcoholic Fatty Liver Disease (NAFLD). *Metabolism* (2016) 65(8):1038–48. doi: 10.1016/j.metabol.2015.12.012S0026-0495(15)00383-2
6. Bartold PM, Van Dyke TE. Host Modulation: Controlling the Inflammation to Control the Infection. *Periodontol 2000* (2017) 75(1):317–29. doi: 10.1111/prd.12169
7. Yamazaki K. New Paradigm in the Relationship Between Periodontal Disease and Systemic Diseases: Effects of Oral Bacteria on the Gut Microbiota and Metabolism. In: L Nibali, B Henderson, editors. *The Human Microbiota and Chronic Disease: Dysbiosis as Cause of Human Pathology*. irst ed. Hoboken, New Jersey: John Wiley & Sons, Inc (2016). p. 243–61.
8. Akinkugbe AA, Slade GD, Barritt AS, Cole SR, Offenbacher S, Petersmann A, et al. Periodontitis and Non-Alcoholic Fatty Liver Disease, A Population-Based Cohort Investigation in the Study of Health in Pomerania. *J Clin Periodontol* (2017) 44(11):1077–87. doi: 10.1111/jcpe.12800
9. Alazawi W, Bernabe E, Tai D, Janicki T, Kemos P, Samsuddin S, et al. Periodontitis Is Associated With Significant Hepatic Fibrosis in Patients With Non-Alcoholic Fatty Liver Disease. *PloS One* (2017) 12(12):e0185902. doi: 10.1371/journal.pone.0185902PONE-D-17-25484
10. Yoneda M, Naka S, Nakano K, Wada K, Endo H, Mawatari H, et al. Involvement of a Periodontal Pathogen, *Porphyromonas Gingivalis* on the Pathogenesis of Non-Alcoholic Fatty Liver Disease. *BMC Gastroenterol* (2012) 12:16. doi: 10.1186/1471-230X-12-161471-230X-12-16
11. Hajishengallis G, Lamont RJ. Breaking Bad: Manipulation of the Host Response by *Porphyromonas Gingivalis*. *Eur J Immunol* (2014) 44(2):328–38. doi: 10.1002/eji.201344202
12. Kuraji R, Ito H, Fujita M, Ishiguro H, Hashimoto S, Numabe Y. Porphyromonas Gingivalis Induced Periodontitis Exacerbates Progression of Non-Alcoholic Steatohepatitis in Rats. *Clin Exp Dent Res* (2016) 2(3):216–25. doi: 10.1002/cre2.41CRE241
13. Sasaki N, Katagiri S, Komazaki R, Watanabe K, Maekawa S, Shiba T, et al. Endotoxemia by *Porphyromonas Gingivalis* Injection Aggravates Non-Alcoholic Fatty Liver Disease, Disrupts Glucose/Lipid Metabolism, and Alters Gut Microbiota in Mice. *Front Microbiol* (2018) 9:2470. doi: 10.3389/fmicb.2018.02470
14. Que YA, Moreillon P. Infective Endocarditis. *Nat Rev Cardiol* (2011) 8 (6):322–36. doi: 10.1038/nrcardio.2011.43nrcardio.2011.43

15. Ebersole JL, Stevens J, Steffen MJ, Dawson Iii D, Novak MJ. Systemic Endotoxin Levels in Chronic Indolent Periodontal Infections. *J Periodontal Res* (2010) 45(1):1–7. doi: 10.1111/j.1600-0765.2008.01169.xJRE1169
16. Armingohar Z, Jorgensen JJ, Kristoffersen AK, Abesha-Belay E, Olsen I. Bacteria and Bacterial DNA in Atherosclerotic Plaque and Aneurysmal Wall Biopsies From Patients With and Without Periodontitis. *J Oral Microbiol* (2014) 6:23408. doi: 10.3402/jom.v6.23408
17. Boursier J, Mueller O, Barret M, Machado M, Fizanne L, Araujo-Perez F, et al. The Severity of Nonalcoholic Fatty Liver Disease is Associated With Gut Dysbiosis and Shift in the Metabolic Function of the Gut Microbiota. *Hepatology* (2016) 63(3):764–75. doi: 10.1002/hep.28356
18. Loomba R, Seguritan V, Li W, Long T, Klitgord N, Bhatt A, et al. Gut Microbiome-Based Metagenomic Signature for Non-Invasive Detection of Advanced Fibrosis in Human Nonalcoholic Fatty Liver Disease. *Cell Metab* (2017) 25(5):1054–62 e5. doi: 10.1016/j.cmet.2017.04.001
19. Ponziani FR, Bhoori S, Castelli C, Putignani L, Rivoltini L, Del Chierico F, et al. Hepatocellular Carcinoma Is Associated With Gut Microbiota Profile and Inflammation in Nonalcoholic Fatty Liver Disease. *Hepatology* (2019) 69 (1):107–20. doi: 10.1002/hep.30036
20. Fei N, Bruneau A, Zhang X, Wang R, Wang J, Rabot S, et al. Endotoxin Producers Overgrowing in Human Gut Microbiota as the Causative Agents for Nonalcoholic Fatty Liver Disease. *mBio* (2020) 11(1):e3263–19. doi: 10.1128/mBio.03263-19
21. Zhang X, Coker OO, Chu ES, Fu K, Lau HCH, Wang YX, et al. Dietary Cholesterol Drives Fatty Liver-Associated Liver Cancer by Modulating Gut Microbiota and Metabolites. *Gut* (2020) 70(4):761–74. doi: 10.1136/gutjnl-2019-319664
22. Arimatsu K, Yamada H, Miyazawa H, Minagawa T, Nakajima M, Ryder MI, et al. Oral Pathobiont Induces Systemic Inflammation and Metabolic Changes Associated With Alteration of Gut Microbiota. *Sci Rep* (2014) 4:4828. doi: 10.1038/srep04828srep04828
23. Nakajima M, Arimatsu K, Kato T, Matsuda Y, Minagawa T, Takahashi N, et al. Oral Administration of *P. Gingivalis* Induces Dysbiosis of Gut Microbiota and Impaired Barrier Function Leading to Dissemination of Enterobacteria to the Liver. *PloS One* (2015) 10(7):e0134234. doi: 10.1371/journal.pone.0134234PONE-D-15-15324[pii
24. Sato K, Takahashi N, Kato T, Matsuda Y, Yokoji M, Yamada M, et al. Aggravation of Collagen-Induced Arthritis by Orally Administered *Porphyromonas Gingivalis* Through Modulation of the Gut Microbiota and Gut Immune System. *Sci Rep* (2017) 7(1):6955. doi: 10.1038/s41598-017-07196-710.1038/s41598-017-07196-7
25. Kato T, Yamazaki K, Nakajima M, Date Y, Kikuchi J, Hase K, et al. Oral Administration of Porphyromonas Gingivalis Alters the Gut Microbiome and Serum Metabolome. *mSphere* (2018) 3(5):e00460–18. doi: 10.1128/mSphere.00460-18
26. Boutaga K, Savelkoul PH, Winkel EG, van Winkelhoff AJ. Comparison of Subgingival Bacterial Sampling With Oral Lavage for Detection and Quantification of Periodontal Pathogens by Real-Time Polymerase Chain Reaction. *J Periodontol* (2007) 78(1):79–86. doi: 10.1902/jop.2007.060078
27. Saygun I, Nizam N, Keskiner I, Bal V, Kubar A, Acikel C, et al. Salivary Infectious Agents and Periodontal Disease Status. *J Periodontal Res* (2011) 46 (2):235–9. doi: 10.1111/j.1600-0765.2010.01335.x
28. von Troil-Linden B, Torkko H, Alaluusua S, Jousimies-Somer H, Asikainen S. Salivary Levels of Suspected Periodontal Pathogens in Relation to Periodontal Status and Treatment. *J Dent Res* (1995) 74(11):1789–95. doi: 10.1177/00220345950740111201
29. Masuoka H, Suda W, Tomitsuka E, Shindo C, Takayasu L, Horwood P, et al. The Influences of Low Protein Diet on the Intestinal Microbiota of Mice. *Sci Rep* (2020) 10(1):17077. doi: 10.1038/s41598-020-74122-9
30. Morita H, Kuwahara T, Ohshima K, Sasamoto H, Itoh K, Hattori M, et al. An Improved DNA Isolation Method for Metagenomic Analysis of the Microbial Flora of the Human Intestine. *Microbes Environ* (2007) 22(3):214–22. doi: 10.1264/jsme2.22.214
31. Hyatt D, Chen GL, Locascio PF, Land ML, Larimer FW, Hauser LJ. Prodigal: Prokaryotic Gene Recognition and Translation Initiation Site Identification. *BMC Bioinf* (2010) 11:119. doi: 10.1186/1471-2105-11-119
32. Murtagh F, Legendre P. Ward's Hierarchical Agglomerative Clustering Method: Which Algorithms Implement Ward's Criterion? *J Classification* (2014) 31(3):274–95. doi: 10.1007/s00357-014-9161-z
33. Huang da W, Sherman BT, Lempicki RA. Systematic and Integrative Analysis of Large Gene Lists Using DAVID Bioinformatics Resources. *Nat Protoc* (2009) 4(1):44–57. doi: 10.1038/nprot.2008.211
34. Benjamini Y, Hochberg Y. Controlling the False Discovery Rate: A Practical and Powerful Approach to Multiple Testing. *J R Stat Sciety Ser B (Methodological)* (1995) 57(1):289–300. doi: 10.1111/j.2517-6161.1995.tb02031.x
35. Motegi H, Tsuboi Y, Saga A, Kagami T, Inoue M, Toki H, et al. Identification of Reliable Components in Multivariate Curve Resolution-Alternating Least Squares (MCR-ALS): A Data-Driven Approach Across Metabolic Processes. *Sci Rep* (2015) 5:15710. doi: 10.1038/srep15710
36. Sekiyama Y, Chikayama E, Kikuchi J. Profiling Polar and Semipolar Plant Metabolites Throughout Extraction Processes Using a Combined Solution-State and High-Resolution Magic Angle Spinning NMR Approach. *Anal Chem* (2010) 82(5):1643–52. doi: 10.1021/ac9019076
37. Shiokawa Y, Misawa T, Date Y, Kikuchi J. Application of Market Basket Analysis for the Visualization of Transaction Data Based on Human Lifestyle and Spectroscopic Measurements. *Anal Chem* (2016) 88(5):2714–9. doi: 10.1021/acs.analchem.5b04182
38. Shima H, Masuda S, Date Y, Shino A, Tsuboi Y, Kajikawa M, et al. Exploring the Impact of Food on the Gut Ecosystem Based on the Combination of Machine Learning and Network Visualization. *Nutrients* (2017) 9(12):1307. doi: 10.3390/nu9121307
39. Misawa T, Date Y, Kikuchi J. Human Metabolic, Mineral, and Microbiota Fluctuations Across Daily Nutritional Intake Visualized by a Data-Driven Approach. *J Proteome Res* (2015) 14(3):1526–34. doi: 10.1021/pr501194k
40. Kikuchi J, Tsuboi Y, Komatsu K, Gomi M, Chikayama E, Date Y. SpinCouple: Development of a Web Tool for Analyzing Metabolite Mixtures *via* Two-Dimensional J-Resolved NMR Database. *Anal Chem* (2016) 88(1):659–65. doi: 10.1021/acs.analchem.5b02311
41. Yamada S, Ito K, Kurotani A, Yamada Y, Chikayama E, Kikuchi J. InterSpin: Integrated Supportive Webtools for Low- and High-Field NMR Analyses Toward Molecular Complexity. *ACS Omega* (2019) 4(2):3361–9. doi: 10.1021/acsomega.8b02714
42. Bolyen E, Rideout JR, Dillon MR, Bokulich NA, Abnet CC, Al-Ghalith GA, et al. Reproducible, Interactive, Scalable and Extensible Microbiome Data Science Using QIIME 2. *Nat Biotechnol* (2019) 37(8):852–7. doi: 10.1038/s41587-019-0209-9
43. Callahan BJ, McMurdie PJ, Rosen MJ, Han AW, Johnson AJ, Holmes SP. DADA2: High-Resolution Sample Inference From Illumina Amplicon Data. *Nat Methods* (2016) 13(7):581–3. doi: 10.1038/nmeth.3869
44. Quast C, Pruesse E, Yilmaz P, Gerken J, Schweer T, Yarza P, et al. The SILVA Ribosomal RNA Gene Database Project: Improved Data Processing and Web-Based Tools. *Nucleic Acids Res* (2013) 41(Database issue):D590–6. doi: 10.1093/nar/gks1219
45. Su J, You P, Zhao JP, Zhang SL, Song SH, Fu ZR, et al. A Potential Role for the Homeoprotein Hhex in Hepatocellular Carcinoma Progression. *Med Oncol* (2012) 29(2):1059–67. doi: 10.1007/s12032-011-9989-6
46. Leung C, Rivera L, Furness JB, Angus PW. The Role of the Gut Microbiota in NAFLD. *Nat Rev Gastroenterol Hepatol* (2016) 13(7):412–25. doi: 10.1038/nrgastro.2016.85nrgastro.2016.85
47. Jang HR, Park HJ, Kang D, Chung H, Nam MH, Lee Y, et al. A Protective Mechanism of Probiotic Lactobacillus Against Hepatic Steatosis *via* Reducing Host Intestinal Fatty Acid Absorption. *Exp Mol Med* (2019) 51(8):1–14. doi: 10.1038/s12276-019-0293-4
48. Ritze Y, Bardos G, Claus A, Ehrmann V, Bergheim I, Schwiertz A, et al. Lactobacillus Rhamnosus GG Protects Against Non-Alcoholic Fatty Liver Disease in Mice. *PloS One* (2014) 9(1):e80169. doi: 10.1371/journal.pone.0080169
49. Zhu L, Baker SS, Gill C, Liu W, Alkhouri R, Baker RD, et al. Characterization of Gut Microbiomes in Nonalcoholic Steatohepatitis (NASH) Patients: A Connection Between Endogenous Alcohol and NASH. *Hepatology* (2013) 57 (2):601–9. doi: 10.1002/hep.26093
50. Wang M, Zhang S, Zhong R, Wan F, Chen L, Liu L, et al. Olive Fruit Extracts Supplement Improve Antioxidant Capacity *via* Altering Colonic Microbiota Composition in Mice. *Front Nutr* (2021) 8:645099. doi: 10.3389/fnut.2021.645099
51. Duan R, Guan X, Huang K, Zhang Y, Li S, Xia J, et al. Flavonoids From Whole-Grain Oat Alleviated High-Fat Diet-Induced Hyperlipidemia *via*

Regulating Bile Acid Metabolism and Gut Microbiota in Mice. *J Agric Food Chem* (2021) 69(27):7629–40. doi: 10.1021/acs.jafc.1c01813
52. Du K, Chitneni SK, Suzuki A, Wang Y, Henao R, Hyun J, et al. Increased Glutaminolysis Marks Active Scarring in Nonalcoholic Steatohepatitis Progression. *Cell Mol Gastroenterol Hepatol* (2020) 10(1):1–21. doi: 10.1016/j.jcmgh.2019.12.006
53. Muraki K, Imaizumi Y. A Novel Action of Palmitoyl-L-Carnitine in Human Vascular Endothelial Cells. *J Pharmacol Sci* (2003) 92(3):252–8. doi: 10.1254/jphs.92.252
54. Tiwari S, Jamal SB, Hassan SS, Carvalho P, Almeida S, Barh D, et al. Two-Component Signal Transduction Systems of Pathogenic Bacteria As Targets for Antimicrobial Therapy: An Overview. *Front Microbiol* (2017) 8:1878. doi: 10.3389/fmicb.2017.01878
55. Wang TJ, Larson MG, Vasan RS, Cheng S, Rhee EP, McCabe E, et al. Metabolite Profiles and the Risk of Developing Diabetes. *Nat Med* (2011) 17(4):448–53. doi: 10.1038/nm.2307nm.2307
56. Magnusson M, Lewis GD, Ericson U, Orho-Melander M, Hedblad B, Engstrom G, et al. A Diabetes-Predictive Amino Acid Score and Future Cardiovascular Disease. *Eur Heart J* (2013) 34(26):1982–9. doi: 10.1093/eurheartj/ehs424ehs424
57. Gaggini M, Carli F, Rosso C, Buzzigoli E, Marietti M, Della Latta V, et al. Altered Amino Acid Concentrations in NAFLD: Impact of Obesity and Insulin Resistance. *Hepatology* (2018) 67(1):145–58. doi: 10.1002/hep.29465
58. Hoyles L, Fernandez-Real JM, Federici M, Serino M, Abbott J, Charpentier J, et al. Molecular Phenomics and Metagenomics of Hepatic Steatosis in Non-Diabetic Obese Women. *Nat Med* (2018) 24(7):1070–80. doi: 10.1038/s41591-018-0061-3
59. Zeisel SH, da Costa KA. Choline: An Essential Nutrient for Public Health. *Nutr Rev* (2009) 67(11):615–23. doi: 10.1111/j.1753-4887.2009.00246.xNURE246
60. Sherriff JL, O'Sullivan TA, Properzi C, Oddo JL, Adams LA. Choline, Its Potential Role in Nonalcoholic Fatty Liver Disease, and the Case for Human and Bacterial Genes. *Adv Nutr* (2016) 7(1):5–13. doi: 10.3945/an.114.0079557/1/5
61. Sharpton SR, Yong GJM, Terrault NA, Lynch SV. Gut Microbial Metabolism and Nonalcoholic Fatty Liver Disease. *Hepatol Commun* (2019) 3(1):29–43. doi: 10.1002/hep4.1284HEP41284
62. Romano KA, Vivas EI, Amador-Noguez D, Rey FE. Intestinal Microbiota Composition Modulates Choline Bioavailability From Diet and Accumulation of the Proatherogenic Metabolite Trimethylamine-N-Oxide. *MBio* (2015) 6(2):e02481. doi: 10.1128/mBio.02481-14e02481-14
63. Koeth RA, Wang Z, Levison BS, Buffa JA, Org E, Sheehy BT, et al. Intestinal Microbiota Metabolism of L-Carnitine, a Nutrient in Red Meat, Promotes Atherosclerosis. *Nat Med* (2013) 19(5):576–85. doi: 10.1038/nm.3145nm.3145
64. Lebeaupin C, Vallee D, Hazari Y, Hetz C, Chevet E, Bailly-Maitre B. Endoplasmic Reticulum Stress Signalling and the Pathogenesis of Non-Alcoholic Fatty Liver Disease. *J Hepatol* (2018) 69(4):927–47. doi: 10.1016/j.jhep.2018.06.008
65. Willy JA, Young SK, Stevens JL, Masuoka HC, Wek RC. CHOP Links Endoplasmic Reticulum Stress to NF-kappaB Activation in the Pathogenesis of Nonalcoholic Steatohepatitis. *Mol Biol Cell* (2015) 26(12):2190–204. doi: 10.1091/mbc.E15-01-0036
66. Lebeaupin C, Vallee D, Rousseau D, Patouraux S, Bonnafous S, Adam G, et al. Bax Inhibitor-1 Protects From Nonalcoholic Steatohepatitis by Limiting Inositol-Requiring Enzyme 1 Alpha Signaling in Mice. *Hepatology* (2018) 68(2):515–32. doi: 10.1002/hep.29847
67. Prudente S, Sesti G, Pandolfi A, Andreozzi F, Consoli A, Trischitta V. The Mammalian Tribbles Homolog TRIB3, Glucose Homeostasis, and Cardiovascular Diseases. *Endocr Rev* (2012) 33(4):526–46. doi: 10.1210/er.2011-1042
68. Kimball SR, Jefferson LS. Induction of REDD1 Gene Expression in the Liver in Response to Endoplasmic Reticulum Stress is Mediated Through a PERK, Eif2alpha Phosphorylation, ATF4-Dependent Cascade. *Biochem Biophys Res Commun* (2012) 427(3):485–9. doi: 10.1016/j.bbrc.2012.09.074S0006-291X(12)01821-9
69. Mazzoccoli G, De Cosmo S, Mazza T. The Biological Clock: A Pivotal Hub in Non-Alcoholic Fatty Liver Disease Pathogenesis. *Front Physiol* (2018) 9:193. doi: 10.3389/fphys.2018.00193
70. Leone V, Gibbons SM, Martinez K, Hutchison AL, Huang EY, Cham CM, et al. Effects of Diurnal Variation of Gut Microbes and High-Fat Feeding on Host Circadian Clock Function and Metabolism. *Cell Host Microbe* (2015) 17(5):681–9. doi: 10.1016/j.chom.2015.03.006
71. Jahn D, Kircher S, Hermanns HM, Geier A. Animal Models of NAFLD From a Hepatologist's Point of View. *Biochim Biophys Acta Mol Basis Dis* (2019) 1865(5):943–53. doi: 10.1016/j.bbadis.2018.06.023

Conflict of Interest: The authors declare that the research was conducted in the absence of any commercial or financial relationships that could be construed as a potential conflict of interest.

Publisher's Note: All claims expressed in this article are solely those of the authors and do not necessarily represent those of their affiliated organizations, or those of the publisher, the editors and the reviewers. Any product that may be evaluated in this article, or claim that may be made by its manufacturer, is not guaranteed or endorsed by the publisher.

frontiers in Microbiology

ORIGINAL RESEARCH
published: 13 January 2022
doi: 10.3389/fmicb.2021.785411

Comparison of Extended-Spectrum Beta-Lactamase-Producing *Escherichia coli* Isolates From Rooks (*Corvus frugilegus*) and Contemporary Human-Derived Strains: A One Health Perspective

*Bálint József Nagy[1,2], Bence Balázs[1,2], Isma Benmazouz[1,3], Péter Gyüre[3], László Kövér[3], Eszter Kaszab[4], Krisztina Bali[4], Ádám Lovas-Kiss[5], Ivelina Damjanova[6], László Majoros[1], Ákos Tóth[6], Krisztián Bányai[4,7] and Gábor Kardos[1,7]**

[1] Department of Medical Microbiology, Faculty of Medicine, University of Debrecen, Debrecen, Hungary, [2] Doctoral School of Pharmaceutical Sciences, University of Debrecen, Debrecen, Hungary, [3] Department of Nature Conservation, Zoology and Game Management, Faculty of Agricultural and Food Sciences and Environmental Management, University of Debrecen, Debrecen, Hungary, [4] Institute for Veterinary Medical Research, Budapest, Hungary, [5] Department for Tisza River Research, Centre for Ecological Research–DRI, Hungarian Academy of Sciences, Budapest, Hungary, [6] National Public Health Center, Budapest, Hungary, [7] Department of Pharmacology and Toxicology, University of Veterinary Medicine Budapest, Budapest, Hungary

OPEN ACCESS

Edited by:
Alain Hartmann,
Institut National de Recherche pour l'Agriculture, l'Alimentation et l'Environnement (INRAE), France

Reviewed by:
Arif Hussain,
International Centre for Diarrhoeal Disease Research, Bangladesh (icddr,b), Bangladesh
Carlos Henrique Camargo,
Center for Bacteriology, Adolfo Lutz Institute, Brazil

***Correspondence:**
Gábor Kardos
kg@med.unideb.hu

Specialty section:
This article was submitted to Antimicrobials, Resistance and Chemotherapy, a section of the journal Frontiers in Microbiology

Received: 29 September 2021
Accepted: 09 December 2021
Published: 13 January 2022

Citation:
Nagy BJ, Balázs B, Benmazouz I, Gyüre P, Kövér L, Kaszab E, Bali K, Lovas-Kiss Á, Damjanova I, Majoros L, Tóth Á, Bányai K and Kardos G (2022) Comparison of Extended-Spectrum Beta-Lactamase-Producing Escherichia coli Isolates From Rooks (Corvus frugilegus) and Contemporary Human-Derived Strains: A One Health Perspective. Front. Microbiol. 12:785411. doi: 10.3389/fmicb.2021.785411

During winter, a large number of rooks gather and defecate at the park of a university clinic. We investigated the prevalence of extended-spectrum beta-lactamase (ESBL)–producing *Escherichia coli* in these birds and compared recovered isolates with contemporary human isolates. In 2016, fecal samples were collected from 112 trap-captured rooks and investigated for presence of ESBL producers using eosin methylene blue agar supplemented by 2 mg/L cefotaxime; 2,455 contemporary human fecal samples of patients of the clinics sent for routine culturing were tested similarly. In addition, 42 ESBL-producing *E. coli* isolates collected during the same period from inpatients were also studied. ESBL genes were sought for by PCR and were characterized by sequencing; *E. coli* ST131 clones were identified. Epidemiological relatedness was determined by pulsed-field gel electrophoresis and confirmed using whole genome sequencing in selected cases. Thirty-seven (33%) of sampled rooks and 42 (1.7%) of human stools yielded ESBL-producing *E coli*. Dominant genes were $bla_{\text{CTX-M-55}}$ and $bla_{\text{CTX-M-27}}$ in corvid, $bla_{\text{CTX-M-15}}$ and $bla_{\text{CTX-M-27}}$ in human isolates. ST162 was common among rooks. Two rook-derived *E. coli* belonged to ST131 C1-M27, which was also predominant (10/42) among human fecal and (15/42) human clinical isolates. Another potential link between rooks and humans was a single ST744 rook isolate grouped with one human fecal and three clinical isolates. Despite possible contact, genotypes shared between rooks and humans were rare. Thus, rooks are important as long-distance vectors and reservoirs of ESBL-producing *E. coli* rather than direct sources of infections to humans in our setting.

Keywords: ESBL carriage, *E. coli* ST131, *E. coli* ST162, *E. coli* ST744, long-distance dispersal, bird migration, CTX-M-55

INTRODUCTION

Antibiotic resistance is a global problem impacting both human and animal health. The One Health concept sets forth that the health of people, animals, and the environment is interconnected, which fully applies to antibiotic resistance as well, as exemplified by the relationship between avoparcin usage and the spread of vancomycin-resistant *Enterococci* in Europe (Bager et al., 1997). Besides spread of resistant strains, gene flow between bacteria of human and animal origin drives the dissemination of resistance genes (Graham et al., 2019). Zoonotic or environmental reservoirs served as sources for emerging resistance genes, e.g., *Kluyvera* spp. as source for $bla_{\text{CTX-M}}$ genes, *Shewanella algae* as source for $bla_{\text{OXA-48}}$, or *Acinetobacter radioresistens* as source for $bla_{\text{OXA-23-like}}$ genes (Livermore et al., 2007; Poirel et al., 2008; Tacão et al., 2018). Resistant bacteria can spread between humans and their households involving their companion animals, and the environment and wildlife. International travel, trade of animal food products, and wildlife migration further contribute to the global dissemination of antibiotic resistance (Guenther et al., 2011; Hussain et al., 2017, 2019; Zendri et al., 2020).

Escherichia coli is a characteristic example linking One Health and antibiotic resistance, being a frequent and abundant member of both human and animal gut microbiome as well as an important pathogen of humans and animals. The massive usage of antibiotics both in human medicine and animal industry led to contamination of natural environments with antimicrobials, antibiotic resistance genes, and resistant human pathogens (Graham et al., 2014, 2019). Wildlife living in contaminated habitats such as landfills, wastewater, sewage sludge of farms, or exposed directly to feces from livestock and companion animals can acquire resistant bacteria or resistance genes (Graham et al., 2014, 2019). These animals, particularly the highly mobile species, may scatter the resistant bacteria. Wild birds were shown to carry antibiotic resistant bacteria; typical carriers are crows (Loncaric et al., 2013; Jamborova et al., 2015) and gulls (Báez et al., 2015; Zendri et al., 2020), which often utilize human waste as food source. These birds are frequently urbanized, and their droppings pollute the cities, potentially reintroducing strains into the human environment. Because of their migration and/or vagrant behavior, these birds may serve as reservoirs and long-distance vectors both for antibiotic-resistant strains and antibiotic resistance genes (Wang et al., 2017).

Our aim was to investigate the prevalence of ESBL-producing *E. coli* carried by rooks (*Corvus frugilegus* ssp. *frugilegus*, Linnaeus 1758) gathering in a university clinic and to compare these isolates with contemporary and geographically related human-derived isolates.

MATERIALS AND METHODS

Samples and Bacterial Isolates

Cloacal swabs were taken from 112 trap-captured rooks wintering in a suburban environment close to the clinical campus of the University of Debrecen between October 2016 and March 2017. The trapping and capturing process was conducted as previously described (Kövér et al., 2018); recapturing did not occur. In parallel, we screened all 2,455 contemporary human fecal samples of the patients of the university clinics sent for routine fecal culture during the study period to assess human asymptomatic fecal carriage of ESBL-producing bacteria using the same culture methodology. Third-generation cephalosporin (3GC)–resistant isolates were recovered using eosin–methylene blue media supplemented with 2 mg/L cefotaxime. One to three colonies per different morphologies were processed further from each sample and identified by matrix-assisted laser desorption ionization (MALDI)–time of flight (TOF) mass spectrometry (Bruker, Bremen, Germany). We also characterized 42 contemporary extended-spectrum beta-lactamase (ESBL)–producing *E. coli* isolates from various samples of inpatients of the university clinics sent for microbiological diagnostic purposes for comparison with isolates carried by rooks and humans. Production of ESBL was examined by double-disk synergy test using cefotaxime, ceftazidime, and cefepime. Susceptibility to ertapenem, ciprofloxacin, trimethoprim–sulfamethoxazole, amikacin, gentamicin, and tobramycin was determined by disk diffusion method following EUCAST guidelines.

Resistance Gene Characterization

Each isolate showing ESBL phenotype was screened by PCR for bla_{SHV}, $bla_{\text{CTX-M}}$, and for CTX-M-1, 2, 8, and 9 subgroups (Ebrahimi et al., 2014, 2016a,b). All amplicons were purified by QIAquick Gel Extraction Kit (Qiagen, Hilden, Germany) and further characterized by sequencing (Macrogen Europe, Amsterdam, Netherlands). Sequences were analyzed by CLC Main Workbench (CLC Bio, Aarhus, Denmark).

To investigate the presence of plasmid-mediated colistin resistance genes *mcr-1*, *mcr-2*, *mcr-3*, *mcr-4*, and *mcr-5*, a multiplex PCR assay was used (Rebelo et al., 2018).

Genetic Diversity and Relatedness of the Strains

We determined the different *E. coli* phylogenetic groups by the multiplex PCR method developed by Clermont et al. (2013). A multiplex PCR assay was performed to detect the presence of virulence factor genes characteristic for enterovirulent *E. coli* pathotypes (Persson et al., 2007). To identify the *E. coli* sequence type (ST) 131 clonal lineage and its members [clades A, B, C, and C subclades (C1-M27, C1-non-M27, and C2)], we used the multiplex PCR developed by Matsumura et al. (2017).

To analyze the epidemiological relationship, we used pulsed-field gel electrophoresis (PFGE) as previously described (Ebrahimi et al., 2014). The threshold for probable genetic relatedness was set to a similarity of $>85\%$.

Whole Genome Sequencing

Based on the results of the PFGE, 20 isolates were selected for whole genome sequencing (WGS) to represent major pulsotypes carried by birds as well as pulsotypes that contained both human and bird isolates to reveal possible connections. Genomic DNA was extracted using Zixpress-32 Bacterial DNA Extraction Kit on Zixpress-32 Automated Nucleic Acid Purification

Instrument (Zinexts Life Science Corporation) following the manufacturer's instructions. WGS was performed using Nextera XT DNA Library Preparation Kit followed by 150-bp single-end sequencing on Illumina NextSeq500 platform. FASTQ files were quality trimmed then assembled *de novo* using Velvet (v1.0.0.); these are available under BioProject ID PRJNA693168. ResFinder (Camacho et al., 2009; Bortolaia et al., 2020; Zankari et al., 2020), PlasmidFinder (Camacho et al., 2009; Carattoli et al., 2014), and VirulenceFinder (Joensen et al., 2014; Malberg Tetzschner et al., 2020) available from the Center for Genomic Epidemiology[1] were used to identify resistance genes, plasmid replicon types, and virulence factors. Multi-locus sequence typing (MLST) and core genome MLST (cgMLST) were performed using SeqSphere + (Ridom, Münster, Germany) according to the "*E. coli* MLST Warwick v1.0" and "*E. coli* cgMLST" version 1.0 scheme.

RESULTS

Occurrence and Characteristics of Extended-Spectrum Beta-Lactamase-Producing *E. coli* in Rooks

Extended-spectrum beta-lactamase-producing bacteria were carried by 37 (33%) of 112 sampled birds and a total of 43 isolates have been recovered, all of which were *E. coli*; six samples (8544, 8551, 8557, 8578, 8583, and HOR3) yielded two different morphologies and during further analysis they turned to be pheno- and genotypically different ESBL-producing *E. coli* isolates (**Supplementary Figure 2**). The predominant ESBL genes were $bla_{\text{CTX-M-55}}$ (16/43) followed by $bla_{\text{CTX-M-27}}$ (n = 15/43) (**Supplementary Figure 1**). Fluoroquinolone (17/43) and sulfonamide (23/43) resistance was frequent whereas all isolates were susceptible to aminoglycosides; 40% (17/43) of the isolates were susceptible to examined non-beta-lactam antibiotics including all $bla_{\text{CTX-M-15}}$ producers. The majority of the isolates carried by birds belonged to commensal phylogroups A (2.3%, 1/43), B1 (51.2%, 22/43), and C (7%, 3/43), B1 being the dominant phylogroup. However, a high proportion (40%, 17/43) of rook isolates belonged to phylogroups associated with human disease, B2 (34.9%, 15/43) and D (4.7%, 2/43) (**Supplementary Figure 1**). Two of B2 CTX-M-27-producing *E. coli* isolates proved to belong to the pandemic ST131 clonal lineage, to the recently emerged C1-M27 subclone. In addition, 21% (9/43) of the isolates carried the intimin coding *eae* gene.

Fecal Carriage Rate and Characteristics of Extended-Spectrum Beta-Lactamase-Producing *E. coli* in Humans

In 2,455 human fecal samples, 42 ESBL-producing *E. coli* were found corresponding to a fecal carriage rate of 1.7%. The dominant ESBL genotypes were $bla_{\text{CTX-M-15}}$ (20/42) followed by $bla_{\text{CTX-M-27}}$ (10/42) (**Supplementary Figure 1**). Resistance to fluoroquinolones (24/42), sulfonamides (29/42), amikacin (14/42), gentamicin (12/42), and to tobramycin (14/42) was common. Isolates of commensal phylogroups were more prevalent; four, three, eight, and eight isolates belonged to phylogroup A, B1, C, and E, but overall B2 (17/42) was the dominant phylogroup. Of the B2 isolates, two, one, one, and ten belonged to ST131 clade A, B, subclade C2, and subclade C1-M27, respectively.

Characteristics of Extended-Spectrum Beta-Lactamase-Producing *E. coli* From Inpatients

The dominant ESBL genes were $bla_{\text{CTX-M-15}}$ (18/42) and $bla_{\text{CTX-M-27}}$ (13/42) (**Supplementary Figure 1**). As sole ESBL gene, $bla_{\text{SHV-12}}$ was present in two isolates. Co-resistance rates were high; 60% (25/42) of isolates were resistant to fluoroquinolones, sulfonamides, and aminoglycosides, mostly the $bla_{\text{CTX-M-15}}$ producers. The majority (74%, 31/42) of the isolates belonged to B2 phylogroup with high prevalence (62%, 26/42) of ST131 clones. Among ST131 isolates, one, nine, and 16 belonged to clade B, subclade C2, and subclade C1-M27, respectively. Curiously, three ST131 C1-M27 isolates were $bla_{\text{CTX-M-15}}$ producers.

Comparing the Characteristics of Rook, Human Fecal, and Human Clinical Isolates

In rooks, $bla_{\text{CTX-M-55}}$ was the dominant ESBL gene while in humans it was $bla_{\text{CTX-M-15}}$; $bla_{\text{CTX-M-27}}$ was the second most common ESBL gene in all three isolate collections (**Supplementary Figure 1**). Group 2 and group 8 CTX-M types were not detected. Rook-derived isolates showed lower co-resistance rates to non-beta-lactam antibiotics than human clinical isolates. Isolates resistant to aminoglycosides, fluoroquinolones, and trimethoprim–sulfamethoxazole tend to carry CTX-M-1 group, particularly $bla_{\text{CTX-M-15}}$, except for rooks where $bla_{\text{CTX-M-15}}$ producers were susceptible; $bla_{\text{CTX-M-27}}$ producers were resistant to fluoroquinolones and to trimethoprim–sulfamethoxazole but not to aminoglycosides. Carbapenem resistance was not detected in the recovered isolates. The majority of rook and human fecal isolates belonged to commensal phylogroups while B2 was dominant among human clinical isolates. The pandemic ST131 *E. coli* clonal lineage was present in isolates of rooks and humans with the dominance of C1-M27 subclade. All isolates were negative for plasmid-mediated colistin resistance genes tested.

Molecular Epidemiology of the Isolates

Pulsed-field gel electrophoresis revealed that human clinical and fecal isolates clustered frequently together whereas the vast majority of rook isolates tended to cluster separately from human isolates (**Supplementary Figure 2**), although clusters containing both rook and human isolates were also found. Out of these, a cluster of eight human fecal, ten human clinical, and two rook isolates (EC069) was the largest, which belonged to the

[1] http://www.genomicepidemiology.org

ST131 clone. Most isolates of the ST131 clone were grouped into three clusters (EC003, EC069, and EC380) although a few other ST131 isolates were randomly distributed. The EC003 cluster exclusively consisted of human clinical ST131 isolates while EC380 cluster contained human fecal ST131 isolates. In the EC069 cluster, the two corvid ST131 isolates showed PFGE profiles indistinguishable from human clinical and human fecal isolates. A smaller cluster of three human clinical, one human fecal, and one rook isolate (EC088) was also detected. In addition, clusters EC147 and EC183 each comprised one rook and one human fecal isolate.

A total of eleven, four, and five of rook, human clinical, and human fecal isolates, respectively, were characterized by WGS (**Table 1**). The results of the cgMLST are shown in **Figure 1**. The relatedness of isolates in PFGE clusters of EC183 and EC399 were not supported by the results of the WGS (**Table 1** and **Supplementary Figure 2**). Both ST24 and ST162 rook isolates were highly uniform genetically; distance based on allele presence was $\leq$1, although these isolates have been recovered from various birds in November and December. Human-derived ST744 isolates were closely related, but the rook one was relatively distant from this cluster; ST131 C1-M27 rook isolates were identical and in close connection with human strains ($\leq$7 alleles) (**Figure 1**).

DISCUSSION

An increasing number of studies reported high prevalence of ESBL-producing *E. coli* in wild animals (Wang et al., 2017). Birds are the most studied hosts, where the most frequently found genes are $bla_{\text{CTX-M-1}}$ and $bla_{\text{CTX-M-15}}$ (Wang et al., 2017). Birds may serve as long distance vectors of strains/genes of human origin. Franklin's gulls (*Leucophaeus pipixcan*) sampled in Chile frequently carried pandemic ST131 CTX-M-15-producing strains, which are highly prevalent in humans in the United States but rarely found in Chile (Báez et al., 2015). Similarly, $bla_{\text{CTX-M-1}}$ and $bla_{\text{CTX-M-15}}$ were previously dominant in rooks wintering in Europe (Loncaric et al., 2013; Jamborova et al., 2015). A few recent European studies also reported a low prevalence of $bla_{\text{CTX-M-55}}$ and $bla_{\text{CTX-M-24}}$ in rooks (Jamborova et al., 2015; Söderlund et al., 2019). Importantly, an earlier study from 2005 reported lack of ESBL producers in wintering rooks in the Czech Republic (Literak et al., 2007).

Rooks wintering in Hungary and in neighboring countries belong to a large population migrating from Russia and Western Asia, belonging to subspecies Western Rook (*Corvus frugilegus frugilegus*) with a breeding area stretching from the East European Plain to the West Siberian Plain. These populations migrate through the Black Sea–Mediterranean flyway and usually winter in European countries (Madge, 2020). The other rook subspecies Eastern Rook (*Corvus frugilegus pastinator*) nests in the Central Siberian Plateau and the Manchurian Plain and migrates to China and to Japan through the East Asian–Australasian flyway. On the border of West Siberian Plain and Central Siberian Plateau, there is a hybrid zone of the two subspecies, where birds may intermingle (Madge, 2020).

In the present work, $bla_{\text{CTX-M-55}}$ and $bla_{\text{CTX-M-27}}$ were predominant in rooks; $bla_{\text{CTX-M-55}}$ is rarely reported in Europe from humans but highly prevalent in Southeast Asia (Lupo et al., 2018). It has been suggested that $bla_{\text{CTX-M-55}}$ in humans in Asia arose from food animal sources, highlighting the importance of One Health (Bevan et al., 2017). Previously, $bla_{\text{CTX-M-14}}$ and, to a lesser extent, $bla_{\text{CTX-M-15}}$ were dominant ESBL genes in Asia; recently, $bla_{\text{CTX-M-55}}$ emerged as the most common ESBL gene in human and animal isolates, while $bla_{\text{CTX-M-27}}$ started to outcompete $bla_{\text{CTX-M-14}}$ (Bevan et al., 2017). As $bla_{\text{CTX-M-55}}$ is dominant in livestock in Asia (Bevan et al., 2017), and manure is often used to fertilize crop fields and may contain ESBL-producing *E. coli*, rooks foraging in these may acquire $bla_{\text{CTX-M-55}}$ producers. This shift in the epidemiology of ESBL genes in Asia may be the cause of the alteration of ESBL genes in rooks as compared with earlier studies (Loncaric et al., 2013; Jamborova et al., 2015).

We hypothesized that Eastern Rooks acquire strains carrying resistance genes prevalent in animals and humans in China and transmit them to Western Rook individuals interacting with carrier Eastern Rooks in the hybrid area. Thus, intermingling rooks may become long-distance vectors mediating spread of strains/genes from Asia to Europe. Similarly, this may have been the route for clade C1-M27 described first in Japan in 2006 then in Korea in 2008 spreading since to Europe and to America (Matsumura et al., 2016). Similar spread routes of H5N1 avian influenza virus was reported extensively in different bird species (Gauthier-Clerc et al., 2007). High similarity between ST131 C1-M27 isolates of rook and human origin may also be explained by acquisition of these strains by rooks in Hungary, suggesting bidirectional transfer. Food importation may be another potential pathway where $bla_{\text{CTX-M-55}}$ can spread from animals to humans toward Europe as exemplified by the dissemination mcr-1 resistance gene since a lot of poultry and pork are imported from China to Europe (Hasman et al., 2015) and the detection of these genes can often be traced back there (Lupo et al., 2018).

The majority of rook isolates of phylogroup B2 had indistinguishable macrorestriction profile (**Supplementary Figure 2**) identified as ST24 carrying $bla_{\text{CTX-M-27}}$. ST24 was reported rarely, mainly from diarrheic rabbits, cattle, and humans (Moura et al., 2009; Xiong et al., 2012). All ST24 isolates carried the *eae* gene (**Supplementary Table 1**), which encodes a major virulence gene of enteropathogenic *E. coli* (EPEC); lack of the *bfp* gene indicates that these isolates are atypical EPEC strains, which are reported both from humans and animals (Moura et al., 2009). A study found that atypical EPEC strains of animal origin have potential to cause diarrhea in humans and revealed a close clonal relationship between human and animal isolates (Moura et al., 2009).

The main phylogroup was B1 among rook isolates, forming a large cluster belonging to ST162 and carrying $bla_{\text{CTX-M-55}}$ (**Supplementary Table 1**). ST162 was found previously in rooks wintering in Europe with low occurrence (Loncaric et al., 2013; Jamborova et al., 2015). This emerging multiresistant *E. coli* lineage is now found worldwide colonizing different hosts including livestock, wild animals, humans, rivers, and sewage

TABLE 1 | Results of whole genome sequencing of the selected isolates.

PFGE	Strain source	ST	Resistance genes								Plasmid replicons
			Bl	Qui	Agl	Tri	Sul	Mac	Phe	Tet	
EC088	857 Clinical	744	*bla*CTX-M-1 *bla*CTX-M-14	gyrA p.S83L gyrA p.D87N parC p.A56T parC p.S80I	aadA5 aph(6)-Id aph(3″)-Ib	dfrA17	sul2	mdf(A)	catA1	tet(B)	IncFII IncI1-I IncQ1
	1254 Fecal	744	*bla*CTX-M-1 *bla*CTX-M-14	gyrA p.S83L gyrA p.D87N parC p.A56T	aadA5 aph(6)-Id aph(3″)-Ib	dfrA17	sul1 sul2	mdf(A)	catA1	tet(B)	IncFII IncI1-I IncQ1
	1418 Clinical	744	*bla*CTX-M-14	gyrA p.S83L gyrA p.D87N parC p.A56T parC p.S80I	aadA5 aph(6)-Id aph(3″)-Ib	dfrA17	sul1 sul2	mdf(A)	catA1	tet(B)	IncFII IncQ1
	8544sz Rook	744	*bla*CTX-M-55	qnrS1 gyrA p.S83L gyrA p.D87N parC p.A56T parC p.S80I	aadA5 aph(6)-Id aph(3″)-Ib	dfrA17	sul1	mdf(A) mph(A)	catA1	tet(A) tet(B)	IncFIA IncFIB IncFIC IncI1-I IncN
	42081 Clinical	744	*bla*CTX-M-14	gyrA p.S83L gyrA p.D87N parC p.A56T parC p.S80I	aadA5 aph(6)-Id aph(3″)-Ib	dfrA17	sul1 sul2		catA1	tet(B)	IncFII IncI1-I IncQ1
EC378	8579 Rook	24	*bla*CTX-M-27					mdf(A)			IncFIB IncFII
	8550 Rook	24	*bla*CTX-M-27					mdf(A)			IncFIB IncFII
	HOR3sz Rook	24	*bla*CTX-M-27					mdf(A)			IncFIB IncFII
EC069	5386 Clinical	131	*bla*CTX-M-27 *bla*TEM-1B	qnrS1 gyrA p.S83L gyrA p.D87N parC p.S80I parC p.E84V parE p.I529L	aadA5 aph(6)-Id aph(3″)-Ib	dfrA17	sul1 sul2	mdf(A) mph(A)		tet(A)	IncFIA IncFIB IncFII IncN
	42532 Fecal	131	*bla*CTX-M-27 *bla*TEM-1B	qnrS1 gyrA p.S83L gyrA p.D87N parC p.S80I parC p.E84V parE p.I529L	aadA5 aph(6)-Id aph(3″)-Ib	dfrA17	sul1 sul2	mdf(A)			IncFIA IncFIB IncFII IncN
	8578sz Rook	131	*bla*CTX-M-27	gyrA p.S83L gyrA p.D87N parC p.S80I parC p.E84V parE p.I529L	aadA5 aph(6)-Id aph(3″)-Ib	dfrA17	sul1 sul2	mdf(A) mph(A)		tet(A)	Col156 IncFIA IncFIB IncFII
	2647 Fecal	69	*bla*CTX-M-15	gyrA p.S83L		dfrA14		erm(B) mdf(A) mph(A)		tet(B)	Col156 IncFIA IncFIB IncFII IncX1
	8546 Rook	131	*bla*CTX-M-27	gyrA p.S83L gyrA p.D87N parC p.S80I parC p.E84V parE p.I529L	aadA5 aph(6)-Id aph(3″)-Ib	dfrA17	sul1 sul2	mdf(A) mph(A)		tet(A)	Col156 IncFIA IncFIB IncFII
EC183	40242k Fecal	131	*bla*CTX-M-15 *bla*TEM-1B	gyrA p.S83L parE p.I529L	aadA5 aph(6)-Id aph(3″)-Ib	dfrA17	sul1 sul2	mdf(A) mph(A)		tet(A)	Col156 IncFIB IncFII
	8563 Rook	162	*bla*CTX-M-1				sul2	mdf(A)		tet(A)	IncFIB IncFII IncI1-I IncX1

(Continued)

TABLE 1 | (Continued)

PFGE	Strain source	ST	Resistance genes							Plasmid replicons
			Bl	Qui	Agl	Tri	Sul	Mac	Phe	Tet	
EC399	2909 Fecal	23	*bla*CTX-M-3					mdf(A)			IncFIB IncFIC IncI1-I
EC382	8523 Rook	162	*bla*CTX-M-55 *bla*TEM-1B	qnrS1	aph(6)-Id aph(3″)-Ib	dfrA7	sul1 sul2	mdf(A)		tet(A)	IncN IncQ1 p0111
	8583F Rook	162	*bla*CTX-M-55 *bla*TEM-1B	qnrS1	aph(6)-Id aph(3″)-Ib	dfrA7	sul1 sul2	mdf(A)		tet(A)	IncN IncQ1 p0111
	HOR3F Rook	162	*bla*CTX-M-55 *bla*TEM-1B	qnrS1	aph(6)-Id aph(3″)-Ib	dfrA7	sul1 sul2	mdf(A)		tet(A)	IncN IncQ1 p0111
	8551F Rook	162	*bla*CTX-M-55 *bla*TEM-1B	qnrS1	aph(6)-Id aph(3″)-Ib	dfrA7	sul1 sul2	mdf(A)		tet(A)	IncN IncQ1 p0111

Bl, beta-lactam; Fq, fluoroquinolone; Agl, aminoglycoside; Tri, trimethoprim; Sul, sulfonamide; Mac, macrolide; Phe, phenicol; Tet, tetracycline.

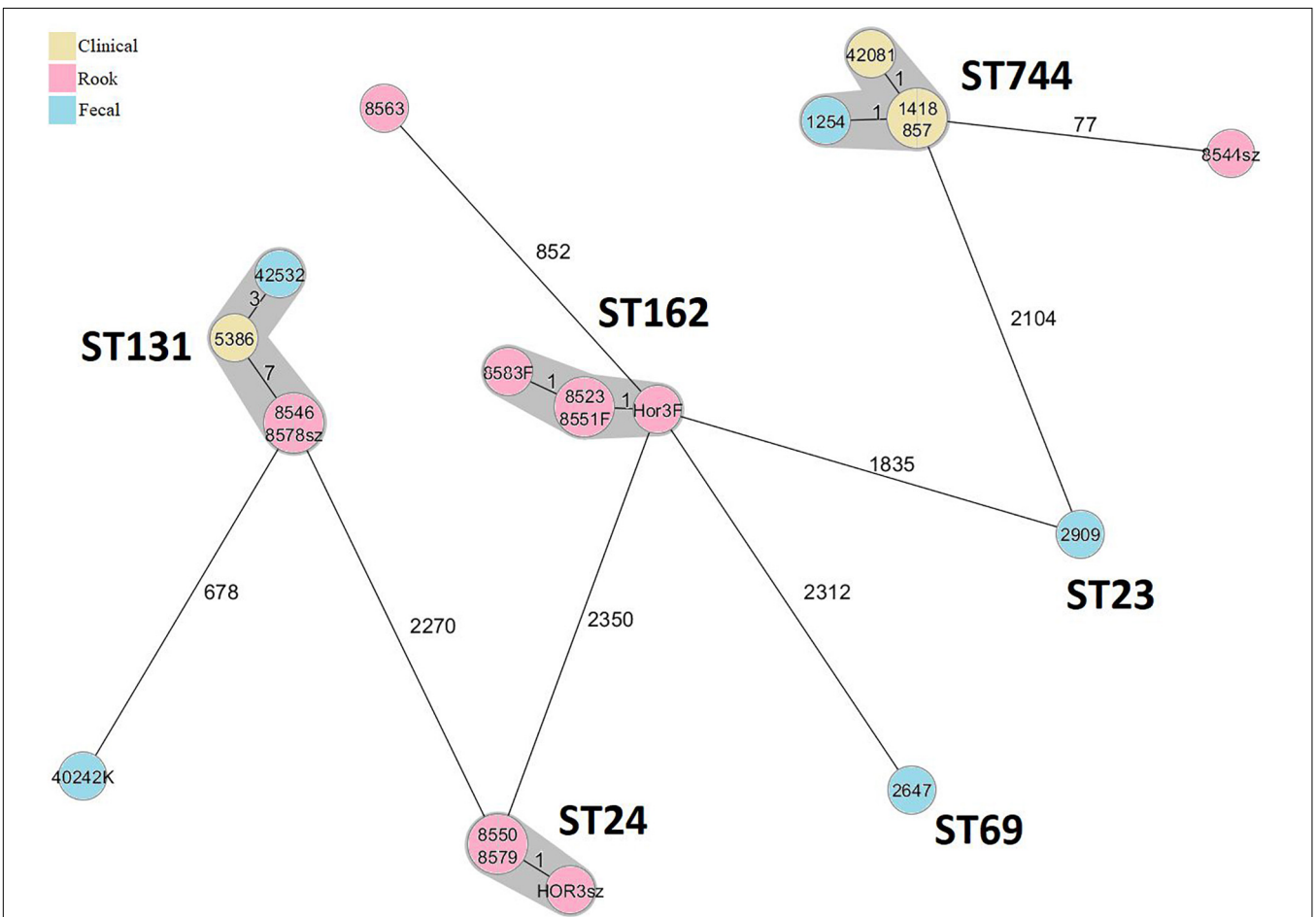

FIGURE 1 | Minimum spanning tree based on cgMLST allelic profiles of 20 sequenced *E. coli* isolates. Each circle represents an allelic profile based on sequence analysis of 2,513 cgMLST target genes. The numbers on the connecting lines illustrate the numbers of target genes with different alleles. Closely related genotypes (<10 alleles difference) are shaded.

(Fuentes-Castillo et al., 2020). ST162 was reported from dairy cows with mastitis (Tahar et al., 2020) and from human clinical samples, even associated with $bla_{\text{NDM-5}}$ in humans (Yoon et al., 2018). These associations raise the concern of dissemination of commensal multiresistant strains in human populations and the diffusion of the antibiotic resistance carried by these strains to other non-commensal, pathogenic strains (Zhuge et al., 2019). Moreover, ST162 *E. coli* recovered from poultry was identified as a highly virulent clone, despite belonging to phylogroup B1, capable of causing bloodstream infections and meningitis in animal models (Zhuge et al., 2019). In our study, ST162 and ST24 isolates seemed to have clonally expanded in rooks, which is notable as the clonal spread of ESBL-producing *E. coli* is scarcely documented in wild animals (Lupo et al., 2018).

Sequence types with human importance ST744 and ST131 C1-M27 were found seldom. ST744 is an international high-risk clone identified in our rook, human fecal, and clinical isolates (**Table 1**). ST744 carrying $bla_{\text{CTX-M-55}}$ was previously reported from diseased pigs in the United States and from healthy and diseased bovines in France, from wastewater, birds of prey (Guenther et al., 2012; Lupo et al., 2018; Hayer et al., 2020) as well as from healthy and diseased companion animals, and humans (Tacão et al., 2017; Zhong et al., 2017; Zogg et al., 2018). Besides ESBLs, ST744 was sporadically associated with mcr-1, mcr-3, $bla_{\text{KPC-3}}$, and bla_{NDM} genes from patients, healthy individuals, and livestock worldwide (Tacão et al., 2017; Zhong et al., 2017; Lupo et al., 2018; Zogg et al., 2018; Li et al., 2019). ST744 isolates of phylogroup A are not as virulent as those belonging to phylogroup B2 and D, but our ST744 rook isolate carried 15 virulence factors (**Supplementary Table 1**) commonly found in extraintestinal pathogenic *E. coli* (ExPEC) isolates.

Presence of key virulence genes (*iss*, *iroN*, *hlyF* and *ompT*, *iutA* and *cvaC*) and phylogroup A indicates that our rook ST744 is an avian pathogenic *E. coli* (APEC) strain, which is the main cause of avian colibacillosis (Johnson et al., 2008). Therefore, wild birds carrying APEC strains might pose a potential economic risk toward poultry; these genes are also frequently found among human ExPEC strains, raising the possibility of zoonotic transmission (Johnson et al., 2008; Zhuge et al., 2019). These suggest that ST744 may be a zoonotic strain capable of colonizing and infecting multiple host species including humans. Moreover, its potential to carry multiple plasmids predisposes it to be involved in transmission of resistance plasmids to other *E. coli* STs.

Subclade ST131 C1-M27 is associated with clonal spread in humans, and was also reported from great cormorants (*Phalacrocorax carbo*), mallards (*Anas platyrhynchos*) (Tausova et al., 2012), gulls (Zendri et al., 2020), companion animals, freshwater, and wastewater (Bevan et al., 2017). Similarly, it occurred in rooks and was also prevalent in human isolates in our study.

Although $bla_{\text{CTX-M-15}}$ remained the predominant ESBL gene among asymptomatically carried human isolates in this study, the prevalence of ST131-CTX-M-15 *E. coli* was lower compared with earlier findings (Ebrahimi et al., 2014, 2016a,b), suggesting a slow replacement of C2 subclade carrying $bla_{\text{CTX-M-15}}$ by the C1-M27 subclade (Merino et al., 2018). ST131 C1-M27 had a higher transmission rate than CTX-M-15-producing ST131 C2 (Merino et al., 2018). C1-M27 isolates often show lower co-resistance to other antimicrobial agents than C2 isolates (Jamborova et al., 2018), which may be advantageous in an antibiotic landscape dominated by beta-lactams as seen in many European countries including Hungary, and particularly the setting where this study was conducted (Tóth et al., 2019).

Both $bla_{\text{CTX-M-27}}$ and $bla_{\text{CTX-M-55}}$ are associated with a wide range of plasmid replicons in animal isolates and certain plasmids showed epidemic spread in Asia in humans (Bevan et al., 2017; Lupo et al., 2018). Unlike $bla_{\text{CTX-M-27}}$ associated with ST131 C1-M27, horizontal transmission is considered to be the main factor driving the dissemination of $bla_{\text{CTX-M-55}}$ in China (Ho et al., 2013). In our work, $bla_{\text{CTX-M-55}}$ have been associated with IncN replicon type (**Table 1**), which often harbors various ESBL genes but rarely $bla_{\text{CTX-M-55}}$[2]. This association of $bla_{\text{CTX-M-55}}$ with IncN plasmids carried by ST162 may open a new way to the dissemination of $bla_{\text{CTX-M-55}}$ in and from Asia toward Europe by bird migration or vagrancy as it may have earlier happened in the case of ST131 C1-M27 (Matsumura et al., 2016).

In summary, increased carriage of ESBL-producing *E. coli* was found in rooks than reported in previous years. Despite the possibilities for contact, birds and humans shared a low proportion of genotypes. The presence of high-risk clones (ST131 and ST744), high prevalence of Asia-related ESBL genes ($bla_{\text{CTX-M-55}}$ and $bla_{\text{CTX-M-27}}$) together with the epidemiological history of ST131 C1-M27 clone suggests that rooks are among the potential vectors for the dissemination of antibiotic resistance genes and resistant strains.

DATA AVAILABILITY STATEMENT

The datasets presented in this study can be found in online repositories. The names of the repository/repositories and accession number(s) can be found in the article/**Supplementary Material**.

ETHICS STATEMENT

Ethical review and approval was not required for the animal study because the birds were captured for the purpose of bird ringing. Bird ringing permission number 309 (Birdlife Hungary MME).

AUTHOR CONTRIBUTIONS

GK, LK, ÁL-K, and ÁT: conceptualization. BN, BB, and PG: data curation. BN, EK, KBl, and ÁT: formal analysis. BN, BB, IB, ID, and KBl: investigation. PG, LK, ÁL-K, ID, BN, LM, ÁT, and KBn: methodology. LK, ÁT, KBn, and GK: resources. EK, KBl, ID, and ÁT: software. ÁT and GK: supervision. PG, ÁL-K, ID,

[2]https://pubmlst.org/organisms/plasmid-mlst

LM, ÁT, and KBn: validation. ID and ÁT: visualization. BN and GK: writing—original draft. BN, ÁT, and GK: writing—review and editing. All authors contributed to the article and approved the submitted version.

FUNDING

GK was supported by a Bolyai Scholarship of the Hungarian Academy of Sciences. BB was supported by the New National Excellence Program of the Ministry of Human Capacities (ÚNKP-19-3-I).

ACKNOWLEDGMENTS

The help of the technicians of Medical Microbiology during screening work and National Public Health Center with PFGE are gratefully acknowledged.

SUPPLEMENTARY MATERIAL

The Supplementary Material for this article can be found online at: https://www.frontiersin.org/articles/10.3389/fmicb.2021.785411/full#supplementary-material

REFERENCES

Báez, J., Hernández-García, M., Guamparito, C., Díaz, S., Olave, A., Guerrero, K., et al. (2015). Molecular characterization and genetic diversity of ESBL-producing *Escherichia coli* colonizing the migratory Franklin's gulls (*Leucophaeus pipixcan*) in Antofagasta, North of Chile. *Microb. Drug Resist.* 21, 111–116. doi: 10.1089/mdr.2014.0158

Bager, F., Madsen, M., Christensen, J., and Aarestrup, F. M. (1997). Avoparcin used as a growth promoter is associated with the occurrence of vancomycin-resistant *Enterococcus faecium* on Danish poultry and pig farms. *Prev. Vet. Med.* 31, 95–112. doi: 10.1016/s0167-5877(96)01119-1

Bevan, E. R., Jones, A. M., and Hawkey, P. M. (2017). Global epidemiology of CTX-M β-lactamases: temporal and geographical shifts in genotype. *J. Antimicrob. Chemother.* 72, 2145–2155. doi: 10.1093/jac/dkx146

Bortolaia, V., Kaas, R. F., Ruppe, E., Roberts, M. C., Schwarz, S., Cattoir, V., et al. (2020). ResFinder 4.0 for predictions of phenotypes from genotypes. *J. Antimicrob. Chemother.* 75, 3491–3500. doi: 10.1093/jac/dkaa345

Camacho, C., Coulouris, G., Avagyan, V., Ma, N., Papadopoulos, J., Bealer, K., et al. (2009). BLAST+: architecture and applications. *BMC Bioinformatics* 10:421. doi: 10.1186/1471-2105-10-421

Carattoli, A., Zankari, E., Garcia-Fernandez, A., Voldby Larsen, M., Lund, O., Villa, L., et al. (2014). *In silico* detection and typing of plasmidsusing PlasmidFinder and plasmid multilocus sequence typing. *Antimicrob. Agents Chemother.* 58, 3895–3903. doi: 10.1128/AAC.02412-14

Clermont, O., Christenson, J. K., Denamur, E., and Gordon, D. M. (2013). The Clermont *Escherichia coli* phylo-typing method revisited: improvement of specificity and detection of new phylo-groups. *Environ. Microbiol. Rep.* 5, 58–65. doi: 10.1111/1758-2229.12019

Ebrahimi, F., Mózes, J., Mészáros, J., Juhász, Á., and Kardos, G. (2014). Carriage rates and characteristics of *Enterobacteriaceae* producing extended-spectrum beta-lactamases in healthy individuals: comparison of applicants for long-term care and individuals screened for employment purposes. *Chemotherapy* 60, 239–249. doi: 10.1159/000375407

Ebrahimi, F., Mózes, J., Monostori, J., Gorácz, O., Fésűs, A., Majoros, L., et al. (2016a). Comparison of rates of fecal colonization with extended-spectrum beta-lactamase-producing enterobacteria among patients in different wards, outpatients and medical students. *Microbiol. Immunol.* 60, 285–294. doi: 10.1111/1348-0421.12373

Ebrahimi, F., Mózes, J., Mészáros, J., Juhász, Á., Majoros, L., Szarka, K., et al. (2016b). Asymptomatic fecal carriage of ESBL producing *Enterobacteriaceae* in Hungarian healthy individuals and in long-term care applicants: a shift towards CTX-M producers in the community. *Infect. Dis.* 48, 557–559. doi: 10.3109/23744235.2016.1155734

Fuentes-Castillo, D., Esposito, F., Cardoso, B., Dalazen, G., Moura, Q., Fuga, B., et al. (2020). Genomic data reveal international lineages of critical priority *Escherichia coli* harboring wide resistome in Andean condors (*Vultur gryphus* Linnaeus, 1758). *Mol. Ecol.* 29, 1919–1935. doi: 10.1111/mec.15455

Gauthier-Clerc, M., Lebarbenchon, C., and Thomas, F. (2007). Recent expansion of highly pathogenic avian influenza H5N1: a critical review. *Ibis* 149, 202–214. doi: 10.1111/j.1474-919X.2007.00699.x

Graham, D. W., Bergeron, G., Bourassa, M. W., Dickinson, J., Gomes, F., Howe, A., et al. (2019). Complexities in understanding antimicrobial resistance across domesticated animal, human, and environmental systems. *Ann. N. Y. Acad. Sci.* 1441, 17–30. doi: 10.1111/nyas.14036

Graham, D. W., Collignon, P., Davies, J., Larsson, D. G. J., and Snape, J. (2014). Underappreciated role of regionally poor water quality on globally increasing antibiotic resistance. *Environ. Sci. Technol.* 48, 11746–11747. doi: 10.1021/es504206x

Guenther, S., Aschenbrenner, K., Stamm, I., Bethe, A., Semmler, T., Stubbe, A., et al. (2012). Comparable high rates of extended-spectrum-beta-lactamase-producing *Escherichia coli* in birds of prey from Germany and Mongolia. *PLoS One* 7:e53039. doi: 10.1371/journal.pone.0053039

Guenther, S., Ewers, C., and Wieler, L. H. (2011). Extended-spectrum beta-lactamases producing *E. coli* in wildlife, yet another form of environmental pollution? *Front. Microbiol.* 2:246. doi: 10.3389/fmicb.2011.00246

Hasman, H., Hammerum, A. M., Hansen, F., Hendriksen, R. S., Olesen, B., Agersø, Y., et al. (2015). Detection of mcr-1 encoding plasmid-mediated colistin-resistant *Escherichia coli* isolates from human bloodstream infection and imported chicken meat, Denmark. *Euro Surveill.* 20:30085. doi: 10.2807/1560-7917.ES.2015.20.49.30085

Hayer, S. S., Lim, S., Hong, S., Elnekave, E., Johnson, T., Rovira, A., et al. (2020). Genetic Determinants of Resistance to Extended-Spectrum Cephalosporin and Fluoroquinolone in *Escherichia coli* Isolated from Diseased Pigs in the United States. *mSphere* 5:e00990-20. doi: 10.1128/mSphere.00990-20

Ho, P. L., Chan, J., Lo, W. U., Law, P. Y., Li, Z., Lai, E. L., et al. (2013). Dissemination of plasmid-mediated fosfomycin resistance fosA3 among multidrug-resistant *Escherichia coli* from livestock and other animals. *J. Appl. Microbiol.* 114, 695–702. doi: 10.1111/jam.12099

Hussain, A., Shaik, S., Ranjan, A., Nandanwar, N., Tiwari, S. K., Majid, M., et al. (2017). Risk of transmission of antimicrobial resistant *Escherichia coli* from commercial broiler and free-range retail chicken in India. *Front. Microbiol.* 8:2120. doi: 10.3389/fmicb.2017.02120

Hussain, A., Shaik, S., Ranjan, A., Suresh, A., Sarker, N., Semmler, T., et al. (2019). Genomic and functional characterization of poultry *Escherichia coli* from India revealed diverse Extended-spectrum β-lactamase-producing lineages with shared virulence profiles. *Front. Microbiol.* 10:2766. doi: 10.3389/fmicb.2019.02766

Jamborova, I., Dolejska, M., Vojtech, J., Guenther, S., Uricariu, R., Drozdowska, J., et al. (2015). Plasmid-mediated resistance to cephalosporins and fluoroquinolones in various *Escherichia coli* sequence types isolated from rooks wintering in Europe. *Appl. Environ. Microbiol.* 81, 648–657. doi: 10.1128/AEM.02459-14

Jamborova, I., Johnston, B. D., Papousek, I., Kachlikova, K., Micenkova, L., Clabots, C., et al. (2018). Extensive genetic commonality among wildlife, wastewater, community, and nosocomial isolates of *Escherichia coli* sequence type 131 (H30R1 and H30Rx Subclones) that carry $bla_{CTX-M-27}$ or $bla_{CTX-M-15}$. *Antimicrob Agents Chemother.* 62:e00519-18. doi: 10.1128/AAC.00519-18

Joensen, K. G., Scheutz, F., Lund, O., Hasman, H., Kaas, R. S., Nielsen, E. M., et al. (2014). Real-time whole-genome sequencing for routine typing, surveillance, and outbreak detection of verotoxigenic *Escherichia coli*. *J. Clin. Micobiol.* 52, 1501–1510. doi: 10.1128/JCM.03617-13

Johnson, T. J., Wannemuehler, Y., Johnson, S. J., Stell, A. L., Doetkott, C., Johnson, J. R., et al. (2008). Comparison of extraintestinal pathogenic *Escherichia coli* strains from human and avian sources reveals a mixed subset representing

potential zoonotic pathogens. *Appl. Environ. Microbiol.* 74, 7043–7050. doi: 10.1128/AEM.01395-08

Kövér, L., Tóth, N., Lengyel, S. Z., and Juhász, L. (2018). Corvid control in urban environments: a comparison of trap types. *North West. J. Zool.* 14, 85–90.

Li, J., Bi, Z., Ma, S., Chen, B., Cai, C., He, J., et al. (2019). Inter-host transmission of carbapenemase-producing *Escherichia coli* among humans and backyard animals. *Environ. Health Perspect.* 127:107009. doi: 10.1289/EHP5251

Literak, I., Vanko, R., Dolejska, M., Cízek, A., and Karpísková, R. (2007). Antibiotic resistant *Escherichia coli* and *Salmonella* in Russian rooks (*Corvus frugilegus*) wintering in the Czech Republic. *Lett. Appl. Microbiol.* 45, 616–621. doi: 10.1111/j.1472-765X.2007.02236.x

Livermore, D. M., Canton, R., Gniadkowski, M., Nordmann, P., Rossolini, G. M., Arlet, G., et al. (2007). CTX-M: changing the face of ESBLs in Europe. *J. Antimicrob. Chemother.* 59, 165–174. doi: 10.1093/jac/dkl483

Loncaric, I., Stalder, G. L., Mehinagic, K., Rosengarten, R., Hoelzl, F., Knauer, F., et al. (2013). Comparison of ESBL–and AmpC producing *Enterobacteriaceae* and methicillin-resistant Staphylococcus aureus (MRSA) isolated from migratory and resident population of rooks (*Corvus frugilegus*) in Austria. *PLoS One* 8:e84048. doi: 10.1371/journal.pone.0084048

Lupo, A., Saras, E., Madec, J. Y., and Haenni, M. (2018). Emergence of blaCTX-M-55 associated with fosA, rmtB and mcr gene variants in *Escherichia coli* from various animal species in France. *J. Antimicrob. Chemother.* 73, 867–872. doi: 10.1093/jac/dkx489

Madge, S. (2020). "Rook (Corvus frugilegus), version 1.0," in *Birds of the World*, eds J. del Hoyo, A. Elliott, J. Sargatal, D. A. Christie, and E. de Juana (Ithaca, NY: Cornell Lab of Ornithology). doi: 10.2173/bow.rook1.01

Malberg Tetzschner, A. M., Johnson, J. R., Johnston, B. D., Lund, O., and Scheutz, F. (2020). In Silico Genotyping of *Escherichia coli* Isolates for Extraintestinal Virulence Genes by Use of Whole-Genome Sequencing Data. *J. Clin. Microbiol.* 58:e01269-20. doi: 10.1128/JCM.01269-20

Matsumura, Y., Pitout, D. D. J., Peirano, G., DeVinney, R., Noguchi, T., Yamamoto, M., et al. (2017). Rapid identification of different *Escherichia coli* sequence type 131 clades. *Antimicrob. Agents Chemother.* 61:e00179-17. doi: 10.1128/AAC.00179-17

Matsumura, Y., Pitout, J. D., Gomi, R., Matsuda, T., Noguchi, T., Yamamoto, M., et al. (2016). Global *Escherichia coli* sequence type 131 clade with blaCTX-M-27 gene. *Emerg. Infect. Dis.* 22, 1900–1907. doi: 10.3201/eid2211.160519

Merino, I., Hernández-García, M., Turrientes, M. C., Pérez-Viso, B., López-Fresneña, N., Diaz-Agero, C., et al. (2018). Emergence of ESBL-producing *Escherichia coli* ST131-C1-M27 clade colonizing patients in Europe. *J. Antimicrob. Chemother.* 73, 2973–2980. doi: 10.1093/jac/dky296

Moura, R. A., Sircili, M. P., Leomil, L., Matté, M. H., Trabulsi, L. R., Elias, W. P., et al. (2009). Clonal relationship among atypical enteropathogenic *Escherichia coli* strains isolated from different animal species and humans. *Appl. Environ. Microbiol.* 75, 7399–7408. doi: 10.1128/AEM.00636-09

Persson, S., Olsen, K. E. P., Scheutz, F., Krogfelt, K. A., and Gerner-Smidt, P. (2007). A method for fast and simple detection of major diarrhoeagenic *Escherichia coli* in the routine diagnostic laboratory. *Clin. Microbiol. Infect.* 13, 516–524. doi: 10.1111/j.1469-0691.2007.01692

Poirel, L., Figueiredo, S., Cattoir, V., Carattoli, A., and Nordmann, P. (2008). Acinetobacter radioresistens as a silent source of carbapenem resistance for *Acinetobacter* spp. *Antimicrob. Agents Chemother.* 52, 1252–1256. doi: 10.1128/AAC.01304-07

Rebelo, A. R., Bortolaia, V., Kjeldgaard, J. S., Pedersen, S. K., Leekitcharoenphon, P., Hansen, I. M., et al. (2018). Multiplex PCR for detection of plasmid-mediated colistin resistance determinants, mcr-1, mcr-2, mcr-3, mcr-4 and mcr-5 for surveillance purposes. *Eurosurveillance* 23, 17–00672. doi: 10.2807/1560-7917.ES.2018.23.6.17-00672

Söderlund, R., Skarin, H., Börjesson, S., Sannö, A., Jernberg, T., Aspán, A., et al. (2019). Prevalence and genomic characteristics of zoonotic gastro-intestinal pathogens and ESBL/pAmpC producing *Enterobacteriaceae* among Swedish corvid birds. *Infect. Ecol. Epidemiol.* 9:1701399. doi: 10.1080/20008686.2019.1701399

Tacão, M., Araújo, S., Vendas, M., Alves, et al. (2018). Shewanella species as the origin of blaOXA-48 genes: insights into gene diversity, associated phenotypes and possible transfer mechanisms. *Int. J. Antimicrob. Agents* 51, 340–348. doi: 10.1016/j.ijantimicag.2017.05.014

Tacão, M., dos Santos Tavares, R., Teixeira, P., Roxo, I., Ramalheira, E., Ferreira, S., et al. (2017). mcr-1 and blaKPC-3 in *Escherichia coli* sequence type 744 after meropenem and colistin therapy, Portugal. *Emerg. Infect. Dis.* 23, 1419–1421. doi: 10.3201/eid2308.170162

Tahar, S., Nabil, M. M., Safia, T., Ngaiganam, E. P., Omar, A., Hafidha, C., et al. (2020). Molecular Characterization of Multidrug-Resistant *Escherichia coli* Isolated from Milk of Dairy Cows with Clinical Mastitis in Algeria. *J. Food Prot.* 83, 2173–2178. doi: 10.4315/JFP-20-198

Tausova, D., Dolejska, M., Cizek, A., Hanusova, L., Hrusakova, J., Svoboda, O., et al. (2012). *Escherichia coli* with extended-spectrum β-lactamase and plasmid-mediated quinolone resistance genes in great cormorants and mallards in Central Europe. *J. Antimicrob. Chemother.* 67, 1103–1107. doi: 10.1093/jac/dks017

Tóth, H., Fésűs, A., Kungler-Gorácz, O., Balázs, B., Majoros, L., Szarka, K., et al. (2019). Utilization of vector autoregressive and linear transfer models to follow up the antibiotic resistance spiral in gram-negative bacteria from cephalosporin consumption to colistin resistance. *Clin. Infect. Dis.* 69, 1410–1421. doi: 10.1093/cid/ciy1086

Wang, J., Ma, Z. B., Zeng, Z. L., Yang, X. W., Huang, Y., and Liu, J. H. (2017). The role of wildlife (wild birds) in the global transmission of antimicrobial resistance genes. *Zool. Res.* 38, 55–80. doi: 10.24272/j.issn.2095-8137.2017.003

Xiong, Y., Wang, P., Lan, R., Ye, C., Wang, H., Ren, J., et al. (2012). A novel *Escherichia coli* O157: H7 clone causing a major hemolytic uremic syndrome outbreak in China. *PLoS One* 7:e36144. doi: 10.1371/journal.pone.0036144

Yoon, E. J., Kang, D. Y., Yang, J. W., Kim, D., Lee, H., Lee, K. J., et al. (2018). New Delhi metallo-beta-lactamase-producing *Enterobacteriaceae* in South Korea between 2010 and 2015. *Front. Microbiol.* 9:571. doi: 10.3389/fmicb.2018.00571

Zankari, E., Allesøe, R., Joensen, K. G., Cavaco, L. M., Lund, O., and Aarestrup, F. M. (2020). PointFinder: a novel web tool for WGS-based detection of antimicrobial resistance associated with chromosomal point mutations in bacterial pathogens. *J. Antimicrob. Chemother.* 72, 2764–2768. doi: 10.1093/jac/dkx217

Zendri, F., Maciuca, I. E., Moon, S., Jones, P. H., Wattret, A., Jenkins, R., et al. (2020). Occurrence of ESBL-Producing *Escherichia coli* ST131, Including the H30-Rx and C1-M27 Subclones, Among Urban Seagulls from the United Kingdom. *Microb. Drug Resist.* 26, 697–708. doi: 10.1089/mdr.2019.0351

Zhong, L. L., Zhang, Y. F., Doi, Y., Huang, X., Zhang, X. F., Zeng, K. J., et al. (2017). Coproduction of MCR-1 and NDM-1 by colistin-resistant *Escherichia coli* isolated from a healthy individual. *Antimicrob. Agents Chemother.* 61:e01962-16. doi: 10.1128/AAC.01962-16

Zhuge, X., Jiang, M., Tang, F., Sun, Y., Ji, Y., Xue, F., et al. (2019). Avian-source mcr-1-positive *Escherichia coli* is phylogenetically diverse and shares virulence characteristics with *E. coli* causing human extra-intestinal infections. *Vet. Microbiol.* 239:108483. doi: 10.1016/j.vetmic.2019.108483

Zogg, A. L., Zurfluh, K., Schmitt, S., Nüesch-Inderbinen, M., and Stephan, R. (2018). Antimicrobial resistance, multilocus sequence types and virulence profiles of ESBL producing and non-ESBL producing uropathogenic *Escherichia coli* isolated from cats and dogs in Switzerland. *Vet. Microbiol.* 216, 79–84. doi: 10.1002/mbo3.845

Conflict of Interest: The authors declare that the research was conducted in the absence of any commercial or financial relationships that could be construed as a potential conflict of interest.

Publisher's Note: All claims expressed in this article are solely those of the authors and do not necessarily represent those of their affiliated organizations, or those of the publisher, the editors and the reviewers. Any product that may be evaluated in this article, or claim that may be made by its manufacturer, is not guaranteed or endorsed by the publisher.

frontiers in Microbiology

ORIGINAL RESEARCH
published: 07 March 2022
doi: 10.3389/fmicb.2022.853762

Insights From the *Lactobacillus johnsonii* Genome Suggest the Production of Metabolites With Antibiofilm Activity Against the Pathobiont *Candida albicans*

*Roberto Vazquez-Munoz[1], Angela Thompson[1], Jordan T. Russell[2], Takanori Sobue[1], Yanjiao Zhou[2] and Anna Dongari-Bagtzoglou[1]**

[1]Department of Periodontology, University of Connecticut Health Center, Farmington, CT, United States, [2]Department of Psychiatry/Medicine, University of Connecticut Health Center, Farmington, CT, United States

OPEN ACCESS

Edited by:
Harold J. Schreier,
University of Maryland,
Baltimore County, United States

Reviewed by:
Melyssa Negri,
State University of Maringá,
Brazil
Qi-Lin Zhang,
Kunming University of Science and Technology, China

***Correspondence:**
Anna Dongari-Bagtzoglou
adongari@uchc.edu

Specialty section:
This article was submitted to Microbial Physiology and Metabolism, a section of the journal Frontiers in Microbiology

Received: 13 January 2022
Accepted: 14 February 2022
Published: 07 March 2022

Citation:
Vazquez-Munoz R, Thompson A, Russell JT, Sobue T, Zhou Y and Dongari-Bagtzoglou A (2022) Insights From the Lactobacillus johnsonii Genome Suggest the Production of Metabolites With Antibiofilm Activity Against the Pathobiont Candida albicans.
Front. Microbiol. 13:853762.
doi: 10.3389/fmicb.2022.853762

Lactobacillus johnsonii is a probiotic bacterial species with broad antimicrobial properties; however, its antimicrobial activities against the pathobiont *Candida albicans* are underexplored. The aim of this study was to study the interactions of *L. johnsonii* with *C. albicans* and explore mechanisms of bacterial anti-fungal activities based on bacterial genomic characterization coupled with experimental data. We isolated an *L. johnsonii* strain (MT4) from the oral cavity of mice and characterized its effect on *C. albicans* growth in the planktonic and biofilm states. We also identified key genetic and phenotypic traits that may be associated with a growth inhibitory activity exhibited against *C. albicans*. We found that *L. johnsonii* MT4 displays pH-dependent and pH-independent antagonistic interactions against *C. albicans*, resulting in inhibition of *C. albicans* planktonic growth and biofilm formation. This antagonism is influenced by nutrient availability and the production of soluble metabolites with anticandidal activity.

Keywords: ***L. johnsonii***, ***Candida abicans***, **biofilm**, ***Lactobacillus***, **bacteriocin, anticandida**

INTRODUCTION

Candida albicans is the most common opportunistic fungal pathogen in immunocompromised hosts (Pfaller and Diekema, 2010; Pfaller et al., 2019). Although it is a member of the mucosal microbiota at different body sites in health, under certain conditions, it can cause invasive mucosal infections (Pendleton et al., 2018). The ability of *C. albicans* to switch from yeast to hyphal morphotypes and form biofilms increases its virulence on mucosal tissues (Pappas et al., 2018). The biofilm growth form also increases resistance to innate immune effector cells and antimicrobial treatments (Dongari-Bagtzoglou et al., 2009; Vazquez-Munoz et al., 2020).

The clinical outcome of mucosal candidiasis has been adversely affected by the rise of drug-resistant *C. albicans* strains which have become a serious threat to human health (Centers for Disease Control and Prevention, 2019). As the effectiveness of conventional antifungals is diminished, novel strategies are being developed, such as probiotic therapies (Mundula et al., 2019). In this regard, several species from the *Lactobacillus* complex genus have been studied

as probiotic therapies in gastrointestinal, vulvovaginal, and oral *Candida* infections in mouse models and human clinical trials (Vazquez-Munoz and Dongari-Bagtzoglou, 2021). This is due to the fact that certain lactobacilli produce soluble metabolites—i.e., bacteriocins, weak organic acids (such as lactic and acetic acids), and biosurfactants with anticandidal properties (Vazquez-Munoz and Dongari-Bagtzoglou, 2021). Antifungal activities vary across *Lactobacillus* species and even among strains (Strus et al., 2005; Jang et al., 2019); hence, the studies on relatively unexplored species, such as *Lactobacillus johnsonii*, and newly isolated strains within this species are novel and can unravel potentially significant probiotic properties.

Recently our group reported that the virulence of *C. albicans* in a mouse model of oropharyngeal candidiasis is attenuated by dietary sucrose. Sucrose significantly enriched the *L. johnsonii* communities on the oral mucosa during infection with *C. albicans* and caused a reduction in fungal burdens (Bertolini et al., 2021). Since other *Lactobacillus* species are antagonistic to *Candida* (Vazquez-Munoz and Dongari-Bagtzoglou, 2021), we hypothesized that *L. johnsonii* might exert a growth inhibitory effect on *C. albicans*. *Lactobacillus johnsonii* are Gram-positive, facultatively anaerobic, non-motile bacteria that are part of the *L. acidophilus* group. Like other lactobacilli, *L. johnsonii* is considered as a GRAS (generally recognized as safe) microorganism and is regarded as a probiotic (Marcial et al., 2017; Zheng et al., 2020). *Lactobacillus johnsonii* is a member of the human health-associated gastrointestinal and vaginal mucosal microbiota, two sites afflicted by mucosal candidiasis (Fujisawa et al., 1992; Assefa et al., 2015; Zheng et al., 2020). However, there is scant information on the interactions between *L. johnsonii* and *C. albicans*, and the limited available information is contradictory (Gil et al., 2010; Assefa et al., 2015; Eryilmaz et al., 2019).

We recently isolated *L. johnsonii* strain MT4 from the oral mucosa of mice receiving a sucrose-enriched diet. This strain was identified as *L. johnsonii via* whole 16S rRNA gene sequencing (Bertolini et al., 2021). Human clinical trials suggest that *L. johnsonii*-based probiotics may reduce the burden of certain infections and metabolic disorders (Cruchet et al., 2003). In this work, our aim was to functionally characterize the genome of strain MT4, assess its effects on the planktonic and biofilm growth of the pathobiont *C. albicans*, and explore relevant mechanisms of antifungal activity. We discovered that *L. johnsonii* MT4 displays pH-dependent and pH-independent anticandidal properties, mediated by the release of soluble metabolites, resulting in inhibition of *C. albicans* planktonic growth and biofilm formation. Our results also shed new light on existing contradictory data regarding the impact of lactic acid-mediated acidification on *C. albicans* growth.

MATERIALS AND METHODS

Strains

Lactobacillus johnsonii strain MT4 was reactivated from frozen stocks in 5 ml MRS broth (Difco™) in an anaerobic chamber at 37°C overnight. *Candida albicans* SC5314 (ATCC MYA-2876), also reactivated from frozen stocks, was sub-cultured in YPD broth (Yeast Extract, Sigma®; Bacto™ Peptone, Gibco; and Dextrose, J.T.Baker®), and incubated aerobically at 30°C in an orbital shaker, overnight. Bacterial and fungal overnight cultures were washed in PBS and adjusted to their final concentration in either MRS, MRS w/o dextrose (USbiological), BHI (BBL™, BD), or biofilm medium (RPMI medium 1640 [Gibco] supplemented with 10% BHI, and 10% Fetal Bovine Serum [Gibco]), as described below. In some experiments, *L. johnsonii* type strain ATCC 33200 was used for comparison.

Genomic Characterization of *Lactobacillus johnsonii* MT4 Strain

Genome sequencing, taxonomy, and comparative genomics of *L. johnsonii* MT4 strain were assessed as follows: (I) *Sequencing*: DNA was extracted using the DNeasy® Blood & Tissue Kit (Qiagen, United States; Bertolini et al., 2021). The extracted genomic DNA was assessed for concentration and size using the Qubit 3.0 HS dsDNA assay (Life Technologies, Carlsbad, CA, United States) and the Tapestation 4200 genomic DNA assay (Agilent Technologies, Santa Clara, CA, United States), respectively. The DNA sample was diluted to 0.2 ng/μl, and the sequencing library was prepared using the Illumina Nextera XT DNA kit (Illumina, San Diego, CA, United States) according to the manufacturer's instructions. The library was again checked for concentration and size (450 bp average library length; average insert size of 315 bp) as before, and the sequencing library was prepared using the Illumina Nextera XT DNA kit (Illumina, San Diego, CA, United States) and sequenced using 2 × 150 bp format on an Illumina NovaSeq 6000 at the Center for Genome Innovation (Institute for Systems Genomics, University of Connecticut). Reads pertaining to 1% PhiX control spike-in were filtered and removed *via* USEARCH v11.0.667. The Whole Genome Sequence (WGS) of MT4 was assembled using Unicycler v0.4.8, which utilizes the SPAdes assembler v3.15.2 (Bankevich et al., 2012), at the University of Connecticut's Xanadu High-Performance Computing Cluster; (II) *Taxonomy*: the contigs resulting from the assembly of MT4 were taxonomically classified using Kraken2 v2.0.8-beta (Wood et al., 2019). Phylogenetic analysis on core genes was performed to find the closest *L. johnsonii* MT4 strain relatives. Seventeen whole-Genome Sequences of *L. johnsonii* strains from the NCBI database (strains NCK2677, ATCC 33200, N6.2, 3DG, BS15, Byun_jo_01, DC22.2, DPC_6026, FI9785, G2A, GHZ10a, IDCC9203, NCC_533, UMNLJ21, UMNLJ22, ZLJ010, and pf01) were compared. The assembled MT4 genome and the NCBI genomes were annotated with Prokka v1.14.6 (Seemann, 2014), and the comparative genomics analysis was performed with Roary v3.13.0 (Page et al., 2015) to identify genes unique and in common between our MT4 isolate and the other 17 NCBI genomes of *L. johnsonii* strains. Roary generates an alignment of the core genes using PRANK (Löytynoja, 2014). Phylogenetic analysis of the *L. johnsonii* strains was done using SeaView v5.0.4 (Gouy et al., 2010). The core gene alignment was curated for further analysis using GBlocks (Castresana, 2000) to remove poorly aligned regions, including large gaps. The phylogeny

was generated with PhyML (Guindon et al., 2010) using the GTR DNA substitution model, which was determined as the optimal model using the Smart Model Selection (SMS) tool web server (Lefort et al., 2017) and branch support values calculated using the aLRT method.[1] Nucleotide equilibrium frequencies, invariable sites, and across-site rate variation were set to "optimized," with the BioNJ option selected (Gascuel, 1997). Finally, SeaView uses the PHYLIP package (Felsenstein, 1993) for tree parsimony. The presence or absence of genes and proteins in MT4 was also verified with searches using BLAST (Altschul et al., 1990) and tblastn, respectively.

Phenotypic Characterization of *Lactobacillus johnsonii*

Growth on Different Culture Media

Lactobacillus johnsonii was grown on MRS (BD), BHI (BD), YPD, KSFM (Gibco), and F-12 (Gibco). Lactobacilli were incubated static, aerobically with 5% CO_2, at 37°C. Optical density ($\lambda = 600$ nm) was measured every 90 min. The pH of growth media was measured at $t = 24$ h.

Aggregation

Lactobacillus johnsonii MT4 auto-aggregation phenotype was assessed in MRS broth after growth under aerobic conditions with 5% CO_2, at 37°C, for 24 h. Auto-aggregation phenotype was defined as positive if the overnight cultures settled at the bottom with no turbidity and negative if they showed turbidity (Jankovic et al., 2003). The non-aggregating *L. johnsonii* ATCC 33200 strain was used as a negative control.

Assessment of D/L-Lactate Production

The DL-lactate kit (Megazyme) was used following the manufacturer's recommendations with minor changes. Briefly, supernatants from overnight *L. johnsonii* and *C. albicans* in single-or dual-species cultures were deproteinized with ice-cold 1 M hydrochloric acid 1 M NaOH, and 20 µl of each sample was tested in duplicate. Standard curves were prepared in the corresponding culture medium. Absorbance was measured at $\lambda = 340$ nm, and D−/L-lactate concentrations were calculated in two independent experiments.

Effect of *Lactobacillus johnsonii* on *Candida albicans* Planktonic Growth

C. albicans (5×10^4 cells ml^{-1}) and *L. johnsonii* (5×10^4 to 5×10^8 cells ml^{-1}) were cocultured in MRS or BHI broth aerobically with 5% CO_2 for 24 h, at 37°C. These growth conditions allow planktonic growth of *C. albicans* exclusively in the yeast form. The influence of media acidification on *C. albicans* growth was assessed in lactic acid-(DL-LA, Sigma-Aldrich)-supplemented MRS broth (pH 4.0 ± 0.05, 142 mM) or BHI broth (pH 5.5 ± 0.08, 28.3 mM). To assess the influence of carbohydrate availability, single- or dual-species cultures were tested in MRS broth without dextrose (MRSm) or with added carbohydrates (2% sucrose or 2% dextrose). At the end of each culture period, *L. johnsonii* viable counts (CFU) were estimated by plating serially 10-fold diluted cultures onto MRS agar plates, incubated anaerobically at 37°C, for 48 h. *C. albicans* yeast cell numbers were assessed by counting in a Neubauer chamber after fixation in 1% paraformaldehyde (PFA, Sigma).

Preparation of Non-viable *Lactobacillus johnsonii*

Some studies have reported that exopolysaccharides from the cell wall of UV-inactivated bacterial cells may decrease the burden of *Candida* infections (Wagner et al., 2000) and reduce the dimorphic transition (Allonsius et al., 2019). Thus, the impact of inactivated *L. johnsonii* cells on *C. albicans* was evaluated. *Lactobacillus johnsonii* cells were UV-light-inactivated in a UVP crosslinker instrument (Analytik Jena; 254 nm, 1,500 mJ cm^{-2}, at 8 cm from the UV lamp) for 12 cycles; Heat-killed organisms were prepared at 95°C for 30 min on a heat block (VWR). To verify that bacteria were killed, 10 µl from each suspension were transferred into 1 ml of MRS and incubated at 37°C for 48 h. *Candida albicans* (~5×10^4 cells ml^{-1}) with killed lactobacilli (~5×10^6 cells ml^{-1}) were suspended in BHI broth and were incubated as described above.

Preparation of Cell-Free Supernatants

Supernatants from *L. johnsonii* single-species cultures (Lj-cell-free supernatant (CFS), starting at 5×10^7 cell ml^{-1}) or in cocultures with *Candida albicans* (CC-CFS, starting at 5×10^4 cell ml^{-1}) were prepared in MRS broth, BHI broth, or biofilm medium under aerobic conditions with 5% CO_2, at 37°C, for 24 h. CFS were collected by centrifugation at 4,000 rpm for 20 min. The pH of supernatants was measured, and each supernatant was divided into two aliquots; one was kept at the original pH (acidic-CFS, pH 3.87 ± 0.03 for MRS broth, 5.40 ± 0.04 for BH, and pH 6.08 ± 0.18 for biofilm medium), while the other was pH-adjusted with a 1 M NaOH solution (neutralized-CFS, pH 6.6 ± 0.14 for MRS, pH 7.4 ± 0.06 for BHI, and pH 8.68 ± 0.04 for biofilm medium). CFS were sterile filtered using a 0.2 µm filter (Corning). CFS were stored at 4°C. The effect of CFS on *C. albicans* (~5×10^4 cells ml^{-1}) was tested in growth media supplemented with 50% CFS or PBS as control.

Impact of *Lactobacillus johnsonii* on *Candida albicans* Biofilm Growth

Biofilm Growth

Lactobacillus johnsonii (5×10^5 to 5×10^7 cells ml^{-1}) and *C. albicans* (5×10^4 cells ml^{-1}) were suspended in biofilm medium (80% RPMI, 10% BHI, and 10% FBS) and seeded in multiwell plates or into µ-Slide 8-well chambered slides (IBIDI GmbH, Gräfelfing, Germany) and incubated statically, aerobically with 5% CO_2 at 37°C for up to 48 h. Single-species cultures were used as control. To visualize *L. johnsonii*, bacteria were stained with 1 mM CellTracker™ Deep Red dye (Thermo Fisher Scientific). Fungal cells were stained

[1] http://www.atgc-montpellier.fr/sms/

with Calcofluor White for 10 min, washed in PBS, and fixed with 4% paraformaldehyde (PFA). The impact of physical contact between the lactobacilli and *Candida* on fungal biofilm growth was assessed by seeding *L. johnsonii* (5×10^6 cell ml^{-1}) into a Millicell® 0.4 µm PCF Cell Culture Insert (Millipore, United States). The inserts were placed into the wells of 24-well plates (Corning) containing *C. albicans* (5×10^4 cell ml^{-1}). Biofilms were grown for 24 h, as above. Exclusion and displacement experiments were performed to assess the effect of preformed biofilms on the ability of the other microbial species to form a biofilm. The supernatant was removed, and preformed biofilms were washed twice with PBS. In exclusion assays, *C. albicans* (5×10^4 cells ml^{-1}) suspended in fresh biofilm medium was transferred to preformed *L. johnsonii* biofilms. In displacement assays, *L. johnsonii* (5×10^7 cells ml^{-1}) suspended in fresh medium was added to preformed *C. albicans* biofilms. For negative controls, cell-free medium was added to the single-species 24 h-old preformed biofilms. Plates were incubated for an additional 24 h, as described above.

Biofilm Analyses

Biovolumes and Thickness

Micrographs were obtained at a ×400 magnification in a Microscope (Zeiss), with the DAPI ($\lambda_{exc} = 358$ nm, $\lambda_{em} = 463$ nm) and CY3 ($\lambda_{exc} = 549$ nm, $\lambda_{em} = 562$ nm) fluorescence channels and using the Z-stack mode. Images were post-processed in Zen Blue (v.3.0, Zeiss) and analyzed with IMARIS Cell Imaging Software (Oxford Instruments) using the Create Surface tool to reconstruct 3D images from the biofilms and assess their volumes.

Biomass

Fungal biomass was quantified by qPCR. DNA from biofilms grown on 24-multiwell plates was extracted using the Yeast DNA Extraction Kit (Thermo Scientific), following the manufacturer's recommendations. A region from the fungal rRNA operon was amplified using the primers 5.8S GTGAATCATCGARTC TTTGAAC (forward primer) and 28S-1 TATGCTTAAGTT CAGCGGGTA (reverse primer) under the qPCR conditions reported by Khot et al. (2009). Fungal biomass was directly correlated to the number of amplicons. Each experiment contained untreated biofilms and cell-free media as controls.

Metabolic Activity

The fungal metabolic activity was assessed *via* XTT as described elsewhere (Pierce et al., 2008). Briefly, biofilms were incubated for 30 min with Penicillin G/Streptomycin (100 µg ml^{-1}, Gibco) to remove the metabolic signal from lactobacilli. Then, biofilms were washed with BPS, XTT/menadione was added, and samples were incubated for 2.5 h. Absorbance was read at 490 nm.

Reproducibility and Statistical Analyses

Data from at least two independent experiments with technical replicates were analyzed for statistical significance using One-Way ANOVA with Kruskal-Wallis posttest in Prism v9.2.0 (GraphPad Software, LLC).

RESULTS

Genomic Characterization of *Lactobacillus johnsonii* Strain MT4

The MT4 genome assembly resulted in 68 contigs with an N50 of 90.96 kb. All but 1 contig were classified as *L. johnsonii*, with a single contig classified as *L. crispatus* based on the Kraken2 results (**Supplementary Table 1**). The 1,883,026 bp genome has a GC content of 34.4%. In total, 1,865 genes were predicted, including 1,772 protein-coding genes and 93 RNA genes (34 miscellaneous/non-coding RNA, 3 rRNA, 55 tRNA, and one tmRNA). Phylogenetic analysis on core genes shows the relation of this strain to 17 *Lactobacillus johnsonii* strains deposited in the NCBI database (**Figure 1**), indicating that strain MT4 is almost identical to strain NCK2677, also isolated from the GI

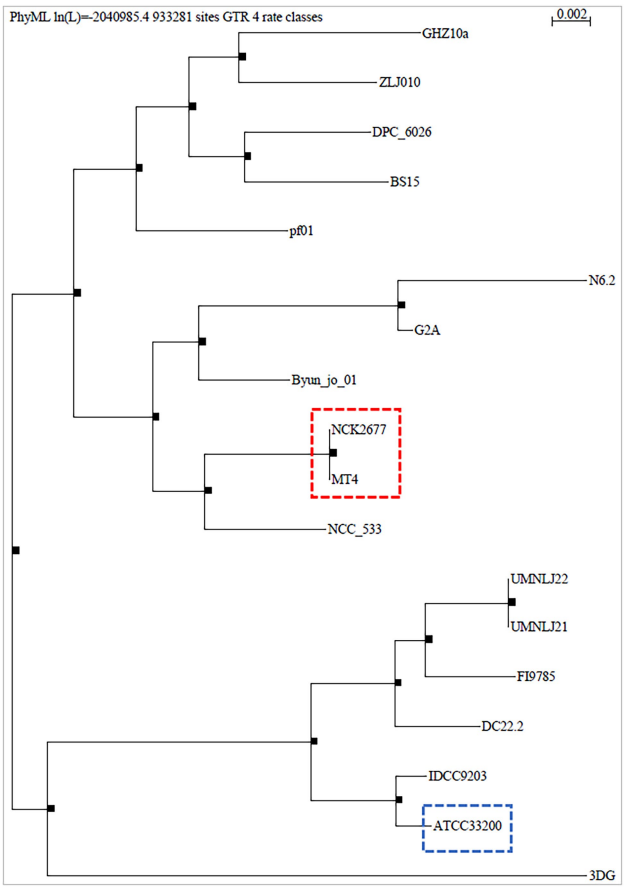

FIGURE 1 | Phylogenetic analysis of *Lactobacillus johnsonii* MT4. The whole genome of the *L. johnsonii* MT4 strain was analyzed to assess its phylogeny. The phylogenetic analysis of the MT4 strain shows the relation of our strains with other 17 *L. johnsonii* strains (genomes from the NCBI database). The analyzed *L. johnsonii* strains are NCK2677, ATCC 33200, N6.2, 3DG, BS15, Byun_jo_01, DC22.2, DPC_6026, FI9785, G2A, GHZ10a, IDCC9203, NCC_533, UMNLJ21, UMNLJ22, ZLJ010, and pf01. All branch support values are 1. The phylogenetic analysis shows that MT4 and NCK2677 share >99.96% of identity (red square). The closest relative to strain MT4/NCK2677 is NCC_533 (La1). ATCC 33200 strain (blue square) was used for some experiments as a comparison.

tract of C57BL/6 mice (O'Flaherty et al., 2020), sharing more than 99.96% identity of their genomes. The closest relative to the MT4/NCK2677 strains is NCC 533 (La1), a strain with probiotic properties (Yamano et al., 2006). Functional genomics analysis revealed that strain MT4 possesses genes encoding products that are similar to reported anticandidal metabolites (a bacteriocin, two hydrolases, and a biosurfactant; **Table 1**). The alignment analysis is listed in **Supplementary Table 2**. MT4 also possesses genes for both D- and L-Lactate synthesis and other metabolites of interest, such as the bacteriocins lactacin-F and helveticin J, and a glucanase (glycoside hydrolase family 8).

TABLE 1 | *Lactobacillus johnsonii* strain MT4 possesses genes encoding for metabolites similar to products reported to display anticandidal activity.

Metabolite	Type	Reported anticandidal effect	References
Bacillomycin D	Lipopeptide, Bacteriocin	Disruption of the fungal cell membrane by forming ion-conducting pores. Bacillomycin D-like peptides inhibit the β-1,3-glucan synthesis.	Olfa et al., 2015; Hajare et al., 2016
Surfactin	Cyclo-lipopeptide biosurfactant	Prevent fungal adhesion to surfaces, reducing biofilm formation	Nelson et al., 2020
Glucanase	Glycoside hydrolase family 8	Hydrolysis of O-glycosyl compounds from *Candida* cell wall.	Jung, 2018
Msp1/p75	Peptidoglycan hydrolase	Chitinase activity; degrades *Candida* cell wall and inhibits hyphal morphogenesis	Allonsius et al., 2019

Phenotypic Traits of *Lactobacillus johnsonii* MT4

Growth on Different Media

Lactobacillus johnsonii MT4 displayed the best aerobic growth rate on MRS broth, followed by BHI broth, while it displayed poor growth in all other media (**Supplementary Figure 1A**).

Auto- and Co-aggregation

Overnight cultures of *L. johnsonii* strain MT4 showed a partial degree of auto-aggregation, whereas the strain ATCC 33200 did not (**Supplementary Figure 1B**). Additionally, *L. johnsonii* MT4 co-aggregated with *C. albicans* cells in dual-species biofilms, particularly on hyphae (**Figure 2**).

Acidification

Growth of *L. johnsonii* MT4 in MRS, BHI, and biofilm medium (80% RPMI, 10% BHI, 10% FBS) displayed a different degree of acidification in overnight cultures (**Figure 3**, bottom table). Regardless of the starting inoculum size (10^4–10^7 cell ml^{-1} range), lactobacilli acidified MRS broth to pH 3.9 (from 6.5), BHI to pH 5.5 (from 7.5), and biofilm medium to pH 6 (from 8.4). In addition to having different starting pH, the difference in pH at the end of the growth period in the two media may be associated with a different buffering capacity or the production of different amounts of organic acids in each medium. *C. albicans* had a small neutralizing effect on the pH of the growth media in dual-species cultures with *L. johnsonii* in BHI and biofilm medium only (**Figure 3**).

DL-Lactate Production

Lactobacillus johnsonii is reported to produce both the D and L enantiomers of lactate (Fujisawa et al., 1992). The functional genome analysis and a DL-lactate assay confirmed that strain

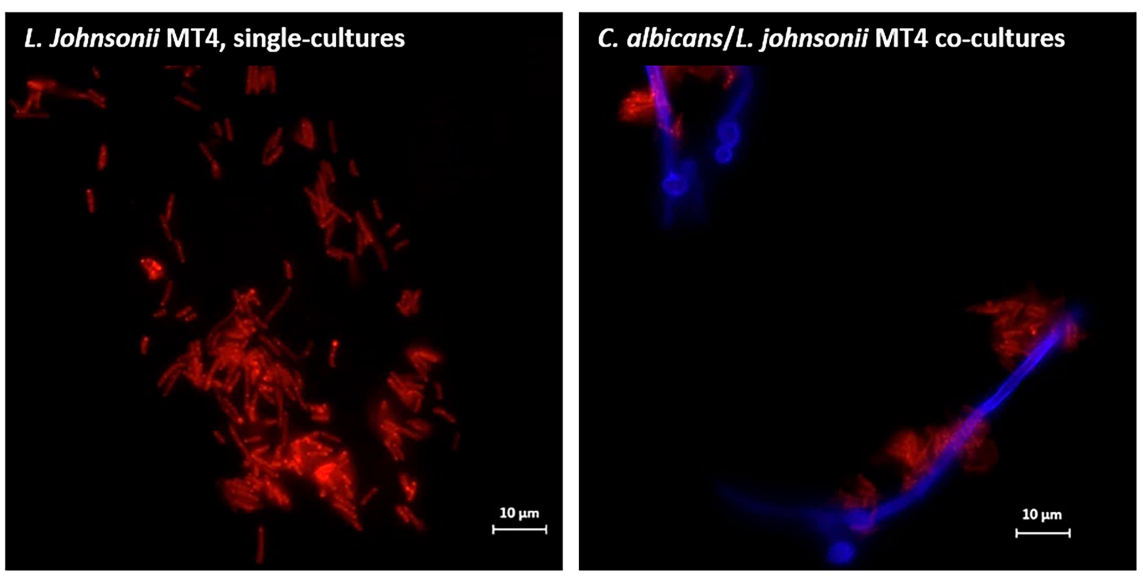

FIGURE 2 | *Lactobacillus johnsonii* co-aggregates with *Candida albicans* cells. *L. johnsonii* (red) auto-aggregates and co-aggregates with *C. albicans* (blue). The yeast and the lactobacilli were grown on biofilm media for 3 h. Lactobacilli were found in physical proximity with *Candida* cells, particularly along the hyphae. Scale bar = 10 µm.

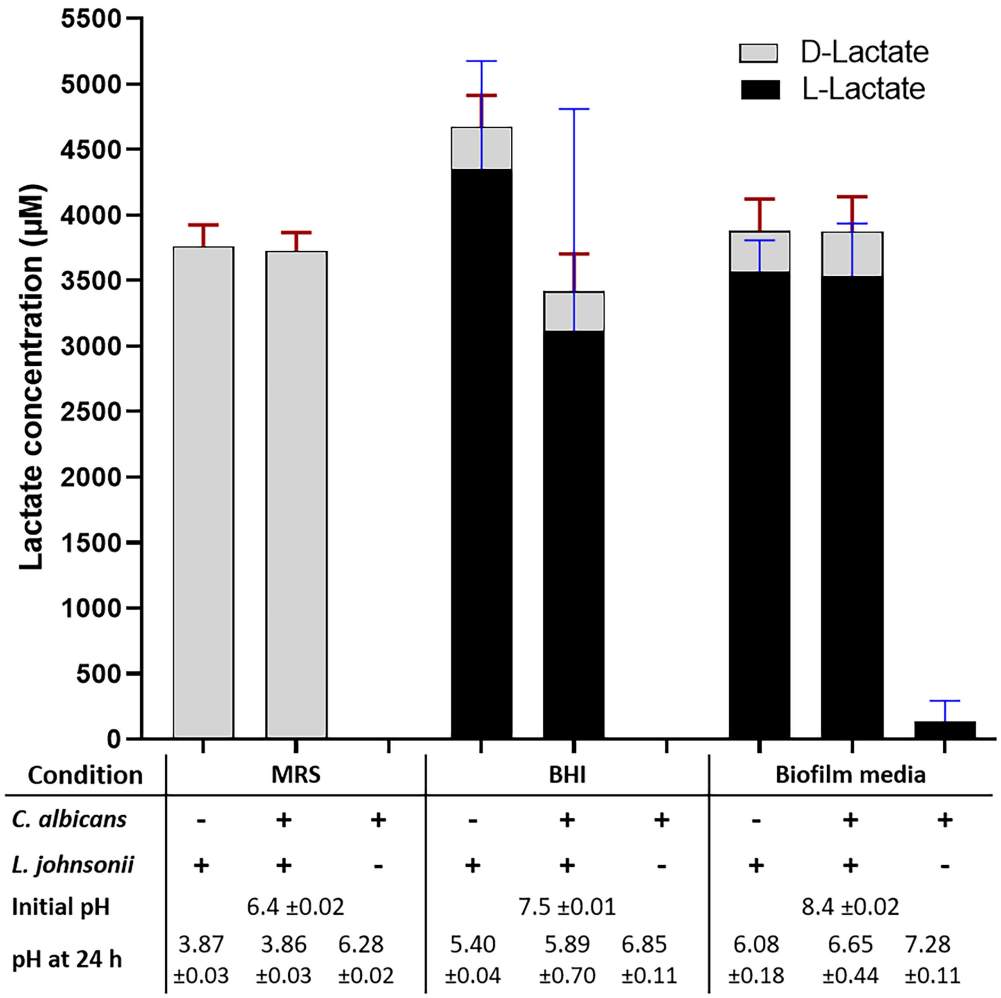

FIGURE 3 | Lactate production and pH on different culture media. The production of DL-lactate by the MT4 strain was measured in various growth media. The growth media influence DL-Lactate production and ratio. In MRS, the D enantiomer is favored, while the L enantiomer production takes over in BHI and biofilm media. Acidification of the culture media does not correspond to the total DL-lactic acid concentration, which may be due to the particular buffering capacity of each growth media and the presence of other organic acids.

MT4 produces both enantiomers (**Figure 3**). Interestingly, the type of growth medium influenced the D−/L-lactate ratio; D-lactate was favored in MRS broth with both MT4 (**Figure 3**) and ATCC 33200 (**Supplementary Figure 2A**) strains, whereas L-lactate was predominant in BHI broth and biofilm medium, representing 93% and 92% of the total production, respectively. The total DL-lactate production was similar in all growth media, ranging between 3.5–4.5 mM (**Figure 3**). *Candida albicans* lactate production was negligible and did not influence the lactate production of *L. johnsonii* (**Figure 3**).

Lactobacillus johnsonii Inhibits *Candida albicans* Planktonic Growth

We first tested the effect of *L. johnsonii* MT4 on *C. albicans* planktonic growth in the two media in which this strain showed the best growth. In both MRS and BHI broth *L. johnsonii* inhibited *C. albicans* growth following a dose-repose trend (**Figures 4A,B**). The inhibition of *C. albicans* growth was more pronounced in MRS, which also showed higher acidification at the end of the coculture period (MRS pH 3.9 vs. BHI pH 5.5). *Lactobacillus johnsonii* ATCC 33200 displayed similar anticandidal activity in MRS broth (**Supplementary Figure 2B**).

To assess the role of acidification in inhibiting fungal growth, we supplemented the media with sufficient amounts of lactic acid to lower the pH to levels comparable with a 24 h culture of *L. johnsonii*. *Candida albicans* growth inhibition in lactic acid-supplemented MRS broth was similar to *L. johnsonii*-induced inhibition, showing that lactic acid-induced acidic pH alone is sufficient to cause growth inhibition in this medium. In contrast, growth inhibition in lactic-acid supplemented BHI was significantly lower than that induced by live bacteria suggesting that acidic pH alone is not responsible for the growth inhibition observed in this medium (**Supplementary Figure 3**).

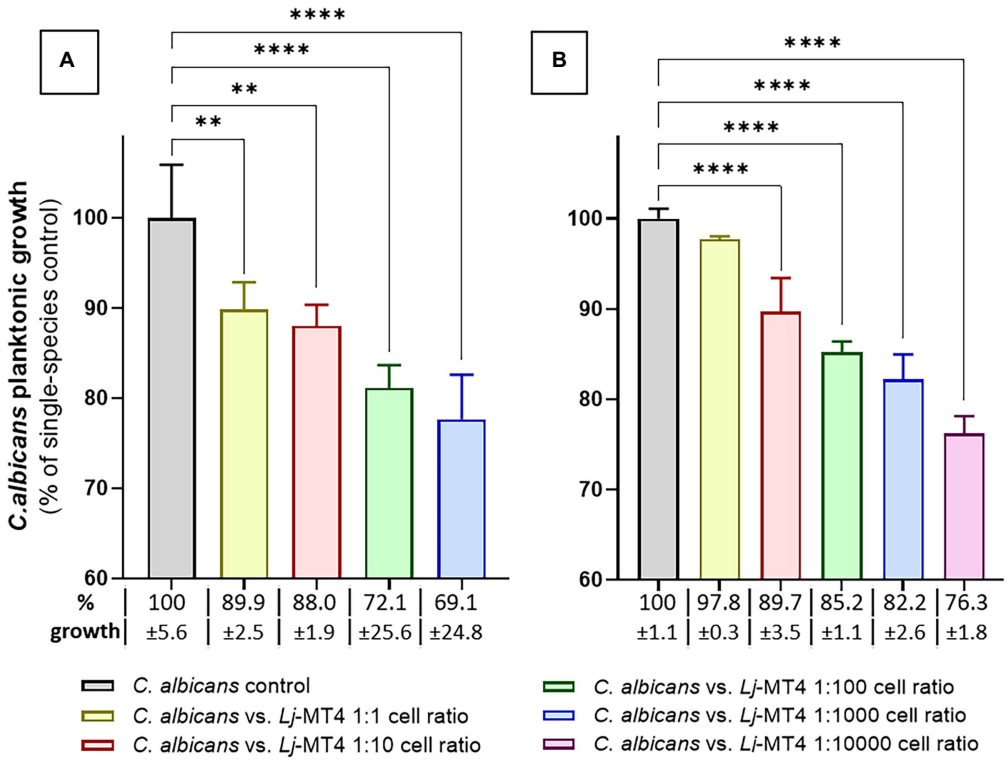

FIGURE 4 | *Lactobacillus johnsonii* inhibits *C. albicans* planktonic growth. The effect of *L. johnsonii* MT4 (Lj) on the planktonic growth of *C. albicans* (Ca) was assessed in two different growth media. *L. johnsonii* at different starting concentrations-inhibited *C. albicans* planktonic growth in a dose–response pattern. **(A)** MRS broth, and **(B)** BHI broth. *Candida albicans* growth inhibition is higher on MRS. One-Way ANOVA, Dunnett posttest, $^{**}p \leq 0.01$ and $^{****}p \leq 0.0001$. In all dual-species cultures, MRS was acidified to pH ~3.9 and BHI to pH ~5.5. 100% growth corresponds to 8.16 ± 0.41 SD and 7.47 ± 0.08 SD yeast cells ml^{-1} (average, log10 values) in MRS and BHI broth, respectively.

Carbohydrate Availability Plays a Role in *Candida albicans* Growth Inhibition in MRS Broth

We next evaluated the impact of carbohydrate availability on *Lactobacillus* fitness and its ability to inhibit *Candida* growth in MRS broth. In carbohydrate-free MRSm, there was a significantly reduced *L. johnsonii* growth rate (**Supplementary Figure 4**), lactate production was significantly curtailed, and the pH of the growth media remained close to the initial pH (**Figure 5A**). As expected, supplementing the media with either 2% dextrose or 2% sucrose fully restored lactate production and caused media acidification, while co-culture with *C. albicans* did not affect the amounts of lactate produced (**Figure 5A**). In MRS broth, growth inhibition of *C. albicans* by *L. johnsonii* MT4 required the availability of carbohydrates (**Figure 5B**), being higher in the 2% dextrose-supplemented MRSm compared to the non-supplemented or 2% sucrose-supplemented MRSm. Since the *Candida*-inhibitory effect of *L. johnsonii* was significantly curtailed when bacterial carbohydrate metabolism was suppressed in MRSm, we hypothesized that bacterial viability is also required for anticandidal activity. As expected, neither UV- nor heat-killed *L. johnsonii* inhibited *C. albicans* yeast growth in MRS broth (**Figure 6A**). Collectively these results indicate that carbohydrate availability influences the ability of *L. johnsonii* to produce weak organic acids and metabolites with anticandidal properties that may be responsible for the growth inhibition of the yeast in MRS.

To further dissect the role of soluble metabolites released in culture media on the growth inhibition observed in MRS broth, we tested the effect of CFS (i.e., *Lactobacillus* spent media) on *C. albicans* growth. CFS from *Lactobacillus* cultures in MRS broth showed significant anticandidal activity, similar to co-cultures with live lactobacilli or lactic acid-acidified media (**Figures 6A,B**). However, the pH-adjusted CFS (pH ~6.5) from *Lactobacillus* cultures in MRS broth had significantly reduced anticandidal activity, suggesting that acidic pH is required for most anticandidal activity of *Lactobacillus* metabolites in MRS broth. Similar results were obtained with CFS prepared from cocultures of *C. albicans* and *L. johnsonii* (**Figure 6B**).

Lactobacillus johnsonii Reduces the Ability of *Candida albicans* to Form Biofilms

Single species *C. albicans* biofilms uniformly covered the well surfaces (**Figure 7A**), while *L. johnsonii* MT4 biofilms consisted of scattered clusters of cells (**Figure 7B**). *Lactobacillus johnsonii* MT4 reduced the metabolic activity of *C. albicans* biofilms in a dose–response pattern (**Supplementary Figure 5**). The ability

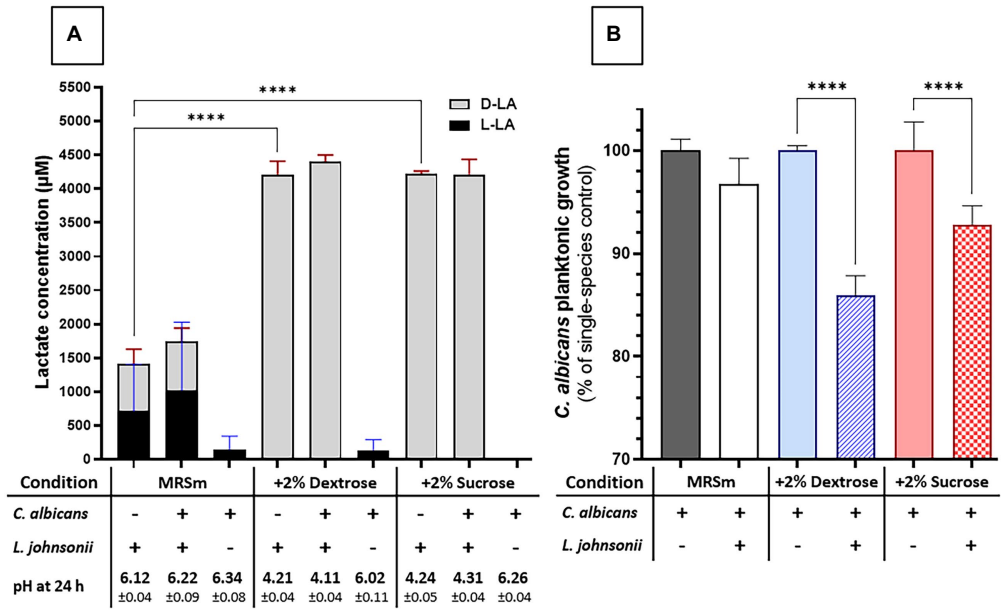

FIGURE 5 | Carbon sources influence *L. johnsonii* anticandidal activity, lactic acid production, and pH. **(A)** Lactate production is impacted by availability but not by the type of carbohydrate (i.e., sucrose vs. glucose). The acidification of the culture media correlates to lactate production; **(B)** The carbohydrate availability and its type influenced the anticandidal activity of *L. johnsonii*. One-Way ANOVA, Dunnett posttest, $^{****}p \leq 0.0001$. 100% growth corresponds to 6.51 ± 0.06 SD, 7.37 ± 0.02 SD, and 6.71 ± 0.06 SD yeast cells ml^{-1} (average, log10 values) in MRSm, MRSm+2% dextrose, and MRSm+2% sucrose, respectively.

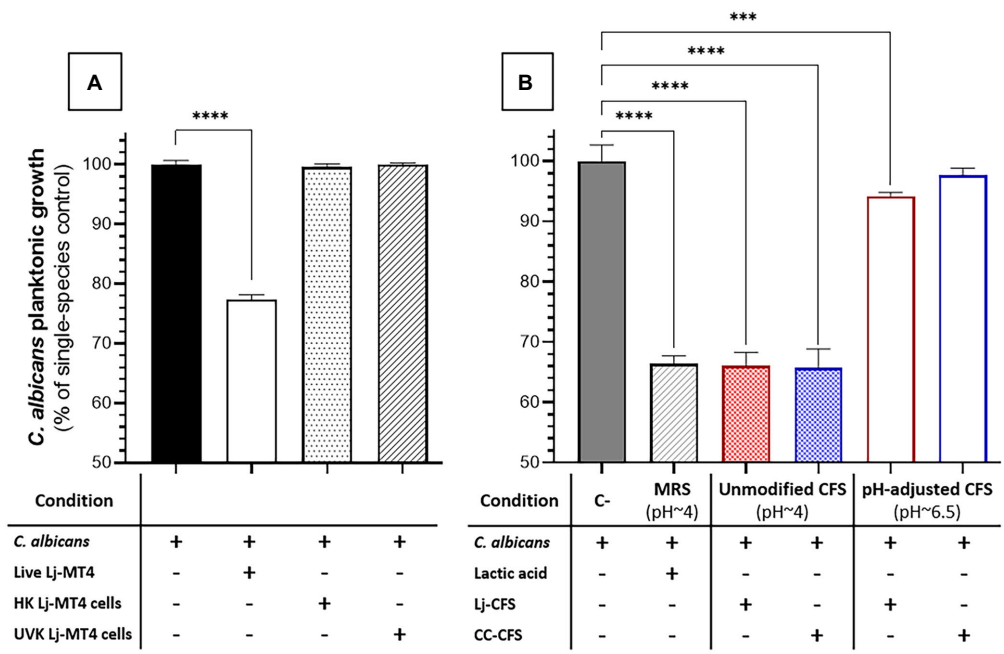

FIGURE 6 | Effect of *L. johnsonii* inactivated cells and soluble metabolites on *C. albicans* growth in MRS broth. **(A)** Inactivated *L. johnsonii* cells did not reduce the growth of *C. albicans*; **(B)** *L. johnsonii* CFS inhibited the growth of *C. albicans* in a pH-dependent manner. HK = heat killed, UVK=UV-killed. CFS = Cell-free supernatant (spent media). One-Way ANOVA, Dunnett posttest, $^{***}p \leq 0.005$, $^{****}p \leq 0.0001$. 100% growth corresponds to 8.16 ± 0.41 SD yeast cells ml^{-1} in MRS broth.

of *C. albicans* to form biofilms was significantly hindered by the MT4 strain (**Figure 7C**), decreasing the fungal biofilm biovolumes (**Figure 7E**), thickness (**Figures 7A,C,F**, *side view*), and biomass as assessed by qPCR (**Figure 7G**). *L. johnsonii* ATCC 33200 displayed similar antibiofilm activity to strain MT4 (**Figures 7D–G**). In addition to hindering the formation

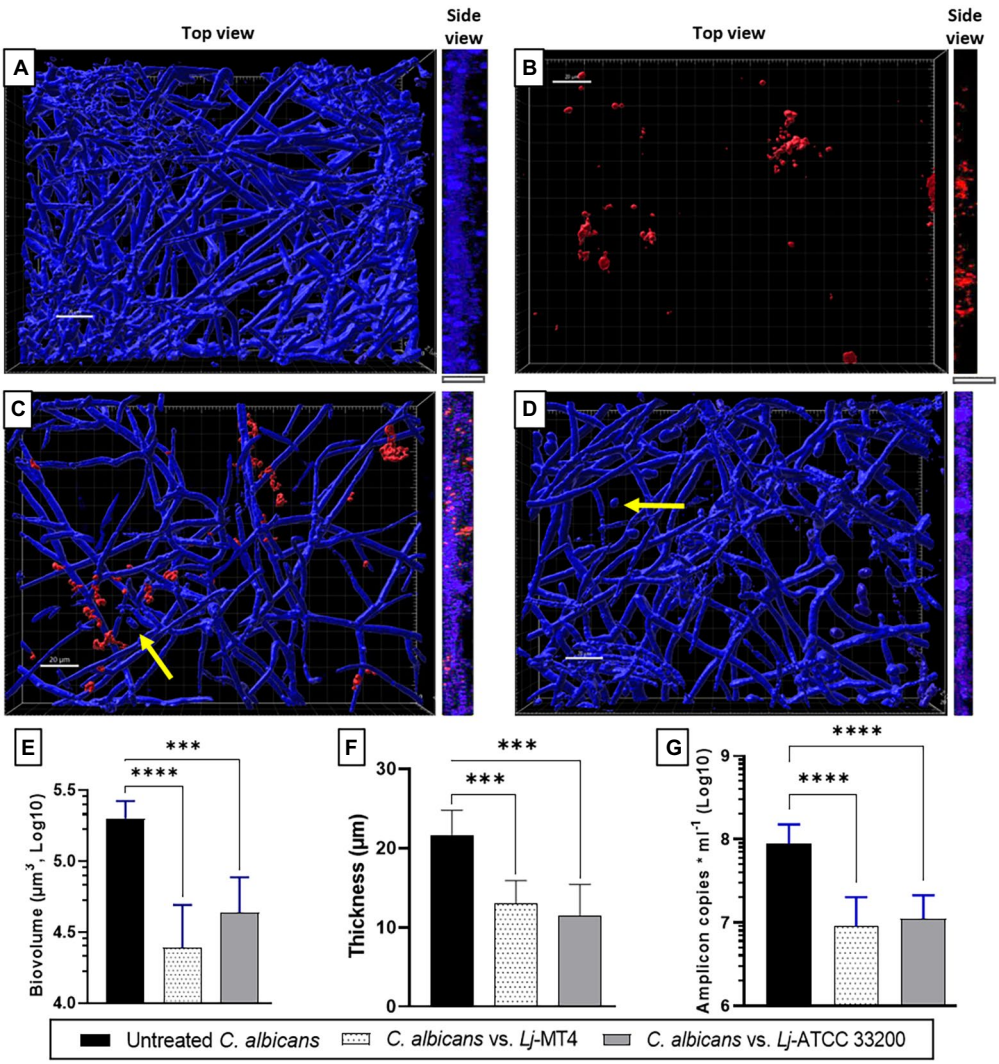

FIGURE 7 | *Lactobacillus johnsonii* reduces the ability of *C. albicans* to form biofilms. **(A)** Single *C. albicans* biofilms uniformly cover the surface; **(B)** Single *L. johnsonii* biofilms consist of scattered clusters of cells; *C. albicans* biofilm formation is reduced by *L. johnsonii* **(C)** MT4 and **(D)** ATCC 33200. Fungal biofilm **(E)** biovolumes, **(F)** thickness, and **(G)** biomass are significantly reduced in the presence of lactobacilli. Yellow arrows indicate the presence of yeast cells. White bar = 20 µ. One-Way ANOVA, Dunnett posttest. $^{***}p \leq 0.005$, $^{****}p \leq 0.0001$.

of fungal biofilms, the yeast morphotype was present in the dual-species biofilms but was rarely observed in the single-species fungal biofilms. The pH of biofilm media at the end of single- and dual-species cultures were 6.08 ± 0.18 and 6.65 ± 0.44, respectively, suggesting that the effect of *L. johnsonii* on biofilm growth is not due to media acidification by the bacteria under these growth conditions.

To examine the role of physical contact between the two organisms in *Candida* biofilm growth inhibition, we used transwell inserts during biofilm growth, allowing passage of soluble metabolites from lactobacilli seeded on the upper transwell compartment. Physical separation of microorganisms with transwell inserts did not significantly impact the reduction in *C. albicans* biofilm biomass, showing that physical contact between *L. johnsonii* and *C. albicans* is not required for inhibiting fungal biofilm growth (**Supplementary Figure 6**). Instead, these data suggested that either nutrient competition during coculture or secreted *L. johnsonii* metabolites are responsible for this effect. These results agree with studies using a similar design that showed other *Lactobacillus* species having biofilm inhibitory activity against *C. albicans* (Poupet et al., 2019) and *Streptococcus mutans* (Wu et al., 2015) in a contact-independent way. To further explore the impact of secreted metabolites, we tested the CFS prepared from biofilm cultures on fungal biofilm growth. CFS did not reduce the fungal biofilm biovolumes compared to the 50% PBS control (**Figure 8A**), but caused a small but statistically significant reduction in the metabolic activity of the fungal biofilms (**Figure 8B**). Importantly, CSF from *L. Johnsonii* alone or from coculture with *C. albicans* hindered its ability to transition into hyphae (**Figures 8C–G**). Surprisingly the yeast morphotype was the most abundant in all CFS-treated biofilms, regardless of whether the pH of the

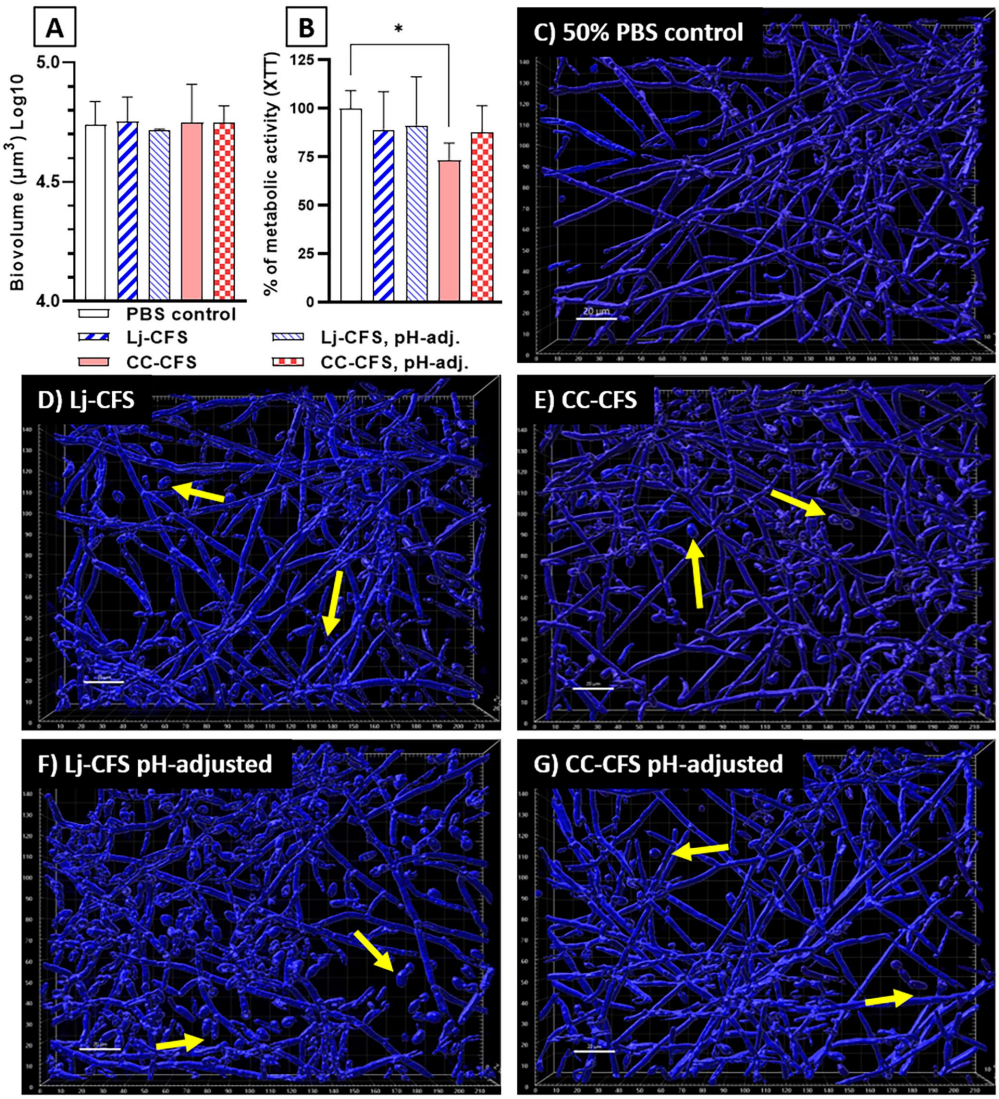

FIGURE 8 | Cell-Free Supernatants reduce the ability of *C. albicans* for hyphal transition in biofilm growth. CFS were prepared from single *L. johnsonii* biofilms (Lj-CFS, panels **D,F**) or from biofilm cocultures with *C. albicans* (CC-CFS, panels **E,G**) in biofilm media and were added during biofilm growth. CSF were used with and without pH neutralization to discern the metabolites' activity beyond acidification. CFS did not reduce the fungal biofilm biovolumes (panel **A**) but reduced the average metabolic activity of the biofilms **(B)**. Additionally, all CFS supplements notably increased the yeast morphotype numbers in biofilms. **(C–G)**. Yellow arrows indicate yeast cells. White bar = 20 µ. One-Way ANOVA, Dunnett posttest. $^{*}p \leq 0.05$. 100% of XTT metabolic activity (panel B) corresponds to $OD_{490} = 0.48 \pm 0.05$ SD of biofilms in 50% PBS.

CSF was adjusted before adding to the culture media or not (**Figures 8D–G**). These results, taken together, suggest that *Lactobacillus* metabolites, accumulating over time during growth in biofilm medium, can negatively impact fungal metabolic activity and hinder the dimorphic transition in a pH-independent manner.

Based on these observations, we next hypothesized that 24 h preformed biofilms of *L. johnsonii* will reduce the ability of *C. albicans* to form biofilms (**Figures 9A,C,E–G**). Indeed there was a significant reduction in biofilm growth as confirmed with biovolume (**Figure 9E**), thickness (**Figures 9A,C,F**, *side view*), and biomass (**Figure 9G**) estimates. As expected, a large number of cells remained in the yeast morphotype, suggesting that the *Lactobacillus* preformed biofilm reduced the dimorphic transition into hyphae, which is an essential stage in biofilm growth on mucosal surfaces (Chandra et al., 2001). Along the same lines, when lactobacilli were added to the 24-h *Candida* preformed biofilms, further growth of *C. albicans* biofilms was prevented (**Figure 9D**) as seen in comparison to 48 h control biofilms (**Figures 9A,B**). Thickness and biomass estimates in this setting were similar to the initial 24 h biofilm control, suggesting arrested biofilm growth. However, fungal biofilm biovolumes (**Figure 9E**) were significantly lower than both the 24 and 48 h control biofilms, possibly due to the fact that lactobacilli-treated biofilms were not uniformly distributed on the surface (**Figure 9D**). The

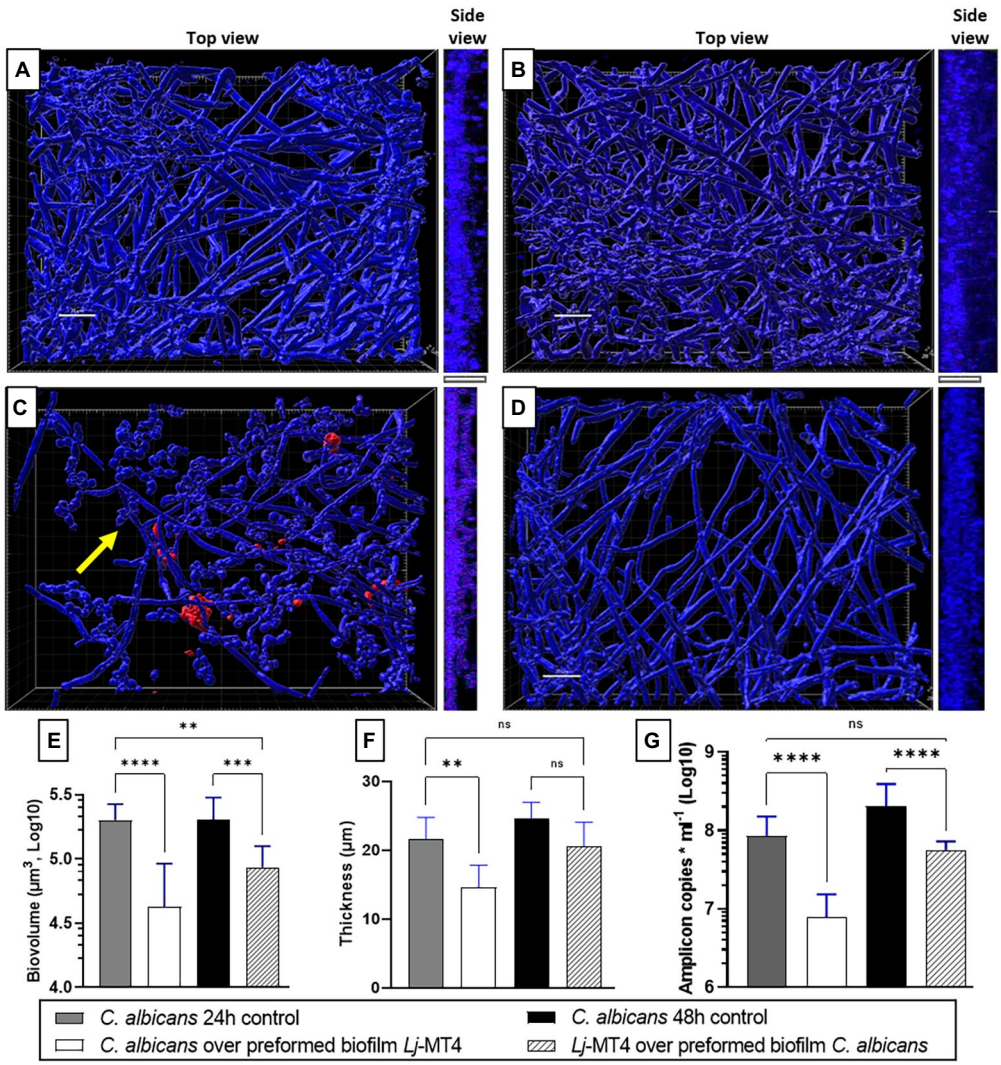

FIGURE 9 | *Lactobacillus johnsonii* displays exclusion and displacement effects against *C. albicans* biofilms. **(A)** 24 h-old and **(B)** 48 h-old single *C. albicans* biofilms; **(C)** Addition of *C. albicans* on preformed *L. johnsonii* biofilm; **(D)** Addition of *L. johnsonii* over preformed *C. albicans* biofilm; Fungal biofilm **(E)** biovolumes, **(F)** thickness, and **(G)** biomass are significantly reduced in the presence of lactobacilli. Yellow arrows indicate the presence of yeast cells. White bar = 20 nm. One-Way ANOVA, Dunnett posttest. $^{*}p \leq 0.05$, $^{**}p \leq 0.01$, $^{***}p \leq 0.005$, $^{****}p \leq 0.0001$.

ability of *L. johnsonii* to alter the fungal biofilm structure and prevent its further growth indicates an antagonistic relationship between these species.

DISCUSSION

In this work, we showed that, like other *Lactobacillus* species (Kang et al., 2018; Jang et al., 2019; Scillato et al., 2021), *L. johnsonii* displays anticandidal properties, reducing *C. albicans* growth and ability to transition into hyphae and establish biofilms on abiotic surfaces. We found that the MT4 strain shows strong dose-dependent anticandidal activity, particularly in the biofilm growth phase. The anticandidal activity of *L. johnsonii* depends on several factors such as viability, cell density, nutrient availability, production of metabolites, and partly on acidification, which are all influenced by growth conditions. Genomic analysis of this strain revealed the presence of several genes that encode metabolites with anticandidal properties, which may explain our results. These metabolites are analogous to other anticandidal compounds isolated and characterized from different bacterial species (i.e., *Bacillus subtilis* and other members of the genus *Lactobacillus*). For example, Bacillomycin D (from *B. subtilis*) is a fungicidal lipopeptide bacteriocin from the iturin group, which targets the cell membrane, creating ion-conducting pores due to the formation of lipopeptide–sterol complexes (Olfa et al., 2015). Additionally, Bacillomycin D-like peptides inhibit β-1,3-glucan synthesis, a major component of the fungal cell wall (Hajare et al., 2016). Surfactin, produced by different *Lactobacillus* species, is a cyclo-lipopeptide biosurfactant that reduces substrate adhesion of *C. albicans*, decreasing its ability to form biofilms

(Nelson et al., 2020). The major secreted protein Msp1 is a hydrolase that cleaves chitin, one of the main biopolymers in the fungal cell wall. Recently, this hydrolase was implicated in inhibiting *C. albicans* morphogenesis into hyphae (Allonsius et al., 2019) and reducing the virulence of *C. glabrata* in a mouse model (Charlet et al., 2020). It is possible that any or all of these metabolites are involved in the anticandidal activities we observed *in vitro*. In addition to these metabolites, data from other lactobacilli (Bergsson et al., 2001; Schaefer et al., 2010; Gomaa, 2013; Charlet et al., 2020) suggest that *L. johnsonii* may encode novel antimicrobial products that require further characterization.

The role of lactate/lactic acid and media acidification on *C. albicans* has been widely discussed in the literature, sometimes with opposite conclusions. Köhler et al. showed that *C. albicans* growth was reduced in lactic acid-supplemented MRS; however, when the supplemented MRS was neutralized, *Candida* resumed its expected growth, suggesting that acidification and not lactate is the leading cause of growth inhibition (Köhler et al., 2012). In contrast, Lourenço et al. showed that *C. albicans* growth is not significantly reduced in lactic acid-supplemented minimal media under acidic conditions (Lourenço et al., 2019), implying that acidification is not relevant under the tested conditions. Our results show that the impact of acidification on *C. albicans* growth inhibition depends on the culture media, as acidification played a key role on MRS broth, but not in BHI or biofilm medium, which did not acidify significantly during co-culture. Also, the D−/L-lactate ratio was different across the growth media, with D-lactate the enantiomer primarily produced in MRS and the L enantiomer in BHI and biofilm medium. *Candida albicans* metabolizes L-lactate produced by the microbiota and the host, but cannot process D-lactate produced only by the microbiota. The ability of *C. albicans* to metabolize L-lactate produced in BHI and biofilm medium and neutralize the pH may be associated with the higher pH we observed in *Candida-Lactobacillus* co-cultures in these media compared to single cultures or cocultures in MRS (Danhof et al., 2016). Beyond its impact on fungal growth, lactic acid/lactate influence fungal physiology and morphology. Exposure for 76 h or longer to lactic acid, and other weak organic acids, turns the yeast cells into a "starvation-like" state, with slow growth rates and RNA-associated metabolism (Cottier et al., 2015). Additionally, lactate reduces the biosynthesis of ergosterol and induces incorrect localization of the transporter Cdr1, reducing the efflux of fluconazole in *C. albicans* cells (Suchodolski et al., 2021), leading to improving the efficacy of azoles, in combined treatments, against *C. albicans* (Alves et al., 2017; Lourenço et al., 2019). Disruption of ergosterol synthesis may interfere with fungal susceptibility to Bacillomycin D, which forms complexes with ergosterol, causing pores on the cell membrane. On the other hand, lactate also contributes to masking *C. albicans* β-glucans (Ene et al., 2013), allowing the fungi to elude the immune system. Yet, β-glucan masking is triggered by L-lactate but not by its D isomer (Ballou et al., 2016). The enantiomer produced by lactobacilli colonizing mucosal sites *in vivo* is unknown, but our results in the serum-supplemented biofilm media suggest that the L-enantiomer may be more physiologically relevant and thus likely to play a significant role in fungal recognition by innate immune cells and the overall host-microbiota-Candida interactions.

Lactobacillus johnsonii MT4 displayed an auto-aggregation phenotype. While not all strains of *L. johnsonii* display this phenotype (Jankovic et al., 2003), aggregation is a relevant trait in several ecological niches, including within the host mucosal sites, as it promotes the interaction between microbial cells. Similarly, as suggested for other *L. johnsonii* strains (Gil et al., 2010), MT4 can co-aggregate with *C. albicans*. In the context of the oral cavity, co-aggregation is a physical interaction mechanism that positively influences colonization and biofilm formation (Kolenbrander, 2000).

We observed that preformed biofilms of lactobacilli significantly inhibited fungal biofilms and the yeast's ability to shift to hyphae. These properties of the mouse MT4 strain may explain the dominant yeast phenotype of *C. albicans* on the oral mucosa of mice receiving a sucrose-rich diet which promotes the growth of lactobacilli (Souza et al., 2020; Bertolini et al., 2021). In addition to preventing *Candida* from forming biofilms, *L. johnsonii* MT4 disrupted preformed fungal biofilms, implying that these bacteria may also curtail further growth of biofilms in colonized surfaces. Quorum sensing (QS) regulates *C. albicans* yeast-to-hyphal transition and biofilm formation (Kruppa, 2009). Diverse QS molecules (i.e., farnesol and fatty acids) can prevent yeast from shifting into hyphae (Lee et al., 2021). Lactobacilli can inhibit QS-induced biofilms in bacteria (Aman et al., 2021), but their impact on *C. albicans* QS responses requires further investigation.

In conclusion, we showed that *L. johnsonii* has an antagonistic relationship with *C. albicans* during planktonic and biofilm growth *in vitro*. Environmental variables, such as the type and amount of nutrients, influence *L. johnsonii* MT4 metabolism, and anticandidal activity. Genomic analysis revealed that beyond acidification and lactate, other soluble metabolites may be responsible for the anticandidal activity and are the focus of current and future investigations. Our findings suggest that this species displays promising probiotic properties to prevent or treat mucosal candidiasis.

DATA AVAILABILITY STATEMENT

The raw FASTQ sequencing data are available at the NCBI Sequence Read Archive under accession SRR17309641. The assembled MT4 genome sequence was submitted to the NCBI Genome database with accession JAJQJG000000000. The MT4 BioSample SAMN23838460 and other associated data listed previously are available under BioProject PRJNA787656.

AUTHOR CONTRIBUTIONS

RV-M: experimental work, analysis, and writing. AT: resources and experimental work. JR: genomic analysis and repositories deposition. TS: resources. YZ: supervision and genomic analysis. AD-B: project administration, funding acquisition, supervision, and writing. All authors contributed to the article and approved the submitted version.

FUNDING

This study was funded by NIH/NIDCR grant RO1 DE013986 and NIH/NIGMS grant RO1 GM127909.

ACKNOWLEDGMENTS

The authors acknowledge the Center for Genome Innovation, Institute for Systems Genomics, University of Connecticut, for the whole genome sequencing of the *L. johnsonii* MT4 strain and CCAM Microscopy Facility, University of Connecticut Health Center, for the access to their quantitative fluorescence imaging applications.

SUPPLEMENTARY MATERIAL

The Supplementary Material for this article can be found online at: https://www.frontiersin.org/articles/10.3389/fmicb.2022.853762/full#supplementary-material

REFERENCES

Allonsius, C. N., Vandenheuvel, D., Oerlemans, E. F. M., Petrova, M. I., Donders, G. G. G., Cos, P., et al. (2019). Inhibition of Candida albicans morphogenesis by chitinase from lactobacillus rhamnosus GG. *Sci. Rep.* 9:2900. doi: 10.1038/s41598-019-39625-0

Altschul, S. F., Gish, W., Miller, W., Myers, E. W., and Lipman, D. J. (1990). Basic local alignment search tool. *J. Mol. Biol.* 215, 403–410. doi: 10.1016/S0022-2836(05)80360-2

Alves, R., Mota, S., Silva, S., Rodrigues, C. F., Brown, A. J. P., Henriques, M., et al. (2017). The carboxylic acid transporters Jen1 and Jen2 affect the architecture and fluconazole susceptibility of *Candida albicans* biofilm in the presence of lactate. *Biofouling* 33, 943–954. doi: 10.1080/08927014.2017.1392514

Aman, M., Aneeqha, N., Bristi, K., Deeksha, J., Afza, N., Sindhuja, V., et al. (2021). Lactic acid bacteria inhibits quorum sensing and biofilm formation of Pseudomonas aeruginosa strain JUPG01 isolated from rancid butter. *C. Agric. Biotechnol.* 36:102115. doi: 10.1016/J.BCAB.2021.102115

Assefa, S., Ahles, K., Bigelow, S., Curtis, J. T., and Köhler, G. A. (2015). Lactobacilli with probiotic potential in the prairie vole (Microtus ochrogaster). *Gut Pathog.* 7:35. doi: 10.1186/s13099-015-0082-0

Ballou, E. R., Avelar, G. M., Childers, D. S., Mackie, J., Bain, J. M., Wagener, J., et al. (2016). Lactate signalling regulates fungal β-glucan masking and immune evasion. *Nat. Microbiol.* 2:16238. doi: 10.1038/NMICROBIOL.2016.238

Bankevich, A., Nurk, S., Antipov, D., Gurevich, A. A., Dvorkin, M., Kulikov, A. S., et al. (2012). SPAdes: A new genome assembly algorithm and its applications to single-cell sequencing. *J. Comput. Biol.* 19, 455–477. doi: 10.1089/CMB.2012.0021

Bergsson, G., Arnfinnsson, J., Steingrímsson, Ó., and Thormar, H. (2001). In vitro killing of Candida albicans by fatty acids and monoglycerides. *Antimicrob. Agents Chemother.* 45, 3209–3212. doi: 10.1128/AAC.45.11.3209-3212.2001

Bertolini, M., Vazquez Munoz, R., Archambault, L., Shah, S., Souza, J. G. S., Costa, R. C., et al. (2021). Mucosal bacteria modulate *Candida albicans* virulence in Oropharyngeal candidiasis. *mBio* 12:e0193721. doi: 10.1128/mBio.01937-21

Castresana, J. (2000). Selection of conserved blocks from multiple alignments for their use in phylogenetic analysis. *Mol. Biol. Evol.* 17, 540–552. doi: 10.1093/oxfordjournals.molbev.a026334

Centers for Disease Control and Prevention (2019). Antibiotic Resistance Threats in the United States, 2019. Atlanta, GA. Available at: www.cdc.gov/DrugResistance/Biggest-Threats.html (Accessed January 24, 2020).

Chandra, J., Kuhn, D. M., Mukherjee, P. K., Hoyer, L. L., McCormick, T., and Ghannoum, M. A. (2001). Biofilm formation by the fungal pathogen Candida albicans: development, architecture, and drug resistance. *J. Bacteriol.* 183, 5385–5394. doi: 10.1128/JB.183.18.5385-5394.2001/ASSET/7682BA16-1CB1-4757-B4AC-81291C643CA8/ASSETS/GRAPHIC/JB1810569007.JPEG

Charlet, R., Bortolus, C., Sendid, B., and Jawhara, S. (2020). Bacteroides thetaiotaomicron and lactobacillus johnsonii modulate intestinal inflammation and eliminate fungi via enzymatic hydrolysis of the fungal cell wall. *Sci. Rep.* 10:11510. doi: 10.1038/s41598-020-68214-9

Cottier, F., Tan, A. S. M., Chen, J., Lum, J., Zolezzi, F., Poidinger, M., et al. (2015). The transcriptional stress response of Candida albicans to weak organic acids. *G3* 5, 497–505. doi: 10.1534/G3.114.015941

Cruchet, S., Obregon, M. C., Salazar, G., Diaz, E., and Gotteland, M. (2003). Effect of the ingestion of a dietary product containing lactobacillus johnsonii La1 on helicobacter pylori colonization in children. *Nutrition* 19, 716–721. doi: 10.1016/S0899-9007(03)00109-6

Danhof, H. A., Vylkova, S., Vesely, E. M., Ford, A. E., Gonzalez-Garay, M., and Lorenz, M. C. (2016). Robust extracellular pH modulation by Candida albicans during growth in carboxylic acids. *mbio* 7, e01646–e01616. doi: 10.1128/MBIO.01646-16

Dongari-Bagtzoglou, A., Kashleva, H., Dwivedi, P., Diaz, P., and Vasilakos, J. (2009). Characterization of mucosal *Candida albicans* biofilms. *PLoS One* 4:e7967. doi: 10.1371/journal.pone.0007967

Ene, I. V., Cheng, S. C., Netea, M. G., and Brown, A. J. P. (2013). Growth of Candida albicans cells on the physiologically relevant carbon source lactate affects their recognition and phagocytosis by immune cells. *Infect. Immun.* 81, 238–248. doi: 10.1128/IAI.01092-12

Eryilmaz, M., Gurpinar, S. S., Palabiyik, I. M., Guriz, H., and Gerceker, D. (2019). Molecular identification and antimicrobial activity of vaginal lactobacillus sp. *Curr. Pharm. Biotechnol.* 19, 1241–1247. doi: 10.2174/1389201020666190110164123

Felsenstein, J. (1993). PHYLIP (Phylogeny Inference Package) version 3.57c. Available at: http://www.dbbm.fiocruz.br/molbiol/main.html (Accessed December 23, 2021).

Fujisawa, T., Benno, Y., Yaeshima, T., and Mitsuoka, T. (1992). Taxonomic study of the *Lactobacillus acidophilus* group, with recognition of *Lactobacillus gallinarum* sp. nov. and *Lactobacillus johnsonii* sp. nov. and synonymy of *Lactobacillus acidophilus* group A3 (Johnson et al. 1980) with the type strain of *Lactobacillus amylovorus* (Nakamura 1981). *Int. J. Syst. Bacteriol.* 42, 487–491. doi: 10.1099/00207713-42-3-487

Gascuel, O. (1997). BIONJ: an improved version of the NJ algorithm based on a simple model of sequence data. *Mol. Biol. Evol.* 14, 685–695. doi: 10.1093/oxfordjournals.molbev.a025808

Gil, N. F., Martinez, R. C. R., Gomes, B. C., Nomizo, A., and de Martinis, E. C. P. (2010). Vaginal lactobacilli as potential probiotics against *Candida* spp. *Brazilian J. Microbiol.* 41, 6–14. doi: 10.1590/S1517-83822010000100002

Gomaa, E. Z. (2013). Antimicrobial and anti-adhesive properties of biosurfactant produced by lactobacilli isolates, biofilm formation and aggregation ability. *J. Gen. Appl. Microbiol.* 59, 425–436. doi: 10.2323/jgam.59.425

Gouy, M., Guindon, S., and Gascuel, O. (2010). SeaView version 4: A multiplatform graphical user Interface for sequence alignment and phylogenetic tree building. *Mol. Biol. Evol.* 27, 221–224. doi: 10.1093/molbev/msp259

Guindon, S., Dufayard, J.-F., Lefort, V., Anisimova, M., Hordijk, W., and Gascuel, O. (2010). New algorithms and methods to estimate maximum-likelihood phylogenies: assessing the performance of PhyML 3.0. *Syst. Biol.* 59, 307–321. doi: 10.1093/sysbio/syq010

Hajare, S. N., Gautam, S., and Sharma, A. (2016). A novel strain of *Bacillus amyloliquefaciens* displaying broad spectrum antifungal activity and its underlying mechanism. *Ann. Microbiol.* 66, 407–416. doi: 10.1007/s13213-015-1123-0

Jang, S. J., Lee, K., Kwon, B., You, H. J., and Ko, G. P. (2019). Vaginal lactobacilli inhibit growth and hyphae formation of Candida albicans. *Sci. Rep.* 9, 8121–8129. doi: 10.1038/s41598-019-44579-4

Jankovic, I., Ventura, M., Meylan, V., Rouvet, M., Elli, M., and Zink, R. (2003). Contribution of aggregation-promoting factor to maintenance of cell shape in *Lactobacillus gasseri* 4B2. *J. Bacteriol.* 185, 3288–3296. doi: 10.1128/JB.185.11.3288-3296.2003

Jung, M. Y. (2018). Complete genome sequence of Lactobacillus sp. CBA3606. EMBL/GenBank/DDBJ. Available at: https://www.uniprot.org/uniprot/A0A2R3JZ49 [Accessed December 24 2021].

Kang, C., Kim, Y. G., Han, S. H., Kim, J. S., Paek, N. S., and So, J. S. (2018). In vitro probiotic properties of vaginal Lactobacillus fermentum MG901 and Lactobacillus plantarum MG989 against Candida albicans. *Eur. J. Obstet. Gynecol. Reprod. Biol.* 228, 232–237. doi: 10.1016/j.ejogrb.2018.07.005

Khot, P. D., Ko, D. L., and Fredricks, D. N. (2009). Sequencing and analysis of fungal rRNA operons for development of broad-range fungal PCR assays. *Appl. Environ. Microbiol.* 75, 1559–1565. doi: 10.1128/AEM.02383-08

Köhler, G. A., Assefa, S., and Reid, G. (2012). Probiotic interference of *Lactobacillus rhamnosus* GR-1 and *Lactobacillus reuteri* RC-14 with the opportunistic fungal pathogen *Candida albicans*. *Infect. Dis. Obstet. Gynecol.* 2012, 1–14. doi: 10.1155/2012/636474

Kolenbrander, P. E. (2000). Oral microbial communities: biofilms, interactions, and genetic systems. *Annu. Rev. Microbiol.* 54, 413–437. doi: 10.1146/annurev.micro.54.1.413

Kruppa, M. (2009). Quorum sensing and Candida albicans. *Mycoses* 52, 1–10. doi: 10.1111/J.1439-0507.2008.01626.X

Lee, J. H., Kim, Y. G., Khadke, S. K., and Lee, J. (2021). Antibiofilm and antifungal activities of medium-chain fatty acids against *Candida albicans* via mimicking of the quorum-sensing molecule farnesol. *Microb. Biotechnol.* 14, 1353–1366. doi: 10.1111/1751-7915.13710

Lefort, V., Longueville, J. E., and Gascuel, O. (2017). SMS: smart model selection in PhyML. *Mol. Biol. Evol.* 34, 2422–2424. doi: 10.1093/MOLBEV/MSX149

Lourenço, A., Pedro, N. A., Salazar, S. B., and Mira, N. P. (2019). Effect of acetic acid and lactic acid at low pH in growth and azole resistance of *Candida albicans* and *Candida glabrata*. *Front. Microbiol.* 9:3265. doi: 10.3389/fmicb.2018.03265

Löytynoja, A. (2014). "Phylogeny-aware alignment with PRANK," in *Multiple Sequence Alignment Methods. Methods in Molecular Biology (Methods and Protocols). Vol. 1079.* ed. D. Russell (Totowa, NJ: Humana Press), 155–170.

Marcial, G. E., Ford, A. L., Haller, M. J., Gezan, S. A., Harrison, N. A., Cai, D., et al. (2017). *Lactobacillus johnsonii* N6.2 modulates the host immune responses: A double-blind, randomized trial in healthy adults. *Front. Immunol.* 8:655. doi: 10.3389/FIMMU.2017.00655

Mundula, T., Ricci, F., Barbetta, B., Baccini, M., and Amedei, A. (2019). Effect of probiotics on oral candidiasis: a systematic review and meta-analysis. *Nutrients* 11:2449. doi: 10.3390/nu11102449

Nelson, J., El-Gendy, A. O., Mansy, M. S., Ramadan, M. A., and Aziz, R. K. (2020). The biosurfactants iturin, lichenysin and surfactin, from vaginally isolated lactobacilli, prevent biofilm formation by pathogenic *Candida*. *FEMS Microbiol. Lett.* 367:126. doi: 10.1093/FEMSLE/FNAA126

O'Flaherty, S., Foley, M. H., Rivera, A. J., Theriot, C. M., and Barrangou, R. (2020). Complete genome sequence of *Lactobacillus johnsonii* NCK2677, isolated from mice. *Microbiol. Resour. Announc.* 9, e00918–e00920. doi: 10.1128/MRA.00918-20

Olfa, T., Antonio, D. G., Sana, A., Imen, B. S., Salem, E., Mohamed Najib, A., et al. (2015). Synergistic fungicidal activity of the lipopeptide bacillomycin D with amphotericin B against pathogenic *Candida* species. *FEMS Yeast Res.* 15:fov022. doi: 10.1093/femsyr/fov022

Page, A. J., Cummins, C. A., Hunt, M., Wong, V. K., Reuter, S., Holden, M. T. G., et al. (2015). Roary: rapid large-scale prokaryote pan genome analysis. *Bioinformatics* 31, 3691–3693. doi: 10.1093/BIOINFORMATICS/BTV421

Pappas, P. G., Lionakis, M. S., Arendrup, M. C., Ostrosky-Zeichner, L., and Kullberg, B. J. (2018). Invasive candidiasis. *Nat. Rev. Dis. Prim.* 4, 1–20. doi: 10.1038/nrdp.2018.26

Pendleton, K. M., Dickson, R. P., Newton, D. W., Hoffman, T. C., Yanik, G. A., and Huffnagle, G. B. (2018). Respiratory tract colonization by Candida species portends worse outcomes in Immunocompromised patients. *Clin. Pulm. Med.* 25, 197–201. doi: 10.1097/CPM.0000000000000279

Pfaller, M. A., and Diekema, D. J. (2010). Epidemiology of invasive mycoses in North America. *Crit. Rev. Microbiol.* 36, 1–53. doi: 10.3109/10408410903241444

Pfaller, M. A., Diekema, D. J., Turnidge, J. D., Castanheira, M., and Jones, R. N. (2019). Twenty years of the SENTRY antifungal surveillance program: results for *Candida* species from 1997-2016. *Open Forum Infect. Dis.* 6, S79–S94. doi: 10.1093/ofid/ofy358

Pierce, C. G., Uppuluri, P., Tristan, A. R., Wormley, F. L., Mowat, E., Ramage, G., et al. (2008). A simple and reproducible 96-well plate-based method for the formation of fungal biofilms and its application to antifungal susceptibility testing. *Nat. Protoc.* 3, 1494–1500. doi: 10.1038/nprot.2008.141

Poupet, C., Saraoui, T., Veisseire, P., Bonnet, M., Dausset, C., Gachinat, M., et al. (2019). *Lactobacillus rhamnosus* Lcr35 as an effective treatment for preventing *Candida albicans* infection in the invertebrate model *Caenorhabditis elegans*: first mechanistic insights. *PLoS One* 14:e0216184. doi: 10.1371/journal.pone.0216184

Schaefer, L., Auchtung, T. A., Hermans, K. E., Whitehead, D., Borhan, B., and Britton, R. A. (2010). The antimicrobial compound reuterin (3-hydroxypropionaldehyde) induces oxidative stress via interaction with thiol groups. *Microbiology* 156, 1589–1599. doi: 10.1099/mic.0.035642-0

Scillato, M., Spitale, A., Mongelli, G., Privitera, G. F., Mangano, K., Cianci, A., et al. (2021). Antimicrobial properties of *Lactobacillus* cell-free supernatants against multidrug-resistant urogenital pathogens. *Microbiology* 10:e1173. doi: 10.1002/mbo3.1173

Seemann, T. (2014). Prokka: rapid prokaryotic genome annotation. *Bioinformatics* 30, 2068–2069. doi: 10.1093/BIOINFORMATICS/BTU153

Souza, J. G. S., Bertolini, M., Thompson, A., Mansfield, J. M., Grassmann, A. A., Maas, K., et al. (2020). Role of glucosyltransferase R in biofilm interactions between *Streptococcus oralis* and *Candida albicans*. *ISME J.* 14, 1207–1222. doi: 10.1038/s41396-020-0608-4

Strus, M., Kucharska, A., Kukla, G., Brzychczy-Włoch, M., Maresz, K., and Heczko, P. B. (2005). The in vitro activity of vaginal *Lactobacillus* with probiotic properties against *Candida*. *Infect. Dis. Obstet. Gynecol.* 13, 69–75. doi: 10.1080/10647440400028136

Suchodolski, J., Muraszko, J., Bernat, P., and Krasowska, A. (2021). Lactate like fluconazole reduces ergosterol content in the plasma membrane and synergistically kills *Candida albicans*. *Int. J. Mol. Sci.* 22:5219. doi: 10.3390/IJMS22105219

Vazquez-Munoz, R., Arellano-Jimenez, M. J., and Lopez-Ribot, J. L. (2020). Bismuth nanoparticles obtained by a facile synthesis method exhibit antimicrobial activity against Staphylococcus aureus and Candida albicans. *BMC Biomed. Eng.* 2:11. doi: 10.1186/s42490-020-00044-2

Vazquez-Munoz, R., and Dongari-Bagtzoglou, A. (2021). Anticandidal activities by lactobacillus species: An update on mechanisms of action. *Front. Oral Heal.* 2:689382. doi: 10.3389/froh.2021.689382

Wagner, R. D., Pierson, C., Warner, T., Dohnalek, M., Hilty, M., and Balish, E. (2000). Probiotic effects of feeding heat-killed lactobacillus acidophilus and lactobacillus casei to Candida albicans-colonized immunodeficient mice. *J. Food Prot.* 63, 638–644. doi: 10.4315/0362-028x-63.5.638

Wood, D. E., Lu, J., and Langmead, B. (2019). Improved metagenomic analysis with Kraken 2. *Genome Biol.* 20:257. doi: 10.1186/S13059-019-1891-0

Wu, C. C., Lin, C. T., Wu, C. Y., Peng, W. S., Lee, M. J., and Tsai, Y. C. (2015). Inhibitory effect of lactobacillus salivarius on *Streptococcus mutans* biofilm formation. *Mol Oral Microbiol* 30, 16–26. doi: 10.1111/OMI.12063

Yamano, T., Tanida, M., Niijima, A., Maeda, K., Okumura, N., Fukushima, Y., et al. (2006). Effects of the probiotic strain lactobacillus johnsonii strain La1 on autonomic nerves and blood glucose in rats. *Life Sci.* 79, 1963–1967. doi: 10.1016/J.LFS.2006.06.038

Zheng, J., Wittouck, S., Salvetti, E., Franz, C. M. A. P., Harris, H. M. B., Mattarelli, P., et al. (2020). A taxonomic note on the genus lactobacillus: description of 23 novel genera, emended description of the genus lactobacillus beijerinck 1901, and union of Lactobacillaceae and Leuconostocaceae. *Int. J. Syst. Evol. Microbiol.* 70, 2782–2858. doi: 10.1099/ijsem.0.004107

Conflict of Interest: The authors declare that the research was conducted in the absence of any commercial or financial relationships that could be construed as a potential conflict of interest.

Publisher's Note: All claims expressed in this article are solely those of the authors and do not necessarily represent those of their affiliated organizations, or those of the publisher, the editors and the reviewers. Any product that may be evaluated in this article, or claim that may be made by its manufacturer, is not guaranteed or endorsed by the publisher.

frontiers | Frontiers in Public Health

ORIGINAL RESEARCH
published: 22 July 2022
doi: 10.3389/fpubh.2022.926641

The Temporal Lagged Relationship Between Meteorological Factors and Scrub Typhus With the Distributed Lag Non-linear Model in Rural Southwest China

Hongxiu Liao[1,2†], Jinliang Hu[1,3†], Xuzheng Shan[1†], Fan Yang[1], Wen Wei[1], Suqin Wang[2], Bing Guo[1] and Yajia Lan[1]*

[1] West China School of Public Health and West China Fourth Hospital, Sichuan University, Chengdu, China, [2] Panzhihua City Center for Disease Control and Prevention, Panzhihua, China, [3] Institute of Health Policy & Hospital Management, Sichuan Academy of Medical Sciences & Sichuan Provincial People's Hospital, Chinese Academy of Sciences Sichuan Translational Medicine Research Hospital, Chengdu, China

OPEN ACCESS

Edited by:
Chao-Yu Guo, National Yang Ming Chiao Tung University, Taiwan

Reviewed by:
Heydar Maleki, Ahvaz Jundishapur University of Medical Sciences, Iran
Manoranjan Ranjit, Regional Medical Research Center (ICMR), India

***Correspondence:**
Yajia Lan
lanyajia2019@163.com

[†] These authors have contributed equally to this work

Specialty section:
This article was submitted to Infectious Diseases – Surveillance, Prevention and Treatment, a section of the journal Frontiers in Public Health

Received: *22 April 2022*
Accepted: *21 June 2022*
Published: *22 July 2022*

Citation:
Liao H, Hu J, Shan X, Yang F, Wei W, Wang S, Guo B and Lan Y (2022) The Temporal Lagged Relationship Between Meteorological Factors and Scrub Typhus With the Distributed Lag Non-linear Model in Rural Southwest China. Front. Public Health 10:926641. doi: 10.3389/fpubh.2022.926641

Background: Meteorological factors can affect the emergence of scrub typhus for a period lasting days to weeks after their occurrence. Furthermore, the relationship between meteorological factors and scrub typhus is complicated because of lagged and non-linear patterns. Investigating the lagged correlation patterns between meteorological variables and scrub typhus may promote an understanding of this association and be beneficial for preventing disease outbreaks.

Methods: We extracted data on scrub typhus cases in rural areas of Panzhihua in Southwest China every week from 2008 to 2017 from the China Information System for Disease Control and Prevention. The distributed lag non-linear model (DLNM) was used to study the temporal lagged correlation between weekly meteorological factors and weekly scrub typhus.

Results: There were obvious lagged associations between some weather factors (rainfall, relative humidity, and air temperature) and scrub typhus with the same overall effect trend, an inverse-U shape; moreover, different meteorological factors had different significant delayed contributions compared with reference values in many cases. In addition, at the same lag time, the relative risk increased with the increase of exposure level for all weather variables when presenting a positive association.

Conclusions: The results found that different meteorological factors have different patterns and magnitudes for the lagged correlation between weather factors and scrub typhus. The lag shape and association for meteorological information is applicable for developing an early warning system for scrub typhus.

Keywords: meteorological factors, scrub typhus, distributed lag non-linear model, early warning, rural areas

INTRODUCTION

Scrub typhus, also known as tsutsugamushi disease, is an acute febrile illness caused by infection with *Orientia (O.) tsutsugamushi* (1). Scrub typhus is a well-known serious public health problem in the Asia-Pacific area that threatens approximately one billion people; moreover, one million people may develop illness from scrub typhus each year globally (2). During the last two decades, scrub typhus has been increasingly reported and has become a significant health concern in eastern Asian countries (3, 4).

Transmission depends on the seasonal activities of both chiggers and humans (5). First, chiggers are most abundant during rainy seasons whereas very few are found during the dry winter months (5). Second, outdoor workers, particularly field workers in rural areas, have a higher risk of acquiring the disease (5, 6). People working in farms and forestry where the chigger-infected rodent cycle occurs have a prolonged duration of exposure and are in danger of infestation with infected mites (3, 7). In China, farmers represent the most commonly infected occupation, accounting for 72.58% of all cases (3).

To date, many studies have evaluated the association between meteorological factors and vector-borne diseases around the world (7, 8) These findings have mainly provided evidence of the association between climate change and diseases. Gage et al. (9) reported that temperature, precipitation, humidity, and other climatic factors were known to affect the reproduction, development, behavior, and population dynamics of the arthropod vectors of these diseases.

Vector mite species can cause different seasonal patterns of scrub typhus as a result of different species and genotypes (2), For example, there are two seasonal peaks of the diseases in China: the summer type and the autumn-early winter type (3), which are primarily caused by the larvae of the chigger mites *Leptotrombidium deliense* and *L. scutellare*, respectively. In Southwest China, the summer seasonal peak is the most common type. Some findings have shown that the seasonality of the disease in these regions is related to the lifecycle of *L. delicense*, which is a predominant vector of Karp-type scrub typhus (8).

The effects of meteorological factors are observed to have two main aspects: lag and non-linear characteristics (10). However, research quantitatively exploring the lag association between weather variables and scrub typhus is sparse (11). Existing studies have validated the non-linear correlation between weather factors (for example, temperature and rainfall) and scrub typhus (12, 13). However, in Southwest China, until now, there has been no report on lag structures and association patterns between weather variation and scrub typhus. The study area in our investigation includes a mountain area, complex terrain, and existing distinguishable dry and rainy seasons. In fact, scrub typhus is hyperendemic in the Panzhihua District, which is located in Southwest China, indicating that its incidence is higher, specifically ∼10 times higher than the average incidence in Sichuan Province overall (3); moreover, the highest incidence occurs in the countryside. Furthermore, the lag structures and association patterns between weekly meteorological variation and scrub typhus require further investigation, particularly in the countryside.

The objective of our work was to explore the lag structures and association patterns between meteorological variables and scrub typhus in rural areas of Panzhihua district, Southwest China. The distributed lag non-linear model (DLNM) was used to study the temporal lagged associations between weekly meteorological factors and weekly scrub typhus cases using data from 2008 to 2017.

METHODS

Study Area

Panzhihua is 7,401 square kilometers in size and is situated at north latitude 26°05'N to 27°21'N and east longitude 101°08'E to 102°15'E. Panzhihua had a registered population of over 1.105 million individuals at the end of 2016 according to the 2017 Sichuan statistical yearbook, including 0.5235 million people comprising the agricultural population. Panzhihua is located at the junction of Sichuan and Yunnan provinces in Southwest China and is the first city in the upper reaches of the Yangtze River, where the Jinsha and Yalong rivers meet. The district is comprised of complex and diverse landform types, 6 of which (flat dam, platform, high hills, low-middle mountains, middle mountains, and mountain plains) account for 88.38% of the total area. The climate is characterized as a stereoscopic climate with a baseband in the south subtropical zone; the most prominent characteristic is the distinction between the dry and rainy seasons. Summers are rainy with high temperatures and a relatively high humidity index. Winters are dry and sunny with a higher temperature compared with other areas, which can also be indicated from the annual mean temperature ranging from 18 to 25°C. There are 5 counties in Panzhihua (**Figure 1**).

Data Collection

Surveillance Data of the Disease

We extracted the computerized dataset on notified scrub typhus cases in rural areas of Panzhihua from the period of January 1, 2008 to December 31, 2017 from the China Information System for Disease Control and Prevention. In China, all scrub typhus cases are diagnosed in terms of the uniform diagnostic criteria described by the Chinese Ministry of Health. Scrub typhus is diagnosed when a sick person displays at least three of the following criteria: a history (traveling to an endemic area and contact with chigger mites within 3 weeks before the onset of illness); sudden-onset high fever at the presence of characteristic eschar or ulcer; skin rash and lymphadenopathy; an agglutination titer >1:160 according to the Weil–Felix test (WF) using the OXK strain of *Proteus mirabilis*; and a 4-fold or larger increase in titres against *O. tsutsugamushi* in the indirect immunofluorescence antibody assay (IFA) (14). Scrub typhus has been a notifiable disease in Sichuan since 2006, similar to other provinces in China (13, 15). Since the notifiable network covers all hospitals and community health centers in Panzhihua, routine case reporting is performed by hospitals or community health centers through the National Notifiable Disease Report System (NNDRS) within 24 h. The notification system records detailed information of each case

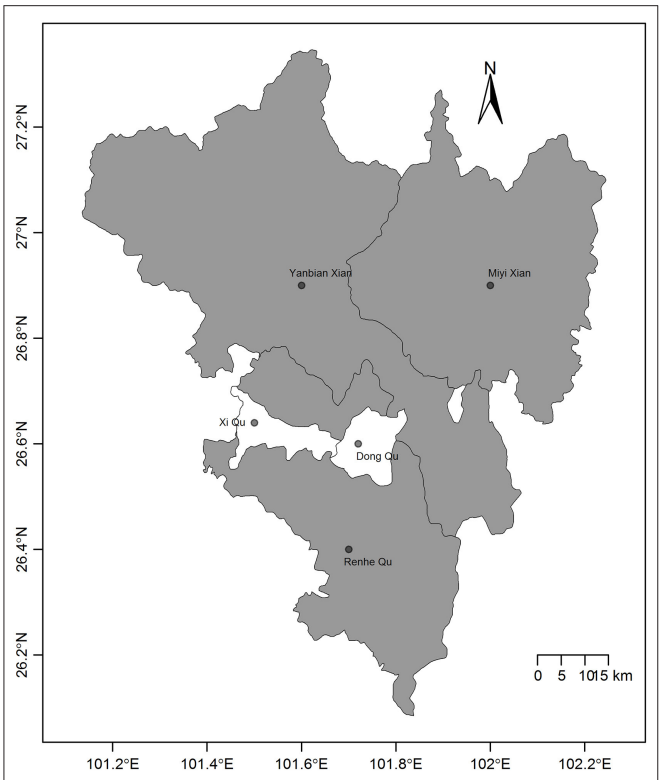

FIGURE 1 | Map of the 5 counties in Panzhihua, Southwest China. The gray counties have a high incidence of scrub typhus and are rural areas whereas the white counties have a low incidence of scrub typhus and are urban areas.

including birth day, gender, address, the onset date, diagnosis date, notification date, etc. The onset date of scrub typhus (15), which is more useful for epidemiological studies than the dates of diagnosis or notification dates, was used in our study. Basic population data for Panzhihua from 2008 to 2017 were obtained from Sichuan Statistical Yearbooks.

Meteorological Data

Meteorological data were obtained from the publicly available Chinese Meteorological Data Sharing Service System (CMDSSS) (16). Eight meteorological data variables were extracted from the CMDSSS during January 2008 to December 2017 for analysis: rainfall, sunshine, mean relative humidity, mean air temperature, mean land surface temperature, mean wind velocity, mean evaporation, and mean air pressure.

Statistical Analysis

After obtaining a descriptive summary of each variable, Spearman's correlation analyses were performed to determine the correlations between meteorological variables. Then, the main study used DLNM (17) to describe the lag non-linear effects between meteorological factors and scrub typhus assuming that the incidence obeyed the Poisson distribution with overdispersion. Furthermore, because weekly scrub typhus cases are commonly sporadic, generalized additive models was used following a quasi-Poisson family (18).

First, the model was constructed for scrub typhus cases according to the basic idea of DLNM. After reviewing a significant amount of relevant research, exploring the cross-basis function was considered for meteorological variables including rainfall, sunshine, relative humidity, air temperature and land surface temperature, which were deemed to have a close relationship with the incidence of scrub typhus (4, 13), to describe effects that vary simultaneously both along the space of these weather variables and in the lag dimension of their occurrence. A natural cubic spline (ns) function was used for the non-linear effect and the lag effect of selected meteorological variables (11, 19, 20). The degrees of freedom (df) (knots) and lag were chosen by the Akaike Information Criterion for quasi-Poisson models (QAIC) (17). When the df of both were 3, the smallest QAIC would be acquired with the following settings completely determined. At this time, the maximum lag for rainfall was set as 14 weeks whereas the maximum lags for the other selected variables were set as 16 weeks. The definition of maximum lags was comprehensively considered according to those characteristics (e.g., times associated with the lifestyle of mites and the incubation period of the disease) and by consulting existing findings (11); however, this study was unique in using weeks as the unit of analysis for time rather than months when DLNM was applied to investigate the effects of weather factors on scrub typhus.

Second, the rest of the collected meteorological variables including mean wind velocity, mean evaporation, and mean air pressure may influence the selected five weather variables above and the incidence of scrub typhus; thus, they were more or less regarded as confounders and were investigated with a flexible modeling tool, using ns functions with an empirical 3 df (18) Consideration was mainly based on the direct interaction of meteorological variables, which was shown via correlation coefficients.

In addition, we did not simply and directly use year or month as variables controlling the variations of the long-term patterns and seasonality of the incidence of scrub typhus in the model. Because our aim was to explore whether short-term variation in scrub typhus cases was explained by exposure to weather factors, the long-term patterns including seasonality were controlled using an ns function with 3 df per year (21). Using week as a time analysis unit provided the advantage of reducing variation caused by the day of the week. After all the settings were determined, the smallest QAIC was 1424.573.

We included all meteorological variables and other potential factors including long-term and seasonal trends in the final model:

$$Y_t \sim quasipoisson(\mu_t, \varnothing\mu_t)$$

$$E\left(y_t\right) = \mu_t Var\left(y_t\right) = \varnothing\mu_t$$

$$\log\left(\mu_t\right) = \alpha + cb\left(P_{t,l}\right) + cb\left(G_{t,l}\right) + cb\left(T_{t,l}\right) + cb\left(R_{t,l}\right) + cb\left(S_{t,l}\right)$$

$$+ns\left(time, 3^{*}year\right) + ns\left(W_t, 3\right) + ns\left(E_t, 3\right) + ns(F_t, 3)$$

Y_t represents the weekly number of scrub typhus cases during week t; μ_t represents the expected number of weekly scrub typhus cases; $\varnothing$ is the dispersion parameter; and α is the intercept. *cb*() is a cross-basis function representing a bi-dimensional exposure-lag-response function for fitting the non-linear and lag effects of relevant weather factors, and $P_{t,l}$, $G_{t,l}$, $T_{t,l}$, $R_{t,l}$ *and* $S_{t,l}$ in brackets represent weekly aggregate rainfall(RF), weekly mean land surface temperature(LST), weekly mean air temperature(AT), weekly mean relative humidity(RH), and weekly aggregate sunshine(SS), respectively. *ns*() represents ns function; time represents 1–522 weeks; W_t, E_t *and* F_t represent weekly mean wind velocity(WV), weekly mean evaporation(ER), and weekly mean air pressure(AP), respectively.

The reference values were also defined for each weather variable before analyzing and estimating the relative risks (RR) which were calculated as well as the 95% confidence intervals for each weather variable when their exposure levels were 50, 60, 70, 75, 80, and 90% compared to the reference values. The reference value of weekly aggregate RF was 0 mm, and the 25th percentiles of the other weather variables were set as the reference values for weekly mean relative RH, weekly mean LST, weekly mean AT and weekly aggregate SS, which corresponded to 40.29%, 19.13°C, 16.90°C and 43.7 h, respectively. The effects of each meteorological factor on the incidence of scrub typhus were analyzed after different exposure levels.

All the implementations above were accomplished with R-3.5.0 using the dlnm (22) and mgcv packages.

RESULTS

Characteristics of Scrub Typhus Cases

During the period of 2008–2017, 1,758 scrub typhus cases were reported in Panzhihua, among which 1,731 cases occurred in the countryside. The annual average incidence in rural areas was 25.77 per 100,000, ranging from 12.38 to 35.02 per 100,000. The highest incidence occurred from 23th to 44th weeks of each year and accounted for 94.74% of the entire year; a single epidemic peak occurred in the summer each year. Of the rural cases, 48.53% (840/1,731) occurred in males and 51.47% (891/1,731) occurred in females, corresponding to a male-to-female ratio of 0.94:1. The largest proportion of patients were in the 18–59-year-old age group (the young and middle-aged population), which accounted for 56.7% (981/1,731) of rural cases. According to occupation, 68.11% (1,179/1,731) of cases occurred in farmers, whereas elementary and nursery children and students accounted for 14.67% (254/1,731) and 12.02% (208/1,731) of cases, respectively.

Characteristics of Meteorological Factors

The weekly aggregate RF ranged from 0 to 223.50 mm, with a median of 1.45 mm. The weekly aggregate SS ranged from 7 to 85.20 h, with a median of 55.8 h. The weekly minimum and maximum mean LSTs were 9.83 and 40.19°C, respectively, with an average of 24.54°C. The weekly minimum and maximum ATs were 8.41 and 33.06°C, respectively, with an average of 21.18°C. The weekly mean relative RH ranged from 17.43 to 85.29%, with an average of 54.64%. The weekly mean WV ranged from 0.54 to 3.11 m/s, with an average of 1.48 m/s. The weekly mean ER ranged from 7 to 106.57 mm, with an average of 39.58 mm. The weekly mean air pressure (AP) ranged from 865.94 to 887.26 hPa, with an average of 875.90 hPa. **Figure 2**, **Table 1** show the weekly time series for the number of cases and meteorological information during the investigation period. We can conclude from **Figure 2** that before the number of scrub typhus cases increased significantly, rainfall, relative humidity, land surface temperature and air temperature displayed obvious fluctuations, and some time after they reached their peak, the number of scrub typhus cases peaked.

As shown in **Table 2**, the weekly rainfall was positively correlated with relative humidity, land surface temperature and air temperature ($P < 0.001$) and was negatively correlated with sunshine and air pressure ($P < 0.001$). The weekly relative humidity was negatively correlated with sunshine, wind velocity and evaporation ($P < 0.001$).

Relationship Between Meteorological Factors and Scrub Typhus Cases

Figure 3 shows the lag-response curves for how different weather variables affect the incidence of scrub typhus at different exposure levels (50, 60, 70, 80, and 90%) according to the model. There were obvious lagged associations between some weather factors (rainfall, relative humidity, and air temperature) and scrub typhus with the same overall trend, an inverse-U shape. The lag effect of land surface temperature on scrub typhus decreased in the beginning; however, after a few weeks, the relationship became significantly positive and then weakened at different hypothetical exposure levels. In addition, at the same lag time, the RR increased with the increase of exposure value for all climate variables when presenting a positive association.

Figures 4A,B showed some of the distributed lag associations between rainfall and scrub typhus cases. First, rainfall had a lag effect during the 0 to 12th weeks, but there was a significant correlation only during the 0 to 6th weeks; when there was less rainfall, the significant correlation range was reduced to ∼0–5 weeks but peaked at the 2nd week. Second, when the rainfall was relatively low, the RR was low, and when the rainfall was relatively large, the RR was greater. Furthermore, the peak value of the RR increased as rainfall increased. For example, when the rainfall was 1.45 mm (50%), there was a significant correlation during the 0 to 5th weeks with the peak RR occurring at the 2nd week with an RR of 1.008 (95% CI: 1.004–1.012) (**Figure 4A**); when the rainfall was 17.88 mm (75%), there was a significant correlation during the 0 to 6th weeks with a peak RR also occurring at the 2nd week (RR: 1.103, 95% CI: 1.050–1.158) (**Figure 4B**).

Figures 4C,D showed some of the distributed lag associations between relative humidity and scrub typhus cases. First, the lag effect ranged from the first to 13th weeks with significance only during the 6th to 11th weeks, which lasted for∼6 weeks and peaked at the 8th week. Second, similar to rainfall, there was a larger RR when the relative humidity was higher, and when the relative humidity increased, the peak RR also increased. For example, when the relative humidity was 59.00% (50%), there was

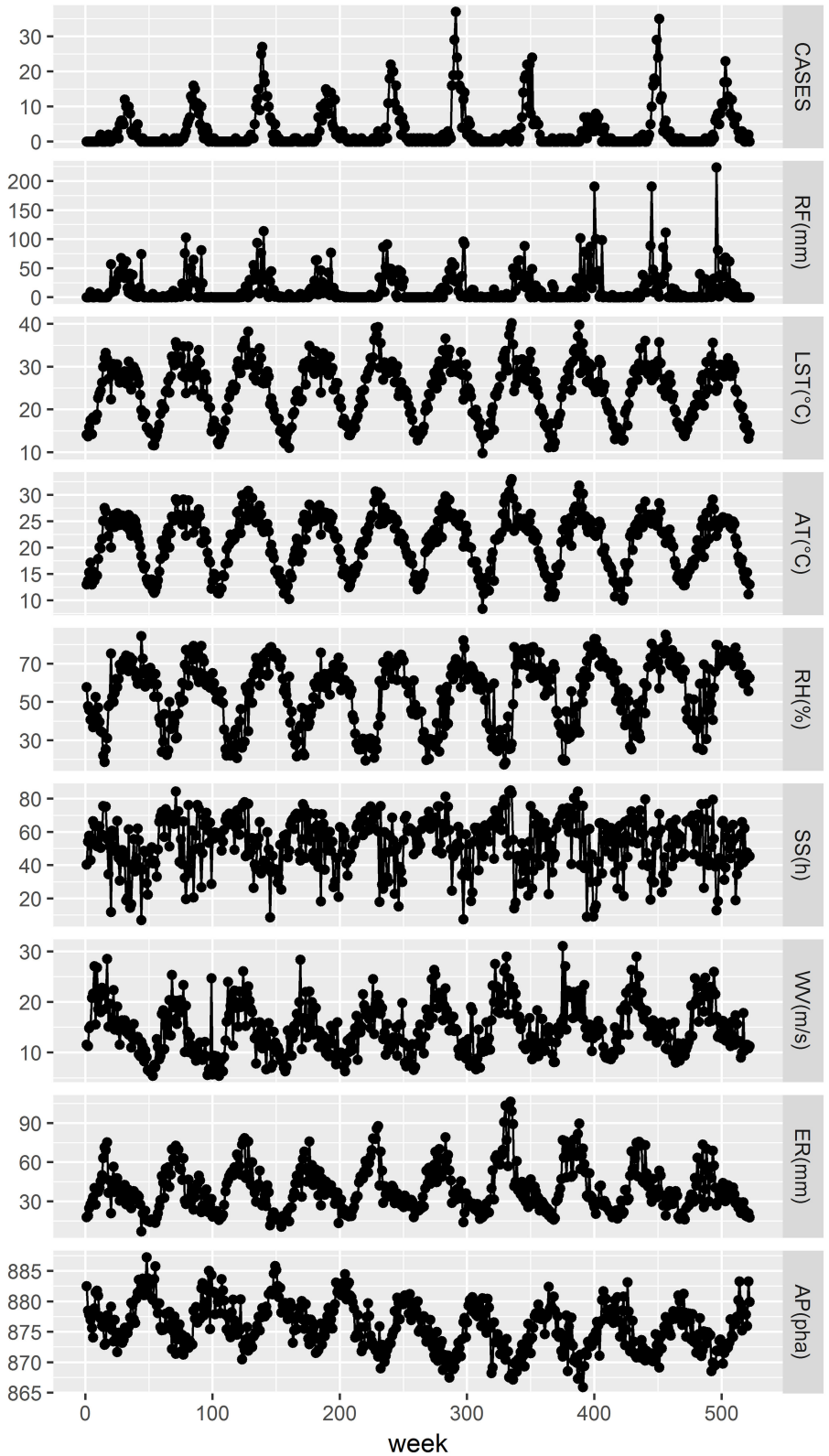

FIGURE 2 | Weekly time series of the number of scrub typhus cases and meteorological variables in rural areas of Panzhihua district, Southwest China, 2008–2017. RF, LST, AT, RH, SS, WV, ER, and AP represent the weekly values of aggregate rainfall, mean land surface temperature, mean air temperature, mean relative humidity, aggregate sunshine, mean wind velocity, mean evaporation, and mean air pressure, respectively.

TABLE 1 | Summary statistics for weekly scrub typhus cases and meteorological variables in rural areas of Panzhihua district, Southwest China, 2008–2017.

	Total	Mean	S.D.	Min	P (25)	Median	P (75)	Max
Aggregate rainfall (mm)	-	14.75	26.88	0	0	1.45	17.88	223.50
Aggregate sunshine (h)	–	53.29	15.94	7.00	43.70	55.80	65.40	85.20
Mean relative humidity (%)	–	54.64	17.02	17.43	40.29	59.00	68.39	85.29
Mean land surface temperature (°C)	–	24.54	6.56	9.83	19.13	25.49	29.65	40.19
Mean air temperature (°C)	–	21.18	5.13	8.41	16.90	22.24	25.20	33.06
Mean wind velocity (m/s)	–	1.48	0.51	0.54	1.09	1.42	1.83	3.11
Mean evaporation (mm)	–	39.58	17.73	7.00	26.61	36.00	49.86	106.57
Mean air pressure (hpa)	–	875.90	3.89	865.94	872.90	875.81	878.50	887.26
No. of cases of scrub typhus	1731	3.32	5.83	0	0	1	4	37

Note: all the data are presented as the weekly aggregate or mean values.
S.D. = Standard deviation.

TABLE 2 | Spearman correlation coefficients between weekly meteorological variables in rural areas of Panzhihua district, Southwest China, 2008–2017.

	Rainfall	Relative humidity	Land surface temperature	Air temperature	Sunshine	Wind velocity	Evaporation
Relative humidity	0.63[a]	1					
Land surface temperature	0.41[a]	−0.06	1				
Air temperature	0.46[a]	−0.03	0.98[a]	1			
Sunshine	−0.54[a]	−0.72[a]	0.26[a]	0.21[a]	1		
Wind velocity	0.07	−0.48[a]	0.45[a]	0.44[a]	0.25[a]	1	
Evaporation	0.05	−0.56[a]	0.78[a]	0.76[a]	0.56[a]	0.75[a]	1
Air pressure	−0.27[a]	0.2[a]	−0.66[a]	−0.71[a]	−0.28[a]	−0.55[a]	−0.68[a]

[a]$p < 0.001$.

a significant correlation during the 6th to 11th weeks with a peak RR occurring during the 8th week (RR: 1.372, 95% CI: 1.135–1.657) (**Figure 4C**). When the relative humidity was 68.39% (75%), a significant correlation also occurred during the 6th to 11th weeks with the peak RR occurring at the 8th week (RR: 1.608, 95% CI: 1.210–2.136) (**Figure 4D**).

Figures 4E,F showed some of the distributed lag associations between land surface temperature and scrub typhus cases. On the one hand, land surface temperature was associated with scrub typhus during the first 2 weeks and during the 6th to 15th weeks, but the significant correlation began at the 7th week and ended at the 13th week with a peak RR near the 9th week and lasting for 7 weeks. On the other hand, a larger RR value was associated with a higher land surface temperature; similarly, the peak RR was associated with the peak land surface temperature. When the land surface temperature was 25.49°C (50%), a significant association appeared during the 7th to 13th weeks with the peak value at the 9th week (RR: 1.589, 95% CI: 1.221–2.068), as shown in **Figure 4E**. When the land surface temperature was 29.65°C (75%), a significant association also appeared during the 7th to 13th weeks with the peak RR occurring at the 9th week (RR: 2.150, 95% CI: 1.391–3.322) (**Figure 4F**).

Figures 4G,H showed some of the distributed lag associations between air temperature and scrub typhus cases. Air temperature showed a similarly shorter and dramatic variation at the beginning of the lag time at different exposure levels; in other words, the zero week and the 8th to 16th weeks showed a statistically negative correlation, whereas the first to the 4th weeks displayed a positive risk peaking at the second week, which was the only statistically significant week. Regardless of whether there was a positive or negative risk, the RR and its corresponding peak value were larger in association with higher air temperatures. As a result, when the air temperature was 22.24°C (50%), a significant risk occurred at the second week, the only statistically significant positive week, with an RR of 1.546 (95% CI: 1.047–2.285), as shown in **Figure 4G**. A similar relationship occurred at 25.2°C (75%), with an RR of 1.970 (95% CI: 1.073–3.616), as shown in **Figure 4H**.

Figures 4I,J showed some of the distributed lag association between sunshine time and scrub typhus cases. At first, sunshine time displayed a negative correlation with no statistical significance during the 0–2nd weeks, and then it displayed a positive relative risk from the 3rd week with no ending time. Furthermore, the magnitude of the increasing trend became larger as sunshine time increased, and there was a significant positive increasing correlation during the 13th to 16th weeks with the largest value occurring at the 16th week. As a result, when the sunshine time was 55.80 h (50%), a significant risk appeared during the 13th to 16th weeks, with the increase of risk lasting the entire time; the largest RR value was 1.111 (95% CI: 1.021–1.209) at the 16th week, (**Figure 4I**); a similar association was displayed at 65.40 h (75%), with a largest RR of 1.208 (95% CI: 1.038–1.406) at the 16th week, as shown in **Figure 4J**.

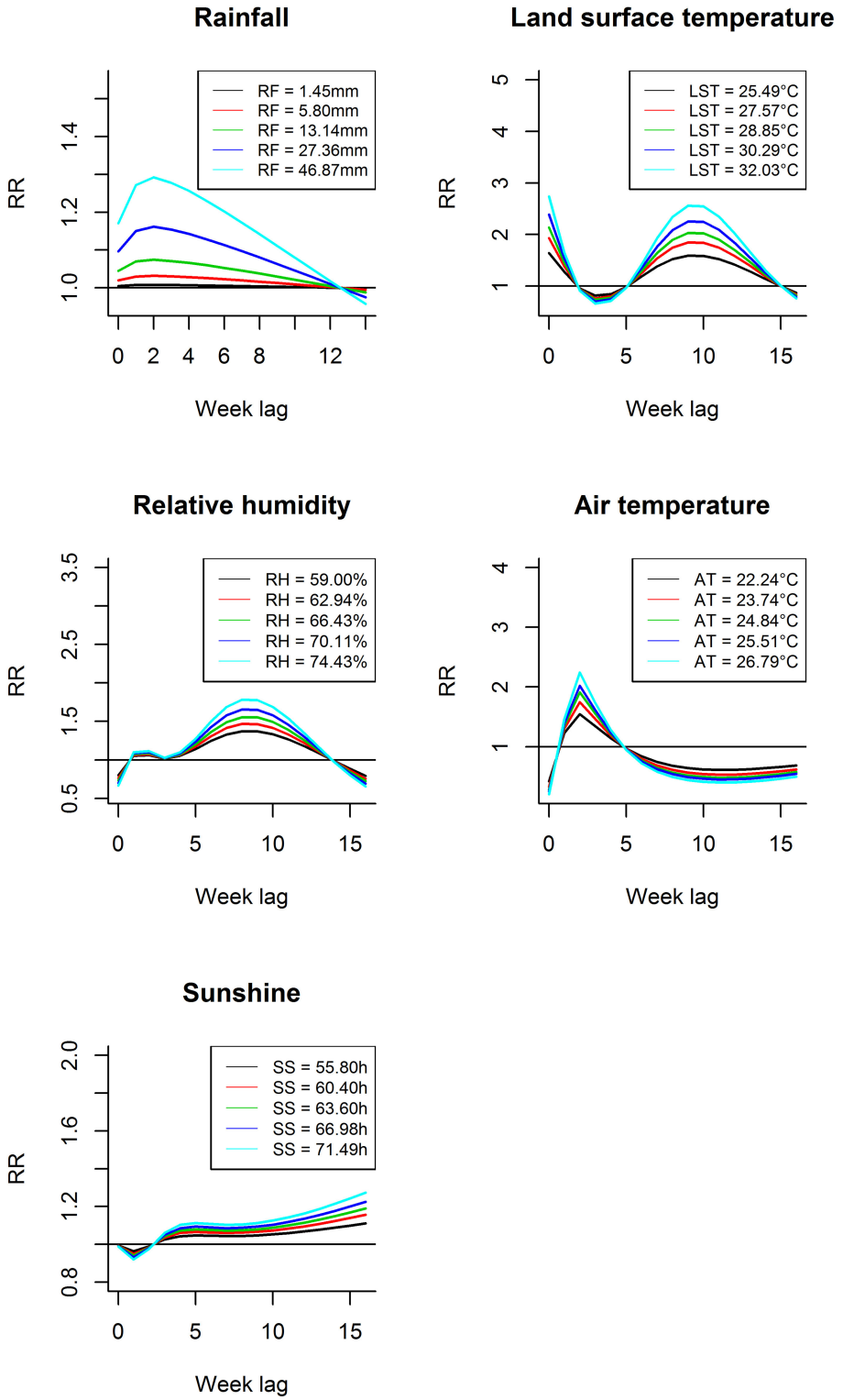

FIGURE 3 | Lag-response curves for different weather variables in their diverse exposure levels (50, 60, 70, 80, and 90%).

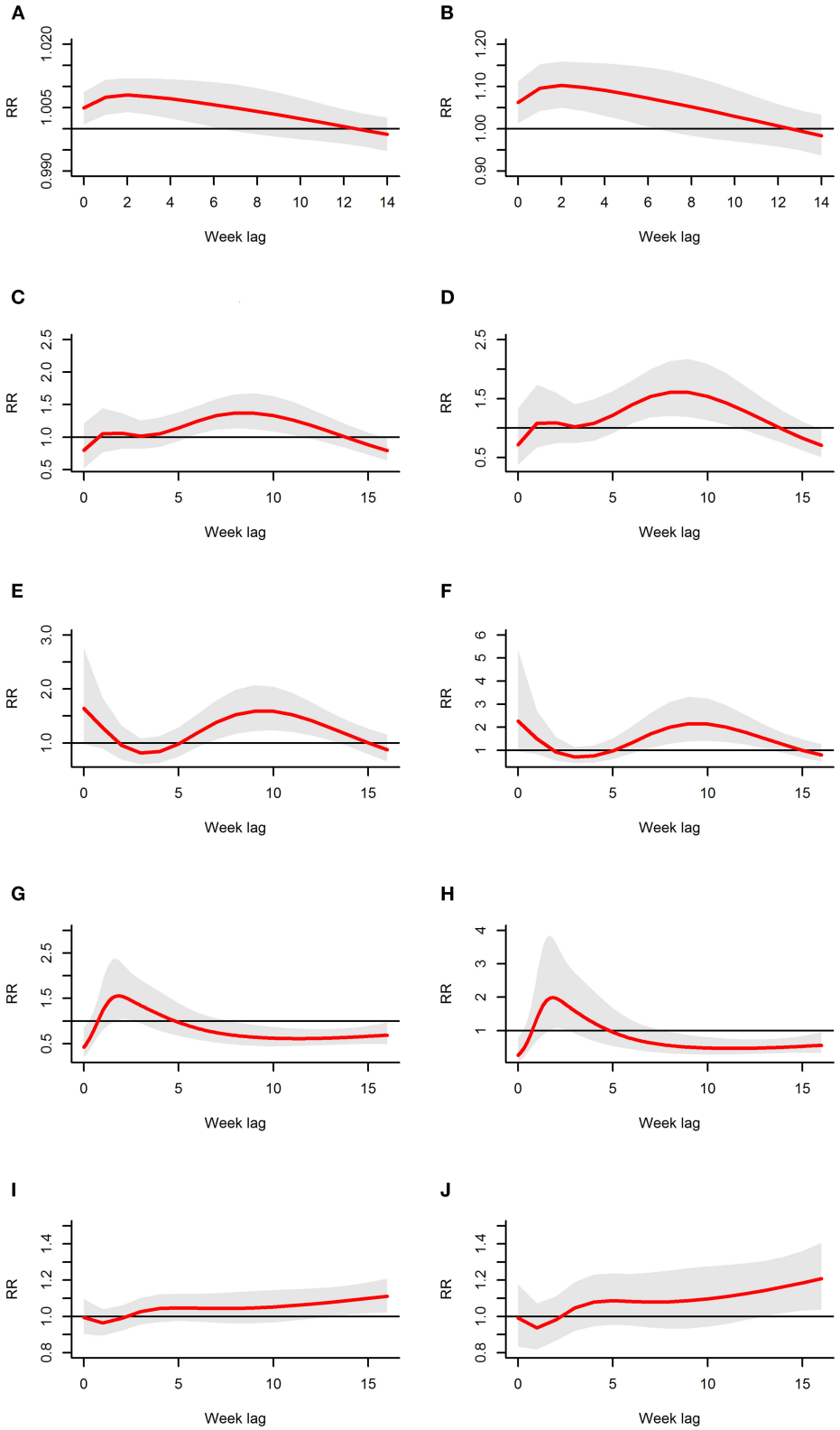

FIGURE 4 | The estimates of distributed lag between meteorological variables and scrub typhus cases. The relative risk for each weather variable is calculated at 50 and 75% exposure levels The estimated distributed lag association is the red line, and the shaded bands indicate its 95% CI. **(A,B)** Show the scenario for rainfall; **(C,D)** show the scenario for relative humidity; **(E,F)** show the scenario for land surface temperature; **(G,H)** show the scenario for air temperature; and **(I,J)** show the scenario for sunshine.

DISCUSSION

Scrub typhus is a life-threatening vector-borne infectious disease that manifests as an acute indiscriminate febrile illness (23–25). Such infections are prevalent worldwide but are often undiagnosed/misdiagnosed, leading to a life-threatening condition (26–28). Meanwhile, no vaccine against *O. tsutsugamushi* is currently available (29). In survivors, immunity does not last long and is poorly cross-reactive amongst numerous strains. Hence, the disease deserves further scrutiny.

Our analysis results show that there is a high incidence of scrub typhus in rural areas in Panzhihua, Southwest China, similar to other regions of China (11, 15, 30, 31). To date, our results show that cases have been reported throughout the year due to the warmer environment.

Since weather factors such as temperature and humidity have been proven to have a significant relationship with the occurrence and transmission of many infectious diseases (9, 32–34), in our study, the association between weather factors and scrub typhus was explored using DLNM (17, 35).

Rainfall, temperature, humidity and other weather variables affect both the vectors and the agents they transmit in many ways (9).

First, certain trombiculid mite species transmit *O. tsutsugamushi*, a causative pathogen of scrub typhus, to humans via bite in the larval stage (12). The optimum temperature for growth, development and activity of the majority of chigger mites is 20–23°C; the growth rate will slow down until death in the presence of temperatures that are too high or too low (12).

Second, chigger mites are considered a class of arthropod vectors and reservoirs of *O. tsutsugamushi* (30). *O. tsutsugamushi* is a very small coccobacillus, an obligate intracellular parasite of infected mites, mammals and human beings (29); this species is also affected by temperature (12).

In summary, meteorological variables can affect scrub typhus cases both through their effects on the vectors and on the pathogens they transmit. In addition, a few studies have shown that there were no significant correlations between meteorological factors and monthly scrub typhus cases in Korea as a whole (8). Another study pointed out that because the seasonal distribution of scrub typhus varies in different geographical areas, it may be too simplistic to investigate the disease at a national level (15). Here, our work was conducted in rural areas of Panzhihua District, a subtropical zone, Southwest China, which may overcome this problem.

The results showed that different meteorological factors including supposedly diverse exposure levels have different patterns and magnitudes of lagged associations. First, rainfall is associated with scrub typhus with a delayed correlation and a relatively long lag range of 13 weeks with 7 weeks being statistically significant at all exposure levels. Second, the current study supports earlier studies from other areas in China (11) that demonstrate that vectors of scrub typhus are more abundant during the wet season.

One study revealed that chiggers survive and reproduce well at a relative humidity above 50% but decrease in number or activity when the relative humidity is below 50% (36); thus, when the assumed exposure level of the relative humidity increases, the RR of the lag association also increases.

Land surface temperature has a longer lag range of 12 weeks with 7 weeks being statistically significant and larger RRs for all assumed exposure levels. Some papers have indicated that land surface temperature affects the growth and development of the vector and pathogens it carries and also influences the abundance and distribution of rodents, which are major parasitic hosts for chigger mites (11). Our study indicates that a higher land surface temperature will introduce a larger RR and peak RR of the correlation compared with the reference level.

Air temperature has a shorter lag range of 4 weeks, but the ∼1-week lag at the 2nd week is statistically significant for all assumed exposure levels. This time is shorter than that reported in previous studies (11, 15). As we know, the incubation period of scrub typhus is ∼6–21 days (mean 10–12 days) after the initial chigger bite; thus, weather variables might not affect scrub typhus emergence immediately (15). We found that a higher temperature results in a greater relative risk at the same lag time from the results. These results coincide with studies conducted in a similar climate region (11).

In our study, sunshine time during the 0–2nd lag weeks was negatively correlated with weekly cases of scrub typhus with no significance, whereas sunshine time during the 3–16th lag weeks was positively correlated with the disease with the last 4 weeks being statistically significant. This can be explained by the abundance of chigger mites (37) and human outdoor activity. A longer sunshine time may have a protective effect for scrub typhus by inhibiting chigger activity, whereas in the long term, human outdoor activities may increase, and thus the occurrence of human infection may also increase.

To our knowledge, this study was the first to use week as a time analysis unit for the relationship between weather factors and scrub typhus rather than month; thus, a more precise lag range was obtained for the predetermined diverse exposure level. Consequently, the results have a greater public health significance for the prevention and control of scrub typhus. Furthermore, this was the first study to apply a mathematical model to analyse the relationship between weather variables and scrub typhus in this region. Additionally, only a few studies have analyzed the delayed effects of weather factors with a distributed lag non-linear model, and our study considered more different weather factors to simultaneously represent the exposure-response relationships and their temporal structure.

Some limitations of this study should be considered. First, there is inevitable underreporting in any infectious disease surveillance system together with less attention paid to scrub typhus; thus, areas of future improvement include training physicians regularly or improving diagnostics with the introduction of sensitive experimental equipment, particularly in rural regions. Second, the occurrence of scrub typhus is complex. It is indeed influenced by climate as shown by previous studies, but it is also influenced by other risk factors such as socioeconomic and behavioral risk factors (38). In addition, the pre-defined maximum lags for weather variables were used. The lag lengths were considered comprehensively according to existing studies (11, 15). These limitations should be evaluated in future studies.

CONCLUSIONS

In summary, our study reveals that rainfall, sunshine, relative humidity, air temperature and land surface temperature have different patterns and magnitudes for the lagged correlation between weather factors and scrub typhus, and when all meteorological factors are at a high level, the potential risk of scrub typhus increases. The lag shape and association for meteorological information is applicable for developing an early warning system for scrub typhus. Public health professionals and medical service providers should pay more attention to preventing and controlling a potential increased risk of scrub typhus under the condition of high-level weather factors.

DATA AVAILABILITY STATEMENT

The raw data supporting the conclusions of this article will be made available by the authors, without undue reservation.

AUTHOR CONTRIBUTIONS

HL and YL: conceptualization. HL, XS, and SW: data curation. JH, FY, and BG: formal analysis. HL, JH, XS, and WW: methodology. YL: project administration and supervision. HL: resources, software, and writing—original draft. JH, XS, and YL: writing—review & editing. All authors contributed to the article and approved the submitted version.

FUNDING

This work was supported by grants from the Health and Family Planning Commission Project of Sichuan Province in China (No. 18PJ576).

ACKNOWLEDGMENTS

We are grateful to Panzhihua City Center for Disease Control and Prevention for providing the disease data.

REFERENCES

1. Jeong YJ, Kim S, Wook YD, Lee JW, Kim KI, Lee SH. Scrub typhus: clinical, pathologic and imaging findings. *Radiographics.* (2007) 27:161–72. doi: 10.1148/rg.271065074
2. Kelly DJ, Fuerst PA, Ching WM, Richards AL. Scrub typhus: the geographic distribution of phenotypic and genotypic variants of orientia tsutsugamushi. *Clin Infect Dis.* (2009) 48 (Suppl 3):S203–30. doi: 10.1086/596576
3. Zhang WY, Wang LY, Ding F, Hu WB, Soares Magalhaes RJ, Sun HL, et al. Scrub typhus in Mainland China, 2006-2012: the need for targeted public health interventions. *PLoS Negl Trop Dis.* (2013) 7:e2493. doi: 10.1371/journal.pntd.0002493
4. Jeung YS, Kim CM, Yun NR, Kim SW, Han MA, Kim DM. Effect of latitude and seasonal variation on scrub typhus, South Korea, 2001-2013. *Am J Tropic Med Hygiene.* (2015) 94:22–5. doi: 10.4269/ajtmh.15-0474
5. Watt G, Parola P. Scrub typhus and tropical rickettsioses. *Curr Opin Infect Dis.* (2003) 16:429–36. doi: 10.1097/00001432-200310000-00009
6. Kweon SS, Choi JS, Lim HS, Kim JR, Kim KY. A community-based case-control study of behavioral factors associated with scrub typhus during the autumn epidemic season in South Korea. *Am Soc Tropic Med Hygiene.* (2009) 80:442–6. doi: 10.4269/ajtmh.2009.80.442
7. Ogawa M, Hagiwara T, Kishimoto T, Shiga S. Scrub typhus in Japan: epidemiology and clinical features of cases reported in 1998. *Am Soc Tropic Med Hygiene.* (2002) 67:162–5. doi: 10.4269/ajtmh.2002.67.162
8. Kwak J, Kim S, Kim G, Singh VP, Hong S, Kim HS. Scrub typhus incidence modeling with meteorological factors in South Korea. *Int J Environ Res Public Health.* (2015) 12:7254–73. doi: 10.3390/ijerph120707254
9. Gage KL, Burkot TR, Eisen RJ, Hayes EB. Climate and vectorborne diseases. *Am J Prev Med.* (2008) 35:436–50. doi: 10.1016/j.amepre.2008.08.030
10. Zhao X, Chen F, Feng ZJ, Li XS, Zhou XH. The temporal lagged association between meteorological factors and malaria in 30 counties in South West China a multilevel distributed lag non linear analysis. *Malar J.* (2014) 13:1–12. doi: 10.1186/1475-2875-13-57
11. Wei Y, Huang Y, Li X, Ma Y, Tao X, Wu X, et al. Climate variability, animal reservoir and transmission of scrub typhus in Southern China. *PLoS Negl Trop Dis.* (2017) 11:e0005447. doi: 10.1371/journal.pntd.0005447
12. Seto J, Suzuki Y, Nakao R, Otani K, Yahagi K, Mizuta K. Meteorological factors affecting scrub typhus occurrence: a retrospective study of yamagata prefecture, Japan, 1984-2014. *Epidemiol Infect.* (2017) 145:462–70. doi: 10.1017/S0950268816002430
13. Li T, Yang Z, Dong Z, Wang M. Meteorological factors and risk of scrub typhus in guangzhou, Southern China, 2006 2012. *BMC Infect Dis.* (2014) 14:139. doi: 10.1186/1471-2334-14-139
14. *China Ministry of Health: Technical Guides for Prevention and Control of Scrub Typhus.* (2022). Available online at: http://www.chinacdc.cn/tzgg/200901/t20090105_40316.htm.
15. Yang LP, Liu J, Wang XJ, Ma W, Jia CX, Jiang BF. Effects of meteorological factors on scrub typhus in a temperate region of China. *Epidemiol Infect.* (2014) 142:2217–26. doi: 10.1017/S0950268813003208
16. *National Science & Technology Infrastructure.* (2022). Available online at: http://data.cma.cn
17. Gasparrini A, Armstrong B, Kenward MG. Distributed lag non-linear models. *Stat Med.* (2010) 29:2224–34. doi: 10.1002/sim.3940
18. Zhu S, Xia L, Wu JL, Chen SB. Ambient air pollutants are associated with newly diagnosed tuberculosis: a time-series study in Chengdu,China. *Sci Total Environ.* (2018) 631-632:47–55. doi: 10.1016/j.scitotenv.2018.03.017
19. Feng Y, Wei J, Hu M, Xu C, Li T, Wang J, et al. Lagged effects of exposure to air pollutants on the risk of pulmonary tuberculosis in a highly polluted region. *Int J Environ Res Public Health.* (2022) 19:5752. doi: 10.3390/ijerph19095752
20. Guo H, Du P, Zhang H, Zhou Z, Zhao M, Wang J, et al. Time series study on the effects of daily average temperature on the mortality from respiratory diseases and circulatory diseases: a case study in Mianyang City. *BMC Public Health.* (2022) 22:1001. doi: 10.1186/s12889-022-13384-6
21. Bhaskaran K, Gasparrini A, Hajat S, Smeeth L, Armstrong B. Time series regression studies in environmental epidemiology. *Int J Epidemiol.* (2013) 42:1187–95. doi: 10.1093/ije/dyt092
22. Gasparrini A. Distributed lag linear and non-linear models the r the package dlnm. *J Stat Softw.* (2011) 43:1–20. doi: 10.18637/jss.v043.i08
23. Paris DH, Shelite TR, Day NP, Walker DH. Unresolved problems related to scrub typhus: a seriously neglected life-threatening disease. *Am J Trop Med Hyg.* (2013) 89:301–7. doi: 10.4269/ajtmh.13-0064
24. Abarca K, Weitzel T, Martínez-Valdebenito C, Acosta-Jamett G. Scrub typhus, an emerging infectious disease in Chile. *Rev Chilena Infectol.* (2018) 35:696–9. doi: 10.4067/S0716-10182018000600696
25. Dorji K, Phuentshok Y, Zangpo T, Dorjee S, Dorjee C, Jolly P, et al. Clinical and epidemiological patterns of scrub typhus, an emerging disease in Bhutan. *Trop Med Infect Dis.* (2019) 4, 56. doi: 10.3390/tropicalmed4020056
26. Dhruva C, Sandeep G. Scrub typhus-resurgence of a forgotten killer. *Indian J Anaesth.* (2013) 57:135–6. doi: 10.4103/0019-5049.111836

27. Koraluru M, Bairy I, Varma M, Vidyasagar S. Diagnostic validation of selected serological tests for detecting scrub typhus. *Microbiol Immunol.* (2015) 59:371–4. doi: 10.1111/1348-0421.12268
28. Richards AL, Jiang J. Scrub typhus: historic perspective and current status of the worldwide presence of orientia species. *Trop Med Infect Dis.* (2020) 5, 49. doi: 10.3390/tropicalmed5020049
29. Xu G, Walker DH, Jupiter D, Melby PC, Arcari CM. A review of the global epidemiology of scrub typhus. *PLoS Negl Trop Dis.* (2017) 11:e0006062. doi: 10.1371/journal.pntd.0006062
30. De W, Jing K, Huan Z, Qiong ZH, Monagin C, Min ZJ, et al. Scrub Typhus, a disease with increasing threat in Guangdong, China. *PLoS ONE.* (2015) 10:e0113968. doi: 10.1371/journal.pone.0113968
31. Lu J, Liu Y, Ma X, Li M, Yang Z. Impact of meteorological factors and southern oscillation index on scrub typhus incidence in Guangzhou, Southern China, 2006-2018. *Front Med.* (2021) 8:667549. doi: 10.3389/fmed.2021.667549
32. Zhang R, Zhang N, Sun W, Lin H, Liu Y, Zhang T, et al. Analysis of the effect of meteorological factors on hemorrhagic fever with renal syndrome in Taizhou City, China, 2008-2020. *BMC Public Health.* (2022) 22:1097. doi: 10.1186/s12889-022-13423-2
33. Ai H, Nie R, Wang X. Evaluation of the effects of meteorological factors on Covid-19 prevalence by the distributed lag nonlinear model. *J Transl Med.* (2022) 20:170. doi: 10.1186/s12967-022-03371-1
34. Lv H, Zhang X, Wang J, Hou Z, Wang H, Li C, et al. Short-term effects of Covid-19 on the risk of traumatic fractures in China cities. *Sci Rep.* (2022) 12:6528. doi: 10.1038/s41598-022-10531-2
35. Michetti M, Adani M, Anav A, Benassi B, Dalmastri C, D'Elia I, et al. From Single to multivariable exposure models to translate climatic and air pollution effects into mortality risk. A Customized Application to the City of Rome, Italy. *MethodsX.* (2022) 9:101717. doi: 10.1016/j.mex.2022.101717
36. Rubio AV, Simonetti JA. Ectoparasitism by eutrombicula alfreddugesi larvae (acari: trombiculidae) on liolaemus tenuis lizard in a chilean fragmented temperate forest. *J Parasitol.* (2009) 2009:244–5. doi: 10.1645/GE-1463.1
37. Tsai PJ, Yeh HC. Scrub Typhus Islands in the Taiwan Area and the association between scrub typhus disease and forest land use and farmer population density: geographically weighted regression. *BMC Infect Dis.* (2013) 13:191. doi: 10.1186/1471-2334-13-191
38. Kuo CC, Huang JL, Ko CY, Lee PF, Wang HC. Spatial analysis of scrub typhus infection and its association with environmental and socioeconomic factors in Taiwan. *Acta Trop.* (2011) 120:52–8. doi: 10.1016/j.actatropica.2011.05.018

Conflict of Interest: The authors declare that the research was conducted in the absence of any commercial or financial relationships that could be construed as a potential conflict of interest.

Publisher's Note: All claims expressed in this article are solely those of the authors and do not necessarily represent those of their affiliated organizations, or those of the publisher, the editors and the reviewers. Any product that may be evaluated in this article, or claim that may be made by its manufacturer, is not guaranteed or endorsed by the publisher.

frontiers | Frontiers in Microbiology

TYPE Original Research
PUBLISHED 04 August 2022
DOI 10.3389/fmicb.2022.912806

OPEN ACCESS

EDITED BY
George Tsiamis,
University of Patras, Greece

REVIEWED BY
Bachar Cheaib,
University of Glasgow, United Kingdom
Amanda Carroll-Portillo,
University of New Mexico,
United States

*CORRESPONDENCE
Morten T. Limborg
morten.limborg@sund.ku.dk

SPECIALTY SECTION
This article was submitted to Systems Microbiology, a section of the journal Frontiers in Microbiology

RECEIVED 04 April 2022
ACCEPTED 06 July 2022
PUBLISHED 04 August 2022

CITATION
Scheuring I, Rasmussen JA, Bozzi D and Limborg MT (2022) A strategic model of a host–microbe–microbe system reveals the importance of a joint host–microbe immune response to combat stress-induced gut dysbiosis. *Front. Microbiol.* 13:912806. doi: 10.3389/fmicb.2022.912806

A strategic model of a host–microbe–microbe system reveals the importance of a joint host–microbe immune response to combat stress-induced gut dysbiosis

István Scheuring[1,2], Jacob A. Rasmussen[3], Davide Bozzi[4,5] and Morten T. Limborg[3]*

[1]Centre for Ecological Research, Institute of Evolution, Budapest, Hungary, [2]MTA-ELTE, Research Group of Theoretical Biology and Evolutionary Ecology, Eötvös University, Budapest, Hungary, [3]Center for Evolutionary Hologenomics, GLOBE Institute, University of Copenhagen, Copenhagen, Denmark, [4]Department of Computational Biology, University of Lausanne, Lausanne, Switzerland, [5]Swiss Institute of Bioinformatics, Lausanne, Switzerland

Microbiomes provide key ecological functions to their host; however, most host-associated microbiomes are too complicated to allow a model of essential host–microbe–microbe interactions. The intestinal microbiota of salmonids may offer a solution since few dominating species often characterize it. Healthy fish coexist with a mutualistic *Mycoplasma* sp. species, while stress allows the spread of pathogenic strains, such as *Aliivibrio* sp. Even after a skin infection, the *Mycoplasma* does not recover; *Aliivibrio* sp. often remains the dominant species, or *Mycoplasma–Aliivibrio* coexistence was occasionally observed. We devised a model involving interactions among the host immune system, *Mycoplasma* sp. plus a toxin-producing pathogen. Our model embraces a complete microbiota community and is in harmony with experimental results that host–*Mycoplasma* mutualism prevents the spread of pathogens. Contrary, stress suppresses the host immune system allowing dominance of pathogens, and *Mycoplasma* does not recover after stress disappears.

KEYWORDS

bistability, mutualism, stress, pathogens, salmonids, microbiome, *Mycoplasma* sp., *Aliivibrio* sp.

Introduction

Almost every eukaryotic organism hosts an associated core microbial community providing key biological functions to the host (McFall-Ngai et al., 2013; Bosch and Miller, 2016; Müller et al., 2016). This has led influential thinkers to coin the term holobiont as describing the sum of a host and its commensal microbes (Margulis, 1990; Baedke et al., 2020). These host–microbiota systems range in complexity from one-to-one symbiotic associations between a host

and a single microorganism, such as the bioluminescent *Aliivibrio* bacteria in light organs of bob-tail squids (Nyholm and McFall-Ngai, 2004), to intricate arrangements between a host and a dynamic community of microorganisms like vertebrates and their gut microbiota (Ley et al., 2008), or plants and their root microbiota (Sasse et al., 2018). The renewed realization that microbes play essential roles for the hosts has catalyzed an increased focus on the study of host–bacteria and bacteria–bacteria dynamics within a holobiont (Zilber-Rosenberg and Rosenberg, 2008; Bordenstein and Theis, 2015; Theis et al., 2016). In extension, the generation of knowledge potentially allowing active manipulation of holobionts has become a global strategic priority across life sciences (Małyska et al., 2019), including food production (Limborg et al., 2018).

One approach to better understand microbiome dynamics is ecological models that include a realistic parameter space for characterizing host–microbe interactions in the holobiont. Microbiomes of animal hosts are generally very complex (Gralka et al., 2020; Alberdi et al., 2021). So far, theoretical studies have achieved limited success in explaining empirical data of these complex systems. Even verification of more simplified feedback and dynamical models describing host–microbe interactions remains scarce (Abbott et al., 2021; Remien et al., 2021). The challenge becomes even more significant if we model how pathogenic microbes interact with the host and the host's commensal and mutualistic contingent of the host–microbiome dynamics (Coyte et al., 2015; Rúa and Umbanhowar, 2015; Jiang et al., 2020). Indeed, to adequately describe realistic host–microbiome dynamics, models must consider at least two key factors that have been ignored in attempts to model realistic holobiont systems reflecting empirical data. First, the host immune system needs to be included as it is known to control microbiome composition (Earley et al., 2018; Zheng et al., 2020). Second, microbial metabolites can act as toxins, common goods, or resources, further shaping the qualitative dynamics of the system (Scheuring and Yu, 2012; Rybicki et al., 2018; Kokou et al., 2019; Gralka et al., 2020). We address this challenge by studying a holobiont system containing relatively few microbial members while covering the complete microbiome community.

Recent investigations have revealed a general trend of low diversity among intestinal microbiota in teleosts compared to warm-blooded animals, including numerous studies from commercially important species such as Atlantic salmon (*Salmo salar*) and rainbow trout (*Oncorhynchus mykiss*) (Huang et al., 2020). Adult salmon are piscivorous and characterized by physiological adaptations necessary to cope with a strictly carnivorous diet. These adaptations may extend to an adaptive composition of its associated gut microbiota. Furthermore, several studies have revealed that the intestinal microbiota of salmonids is characterized by strikingly low diversity, with as little as one or two species dominating the microbial biomass (Holben et al., 2002; Llewellyn et al., 2016; Bozzi et al., 2021; Wang et al., 2021). Together, these observations suggest that salmon and related species are well-suited holobiont systems to study concrete biological interactions between a eukaryotic host and its commensal microbiota (Limborg et al., 2018; Nyholm et al., 2020; Alberdi et al., 2021).

Mycoplasma sp. has recently emerged as a core and often dominating member of the gut microbiome in some salmonid species. This novel *Mycoplasma* species have been reported at high-relative abundances in the gut of different salmonids species in numerous independent studies over the past 20 years (Holben et al., 2002; Zarkasi et al., 2014; Lowrey et al., 2015; Llewellyn et al., 2016; Dehler et al., 2017; Lyons et al., 2017; Brown et al., 2019; Rimoldi et al., 2019; Bozzi et al., 2021; Rasmussen et al., 2022a,b). *Mycoplasma* sp. abundance has been associated with enhanced health conditions (Bozzi et al., 2021), disese resilience (Rasmussen et al., 2022b), and improved growth performances (Rimoldi et al., 2019; Bozzi et al., 2021) of the salmonid host. More detailed studies using genome-resolved metagenomics further point toward a putative mutualistic relationship between *Mycoplasma* sp. and its salmonid hosts (Cheaib et al., 2021a; Rasmussen et al., 2021). For example, *Mycoplasma* sp. can provide the host with a suite of beneficial functions, such as arginine biosynthesis, ammonia detoxification, and degradation of long-chain polymers, which could improve the nutritional value of both chitin-rich diet and strict carnivory during the juvenile and adult life stages of salmon (Rasmussen et al., 2021).

Interestingly, the proposed beneficial role of *Mycoplasma* sp. is further supported by numerous observations where slower-growing or disease-susceptible salmonid cohorts have a reduced abundance of *Mycoplasma* sp. in concomitance with the increase of pathogenic/opportunistic strains (Table 1). These observations, together with the resolved *Mycoplasma* phylogeny (Rasmussen et al., 2021), suggest a mutualistic relationship, thus providing an excellent system to further model and understand adaptively important host–microbe and microbe–microbe interactions. Here, we build upon a previous case study to develop a simple mathematical model describing the dynamics of an observed change in *Mycoplasma* sp. abundance in a sick cohort of Atlantic salmon.

The study of Bozzi et al. (2021) provides a valuable dataset to describe a model involving interactions among the host immune system, *Mycoplasma* sp. plus a toxin-producing pathogenic competitor as the two dominant gut microbes. Bozzi et al. (2021) assessed changes in the composition of the Atlantic salmon distal gut microbiota in the context of a bacterial skin infection caused by the pathogen *Tenacibaculum dicentrarchi*. The infected fish developed an ulcerative skin disease, which would eventually lead to the death of the fish. The researchers collected samples from the distal gut content and the distal gut mucosa tissue of both healthy and diseased salmon. The stressful event was resolved by a water disinfection treatment aimed at killing the skin pathogen.

TABLE 1 A non-exhaustive list of relevant studies showing similar positive correlations with *Mycoplasma* sp. abundance and fish health.

Host species	Type of stress	Microbiota pattern (before and after stress)	References
Atlantic salmon	Tenacibaculosis outbreak	*Mycoplasma* dominates healthy control fish while its abundance is highly reduced in diseased fish.	Bozzi et al., 2021
Rainbow trout	*Yersinia ruckeri* challenge	*Mycoplasma* dominates healthy control fish while its abundance is highly reduced in diseased fish.	Rasmussen et al., 2022b
Atlantic salmon	Tenacibaculosis outbreak	The intestinal microbiota initially dominated by *Mycoplasma* experienced an increase in *Aliivibrio* and *Alcaligenes* abundance in the intestine of fish with ulcerative disorder.	Karlsen et al., 2017
Rainbow trout	Comparison of the microbiome of a selectively bred line resistant to *Flavobacterium psychrophilum* infection with the susceptible line.	*Mycoplasma* sp. was the dominant taxon in the midgut of both groups, although, in the susceptible line, it was present at a decreased abundance, together with an increased abundance of the potential opportunistic pathogen *Brevinema andersonii*.	Brown et al., 2019
Rainbow trout	The Effects of a dietary insect meal	The relative abundance of Aeromonadaceae (a family that includes pathogenic species) decreased in fish fed with higher percentages of insect meal. Concurrently mycoplasmataceae amount increased in these samples.	Rimoldi et al., 2019
Chinook salmon (*Oncorhynchus tshawytscha*)	No stress reported	The mid-intestinal microbiota of the majority of the 30 sampled fish was dominated by the family Vibrionaceae, except two of the individuals which had a microbiota dominated by Mycoplasma.	Ciric et al., 2019

The sampling procedure was then repeated after treatment. The microbiome composition was investigated with 16S rRNA amplicon sequencing and described the relative abundance of dominating microbial species (Figure 1). Before treatment, most healthy fish had a *Mycoplasma*-dominated gut microbiome. The infection, even if it affects the outer skin of the host, allows the spread of an opportunistic and potentially pathogenic *Aliivibrio* strain, leading to its dominance in the gut of the sick fish. These observations were consistent with the gut content and mucosa tissue samples. After treatment of the infection, the *Mycoplasma*-dominated microbiomes of healthy fish do not recover, and *Aliivibrio* sp. remains the dominant species in most of the samples of the gut mucosa tissue. Instead, in the gut content, we observe the presence of some samples showing patterns of *Mycoplasma*–*Aliivibrio* coexistence (Figure 1).

In this study, we consider the study of Bozzi et al. (2021) as a case to model and understand the dynamics of a concrete host–microbe–microbe model exemplified by the *Mycoplasma*-dominated salmonid microbiomes in the context of a stressful event and the emergence of an opportunistic/pathogenic bacteria.

Based on the experimental observations described above, we define the following assumptions about the case study for building our model:

1. Salmon and *Mycoplasma* form a mutualistic relationship (Rasmussen et al., 2021), so we assume that the immune system of the host increases the carrying capacity of the *Mycoplasma* in the distal gut, and vice versa the presence of *Mycoplasma* activates the immune system either directly or indirectly by keeping the host in a healthier state (Cerf-Bensussan and Gaboriau-Routhiau, 2010; Pérez et al., 2010; Koch and Schmid-Hempel, 2011; Earley et al., 2018; Xiong et al., 2019).
2. *Aliivibrio* is a putative toxin-producing pathogen of salmonids. The assumption is based on the fact that the known *Aliivibrio* sp. generally infects its host with the help of a toxin by suppressing the immune system (Shinoda, 1999; Karlsen et al., 2014; Pérez-Reytor et al., 2018). We build our assumption on these studies to allow the pathogenic species to exert a negative impact on mutualistic bacteria in the model.
3. *Mycoplasma* colonizes the intestine of salmonids in the juvenile phase (Cheaib et al., 2021a; Rasmussen et al., 2022b) before the *Aliivibrio* can infect it. Alternatively, it can be the case that *Aliivibrio* infection in the juvenile phase is highly lethal for the host, which does not modify our argument below.
4. *Mycoplasma* and *Aliivibrio* compete in the distal intestine; that is, space and nutrients are common limiting factors of

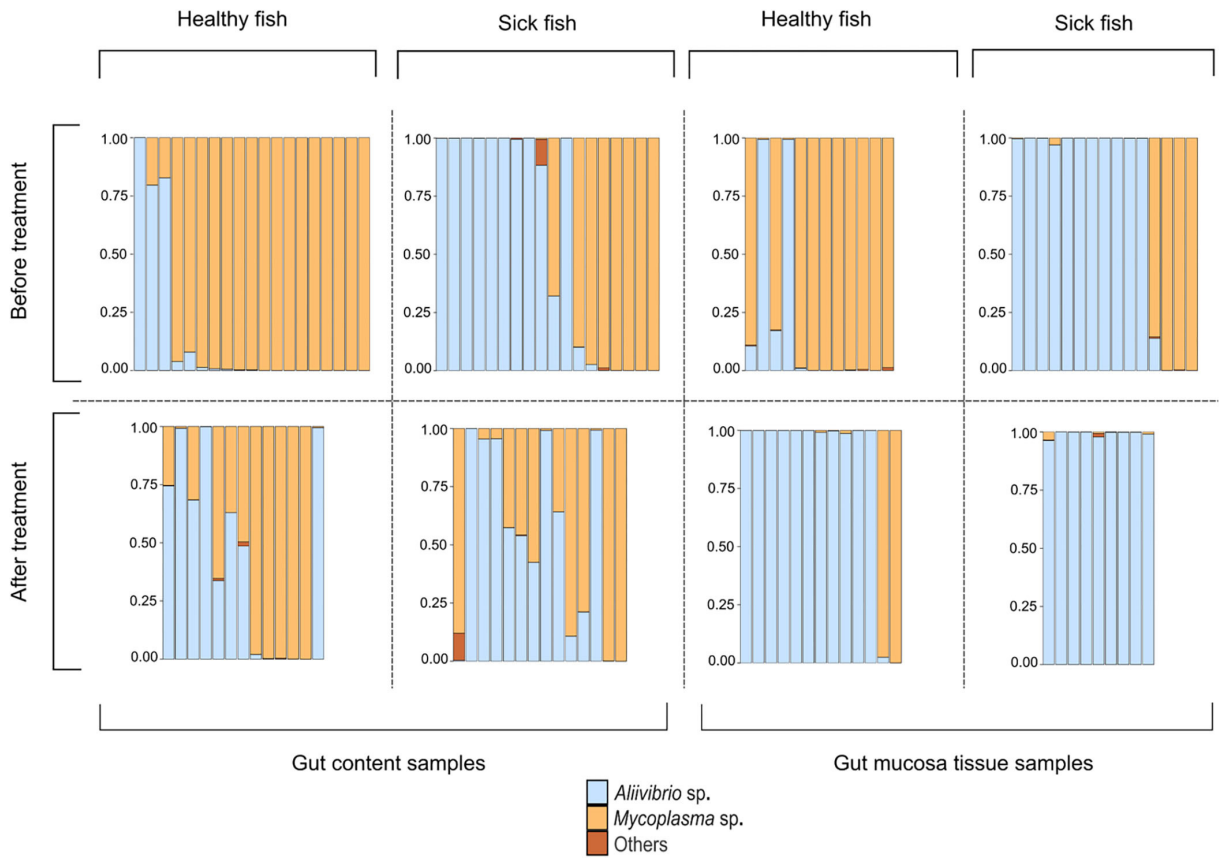

FIGURE 1
Intestinal microbiota composition for the two dominant bacterial species *Mycoplasma* sp. and *Aliivibrio* sp. for eight distinct cohorts of Atlantic salmon during a disease outbreak. Each bar represents one fish. The eight cohorts represent three relevant variables pertaining to the sampled tissue (gut content vs. gut mucosa), the health status during a Tenacibaculosis outbreak (Healthy vs. Sick), and whether fish were sampled before or after treatment against the Tenacibaculosis causing pathogen *Tenacibaculum dicentrarchi* (before vs. after treatment). The figure has been reformatted based on data from Bozzi et al. (2021).

these two species. Additionally, *Aliivibrio* can also be toxic for *Mycoplasma*, which is considered in the model.

5. Infection or other stress factors elicit an acute immune response that will remove resources from other fish metabolic processes, including transcription of host genes usually involved in maintaining gut homeostasis in the host fish (Tort, 2011; Nardocci et al., 2014; Cámara-Ruiz et al., 2021).

Materials and methods

We consider a simple dynamical model to describe the dynamics of the host immune system, the mutualistic microbe, and the invading toxic producing bacterium. As we argued above, in the case of salmonid hosts, the resident microbiome is typically dominated by *Mycoplasma*. Still, after some stress, the microbiome is frequently replaced by an opportunistic pathogenic *Aliivibrio* species. We apply the common Lotka–Volterra competition model to describe the *Mycoplasma*–*Aliivibrio* competition in their common habitat. We define a model where the mutualistic *Mycoplasma* facilitates the immune system of the host; in return, the host's immune system selectively helps to maintain a higher density of *Mycoplasma* in the gut. Furthermore, we use a simple model for the pathogen-immune sub-system, where the *Aliivibrio* pathogen produces toxins that inhibit immune response while immune effectors try to eliminate pathogens (Rybicki et al., 2018). Figure 2 depicts the interactions between the microbes and host, and the corresponding dynamical system is the following:

$$\frac{dA}{dt} = r_A\left(1 - \frac{A}{K_a} - a_{MA}M\right)A - kIA \tag{1a}$$

$$\frac{dM}{dt} = r_M\left(1 - \frac{M}{K_M(I)} - a_{AM}A\right)M \tag{1b}$$

$$\frac{dT}{dt} = sA - mT \tag{1c}$$

$$\frac{dI}{dt} = r(I_0(M) - I) - eIT, \quad (1d)$$

where A and M are the concentration of *Aliivibrio* and *Mycoplasma* species in the gut of the host, T and I are the concentration of toxin and immune effectors, r and s are the growth rates of microbes and the effector cells, and k is the rate at which the immune effector eliminates the pathogen *Aliivibrio*. a_{MA} and a_{AM} are the intraspecific competition coefficients. s and m are the toxin production and decay rates, and e is the rate at which toxin (or any other mechanism by the pathogen) inactivates the active immune effectors. $K_M(I)$, $I_0(M)$ are increasing saturating functions of I and M, in harmony with the assumptions that *Mycoplasma* activates the immune system to reach a higher equilibrium proliferation level, while in return the immune system of the host enhances the carrying capacity of the *Mycoplasma*:

$$I_0(M) = I_0\left(1 + \varepsilon\frac{M}{\sigma + M}\right),$$
$$K_M(I) = K_M\left(1 + \delta\frac{I}{\beta + I}\right).$$

Parameters ε and δ determine the maximal effect of M and I on I_0 and K_M, while β and σ are the half-saturation constants of these functions. If the host can only tolerate *Mycoplasma* (that is immune system neither support nor harm it), then δ and probably ε are zero in the previous functions. In this case, only the direct competition of *Mycoplasma* with *Aliivibrio* has to be taken into account, a situation that we will also analyze later.

We might assume that the dynamics of I and T are much faster than the dynamics of microbes ($s, m, r, e \gg r_A, r_M$), that is, $\frac{dI}{dt} = 0$, $\frac{dT}{dt} = 0$ in Equations (1c,1d) (Rybicki et al., 2018). Consequently, the concentrations of immune effectors and toxins in steady-state are $I^*(A,M) = \frac{I_0\left(1+\varepsilon\frac{M}{\sigma+M}\right)}{1+\frac{es}{mr}A}$, $T^* = \frac{s}{m}A$.

By substituting $I^*(A, M)$ and T^* into (1a, 1b), we receive the following dynamical system for A and M:

$$\frac{dA}{dt} = r_A\left[1 - A - a_{AM}M - I^*(A,M)\right]A \quad (2a)$$
$$\frac{dM}{dt} = r_M\left(1 - \frac{M}{1 + \delta\frac{I^*(A,M)}{\beta + I^*(A,M)}} - a_{MA}A\right)M, \quad (2b)$$

where $I^*(A,M) = \frac{\pi\left(1+\varepsilon\frac{M}{\sigma+M}\right)}{1+\mu A}$, $\pi = \frac{kI_0}{r_A}$, $\mu = \frac{es}{rm}$, are variables, and other parameters are rescaled to $A \to AK_A$, $M \to MK_M, a_{AM} \to a_{AM}K_M$, $a_{MA} \to a_{MA}K_A, \sigma \to \frac{\sigma}{K_M}$. π is the relative immune efficiency, μ is the relative toxin efficiency, and a_{MA} and a_{AM} are the rescaled intraspecific competition coefficients, which are the key parameters of the model.

Results

We examine the condition that the invading *Aliivibrio* could not spread if *Mycoplasma* is the dominant microbial resident of the host. According to the experimental observations, we assume that *Mycoplasma* arrives earlier in the distal intestine [typically in the early juvenile phase (Llewellyn et al., 2016)] than *Aliivibrio* and dominates in this section of the intestine before the infection. *Mycoplasma* reaches its equilibrium density, the stable fixed point of (2b) when $A = 0$. It is easy to show that $1 < M^* < 1 + \delta$, the solution of $1 - \frac{M}{1+\delta\frac{I*(0,M)}{\beta+I*(0,M)}} = 0$, is the only stable fixed point of (2b). *Aliivibrio* could not invade the *Mycoplasma* dominated microbiome if $\frac{dA}{dt} < 0$ in the case of $A \approx 0$ and $M = M^*$. This leads to the following relation:

$$\left(1 - a_{AM}M^* - A\right)(1 + \mu A) - \pi\left(1 + \varepsilon\frac{M^*}{\sigma + M^*}\right) < 0, \quad (3)$$

which is satisfied if

$$\pi > \pi_0(\alpha^*, \varepsilon^*) = \frac{1 - \alpha^*}{1 + \varepsilon^*}, \quad (4)$$

where $\alpha^* = a_{AM}M^*$, $\varepsilon^* = \varepsilon\frac{M^*}{\sigma+M^*}$. However, there are two different cases even if relation (4) is valid. If

$$\mu < \mu_0\left(\pi, \alpha^*, \varepsilon^*\right) = \frac{2\pi\left(1+\varepsilon^*\right) - \left(1-\alpha^*\right) + 2\sqrt{\pi\left(1+\varepsilon^*\right)\left(\pi\left(1+\varepsilon^*\right) - \left(1-\alpha^*\right)\right)}}{(1-\alpha^*)^2}, \quad (5)$$

then *Aliivibrio* can never spread independently to its initial dose. However, if $\mu \geq \mu_0(\pi, \alpha^*, \varepsilon^*)$, then *Aliivibrio* spreads if its initial concentration is above a critical level. So, there is a critical dose of the pathogen above which it can infect the host. Naturally, if (4) is not valid, then $\frac{dA}{dt} > 0$; thus, *Aliivibrio* always spreads independently to its initial concentration.

Mycoplasma defends the host by having a direct competition with *Aliivibrio*, which is manifested in the parameter α^*; however, it also benefits the host indirectly by facilitating its immune response, which is involved in the parameter ε^*. Notably, the direct and the indirect effects both take a role in relations (4) and (5); that is, *Mycoplasma* not only prevents the rare *Aliivibrio* from spreading, but its presence increases the critical dose of *Aliivibrio* above which it can spread (see Figure 3).

According to the experimental results, Aliivibrio cannot expand in healthy hosts where *Mycoplasma* dominates the microbial abundance in the distal intestine (Bozzi et al., 2021) (Figure 1). Hence, this means that relation (4) and probably (5) are valid in most cases in healthy fishes. Assume that infection on the skin or any other external stress suppresses the

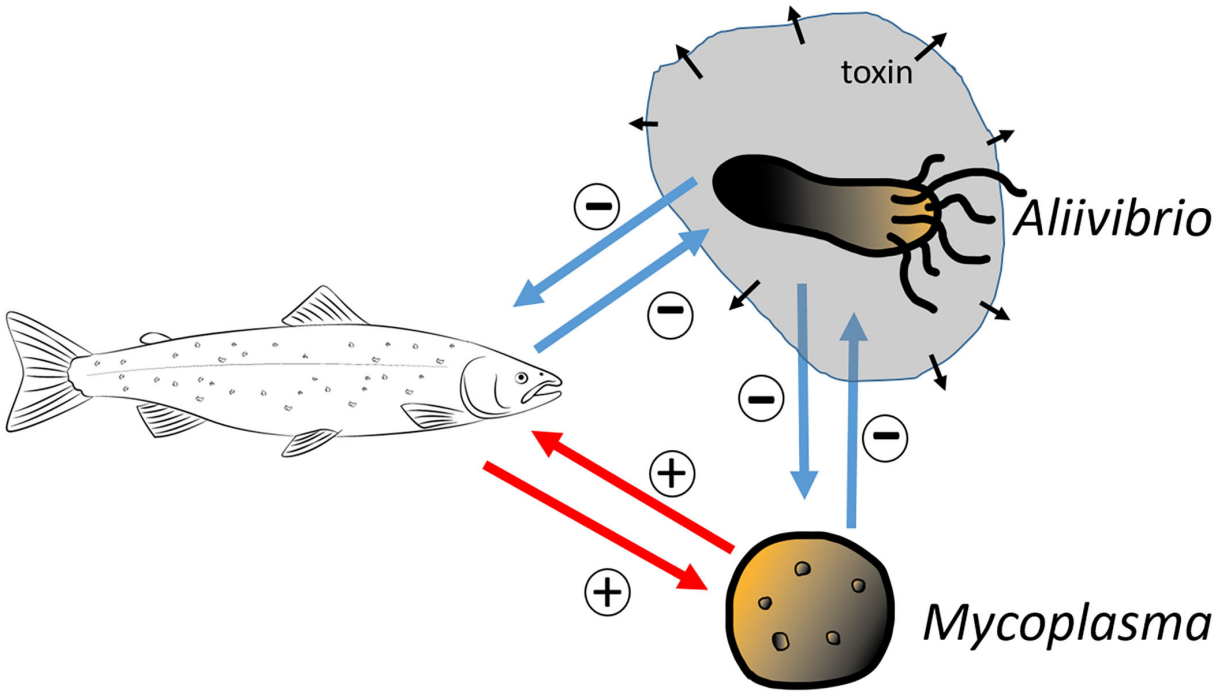

FIGURE 2
A conceptual schematic of the model. The salmon and *Mycoplasma* engaged in mutualistic interaction with each other (+ signs at the red arrows). Conversely, the toxin-producing *Aliivibrio* harms the salmon, which in turn defends itself *via* its immune response (− signs at the blue arrows). The Mycoplasma and Aliivibrio species of the model compete for the same niches and resources so that the expansion of one species is at the expense of the other species (− signs at the blue arrows).

immune system or decreases the health condition of the host, which causes a less effective immune reaction. Thus I_0, and consequently π decreases. It leads to a decrease in M^*, and thus in α^* and in ε^*. Therefore, the right-hand side of (4) increases while the left-hand side decreases.

For the same reason, the right-hand side of (5) decreases too. Consequently, it can happen that π, the actual relative immune efficiency is no longer sufficiently high to prevent the spread of the pathogen. Alternatively, it can happen as well that the decrease of π and M^* keeps the relation (4) valid, but μ, the relative toxin efficiency becomes higher than the threshold level in (5), thus because of the stress a higher dose of pathogens can spread in the host.

The results presented by Bozzi et al. (2021) also suggest that *Mycoplasma* generally cannot spread if *Aliivibrio* becomes the dominant microbe in the distal intestine (Figure 1). This means in our model that $\frac{dM}{dt} < 0$ if $M \approx 0$ when $A = A^* < 1$ is at the equilibrium density. Substituting these values into (2b), we receive that $1 - a_{MA}A^* < 0$ guarantees that *Mycoplasma* invading in a low dose (rare invader) could not spread in an *Aliivibrio* dominated microbiota. Since $A^* < 1$, therefore $a_{MA} > 1$ is necessary to satisfy the previous relation. This means that the negative effect of *Aliivibrio* on *Mycoplasma* should be more intense than the negative effect of *Aliivibrio* on itself (since this constant is normalized to one in the model). This happens if the *Aliivibrio* species actively destroys the living conditions of *Mycoplasma*. Since most *Aliivibrio* strains produce toxin, it is conceivable that toxin harms *Mycoplasma* too, which mapped to the condition $a_{MA} > 1$ in our model. Contrary, if the competing efficiency of *Aliivibrio* is not strong enough, that is if $1 - a_{MA}A^* > 0$ then rare *Mycoplasma* can spread to the *Aliivibrio* dominated state.

Collecting the possible invasion scenarios listed above, there are four qualitatively different competition situations if an invasion of *Mycoplasma* is not possible at lower π-s (higher A^*) but possible at higher π-s (lower A^*): (a) *Aliivibrio* is dominant over *Mycoplasma*, (b) neither rare invaders can spread, so the system is bistable, and (c) *Aliivibrio* can spread above a critical concentration while rare *Mycoplasma* can spread. The two species either are in stable coexistence or *Mycoplasma* is the winner of the competition, (d) *Mycoplasma* is dominant over *Aliivibrio* (Figure 4; Supplementary material).

Importantly, the microbial pattern experienced in Figure 1 can be explained by the behavior of our model. The stress decreases I_0, thus it decreases π as well. This allows *Aliivibrio* to spread and dominate the total microbial abundance

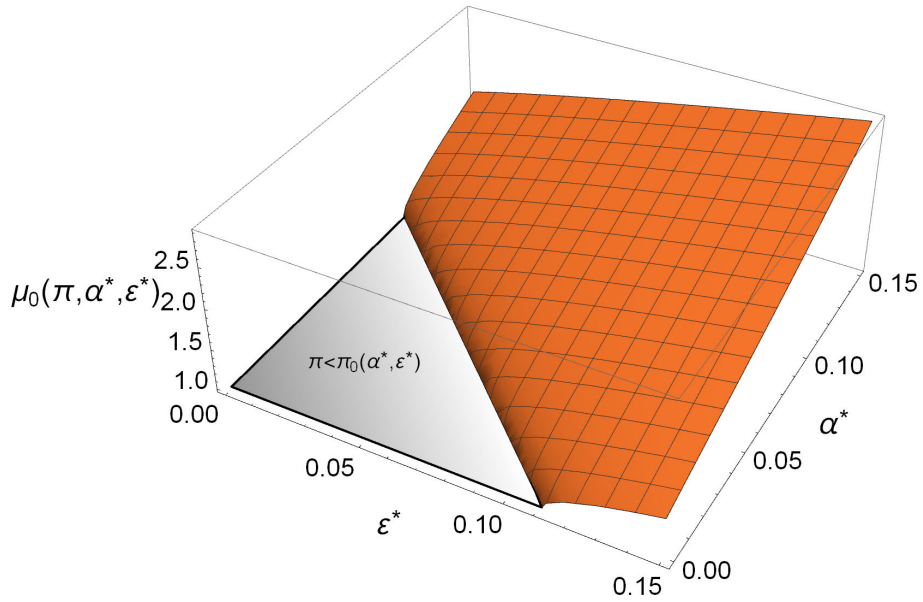

FIGURE 3
The critical toxin efficiency (μ_0) in the function of direct competition (α^*) and immune system facilitation (ε^*). The gray triangle denotes the region where rare *Aliivibrio* always/spreads in the *Mycoplasma*-dominated microbiome [$\pi < \pi_0(\alpha^*,\varepsilon^*)$]. The orange region covers the α^*, ε^* values where rare *Aliivibrio* cannot invade. If the actual $\mu < \mu_0(\pi,\alpha^*,\varepsilon^*)$ which can be satisfied more easily when α^*,ε^* are bigger, then the host is defended from the invasion of even a high dose of *Aliivibrio*, ($\pi = 0.9$).

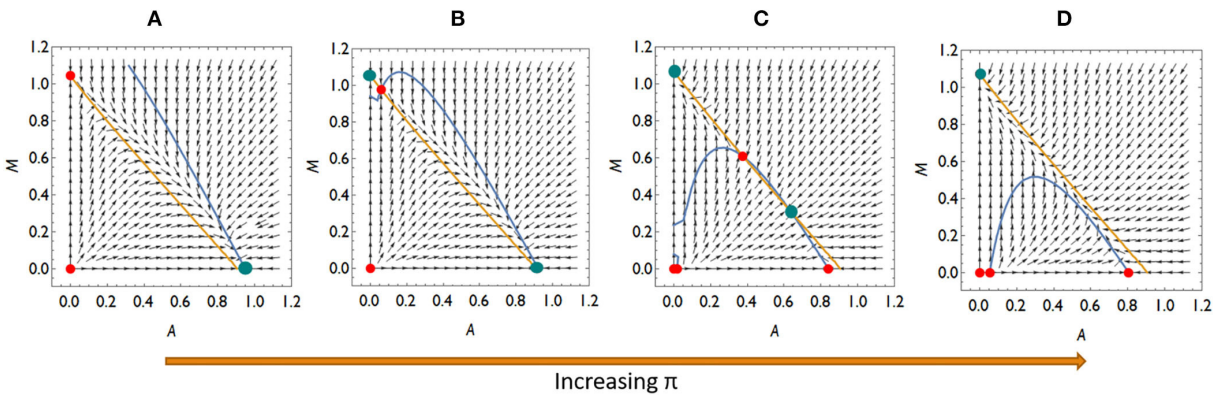

FIGURE 4
The qualitatively different dynamics of the *Mycoplasma*–*Aliivibrio* system when *Aliivibrio* deteriorate *Mycoplasma* living conditions. The nullclines of **(A,B)** are depicted (yellow dM/dt = 0, blue dA/dt = 0), so their intersections define the fixed points of the dynamics. Red points denote the unstable, while green points denote the stable fixed points of the system. At low relative immune efficiency (π) *Aliivibrio* dominates the dynamics **(A)**. At intermediate π the system is bistable **(B,C)**, while at high π *Mycoplasma* dominates the dynamics **(D)**. Parameters: (A) $\pi = 0.4$, (B) $\pi = 0.6$, (C) $\pi = 1.1$, (d) $\pi = 1.3$, other parameters are the same for all subfigures: $r_A = r_M = 1, a_{AM} = 0.5\ a_{MA} = 1.1, \varepsilon = 0.1, \sigma = 0.5, \delta = 0.1, \beta = 0.5, \mu = 7$.

(Figure 4A). After the treatment, parameter I_0 recovers leading to an increase of π again, but if this recovered π is not high enough, then *Aliivibrio* remains dominant (Figure 4B) or the two strains coexist after reinvasion of *Mycoplasma* (Figure 4C). The observation of different microbial states of the hosts after treatment (Figure 1) can be the consequence of different health states, such as the immune efficiency π, of the hosts which, as we have shown, can lead to different microbiome dynamics.

Let us also consider what dynamic cases are possible if *Aliivibrio* cannot significantly hamper the living conditions of *Mycoplasma* even though *Aliivibrio's* toxin suppresses the salmon host's immune system. Then $a_{MA} < 1$, thus rare *Mycoplasma* can always replace the resident *Aliivibrio*

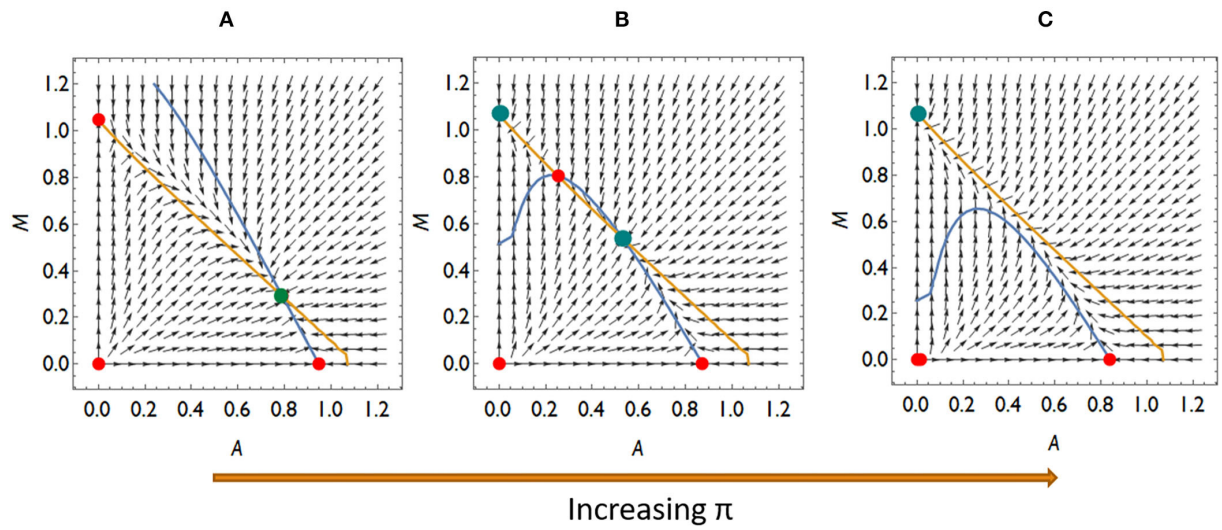

FIGURE 5
The qualitatively different dynamics of the *Mycoplasma–Aliivibrio* system when rare *Mycoplasma* always invades *Aliivibrio*. The nullclines of (1–2) are depicted (yellow dM/dt = 0, blue dA/dt = 0). Red dots denote the unstable fixed points, green ones denote the stable fixed points of the system. At low-relative immune efficiency (π), rare species invade and *Mycoplasma* are in coexistence with *Aliivibrio* **(A)**. At intermediate π the system is bistable **(B)**, while at high π *Mycoplasma* dominates the dynamics **(C)**. Parameters: (A) $\pi = 0.4$, (B) $\pi = 0.9$, (C) $\pi = 1.1$, (D) other parameters are the same for all subfigures: $r_A = r_M = 1$, $a_{AM} = 0.5$ $a_{MA} = 0.9$, $\varepsilon = 0.1$, $\sigma = 0.5, \delta = 0.1, \beta = 0.5, \mu = 7$.

population. There are typically three different dynamical scenarios in this case. There is a stable coexistence of species for weak relative immune efficiency (Figure 5A), while the system is bistable with a coexistence or a *Mycoplasma* only stable state for intermediate relative immune efficiency (Figure 5B). For high relative immune efficiency, *Mycoplasma* will be dominant as in the previous scenario (compare Figure 4D with Figure 5C). Under these conditions, stress does not lead to the displacement of *Mycoplasma*. However, the coexistence of the strains is the expected outcome, which is still compatible with the experimental results for some individuals (see Figure 1). However, assuming this dynamic situation, the *Mycoplasma* concentrations should increase after the stress is removed (after treatment). But this is not what we see in the experiment. Therefore, we can assume that once *Aliivibrio* reaches a particular concentration, it negatively impacts the living conditions of *Mycoplasma*, a scenario following our analyses above (Figures 4A,B) as the typical case.

The model parameters determine which of the above scenarios will play out. The dynamical parameters can be considered constant in a given host–microbiome system, except π, the relative efficiency of the immune system, which can decrease and increase because of stress and treatment. As π increases, we can move from an *Aliivibrio*-dominated stable microbiome to a *Mycoplasma* dominated state *via* bistable behavior, including the stable coexistence of *Mycoplasma* and *Aliivibrio*.

Since the coexistence of *Mycoplasma* and *Aliivibrio* after the stress is occasionally observed and the reinvasion of *Mycoplasma* after the treatment is experienced too, although it is not typical in the Atlantic salmon experiment (Figure 1), it is likely that *Aliivibrio* actively harms *Mycoplasma* ($a_{MA} > 1$). However, according to the experimental results depicted in Figure 1, stress decreases π to a value where *Aliivibrio* becomes dominant (Figure 4A), and after treatment, it can increase only to allow a bistable state (Figures 5B,C) in most cases. Naturally, these observations do not exclude that the scenario presented in Figure 5 occurs in other salmonid-related *Mycoplasma* pathogen systems.

Mycoplasma does not facilitate the immune system, and the immune system does not increase *Mycoplasma* concentration

We consider here the case when *Mycoplasma* and the host conform to a mutualistic interaction or where the host tolerates *Mycoplasma*. However, the immune system is not facilitated by *Mycoplasma*, that is, $\varepsilon = 0$ in the model. These modifications did not lead to qualitative changes compared to the previous analysis. The difference is only quantitative, making *Mycoplasma* stable against invasion of *Aliivibrio* in a narrower

parameter space [see Equations (4 and 5)]. Similarly, suppose the host immune system does not increase the carrying capacity of *Mycoplasma* directly; that is, when $\delta = 0$, then $M^* = 1$, which again does not change the previous derivations except that the invasion of *Aliivibrio* will be more likely [see Equations (4 and 5)].

The invader species (*Aliivibrio*) does not suppress the host immune system

To make a comprehensive analysis, we consider the situation when *Aliivibrio* does not harm the efficiency of the immune system directly. This means formally in the model that $\mu = 0$. The consequence is that the dosage effect disappears in the system; that is, rare *Aliivibrio* simply cannot invade the resident *Mycoplasma* if Equation (4) is valid, and invades if this relationship does not hold. Since it is assumed that *Aliivibrio* does not produce a toxin, *Aliivibrio* does not deteriorate *Mycoplasma* habitat, that is $a_{MA} < 1$ (intraspecific competition is more robust than interspecific) should be valid in the model. So, *Mycoplasma* invariably invades the *Aliivibrio*-dominated community ($dM/dt > 0$ if $M \approx 0$ and $A = A^* < 1$).

Two different dynamical outcomes are possible, either *Mycoplasma* dominates for stronger relative immune efficiency [π is bigger, Equation (4) is invalid], or the two competing strains are in coexistence [π is lower, Equation (4) is valid]. Consequently, stress never leads to *Aliivibrio* dominance which contradicts the experimental results presented in Figure 1.

Discussion

We present one of the first models able to describe a, albeit simple, complete intestinal microbiome community of a vertebrate host. Our model stands out from predecessors by considering realistic parameters of the host immune function, a mutualist microbe able to induce host immune reactions, and a toxin-producing pathogenic microbe. The dynamics explained by our model are in line with multiple empirical observations (Table 1).

Based on the experimental observations described, we assumed that salmon and *Mycoplasma* form a mutualistic relationship in a way that the immune system of the host increases the carrying capacity of *Mycoplasma* in the distal gut, and vice versa, the presence of *Mycoplasma* can boost the immune response of the host. Furthermore, we assume that *Aliivibrio* represents any toxin-producing intestinal pathogen of salmonids. *Mycoplasma* is believed to colonize the intestine of salmon in the juvenile phase before the *Aliivibrio* can infect it. *Mycoplasma* and *Aliivibrio* compete in the distal intestine, where *Aliivibrio* can be toxic for Mycoplasma, which is also considered in the model. The last assumption of the model is that infection or other stress factors elicit an acute immune response that will remove resources from other metabolic processes in the host fish.

Analyzing the mathematical model of the above system, we have shown that *Mycoplasma* helps to prevent the host from the *Aliivibrio* infection. If relative immune efficiency is high enough, *Aliivibrio* cannot invade (Figures 4D, 5C). Suppose the host is infected or stressed in any way that leads to an immuno-deprived state, or the *Mycoplasma* density reduces for any reason, then *Aliivibrio* can spread and replace *Mycoplasma* (Figures 4A,B). We have shown that if *Aliivibrio* becomes dominant in the distal intestine, then *Mycoplasma* cannot invade in low concentrations if the toxin harms *Mycoplasma* growth (Figure 4B). The system is bistable in a wide range of relative immune efficiency: depending on the parameters, the two stable states are: *Mycoplasma* only and *Aliivibrio* only (Figure 4B) or *Mycoplasma* only and coexistence of *Mycoplasma* and *Aliivibrio* (Figures 4C, 5B). The system flips from the *Mycoplasma* only state to the other one if the invader *Aliivibrio* concentration is high enough. *Mycoplasma* and the host immune system define that critical level of invasion. Together, this prevents the pathogen from spreading easily in a way that, besides the level of relative immune efficiency, the level of mutualism helps the competitive ability of *Mycoplasma* involved in the protection from the pathogen (Figure 3). We emphasize here that the behavior of the model explains the observations of a previous experiment (Figure 1). Furthermore, while *Mycoplasma–Aliivibrio* dominant microbiomes are widespread in salmonid hosts (Table 1), it is highly likely that the dynamics covered by our model are common in both these economically important and numerous related species. Our analysis points out that, due to the bistability of the system, the *Aliivibrio* dominant state can only be eliminated by introducing high doses of *Mycoplasma*. A possible solution would be to feed the individuals infected by *Aliivibrio* with the gut content (or shredded intestine) of healthy individuals carrying high intestinal biomass of *Mycoplasma* sp.

Since some assumptions of the model are based only on indirect observations, consequently we examined the robustness of the model to these assumptions. We have shown that the dynamical behavior does not change qualitatively if the immune system of the host and *Mycoplasma* do not help each other directly ($\varepsilon = 0, \delta = 0$); however, the presence of mutual help ($\varepsilon > 0, \delta > 0$) increases the range of conditions where the *Mycoplasma* dominated state is stable against invasion of *Aliivibrio*. Similarly, the dosage effect, the possibility of mutual invasion of *Mycoplasma* and *Aliivibrio,* and stable coexistence of them are possible even if *Aliivibrio* does not harm *Mycoplasma* effectively (Figures 4A,B). Contrary, in a model where *Aliivibrio* does not harm the immune system, the Allee effect (invasion only above a critical concentration of *Aliivibrio*) disappears. Naturally, outer stress suppressing the immune system still facilitates invasion of the pathogen, but successful invasion

always leads to the coexistence of *Mycoplasma* and *Aliivibrio*, which is not compatible with the results of (Bozzi et al., 2021) (see Figure 1).

Naturally, there are simplifications of the study. First, it should be stated that the *Mycoplasma* component in our model represents a single dominant species following the observations listed in Table 1, whereas numerous distinct species of *Mycoplasma* may be associated with their fish hosts, including the skin tissue (Cheaib et al., 2021b). The model neglects the spatial constraints and heterogeneities present in the gut and the non-even distributions of the cells and materials by the finite speed of diffusion of these materials and cells. Based on previous studies, however, it is highly probable that we do not lose the essence of the dynamics with these simplifications (compare e.g., Scheuring and Yu, 2012) with (Boza et al., 2019). To make the model tractable, we consider only the dominant species of the community, and the immune system dynamics are highly simplified. While this is an excellent first step toward developing models that help us move from only studying host–microbe and microbe–microbe interactions to better understand host–microbe–microbe interactions, the effect of our simplifications needs to be further explored in the context of species with more complex gut microbiome communities.

In summary, our model robustly describes the patterns seen in the experiments and remains consistent with other experimental observations. Based on the model, it is expected that the unfavorable *Aliivibrio* dominated microbiome community after stress can, in most cases, only be restored to a favorable *Mycoplasma* dominated state by introducing a high dose of *Mycoplasma*. We propose to test this specific hypothesis and the broader relevance of our model in future experiments.

Data availability statement

The original contributions presented in the study are included in the article/Supplementary material, further inquiries can be directed to the corresponding author/s.

Author contributions

IS designed and analyzed the mathematical model. IS, JR, DB, and ML wrote the paper. IS and ML designed the project. DB crafted Figure 1. DB and JR performed the literature research for Table 1. All authors contributed to the article and approved the submitted version.

Funding

The research was funded by the Hungarian National Fund, NKFI (K128289) to IS, the Independent Research Fund Denmark (HappyFish, Grant No. 8022-00005B), the Danish National Research Foundation Grant No. DNRF143 to ML, and the Two European Union's Horizon 2020 Actions HoloFood (817729) to ML as well as FindingPheno (952914) to IS and ML.

Acknowledgments

We thank Dr. Harald Sveier for helping design the underlying trial and interpreting the empirical results.

Conflict of interest

The authors declare that the research was conducted in the absence of any commercial or financial relationships that could be construed as a potential conflict of interest.

Publisher's note

Supplementary material

The Supplementary Material for this article can be found online at: https://www.frontiersin.org/articles/10.3389/fmicb.2022.912806/full#supplementary-material

References

Abbott, K. C., Eppinga, M. B., Umbanhowar, J., Baudena, M., and Bever, J. D. (2021). Microbiome influence on host community dynamics: conceptual integration of microbiome feedback with classical host-microbe theory. *Ecol. Lett.* 24, 2796–2811. doi: 10.1111/ele.13891

Alberdi, A., Andersen, S. B., Limborg, M. T., Dunn, R. R., and Gilbert, M. T. P. (2021). Disentangling host-microbiota complexity through hologenomics. *Nat. Rev. Genetics.* 21, 23. doi: 10.1038/s41576-021-00421-0

Baedke, J., Fábregas-Tejeda, A., and Nieves Delgado, A. (2020). The holobiont concept before Margulis. *J. Experiment. Zool. Part B Mol. Develop. Evol.* 334, 149–155. doi: 10.1002/jez.b.22931

Bordenstein, S. R., and Theis, K. R. (2015). Host biology in light of the microbiome: ten principles of holobionts and hologenomes. *PLoS Biol.* 13, e1002226. doi: 10.1371/journal.pbio.1002226

Bosch, T. C. G., and Miller, D. J. (2016). *The Holobiont Imperative: Perspectives from Early Emerging Animals*. New York, NY: Springer.

Boza, G., Worsley, S. F., Yu, D. W., and Scheuring, I. (2019). Efficient assembly and long-term stability of defensive microbiomes *via* private resources and community bistability. *PLoS Computat. Biol.* 15, e1007109. doi: 10.1371/journal.pcbi.1007109

Bozzi, D., Rasmussen, J. A., Carøe, C., Sveier, H., Nordøy, K., Gilbert, M. T. P., et al. (2021). Salmon gut microbiota correlates with disease infection status: potential for monitoring health in farmed animals. *Anim. Microb.* 3, 1–17. doi: 10.1186/s42523-021-00096-2

Brown, R. M., Wiens, G. D., and Salinas, I. (2019). Analysis of the gut and gill microbiome of resistant and susceptible lines of rainbow trout (Oncorhynchus mykiss). *Fish Shellfish Immunol.* 86, 497–506. doi: 10.1016/j.fsi.2018.11.079

Cámara-Ruiz, M., Cerezo, I. M., Guardiola, F. A., García-Beltrán, J. M., Balebona, M. C., Moriñigo, M. Á., et al. (2021). Alteration of the immune response and the microbiota of the skin during a natural infection by vibrio harveyi in european seabass (Dicentrarchus labrax). *Microorganisms* 9, 5. doi: 10.3390/microorganisms9050964

Cerf-Bensussan, N., and Gaboriau-Routhiau, V. (2010). The immune system and the gut microbiota: friends or foes? *Nat. Rev. Immunol.* 10, 735–744. doi: 10.1038/nri2850

Cheaib, B., Seghouani, H., Llewellyn, M. (2021b). The yellow perch (Perca flavescens) microbiome revealed resistance to colonisation mostly associated with neutralism driven by rare taxa under cadmium disturbance. *Anim. Microbiome* 3, 3. doi: 10.1186/s42523-020-00063-3

Cheaib, B., Yang, P., Kazlauskaite, R., Lindsay, E., Heys, C., Dwyer, T., et al. (2021a). Genome erosion and evidence for an intracellular niche—exploring the biology of mycoplasmas in Atlantic salmon. *Aquaculture* 21, 736772. doi: 10.1016/j.aquaculture.2021.736772

Ciric, M., Waite, D., Draper, J., and Jones, J., Brian. (2019). Characterization of mid-intestinal microbiota of farmed Chinook salmon using 16S rRNA gene metabarcoding. *Archiv. Biologic. Sci.* 71, 577–587. doi: 10.2298/ABS190402040C

Coyte, K. Z., Schluter, J., and Foster, K. R. (2015). The ecology of the microbiome: networks, competition, and stability. *Science* 350, 663–666. doi: 10.1126/science.aad2602

Dehler, C. E., Secombes, C. J., and Martin, S. A. M. (2017). Environmental and physiological factors shape the gut microbiota of Atlantic salmon parr (Salmo salar L.). *Aquaculture* 467, 149–157. doi: 10.1016/j.aquaculture.2016.07.017

Earley, A. M., Graves, C. L., and Shiau, C. E. (2018). Critical role for a subset of intestinal macrophages in shaping gut microbiota in adult zebrafish. *Cell Rep.* 25, 424–436. doi: 10.1016/j.celrep.2018.09.025

Gralka, M., Szabo, R., Stocker, R., and Cordero, O. X. (2020). Trophic interactions and the drivers of microbial community assembly. *Curr. Biol. CB* 30, R1176–R1188. doi: 10.1016/j.cub.2020.08.007

Holben, W. E., Williams, P., Gilbert, M. A., Saarinen, M., Särkilahti, L. K., and Apajalahti, J. H. A. (2002). Phylogenetic analysis of intestinal microflora indicates a novel Mycoplasma phylotype in farmed and wild salmon. *Microb. Ecol.* 44, 175–185. doi: 10.1007/s00248-002-1011-6

Huang, Q., Sham, R. C., Deng, Y., Mao, Y., Wang, C., Zhang, T., et al. (2020). Diversity of gut microbiomes in marine fishes is shaped by host-related factors. *Mol. Ecol.* 20, 1699. doi: 10.1111/mec.15699

Jiang, J., Abbott, K. C., Baudena, M., Eppinga, M. B., Umbanhowar, J. A., and Bever, J. D. (2020). Pathogens and mutualists as joint drivers of host species coexistence and turnover: implications for plant competition and succession. *Am. Natural.* 195, 591–602. doi: 10.1086/707355

Karlsen, C., Ottem, K. F., Brevik, Ø. J., Davey, M., Sørum, H., and Winther-Larsen, H. C. (2017). The environmental and host-associated bacterial microbiota of Arctic seawater-farmed Atlantic salmon with ulcerative disorders. *J. Fish Dis.* 40, 1645–1663. doi: 10.1111/jfd.12632

Karlsen, C., Vanberg, C., Mikkelsen, H., and Sørum, H. (2014). Co-infection of Atlantic salmon (Salmo salar), by Moritella viscosa and Aliivibrio wodanis, development of disease and host colonization. *Veterin. Microbiol.* 171, 112–121. doi: 10.1016/j.vetmic.2014.03.011

Koch, H., and Schmid-Hempel, P. (2011). Socially transmitted gut microbiota protect bumble bees against an intestinal parasite. *Proceed. Nat. Acad. Sci. USA* 108, 19288–19292. doi: 10.1073/pnas.1110474108

Kokou, F., Sasson, G., Friedman, J., Eyal, S., Ovadia, O., Harpaz, S., et al. (2019). Core gut microbial communities are maintained by beneficial interactions and strain variability in fish. *Nat. Microbiol.* 4, 2456–2465. doi: 10.1038/s41564-019-0560-0

Ley, R. E., Lozupone, C. A., Hamady, M., Knight, R., and Gordon, J. I. (2008). Worlds within worlds: evolution of the vertebrate gut microbiota. *Nat. Rev. Microbiol.* 6, 776–788. doi: 10.1038/nrmicro1978

Limborg, M. T., Alberdi, A., Kodama, M., Roggenbuck, M., Kristiansen, K., and Gilbert, M. T. P. (2018). Applied Hologenomics: feasibility and Potential in Aquaculture. *Trends Biotechnol.* 36, 252–264. doi: 10.1016/j.tibtech.2017.12.006

Llewellyn, M. S., McGinnity, P., Dionne, M., Letourneau, J., Thonier, F., Carvalho, G. R., et al. (2016). The biogeography of the atlantic salmon (Salmo salar) gut microbiome. *The ISME J.* 10, 1280–1284. doi: 10.1038/ismej.2015.189

Lowrey, L., Woodhams, D. C., Tacchi, L., and Salinas, I. (2015). Topographical mapping of the rainbow trout (Oncorhynchus mykiss) microbiome reveals a diverse bacterial community with antifungal properties in the skin. *Appl. Environ. Microbiol.* 81, 6915–6925. doi: 10.1128/AEM.01826-15

Lyons, P. P., Turnbull, J. F., Dawson, K. A., and Crumlish, M. (2017). Phylogenetic and functional characterization of the distal intestinal microbiome of rainbow trout Oncorhynchus mykiss from both farm and aquarium settings. *J. Appl. Microbiol.* 122, 347–363. doi: 10.1111/jam.13347

Małyska, A., Markakis, M. N., Pereira, C. F., and Cornelissen, M. (2019). The microbiome: a life science opportunity for our society and our planet. *Trends Biotechnol.* 37, 1269–1272. doi: 10.1016/j.tibtech.2019.06.008

Margulis, L. (1990). Words as battle cries–symbiogenesis and the new field of endocytobiology. *Bioscience* 40, 673–677. doi: 10.2307/1311435

McFall-Ngai, M., Hadfield, M. G., Bosch, T. C. G., Carey, H. V., Domazet-Lošo, T., Douglas, A. E., et al. (2013). Animals in a bacterial world, a new imperative for the life sciences. *Proceed. Nat. Acad. Sci. USA* 110, 3229–3236. doi: 10.1073/pnas.1218525110

Müller, D. B., Vogel, C., Bai, Y., and Vorholt, J. A. (2016). The plant microbiota: systems-level insights and perspectives. *Ann. Rev. Genetics* 50, 211–234. doi: 10.1146/annurev-genet-120215-034952

Nardocci, G., Navarro, C., Cortés, P. P., Imarai, M., Montoya, M., Valenzuela, B., et al. (2014). Neuroendocrine mechanisms for immune system regulation during stress in fish. *Fish Shellfish Immunol.* 40, 531–538. doi: 10.1016/j.fsi.2014.08.001

Nyholm, L., Koziol, A., Marcos, S., Botnen, A. B., Aizpurua, O., Gopalakrishnan, S., et al. (2020). Holo-omics: integrated host-microbiota multi-omics for basic and applied biological research. *iScience* 23, 101414. doi: 10.1016/j.isci.2020.101414

Nyholm, S. V., and McFall-Ngai, M. J. (2004). The winnowing: establishing the squid-vibrio symbiosis. *Nat. Rev. Microbiol.* 2, 632–642. doi: 10.1038/nrmicro957

Pérez, T., Balcázar, J. L., Ruiz-Zarzuela, I., Halaihel, N., Vendrell, D., de Blas, I., et al. (2010). Host–microbiota interactions within the fish intestinal ecosystem. *Mucosal Immunol.* 3, 355–360. doi: 10.1038/mi.2010.12

Pérez-Reytor, D., Jaña, V., Pavez, L., Navarrete, P., and García, K. (2018). Accessory toxins of vibrio pathogens and their role in epithelial disruption during infection. *Front. Microbiol.* 9, 2248. doi: 10.3389/fmicb.2018.02248

Rasmussen, J. A., Villumsen, K. R., Duchêne, D. A., Puetz, L. C., Delmont, T. O., Sveier, H., et al. (2021). Genome-resolved metagenomics suggests a mutualistic relationship between Mycoplasma and salmonid hosts. *Communicat. Biol.* 4, 579. doi: 10.1038/s42003-021-02105-1

Rasmussen, J. A., Villumsen, K. R., Ernst, M., Hansen, M., Forberg, T., Gopalakrishnan, S., et al. (2022a). A multi-omics approach unravels metagenomic and metabolic alterations of a probiotic and synbiotic additive in rainbow trout (Oncorhynchus mykiss). *Microbiome* 10, 21. doi: 10.1186/s40168-021-01221-8

Rasmussen, J. A., Villumsen, K. R., von Gersdorff Jørgensen, L., Forberg, T., Zuo, S., Kania, P. W., et al. (2022b). Integrative analyses of probiotics, pathogenic infections, and host immune response highlight the importance of gut microbiota in understanding disease recovery in rainbow trout (Oncorhynchus mykiss). *J. Appl. Microbiol.* 22, 1543. doi: 10.1111/jam.15433

Remien, C. H., Eckwright, M. J., and Ridenhour, B. J. (2021). Structural identifiability of the generalized Lotka–Volterra model for microbiome studies. *Royal Soc. Open Sci.* 8, 201378. doi: 10.1098/rsos.201378

Rimoldi, S., Gini, E., Iannini, F., Gasco, L., and Terova, G. (2019). The effects of dietary insect meal from hermetia illucens prepupae on autochthonous gut microbiota of rainbow trout (Oncorhynchus mykiss). *Animals: Open Access J. MDPI* 9, 4. doi: 10.3390/ani9040143

Rúa, M. A., and Umbanhowar, J. (2015). Resource availability determines stability for mutualist–pathogen–host interactions. *Theoretic. Ecol.* 8, 133–148. doi: 10.1007/s12080-014-0237-5

Rybicki, J., Kisdi, E., and Anttila, J. V. (2018). Model of bacterial toxin-dependent pathogenesis explains infective dose. *Proceed. Nat. Acad. Sci. USA* 115, 10690–10695. doi: 10.1073/pnas.1721061115

Sasse, J., Martinoia, E., and Northen, T. (2018). Feed your friends: do plant exudates shape the root microbiome? *Trends Plant Sci.* 23, 25–41. doi: 10.1016/j.tplants.2017.09.003

Scheuring, I., and Yu, D. W. (2012). How to assemble a beneficial microbiome in three easy steps. *Ecology Lett.* 15, 1300–1307. doi: 10.1111/j.1461-0248.2012.01853.x

Shinoda, S. (1999). Protein toxins produced by pathogenic vibrios. *J. Nat. Toxins* 8, 259–269.

Theis, K. R., Dheilly, N. M., Klassen, J. L., Brucker, R. M., Baines, J. F., Bosch, T. C. G., et al. (2016). Getting the hologenome concept right: an eco-evolutionary framework for hosts and their microbiomes. *mSystems* 1, 2. doi: 10.1128/mSystems.00028-16

Tort, L. (2011). Stress and immune modulation in fish. *Development. Comparat. Immunol.* 35, 1366–1375. doi: 10.1016/j.dci.2011.07.002

Wang, J., Jaramillo-Torres, A., Li, Y., Kortner, T. M., Gajardo, K., Brevik, Ø. J., et al. (2021). Microbiota in intestinal digesta of Atlantic salmon (Salmo salar), observed from late freshwater stage until one year in seawater, and effects of functional ingredients: a case study from a commercial sized research site in the Arctic region. *Animal Microbiome* 3, 14. doi: 10.1186/s42523-021-00075-7

Xiong, J.-B., Nie, L., and Chen, J. (2019). Current understanding on the roles of gut microbiota in fish disease and immunity. *Zoologic> Res.* 40, 70–76. doi: 10.24272/j.issn.2095-8137.2018.069

Zarkasi, K. Z., Abell, G. C. J., Taylor, R. S., Neuman, C., Hatje, E., Tamplin, M. L., et al. (2014). Pyrosequencing-based characterization of gastrointestinal bacteria of Atlantic salmon (Salmo salar L.) within a commercial mariculture system. *J. Appl. Microbiol.* 117, 18–27. doi: 10.1111/jam.12514

Zheng, D., Liwinski, T., and Elinav, E. (2020). Interaction between microbiota and immunity in health and disease. *Cell Res.* 30, 492–506. doi: 10.1038/s41422-020-0332-7

Zilber-Rosenberg, I., and Rosenberg, E. (2008). Role of microorganisms in the evolution of animals and plants: the hologenome theory of evolution. *FEMS Microbiol. Rev.* 32, 723–735. doi: 10.1111/j.1574-6976.2008.00123.x

frontiers | Frontiers in Microbiomes

TYPE Original Research
PUBLISHED 20 October 2022
DOI 10.3389/frmbi.2022.1006078

OPEN ACCESS

EDITED BY
Alexey V. Melnik,
University of Connecticut,
United States

REVIEWED BY
Nelly Aku Amenyogbe,
University of Western Australia,
Australia
Sudhanshu P. Raikwar,
Barrow Neurological Institute (BNI),
United States
Renukaradhya J. Gourapura,
The Ohio State University,
United States

*CORRESPONDENCE
Thimmasettappa Thippeswamy
tswamy@iastate.edu

SPECIALTY SECTION
This article was submitted to
Host and Microbe Associations,
a section of the journal
Frontiers in Microbiomes

RECEIVED 28 July 2022
ACCEPTED 20 September 2022
PUBLISHED 20 October 2022

CITATION
Gage M, Vinithakumari AA, Mooyottu S and Thippeswamy T (2022) Gut dysbiosis following organophosphate, diisopropylfluorophosphate, intoxication and saracatinib oral administration.
Front. Microbiom. 1:1006078.
doi: 10.3389/frmbi.2022.1006078

Gut dysbiosis following organophosphate, diisopropylfluorophosphate (DFP), intoxication and saracatinib oral administration

Meghan Gage[1], Akhil A. Vinithakumari[2], Shankumar Mooyottu[2] and Thimmasettappa Thippeswamy[1]*

[1]Interdepartmental Neuroscience, The Departments of Biomedical Sciences, Iowa State University, Ames, IA, United States, [2]Veterinary Pathology, College of Veterinary Medicine, Iowa State University, Ames, IA, United States

Organophosphate nerve agents (OPNAs) act as irreversible inhibitors of acetylcholinesterase and can lead to cholinergic crisis including salivation, lacrimation, urination, defecation, gastrointestinal distress, respiratory distress, and seizures. Although the OPNAs have been studied in the past few decades, little is known about the impact on the gut microbiome which has become of increasing interest across fields. In this study, we challenged animals with the OPNA, diisopropylfluorophosphate (DFP, 4mg/kg, s.c.) followed immediately by 2mg/kg atropine sulfate (i.m.) and 25mg/kg 2-pralidoxime (i.m.) and 30 minutes later by 3mg/kg midazolam (i.m.). One hour after midazolam, animals were treated with a dosing regimen of saracatinib (SAR, 20mg/kg, oral), a src family kinase inhibitor, to mitigate DFP-induced neurotoxicity. We collected fecal samples 48 hours, 7 days, and 5 weeks post DFP intoxication. 16S rRNA genes (V4) were amplified to identify the bacterial composition. At 48 hours, a significant increase in the abundance of *Proteobacteria* and decrease in the abundance of *Firmicutes* were observed in DFP treated animals. At 7 days there was a significant reduction in *Firmicutes* and *Actinobacteria*, but a significant increase in *Bacteroidetes* in the DFP groups compared to controls. The taxonomic changes at 5 weeks were negligible. There was no impact of SAR administration on microbial composition. There was a significant DFP-induced reduction in alpha diversity at 48 hours but not at 7 days and 5 weeks. There appeared to be an impact of DFP on beta diversity at 48 hours and 7 days but not at 5 weeks. In conclusion, acute doses of DFP lead to short-term gut dysbiosis and SAR had no effect. Understanding the role of gut dysbiosis in long-term toxicity may reveal therapeutic targets.

KEYWORDS

organophosphate nerve agent, diisopropylfluorophosphate (DFP), gut microbiome, saracatinib, orally administered drugs

1 Introduction

Organophosphate nerve agents (OPNAs) have been utilized in the past to target both military and civilian populations (Morita et al., 1995; Tucker, 1996; Okumura et al., 1998; Yanagisawa et al., 2006). These nerve agents, including soman, sarin, cyclosarin, VX, tabun, and several others, are irreversible inhibitors of acetylcholinesterase (Mukherjee and Gupta, 2020). One-time exposure to a subacute dose of OPNA can lead to cholinergic crisis which includes symptoms such as salivation, lacrimation, urination, pupillary constriction, gastrointestinal distress, bronchoconstriction, muscle weakness and convulsions (Jett, 2012). In higher doses of OPNA acute exposure, the convulsions can lead to the development of *status epilepticus* (SE) which in turn, initiates epileptogenesis and the development of spontaneously recurring seizures (Jett, 2007; Rojas et al., 2018; Putra et al., 2020c). Currently, medical countermeasures for the short-term effects of OPNA toxicity include cholinergic receptor antagonists (atropine), acetylcholinesterase reactivators (HI-6, 2-pralidoxime (2-PAM)), and GABAergic agonists (benzodiazepines). Although there are many anti-seizure drugs available to aide in the long-term neurological consequences of OPNA toxicity, about 30% of people with epilepsy develop pharmacoresistance and do not respond to current medications (French, 2007). This highlights the need to find new therapeutic avenues.

Although our understanding of the neurological consequences of OPNA-induced neurotoxicity has been of great interest in recent decades, less is known about other short- and long-term toxicity in other biological systems including the gut microbiome. One study, showed that there was a significant effect on the fecal bacteria biota and urine metabolites following soman intoxication (Getnet et al., 2018). Until this study, this was an unknown consequence of OPNA toxicity and has not been studied in other models of OPNA intoxication. In the current study, we investigated the changes in the fecal microbiome following intoxication with the OPNA, diisopropylfluorophosphate (DFP). DFP, though less potent than other OPNAs used in real-world chemical warfare scenarios is often used as a surrogate to model the effects of OPNAs (Lim et al., 1983; Deshpande et al., 2010; Flannery et al., 2016; Puttachary et al., 2016).

In addition to determining the effects of DFP on the fecal microbiome, we also analyzed the fecal microbiome from animals that were administered the potential disease modifier, saracatinib (SAR) *via* the oral route. SAR is a potent inhibitor of src tyrosine family kinases (SFKs) which are involved in a variety of biological processes (Green et al., 2009; Nie et al., 2020). SAR has been previously used in both preclinical and clinical studies of cancer, Alzheimer's disease (AD), and epilepsy (Baselga et al., 2010; Kaufman et al., 2015; Sharma et al., 2018; Smith et al., 2018; Sharma et al., 2021; Luo et al., 2021). We have previously shown that SAR treatment when given soon after DFP intoxication, reduces seizures, some behavioral deficits, as well as both short- and long-term gliosis and neurodegeneration (Gage et al., 2021a; Gage et al., 2021b). Having known the potential disease-modifying effects of orally administered SAR in experimental models, it is important to understand the impact of SAR alone, on the microbiome, as well the impact of SAR in the context of OPNA intoxication from therapeutic perspective.

2 Materials and methods

2.1 Animals, care and ethics

Male Sprague Dawley rats (7-8 weeks) were purchased from Charles River (Wilmington, MA, USA). The fecal samples (n=6/time-point) for this study were from the same animals that were reported in our recent publications on the disease-modifying effects of SAR in the rat DFP model (24, 25). The data on the gut microbiota presented here are novel. Though no post-mortem data is presented here, at the end of experiment, all animals used in this study were euthanized with 100mg/kg pentobarbital sodium (Iowa State University Llyod Veterinary Medical Center Hospital Pharmacy). Procedures were approved by the Iowa State Institutional Care and Use Committee (IACUC-18-159). Animals were single housed at the Iowa State Laboratory of Animal resources, given *ab libitum* access to food and water and light/dark cycles of 12 hours. All procedures were complied with the ARRIVE guidelines (Kilkenny et al., 2010).

2.2 DFP intoxication

The experimental design is outlined in Figures 1A, B. Animals were exposed to 4 mg/kg DFP (s.c.) followed immediately by 2 mg/kg atropine sulfate (ATS, i.m.) and 25 mg/kg 2-PAM (i.m.) to reduce mortality and to counteract the peripheral effects of AChE inhibition. Control animals were administered phosphate buffered saline (PBS). To confirm the toxicity caused by DFP, animals were assessed for seizure score based on a modified Racine sale as described in our previous publications (Racine, 1972; Putra et al., 2020a; Gage et al., 2021a). Stages 1 (salivation, lacrimation, urination, defecation-SLUD), and mastication, and 2 (head nodding, tremors) were considered nonconvulsive seizures (NCS). Stages 3 (rearing, Staub tail, forelimb clonus), 4 (falling, loss of righting reflex), and 5 (repeated falling, abducted limbs, rapid circling) were considered convulsive seizures (CS). To control behavioral seizures, animals were administered 3 mg/kg midazolam (MDZ, i.m.) once the animals spent 20 minutes in CS

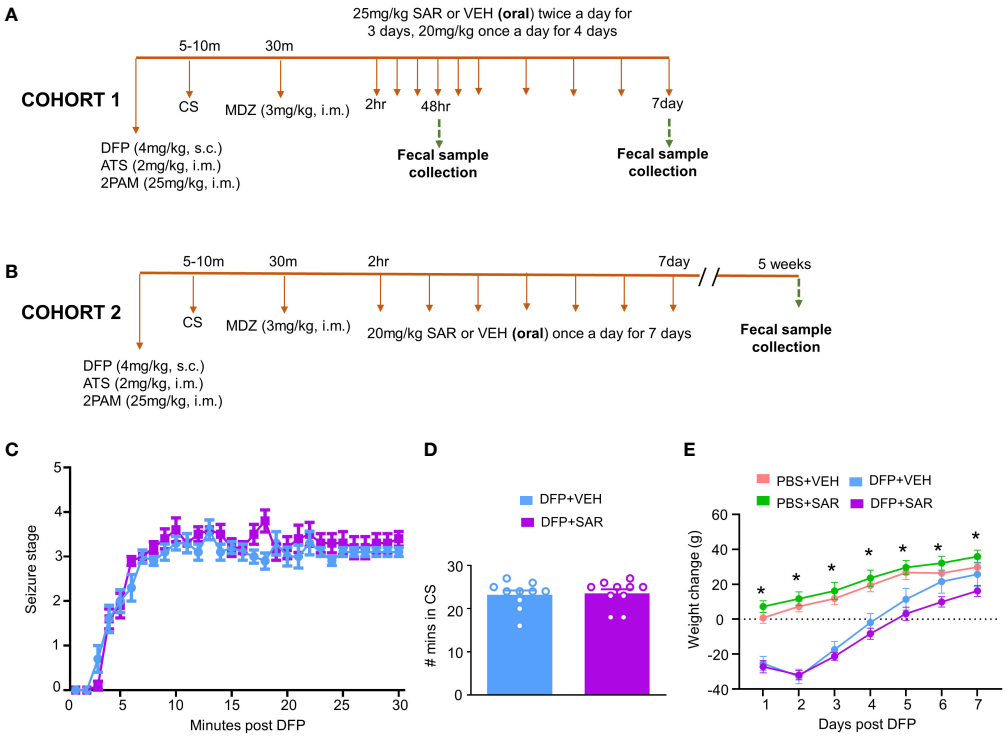

FIGURE 1
Experimental design and impact of DFP and SAR on seizures and bodyweight changes. **(A, B)** Two cohorts of animals were used in this experiment. Both cohorts were challenged with 4mg/kg diisopropylfluorophosphate (DFP, s.c.) followed immediately by 2mg/kg atropine sulfate (ATS, i.m.) and 25mg/kg 2-pralidoxime (2-PAM, i.m.) and one hour later 3mg/kg midazolam (MDZ, i.m.). Two hours after MDZ, saracatinib (SAR) or vehicle (VEH) treatment began. Cohort-1 received 25mg/kg twice a day for the first three days followed by 20mg/kg once a day for four days with fecal collections at 48 hours and 7 days. The second cohort received seven daily doses 20mg/kg SAR and had fecal collections at 5 weeks. **(C)** Seizure response over time, linear mixed effects model. **(D)** Number of minutes animals spent in a convulsive seizure (CS), t-test. **(E)** Bodyweight changes over the treatment period. Linear mixed effects model, *p < 0.05.

(approximately 30 minutes after DFP). SAR or vehicle (VEH) was administered orally 2 hours after MDZ. VEH consisted of 0.5% hydroxypropyl methylcellulose and 0.1% tween 20; preparation as described in our previous publication (Gage et al., 2021a). SAR was left stirring during the experiment to avoid precipitation. Importantly, DFP treated animals were randomly assigned to either SAR or VEH treatment so that the groups had equal SE severity.

Two cohorts of animals were used in this study. In the first cohort, 25 mg/kg SAR or vehicle was administered twice a day for the first 3 days followed by 20 mg/kg once a day for four days. Fecal samples were collected from these animals 48 hours and 7 days post DFP intoxication. In order to understand the long-term impact of DFP and SAR on the microbiome, we collected fecal samples from a second cohort of animals 5 weeks post DFP from animals in another study which has already been published (Gage et al., 2021b) except the microbiome data. In this group, 20 mg/kg SAR or VEH was administered once a day for 7 days to understand the impact of lower doses of SAR effect on the gut microbiome in the long term

2.3 Fecal sample collection and sequencing

Fresh samples were collected from each animal 48 hours, 7 days and 5 weeks after DFP intoxication. Extraction and sequencing have been previously described (Mooyottu et al., 2017). The DNA for 16S rRNA gene sequencing was isolated from 10 to 50 mg fecal pellet from each rat using the DNeasy PowerSoil HTP 96 Kit (Qiagen, Valencia, CA, USA, Cat# 12955-4) according to the manufacturer's instructions. The 16S rRNA sequencing library was created as previously reported (Kozich et al., 2013). The hypervariable V4 region of the 16S rRNA gene was then targeted using PCR with the forward primer 515F (5′ GTGCCAGCMGCCGCGGTAA3′) and the reverse primer 806R (5′GGACTACNNGGGTATCTAAT3′). The 16S rRNA amplicon library was sequenced using the MiSeq technology (Illumina, San Diego, CA). The Sequal Prep normalization plate kit was used to normalize the cleaned amplicons (Thermo Fisher Scientific, Waltham, CA). A sequencing library was built according to the manufacturer's methodology, and sequencing was performed using the Illumina Hiseq 2500 platform.

2.4 Data analysis

Qiime 2 (v2021.11) was used for all sequence processing steps (Bolyen et al., 2019). Noisy sequencing data were removed, including error tags, chimera, and low-quality sequences using cutadapt (Martin, 2011). At 97% identity, the clean data were grouped into operational taxonomic units (OTUs) and compared to Greengenes databases (Release 13.8). Comprehensive differential abundance analyses were performed using the MicrobiomeAnalyst web-based platform (https://www.microbiomeanalyst.ca/) according to the relative abundance of OTUs (Chong et al., 2020). Marker Data Profiling was used to examine gene abundance data (MDP). Data were rarified to a minimum library size and filtered to exclude features with less than four counts and less than 20% prevalence. The alpha and beta diversity data were calculated with the MicrobiomeAnalyst platform according to the relative abundance of OTUs. The linear discriminant analysis (LDA) effect size (LEfSe) was also used to identify the various taxonomies.

2.5 Statistical analysis

Graphpad prism 9.3.0 software and MicrobiomeAnalyst were used to analyze and graph the results. Linear analyses were primarily used to analyze the significance of results. Sharpiro-Wilcox tests were used to assess data normality. Experimenters were blind to treatment where appropriate and treatment groups were randomized with respect to SE severity.

3 Results

3.1 Initial response to DFP

The experimental designs are shown in Figures 1A, B. Animals developed CS within 5-10 minutes of DFP (4mg/kg) and were given MDZ about 30 minutes later so that animals had approximately 20 minutes of CS. There was no difference in SE severity between VEH-treated animals and SAR-treated animals over time (Figure 1C) or in the total number of minutes spent in a CS (Figure 1D). Both DFP treated groups lost weight for at least the first 2 days and began to steadily gain weight thereafter (Figure 1E). SAR administration did not impact the weight loss or weight gain (Figure 1E).

3.2 DFP and SAR short- and long-term impact on major gut microbiota

3.2.1 48 hours post-DFP/SAR

Univariate analysis was performed by MicrobiomeAnalyst software to determine the impact of treatment on phyla at each timepoint. The overall impact of DFP and SAR on gut microbiota phyla at 48 hours is shown in Figure 2A. Class through species levels are represented in Figure S1. The abundance for each phylum is presented in Figures 2B–I. There was a DFP-induced decrease in *Firmicutes* in both VEH and SAR treated groups, but it was only significant in the DFP +SAR group (Figure 2B). In contrast, there was a significant increase in *Proteobacteria* in both DFP treated groups compared to the controls (Figure 2C). However, there were no significant changes in *Bacteroidetes* (Figure 2D), *Actinobacteria* (Figure 2E), *Verrcomicrobia* (Figure 2F), *Tenericutes* (Figure 2G), *Deferrbacteriodetes* (Figure 2H) or *Cyanobacteria* (Figure 2I). Linear discriminant analysis (LDA) effect size (LEfSe) was used to observe group differences on the genus level. Genera with LDA scores above 2.0 are shown in Figure 3A. A heatmap cluster for the genera is presented in Figure 3B. Those with factor level $p< 0.05$ are represented by box plots in Figures 3C–I. In both DFP groups, there was an increase in *Escherichia, Rothia, Corynbacterium* and *Streptococcus* (Figures 3C–F). In the DFP +SAR group there was an increase in *Allobaculum* compared to all other groups (Figure 3H). There was DFP-induced reduction in *Lactobacillus*, and *Oscillospira* regardless of treatment with VEH or SAR (Figures 3G, I). Comparison of the treatment groups at 48 hours by species level is represented in Figure S2. The software, Picrust2, was used to predict the functional composition of the microbiota in the treatment groups; a heatmap is presented in Figure S3.

3.2.2 7 days post-DFP/SAR

The impact of DFP and SAR on gut microbiota at 7 days on the phyla level is shown in Figure 4A. Class to species levels are represented in Figure S4. There was a DFP-induced significant increase in *Bacteroidetes* (Figure 4C). Compared to the PBS +VEH control, the DFP+VEH animals had decreased *Firmicutes* and *Actinobacteria* (Figures 4B, E). There were no changes between the treatment groups on the other phyla levels (Figures 4D, F–H). Following LEfSe analysis, the genera with the highest LDA scores are presented in Figure 5A. A heatmap cluster by genus is presented in Figure 5B. Trends for genera with an overall $p<0.05$ are graphed in Figures 5C–L. In the DFP groups compared to the controls, there was an increased abundance of *Prevotella*, *Bacteroides*, and *Blautia* (Figures 5C, D, F) and a decrease in *Staphylococcus, Allobaculum, Bifidobacterium, Turicibacter, SMB53, Lactobacillus* and *Corynebacterium* (Figures 5E, G, H–L). Comparison of the treatment groups at 7 days by species level is represented in Figure S5.

3.2.3 5 weeks post-DFP/SAR

The overall impact of DFP and SAR on gut microbiota phyla at 5 weeks is shown in Figure 6A. Order to species levels are represented in Figure S6. There were no significant differences

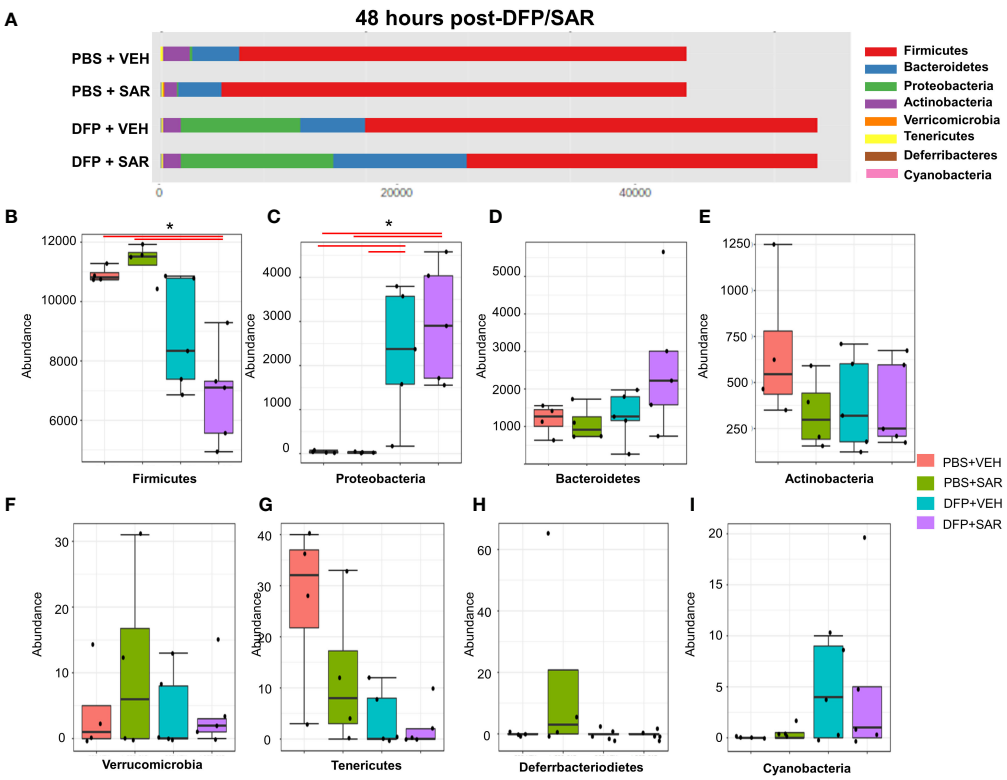

FIGURE 2
Impact of DFP and SAR on the phyla level at 48 hours post-exposure. **(A)** Overall changes and actual abundance in phyla. **(B–I)** Actual abundance by phyla for *Firmicutes* **(B)**, *Bacteroidetes* **(C)**, *Proteobacteria* **(D)**, *Actinobacteria* **(E)**, *Verricomicrobia* **(F)**, *Tenericutes* **(G)**, *Deferrbacteriodietes* **(H)**, and *Cynanobacteria* **(I)**. ANOVA or Kruskal Wallis test, *p<0.05, n=4-5.

between the treatment groups on any phyla level (Figures 6B–H). Following LEfSe analysis, the genera with the highest LDA scores are presented in Figure 7A. A heatmap by genus level is presented in Figure 7B. In the DFP groups compared to the controls, there was an increase in *RC4_4, Blautia, Rothia*, and *Anerostipes* (Figures 7C–F). Heat-trees at the species level are shown in Figure S7.

3.3 Impact of DFP and SAR on alpha and beta diversity at 48hrs, 7 days, and 5 weeks

We utilized observed (richness), chao1 and ACE (richness accounting for unobserved species), and Shannon, Simpson and Fisher (richness and evenness) to assess Alpha diversity among the treatment groups. At 48 hours, there was a significant reduction in observed, Chao1, ACE, and Fisher's alpha diversity in the DFP-treated groups, both VEH and SAR, compared to the PBS+SAR treated group (Figure 8A). There was no significant difference between the treatment groups at 7 days or 5 weeks on any alpha diversity metric (Figures 8B, C). We measured beta diversity using a principal coordinate analysis (PCoA) and nonmetric multidimensional scaling (NMDS). The PERMANOVA results revealed that at all time points, treatment significantly contributed to the clustering (Figure 9). The PERMANOVA values are summarized in Table S1. The most dramatic clustering of samples was observed in the PCoA analysis. The DFP treated groups were clustered separately from the PBS treated groups at 48 hours and 7 days but not at 5 weeks (Figure 9).

4 Discussion

The purpose of the study was to determine the impact of the OPNA, DFP, and saracatinib on the gut microbiome. The SLUD and seizures response to DFP was similar to the previous studies from our lab and others (Rojas et al., 2018; Wu et al., 2018; Guignet et al., 2019; Putra et al., 2020a; Putra et al., 2020b; Gage et al., 2021a). In addition, we observed other DFP-induced changes such as exophthalmos, porphyrin staining, hunched

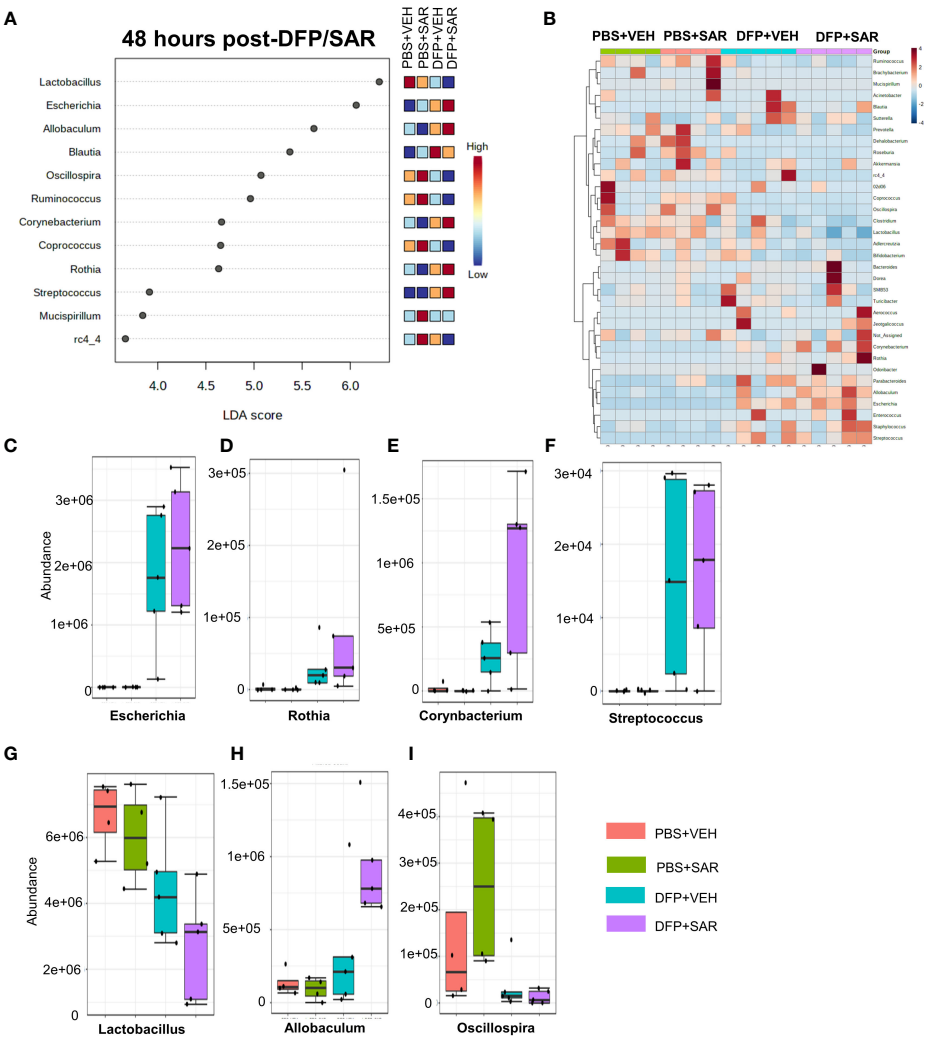

FIGURE 3
Impact of DFP and SAR on the genus level at 48 hours post-exposure. **(A)** LEfSe analysis revealed genera with LDA scores above 2.0. **(B)** Heatmap clustering by genus. **(C–I)**. Trends in actual abundance of the seven genera with an overall $p<0.05$, n=6.

body posture, tremors, muscle weakness, piloerection, and change in fur color in the days immediately following DFP intoxication (Irwin, 1968; Gage et al., 2021b). Animals developed CS 5-10 minutes post insult. Notably, we limited the duration of CS, i.e., SE, to about 20 minutes, similar to our previous studies (Gage et al., 2021a; Gage et al., 2021b). Although the seizure response to acute exposures to OPs and other OP-related consequences are well documented, the impact on the microbiome in not well known. In recent years, there has been increased interest in understanding the gut-brain axis and how neurological injury contributes to changes in the gut and vice versa (Carabotti et al., 2015; Panther et al., 2022).

Prior to this study, one other group did observe alterations in the gut microbiome following soman, an OPNA, intoxication (Getnet et al., 2018). DFP is typically used as a surrogate for soman or other OPNAs and has the same mechanism of action and clinical signs upon exposure (Jett, 2012). Soman. exposure increased in the relative abundance of *Proteobacteria* and *Cyanobacteria* 72 hours post exposure (Getnet et al., 2018). This was also observed in the current study, specifically at 48 hours post-DFP exposure. The mechanisms of DFP-induced gut dysbiosis are unclear. The gut microbiome has been primarily studied with respect to diet and obesity (Hills et al., 2019). Notably, DFP-exposed animals eat less in the 2-3 days following DFP intoxication, and therefore lose bodyweight. A number of bacteria have been found to contain genes implicated in metabolism of OPs, which could explain the increase in abundance of *Proteobacteria* and *Cyanobacteria* (Karpouzas and Singh, 2006; Getnet et al., 2018). Future studies could determine if any of the genera/species identified in this study

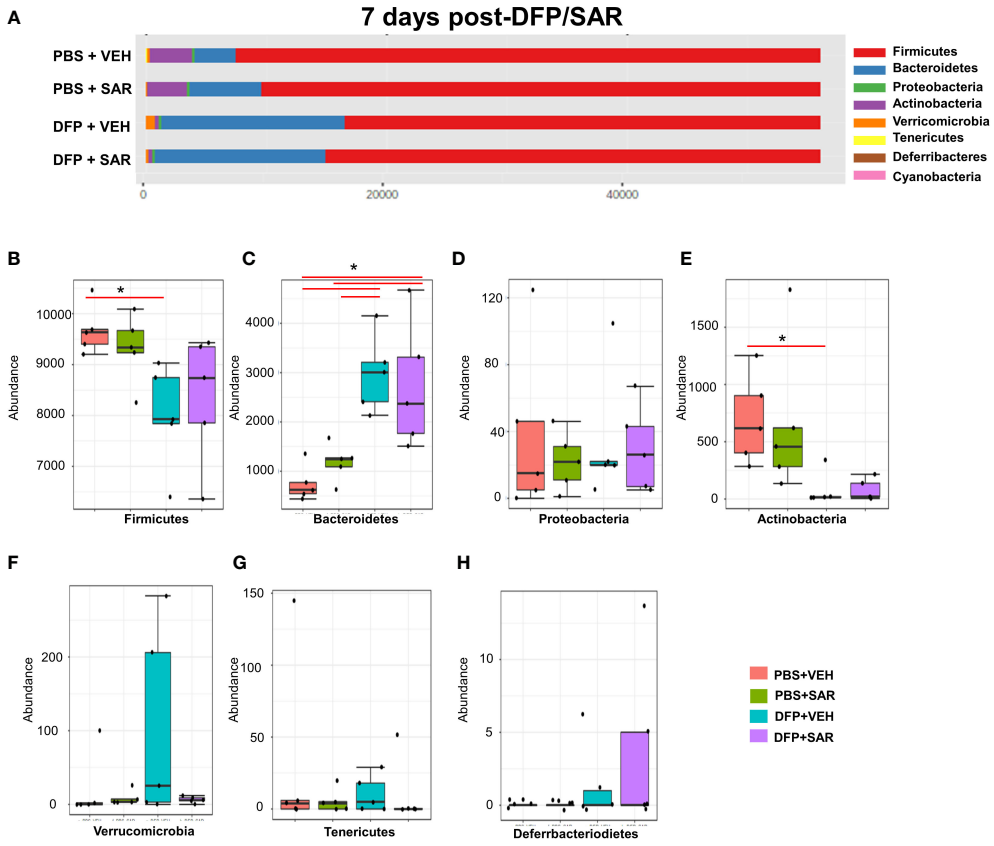

FIGURE 4
Impact of DFP and SAR on the phyla level at 7 days post-exposure. **(A)** Overall changes in actual abundance in phyla. **(B–I)** Actual abundance by phyla for *Firmicutes* **(B)**, *Bacteroidetes* **(C)**, *Proteobacteria* **(D)**, *Actinobacteria* **(E)**, *Verricomicrobia* **(F)**, *Tenericutes* **(G)**, *Deferrbacteriodietes* **(H)**. ANOVA or Kruskal Wallis test, *p < 0.05, n=4-5.

are capable of OP metabolism. Interestingly, in the soman study (Getnet et al., 2018), the change in phyla was dependent upon the initial seizure response to soman which suggests that the gut dysbiosis is more dependent on the gut-brain axis rather than the administration of the organophosphate itself. In our study, all the animals had at least 20 minutes CS during SE, so we were not able to discriminate between the effects of seizures and the impact of DFP. Future studies could determine the impact of SE severity and duration on gut dysbiosis.

On a phyla level, it appears that in the short-term (48 hours), increase in *Proteobacteria* and decrease in *Firmicutes* are primarily responsible for gut dysbiosis. Increase in the abundance of *Proteobacteria* is considered to be a microbial signature of dysbiosis and is implicated in a wide variety of diseases, especially in those involving inflammation or metabolic dysfunction (Shin et al., 2015; Rizzatti et al., 2017). *Proteobacteria* are one of the most abundant phyla and are comprised of organisms with varying physiology (Shin et al., 2015). Upon analysis at the genus level, we found that the *Proteobacteria* increase in the DFP treated animals included *Escherichia*. Certain strains of *Escherichia* can act as an intestinal pathogen and could contribute to the poor health of the animals. In this study, in the days immediately following DFP intoxication there was the loss in bodyweight in the first 2-3 days post intoxication.

Firmicutes are thought to primarily be involved in fermenting short-chain fatty acids which impact the function of the intestinal barrier (Stojanov et al., 2020). The ratio of *Firmicutes* to *Bacteroidetes* has been implicated in several other diseases including obesity, inflammatory bowel syndrome, and major depressive disorder (Huang et al., 2018; Magne et al., 2020; Stojanov et al., 2020). In DFP-treated animals, there was a reduction in *Firmicutes* at 48 hours but an increase in the *Streptococcus* genera. There was a decrease in the *Lactobacillus* and *Oscillospira* genera, which have both been implicated as possible therapeutic targets *via* probiotics in other diseases (Di Cerbo et al., 2016; Yang et al., 2021). Possibly this phylum may be a therapeutic target too in OP intoxication as an adjunct therapy to mitigate DFP-induced gut dysbiosis.

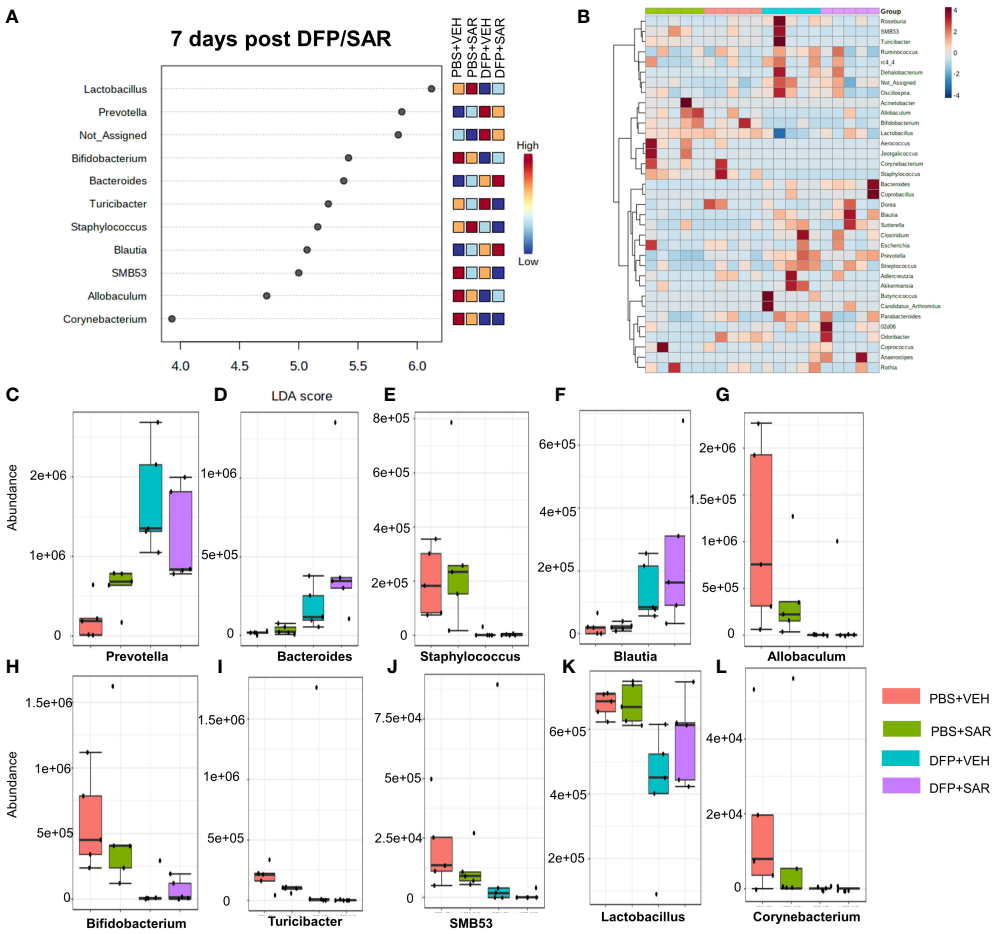

FIGURE 5
Impact of DFP and SAR on the genus level at 7 days post-exposure. **(A)** LEfSe analysis reveals genera with LDA scores above 2.0. **(B)** Heatmap clustering by genus. **(C–L)**. Trends in actual abundance of the seven genera with an overall $p < 0.05$, n=4-5.

Unlike the increase in *Proteobacteria*, the decrease in *Firmicutes* persisted at day 7 post-DFP. Interestingly, the LEfSe analysis revealed a reduction in *Staphylococcus* at 7 days in contrast to 48 hours post exposure. There was also a reduction in *Allobaculum, Lactobacillus, SMB53*, and *Turibacter*. There was also an increase in the *Bacteroidetes* phylum and reduction in *Actinobacteria*. *Bacteroidetes* are most well-known to be involved in the degradation of biopolymers in the intestine (Thomas et al., 2011). Based on the LEfSe analysis, the increase in *Bacteroidetes* seemed to be primarily driven by the increase in *Prevotella* and *Bacteroides* which are both implicated in health and disease (Su et al., 2018; Zafar and Saier, 2021). *Actinobacteria*, though less abundant than *Bacteroidetes* and *Firmicutes*, play an important role in gut homeostasis and are involved in a variety of processes including biotransformation, lipid and nutrient metabolism (Binda et al., 2018). It appears that the most highly affected *Actinobacteria* include *Bifidobacterium* and *Corynebacterim*. Like *Firmicutes, Actinobacteria* have also been the target of probiotics in disease (Binda et al., 2018).

Many of the changes we observed at 7 days were similar to those in previous studies of chronic exposure to less potent OPs such as those found in pesticides (Roman et al., 2019; Giambò et al., 2021). In a chlorpyrifos study, exposure during the gestational period led to alterations in the intestinal villi and changes in the microbiome composition with a reduction in *Lactobacillus* (Condette et al., 2015). Another chronic exposure study in mice, administered chlorpyrifos for 30 days and found a significant increase in the abundance of *Bacteroidetes* and significant decrease in the abundance of *Firmicutes* (Zhao et al., 2016). In an *in vitro* model of the human gut, an increase in *Bacteroides* and a reduction in *Bifidobacteria* have been reported (Reygner et al., 2016). Chronic oral administration of chlorpyrifos in various species led to gut microbiome changes in a diet dependent manner (Fang et al.,

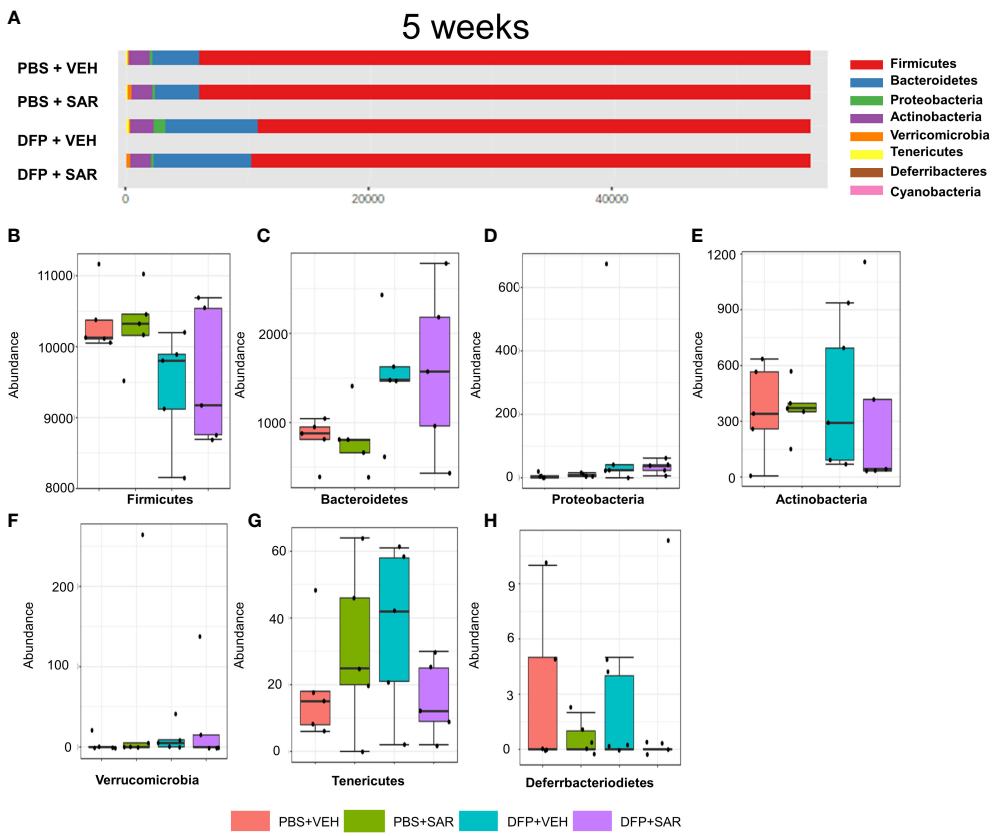

FIGURE 6
Impact of DFP and SAR on the phyla level at 5 weeks post-exposure. **(A)** Overall changes in phyla actual abundance. **(B–I)** Actual abundance by phyla for *Firmicutes* **(B)**, *Bacteroidetes* **(C)**, *Proteobacteria* **(D)**, *Actinobacteria* **(E)**, *Verricomicrobia* **(F)**, *Tenericutes* **(G)**, *Deferrbacteriodietes* **(H)**. ANOVA or Kruskal Wallis test, n=4-5.

2018). Notably, most of these studies did not report the dramatic increase in *Proteobacteria* that observed in 48-hour group in this study, and in soman study (11), suggesting that a high dose of OP that induces seizures is required for this type of gut dysbiosis.

Importantly, with the exception of a few genera, there were minimal taxonomic changes 5 weeks post-DFP intoxication similar to the soman study which reported that taxonomic changes were negligible 75 days post-exposure (Getnet et al., 2018). As we have shown in previous studies, DFP-induced SE leads to the development of spontaneous recurrent seizures in most of the animals (Puttachary et al., 2016; Putra et al., 2020a). Although we did not utilize telemetry devices in these animals to monitor seizures, it is likely that these animals may have been experiencing spontaneous seizures by 5 weeks. Thus, our data would suggest that gut dysbiosis is not contributing to the initiation of seizures during an epileptic phase. In contrast, a study in children with epilepsy found a unique microbial signature that might contribute to drug resistance which might suggest that the microbiome component may be model dependent (Ceccarani et al., 2021). Future studies will further investigate the relationship between gut dysbiosis and spontaneous recurrent seizures in this rodent model.

We also found changes in microbial diversity at 48 hours and 7 days post intoxication which did not persist at 5 weeks. Loss of microbial diversity is generally considered to be indicative of compromised health (Mosca et al., 2016; Eisenstein, 2020). Alpha diversity measures intra-sample diversity while beta diversity measures inter-sample diversity. In our study, DFP treated animals had reduced alpha diversity at 48 hours using the observed, chao1, ACE and Fisher metrics of which the first three only take abundance into account which would suggest that the alpha diversity changes are primarily concerned with abundance rather than evenness (Willis, 2019). Fisher's alpha diversity takes into account the number of species as well as the number of individuals in those species (Fisher et al., 1943). Although there were no statistical differences in alpha diversity at later timepoints, it did appear that the change in Beta diversity persisted at 7 days but not at 5 weeks which agrees with the significant changes we observed at the phylogenetic level.

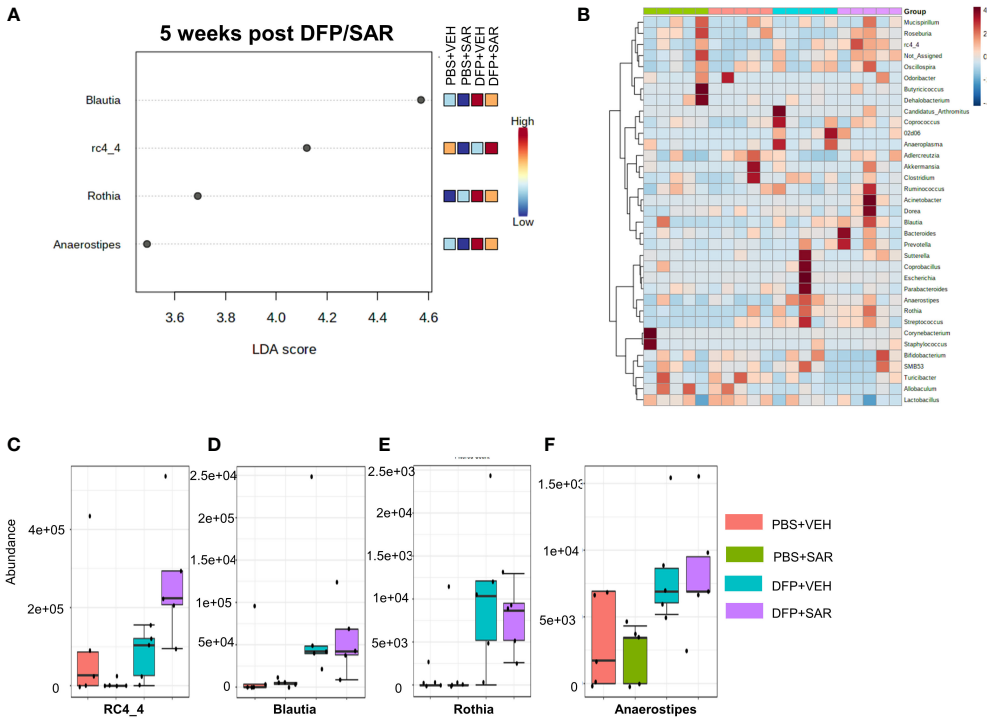

FIGURE 7
Impact of DFP and SAR on the genus level at 5 weeks post-exposure. **(A)** LEfSe analysis reveals genera with LDA scores above 2.0. **(B)** Heatmap clustering by genus. **(C–F)** Trends in actual abundance of the seven genera with an overall p-value<0.05, n=4-5.

Although it is important to understand the impact of acute OP nerve agent toxicity, our study also examined the impact of an orally active disease modifier, SAR, in mediating gut dysbiosis. We thought that the changes in the gut microbiome could influence the metabolism or efficacy of any orally administered disease modifier. It is known that SAR is bioactivated by cytochrome P450, a drug metabolizing enzymes that is known to be expressed in some bacteria (Murphy, 2015; Chen et al., 2016). SAR is a potent inhibitor of src family kinases which have been implicated in various neurological diseases such as Alzheimer's disease, Parkinson's disease, and epilepsy (Green et al., 2009; Nygaard, 2018; Panicker et al., 2019; Putra et al., 2020b; Sharma et al., 2021). We have previously tested SAR in the DFP model and found that, depending on the initial SE severity, early administration can mitigate the epileptogenic markers such as seizures, neuroinflammation and neurodegeneration (Gage et al., 2021a; Gage et al., 2021b). Although we did not quantify, in our previous experiments we occasionally observed increased prevalence of diarrhea in the SAR treated animals with higher doses that were also challenged with DFP which led to some concerns on how higher doses of SAR might have influenced the gut microbiome. Importantly, in this study we did not observe many changes in gut microbiome between the vehicle and the SAR treated groups suggesting that SAR at optimal dose *via* oral route is safe.

In this study, we were able to successfully determine the impact of DFP and SAR on gut dysbiosis. Future studies could further address dysbiosis in this model by considering other factors such as sex and age as both are well known to impact the gut microbiome (Kim et al., 2020; Bosco and Noti, 2021). Also of interest, it is also well known that prolonged seizures, induced by DFP and other chemoconvulsants, impact both cognitive function and motor ability (Hernandez et al., 2002; Holmes, 2015; Helmstaedter and Witt, 2017; Guignet et al., 2019; Putra et al., 2020b). As cognition and motor ability are also associated with the gut microbiome (Sampson et al., 2016; Meyer et al., 2022), it would be interesting to explore their relationship in the DFP model. However, in the DFP model, animals were morbid (required 5-7 days to recover their bodyweight, some animals had spontaneous seizures while handling) (Gage et al., 2021b). Therefore, conducting behavioral tests to determine the early effects of gut dysbiosis was not feasible in this study. However, it is possible that the short-term dysbiosis observed in this study

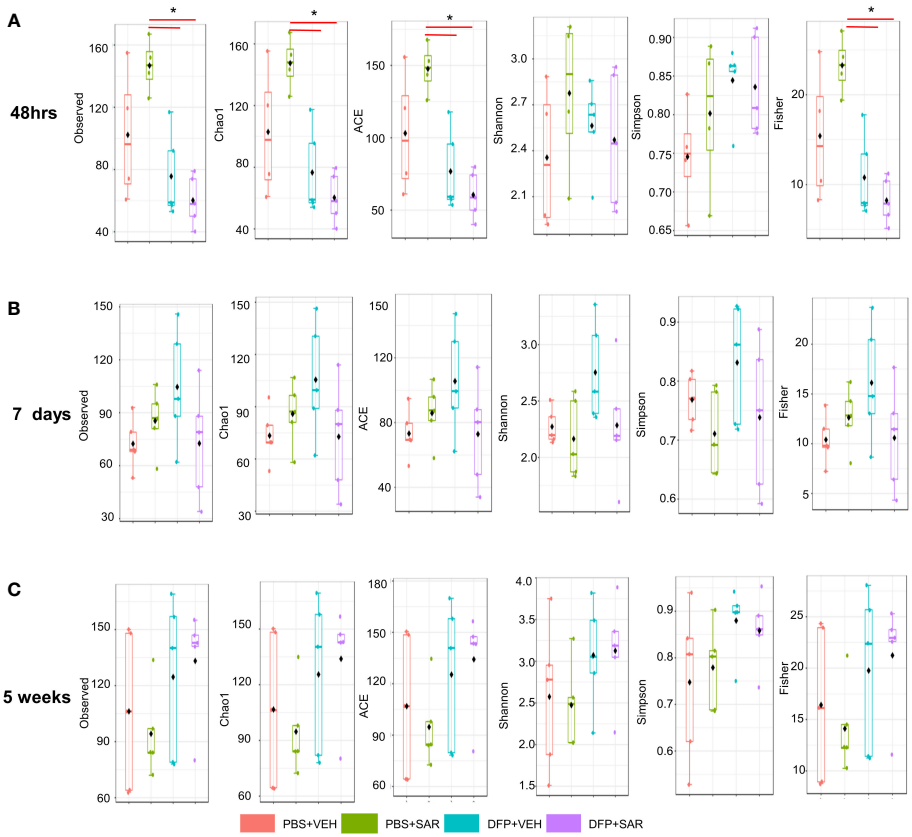

FIGURE 8
Alpha Diversity. Alpha diversity was measured using several metrics including observed, chao1, ACE, Shannon, Simpson, and Fisher at 48 hours **(A)**, 7 days **(B)** and 5 weeks **(C)** post-exposure, ANOVA or Kruskal Wallis test, *p < 0.05, n=4-5.

could contribute to long-term neurobehavioral deficits. Changes in metabolites are also common to both gut dysbiosis and chemoconvulsant-induced epilepsy (Meldrum and Chapman, 1999; Agus et al., 2021). For example, in a recent study, we observed an increased concentration of cresols and alterations in dopaminergic neurotransmission within two days of induction of gut dysbiosis and the resultant secondary proliferation of major cresol-producing bacteria (Vinithakumari et al., 2022). In addition, acute gut permeability changes could increase serum toxic metabolite concentrations (Chakaroun et al., 2020; Ghosh et al., 2020; Ma et al., 2022). It would be interesting to investigate in future studies whether gut-induced changes in critical metabolites contribute to the toxicity caused by OPNAs. It is also important to consider whether the findings in this study are translatable to humans. Although there is no data on the microbiome of humans exposed to OPNAs, pesticides have been implicated in altering the human gut microbiome, mostly using *in vitro* studies (Utembe and Kamng'ona, 2021). It is likely that our findings in rats exposed to DFP might translate to humans exposed to OPNAs.

5 Conclusion

The purpose of the current study was to determine the overall impact of the OP, DFP and the disease modifier, SAR on the gut microbiome. We found that DFP-induced dysbiosis at 48 hours and 7 days were no longer prevalent at 5 weeks post intoxication. We also observed expected changes in alpha and beta diversities. Interestingly, SAR did not affect DFP-induced gut microbiome changes which are required to metabolize DFP. Importantly the function of many of these gut-microbiota is diverse and there are several unknowns about the role of each bacterium in OP-induced gut motility, localized gut immunity, and absorption. As research progresses in the gut microbiome field, we might better understand how these microorganisms are

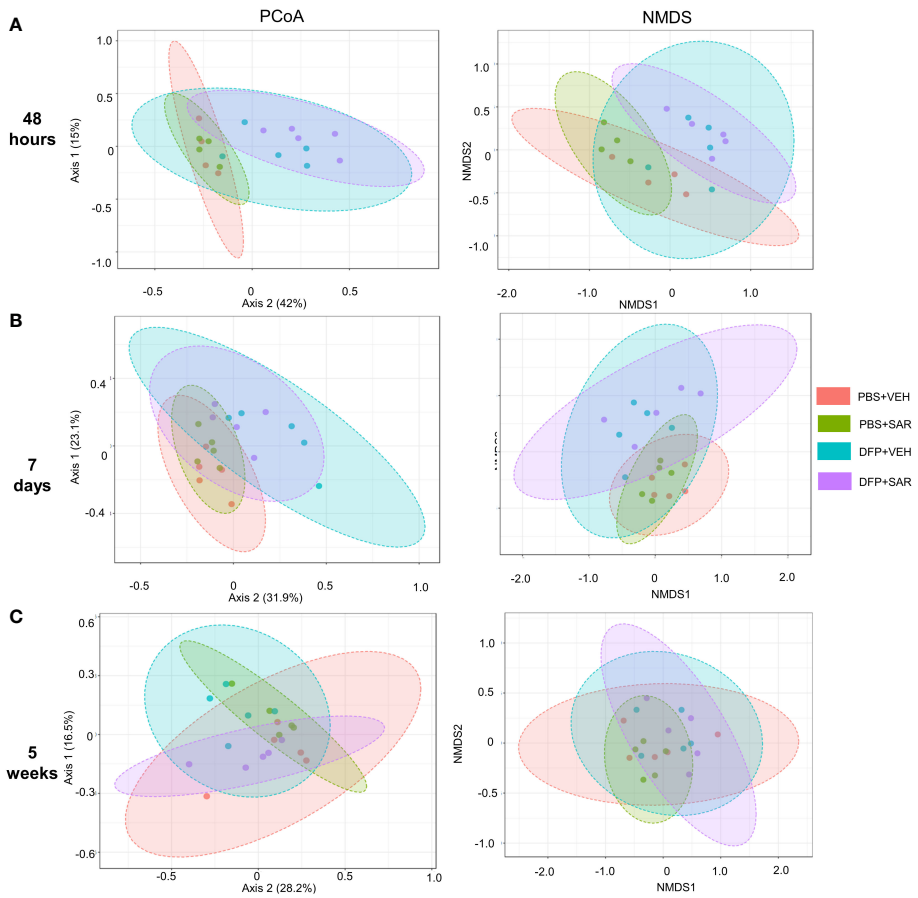

FIGURE 9
Beta diversity. Beta diversity was assed using principle coordinate analysis (PCoA) and multidimensional scaling (NMDS) at 48 hours **(A)**, 7 days **(B)** and 5 weeks **(C)** post-exposure.

contributing to health and epileptogenesis following OP intoxication. Targeting changes in the gut microbiome at an appropriate time might be a future therapeutic approach to improve the efficacy of orally acting drugs.

Data availability statement

The datasets presented in this study can be found in online repositories. The names of the repository/repositories and accession number(s) can be found below: BioProject, accession number PRJNA865374.

Ethics statement

This study was reviewed and approved by Iowa State Institutional Animal Care and Use Committee.

Author contributions

Authors contribution: MG performed the animal experiments, analyzed data, and drafted the manuscript. AV analyzed the data *via* QiimeII and MicrobiomeAnalyst. SM and TT edited the manuscript and oversaw the study. All authors contributed to the article and approved the submitted version.

Funding

The DFP-SAR project is supported by the NINDS CounterACT program (U01NS117284, NS110648) and microbiome aspect of the project was supported by the Dean Faculty Fellowship to TT. AstraZeneca supplied saracatinib for this study under the Open Innovation Program.

Conflict of interest

The authors declare that the research was conducted in the absence of any commercial or financial relationships that could be construed as a potential conflict of interest.

Publisher's note

All claims expressed in this article are solely those of the authors and do not necessarily represent those of their affiliated organizations, or those of the publisher, the editors and the reviewers. Any product that may be evaluated in this article, or claim that may be made by its manufacturer, is not guaranteed or endorsed by the publisher.

Supplementary material

The Supplementary Material for this article can be found online at: https://www.frontiersin.org/articles/10.3389/frmbi.2022.1006078/full#supplementary-material

References

Agus, A., Clément, K., and Sokol, H. (2021). Gut microbiota-derived metabolites as central regulators in metabolic disorders. *Gut* 70 (6), 1174–1182. doi: 10.1136/GUTJNL-2020-323071

Baselga, J., Cervantes, A., Martinelli, E., Chirivella, I., Hoekman, K., Hurwitz, H. I., et al. (2010). Phase I safety, pharmacokinetics, and inhibition of src activity study of saracatinib in patients with solid tumors. *Clin. Cancer Res.* 16 (19), 4876–4883. doi: 10.1158/1078-0432.CCR-10-0748

Binda, C., Lopetuso, L. R., Rizzatti, G., Gibiino, G., Cennamo, V., and Gasbarrini, A. (2018). Actinobacteria: A relevant minority for the maintenance of gut homeostasis. *Digest. Liver Dis.* 50 (5), 421–428. doi: 10.1016/J.DLD.2018.02.012

Bolyen, E., Rideout, J. R., Dillon, M. R., Bokulich, N. A., Abnet, C. C., Al-Ghalith, G. A., et al. (2019). Reproducible, interactive, scalable and extensible microbiome data science using QIIME 2. *Nat. Biotechnol.* 37 (8), 852–857. doi: 10.1038/S41587-019-0209-9

Bosco, N., and Noti, M. (2021). The aging gut microbiome and its impact on host immunity. *Genes Immun. 2021 22:5* 22 (5), 289–303. doi: 10.1038/s41435-021-00126-8

Carabotti, M., Scirocco, A., Maselli, M. A., and Severi, C. (2015). The gut-brain axis: interactions between enteric microbiota, central and enteric nervous systems. *Ann. Gastroenterology : Q. Publ. Hellenic Soc. Gastroenterol.* 28 (2), 203.

Ceccarani, C., Viganò, I., Ottaviano, E., Redaelli, M. G., Severgnini, M., Vignoli, A., et al. (2021). 'Is gut microbiota a key player in epilepsy onset? a longitudinal study in drug-naive children'. *Front. Cell. Infection Microbiol.* 11, 1231. doi: 10.3389/FCIMB.2021.749509/BIBTEX

Chakaroun, R. M., Massier, L., and Kovacs, P. (2020). Gut microbiome, intestinal permeability, and tissue bacteria in metabolic disease: Perpetrators or bystanders? *Nutrients* 12 (4). doi: 10.3390/NU12041082

Chen, J., Peng, Y., and Zheng, J. (2016). Cytochrome P450 mediated bioactivation of saracatinib. *Chem. Res. Toxicol.* 29 (11), 1835–1842. doi: 10.1021/ACS.CHEMRESTOX.6B00242

Chong, J., Liu, P., Zhou, G., and Xia, J. (2020). Using MicrobiomeAnalyst for comprehensive statistical, functional, and meta-analysis of microbiome data. *Nat. Protoc.* 15 (3), 799–821. doi: 10.1038/S41596-019-0264-1

Condette, C., Bach, V., Mayeur, C., Gay-Quéheillard, J., and Khorsi-Cauet, H. (2015). Chlorpyrifos exposure during perinatal period affects intestinal microbiota associated with delay of maturation of digestive tract in rats. *J. Pediatr. Gastroenterol. Nutr.* 61 (1), 30–40. doi: 10.1097/MPG.0000000000000734

Deshpande, L. S., Carter, D. S., Blair, R. E., and DeLorenzo, R. J. (2010). Development of a prolonged calcium plateau in hippocampal neurons in rats surviving status epilepticus induced by the organophosphate diisopropylfluorophosphate. *Toxicol. Sci.* 116 (2), 623–631. doi: 10.1093/toxsci/kfq157

Di Cerbo, A., Palmieri, B., Aponte, M., Morales-Medina, J. C., and Iannitti, T. (2016). 'Mechanisms and therapeutic effectiveness of lactobacilli'. *J. Clin. Pathol.* 69 (3), 187. doi: 10.1136/JCLINPATH-2015-202976

Eisenstein, M. (2020). The hunt for a healthy microbiome. *Nature* 577 (7792). doi: 10.1038/D41586-020-00193-3

Fang, B., Li, J. W., Zhang, M., Ren, F. Z., and Pang, G. F. (2018). Chronic chlorpyrifos exposure elicits diet-specific effects on metabolism and the gut microbiome in rats. *Food Chem. Toxicol.* 111, 144–152. doi: 10.1016/J.FCT.2017.11.001

Fisher, R. A., Corbet, A. S., and Williams, C. B. (1943). 'The relation between the number of species and the number of individuals in a random sample of an animal population'. *J. Anim. Ecol.* 12 (1), 42–58.

Flannery, B. M., Bruun, D. A., Rowland, D. J., Banks, C. N., Austin, A. T., Kukis, D. L., et al. (2016). Persistent neuroinflammation and cognitive impairment in a rat model of acute diisopropylfluorophosphate intoxication. *J. Neuroinflamm.* 13 (1), 267. doi: 10.1186/s12974-016-0744-y

French, J. A. (2007). 'Refractory epilepsy: Clinical overview'. *Epilepsia* 48(suppl. 1), 3–7. doi: 10.1111/j.1528-1167.2007.00992.x

Gage, M., Putra, M., Estrada, C. G., Golden, M., Wachter, L., Gard, M., et al. (2021a). Differential impact of severity and duration of status epilepticus, medical countermeasures, and a disease-modifier, saracatinib (AZD0530), on brain regions in the rat diisopropylfluorophosphate (DFP) model. *Front. Cell. Neurosci.* 0, 426. doi: 10.3389/FNCEL.2021.772868

Gage, M., Putra, M., Wachter, L., Dishman, K., Gard, M., Gomez-Estrada, C., et al. (2021b). 'Saracatinib, a src tyrosine kinase inhibitor, as a disease modifier in the rat DFP model: Sex differences, neurobehavior, gliosis, neurodegeneration, and nitro-oxidative stress'. *Antioxidants* 11 (1), 61. doi: 10.3390/ANTIOX11010061

Getnet, D., Gautam, A., Kumar, R., Hoke, A., Cheema, A. K., Rossetti, F., et al. (2018). Poisoning with soman, an organophosphorus nerve agent, alters fecal bacterial biota and urine metabolites: a case for novel signatures for asymptomatic nerve agent exposure. *Appl. Environ. Microbiol.* 84 (21). doi: 10.1128/AEM.00978-18

Ghosh, S. S., Wang, J., Yannie, P. J., and Ghosh, S. (2020). Intestinal barrier dysfunction, LPS translocation, and disease development. *J. Endoc. Soc.* 4 (2). doi: 10.1210/JENDSO/BVZ039

Giambò, F., Teodoro, M., Costa, C., and Fenga, C. (2021). Toxicology and microbiota: How do pesticides influence gut microbiota? a review. *Int. J. Environ. Res. Public Health* 18 (11). doi: 10.3390/IJERPH18115510

Green, T. P., Fennell, M., Whittaker, R., Curwen, J., Jacobs, V., Allen, J., et al. (2009). Preclinical anticancer activity of the potent, oral src inhibitor AZD0530. *Mol. Oncol.* 3 (3), 248–261. doi: 10.1016/j.molonc.2009.01.002

Guignet, M., Dhakal, K., Flannery, B. M., Hobson, B. A., Zolkowska, D., Dhir, A., et al. (2019). Persistent behavior deficits, neuroinflammation, and oxidative stress in a rat model of acute organophosphate intoxication. *Neurobiol. Dis* V133 (104431). doi: 10.1016/j.nbd.2019.03.019

Helmstaedter, C., and Witt, J. A. (2017). Epilepsy and cognition – a bidirectional relationship? *Seizure* 49, 83–89. doi: 10.1016/J.SEIZURE.2017.02.017

Hernandez, M. T., Sauerwein, H. C., Jambaqué, I., De Guise, E., Lussier, F., Lortie, A., et al. (2002). Deficits in executive functions and motor coordination in children with frontal lobe epilepsy. *Neuropsychologia* 40 (4), 384–400. doi: 10.1016/S0028-3932(01)00130-0

Hills, R. D., Pontefract, B. A., Mishcon, H. R., Black, C. A., Sutton, S. C., and Theberge, C. R. (2019). Gut microbiome: Profound implications for diet and disease. *Nutrients* 11 (7). doi: 10.3390/NU11071613

Holmes, G. L. (2015). Cognitive impairment in epilepsy: The role of network abnormalities. *Epileptic Disord.* 17 (2), 101. doi: 10.1684/EPD.2015.0739

Huang, Y., Shi, X., Li, Z., Shen, Y., Shi, X., Wang, L., et al. (2018). Possible association of firmicutes in the gut microbiota of patients with major depressive disorder. *Neuropsychiatr. Dis. Treat* 14, 3329. doi: 10.2147/NDT.S188340

Irwin, S. (1968). Comprehensive observational assessment: Ia. a systematic, quantitative procedure for assessing the behavioral and physiologic state of the mouse. *Psychopharmacologia* 13 (3), 222–257. doi: 10.1007/BF00401402

Jett, D. A. (2007). Neurological aspects of chemical terrorism. *Ann. Neurol.* 61 (1), 9–13. doi: 10.1002/ana.21072

Jett, D. A. (2012). Chemical toxins that cause seizures. *Neurotoxicology* 33 (6), 1473–1475. doi: 10.1016/j.neuro.2012.10.005

Karpouzas, D. G., and Singh, B. K. (2006). Microbial degradation of organophosphorus xenobiotics: metabolic pathways and molecular basis. *Adv. microbial Physiol.* 51 (SUPPL.). doi: 10.1016/S0065-2911(06)51003-3

Kaufman, A. C., Salazar, S. V., Haas, L. T., Yang, J., Kostylev, M. A., Jeng, A. T., et al. (2015). Fyn inhibition rescues established memory and synapse loss in Alzheimer mice. *Ann. Neurol.* 77 (6), 953–971. doi: 10.1002/ana.24394

Kilkenny, C., Browne, W. J., Cuthill, I. C., Emerson, M., and Altman, D. G. (2010). Improving bioscience research reporting: The ARRIVE guidelines for reporting animal research. *PloS Biol.* 8 (6), e1000412. doi: 10.1371/journal.pbio.1000412

Kim, Y. S., Unno, T., Kim, B. Y., and Park, M. S. (2020). Sex differences in gut microbiota. *World J. Men's Health* 38 (1), 48. doi: 10.5534/WJMH.190009

Kozich, J. J., Westcott, S. L., Baxter, N. T., Highlander, S. K., and Schloss, P. D. (2013). Development of a dual-index sequencing strategy and curation pipeline for analyzing amplicon sequence data on the MiSeq illumina sequencing platform. *Appl. Environ. Microbiol.* 79 (17), 5112–5120. doi: 10.1128/AEM.01043-13

Lim, D. K., Hoskins, B., and Ho, I. K. (1983). Assessment of diisopropylfluorophosphate (DFP) toxicity and tolerance in rats. *Res. Commun. Chem. Pathol. Pharmacol.* 39 (3), 399–418.

Luo, X.-M., Zhao, J., Wu, W.-Y., Fu, J., Li, Z.-Y., Zhang, M., et al. (2021). Post-status epilepticus treatment with the fyn inhibitor, saracatinib, improves cognitive function in mice. *BMC Neurosci.* 22 (1), 1–8. doi: 10.1186/S12868-020-00606-Z

Magne, F., Gotteland, M., Gauthier, L., Zazueta, A., Pesoa, S., Navarrete, P., et al. (2020). The Firmicutes/Bacteroidetes ratio: A relevant marker of gut dysbiosis in obese patients? *Nutrients* 12 (5). doi: 10.3390/NU12051474

Ma, Y., Liu, X., and Wang, J. (2022). Small molecules in the big picture of gut microbiome-host cross-talk. *eBioMedicine* 81, 104085. doi: 10.1016/j.ebiom.2022.104085

Martin, M. (2011). Cutadapt removes adapter sequences from high-throughput sequencing reads. *EMBnet.journal* 17 (1), 10–12. doi: 10.14806/EJ.17.1.200

Meldrum, B., and Chapman, A. (1999) *'Metabolic consequences of seizures'*. Available at: https://www.ncbi.nlm.nih.gov/books/NBK28033/ (Accessed 14 September 2022).

Meyer, K., Lulla, A., Debroy, K., Shikany, J. M., Yaffe, K., Meirelles, O., et al. (2022). Association of the gut microbiota with cognitive function in midlife. *JAMA Network Open* 5 (2), e2143941–e2143941. doi: 10.1001/JAMANETWORKOPEN.2021.43941

Mooyottu, S., Flock, G., Upadhyay, A., Upadhyaya, I., Maas, K., and Venkitanarayanan, K. (2017). Protective effect of carvacrol against gut dysbiosis and clostridium difficile associated disease in a mouse model. *Front. Microbiol.* 8, 625. doi: 10.3389/fmicb.2017.00625

Morita, H., Yanagisawa, N., Nakajima, T., Shimizu, M., Hirabayashi, H., Okudera, H., et al. (1995). Sarin poisoning in Matsumoto, Japan. *Lancet (London England)* 346 (8970), 290–293.

Mosca, A., Leclerc, M., and Hugot, J. P. (2016). Gut microbiota diversity and human diseases: Should we reintroduce key predators in our ecosystem? *Front. Microbiol.* 7, 455. doi: 10.3389/FMICB.2016.00455/BIBTEX

Mukherjee, S., and Gupta, R. D. (2020). Organophosphorus nerve agents: Types, toxicity, and treatments. *J. Toxicol. Hindawi Limit.* 2020, 3007984 doi: 10.1155/2020/3007984

Murphy, C. D. (2015). Drug metabolism in microorganisms. *Biotechnol. Lett.* 37 (1), 19–28. doi: 10.1007/S10529-014-1653-8

Nie, L., Ye, W.-R., Chen, S., Chirchiglia, D., and Wang, M. (2020). Src family kinases in the central nervous system: Their emerging role in pathophysiology of migraine and neuropathic pain. *Curr. Neuropharmacol.* 19 (5), 665–678. doi: 10.2174/1570159X18666200814180218

Nygaard, H. B. (2018). Targeting fyn kinase in alzheimer's disease. *Biol. Psychiatry*, 369–376. doi: 10.1016/j.biopsych.2017.06.004

Okumura, T., Suzuki, K., Fukuda, A., Kohama, A., Takasu, N., Ishimatsu, S., et al. (1998). The Tokyo subway sarin attack: Disaster management, part 1: Community emergency response. *Acad. Emergency Med.* 5 (6), 613–617. doi: 10.1111/j.1553-2712.1998.tb02470.x

Panicker, N., Kanthasamy, A., and Kanthasamy, A. G. (2019). Fyn amplifies NLRP3 inflammasome signaling in parkinson's disease. *Aging* 11(16), 5871–5873. doi: 10.18632/aging.102210

Panther, E. J., Dodd, W., Clark, A., and Lucke-Wold, B. (2022). Gastrointestinal microbiome and neurologic injury. *Biomedicines* 10 (2). doi: 10.3390/BIOMEDICINES10020500

Putra, M., Sharma, S., Gage, M., Gasser, G., Hinojo-Perez, A., Olson, A., et al. (2020c). Inducible nitric oxide synthase inhibitor 1400W, mitigates DFP-induced long-term neurotoxicity in the rat model. *Neurobiol. Dis.* 133. doi: 10.1016/j.nbd.2019.03.031

Putra, M., Gage, M., Sharma, S., Gardner, C., Gasser, G., Anantharam, V., et al. (2020a). Diapocynin, an NADPH oxidase inhibitor, counteracts diisopropylfluorophosphate-induced long-term neurotoxicity in the rat model. *Ann. New York Acad. Sci.*, nyas.14314. doi: 10.1111/nyas.14314

Putra, M., Puttachary, S., Liu, G., Lee, G., and Thippeswamy, T. (2020b). Fyn-tau ablation modifies PTZ-induced seizures and post-seizure hallmarks of early epileptogenesis. *Front. Cell. Neurosci.* 14, 592374. doi: 10.3389/fncel.2020.592374

Puttachary, S., Sharma, S., Verma, S., Yang, Y., Putra, M., Thippeswamy, A., et al. (2016). 1400W, a highly selective inducible nitric oxide synthase inhibitor is a potential disease modifier in the rat kainate model of temporal lobe epilepsy. *Neurobiol. Dis.* 93, 184–200. doi: 10.1016/j.nbd.2016.05.013

Racine, R. J. (1972). 'Modification of seizure activity by electrical stimulation. II. motor seizure'. *Electroencephalograph Clin. Neurophysiol.* 32 (3), 281–294.

Reygner, J., Condette, C. J., Bruneau, A., Delanaud, S., Rhazi, L., Depeint, F., et al. (2016). Changes in composition and function of human intestinal microbiota exposed to chlorpyrifos in oil as assessed by the SHIME® model. *Int. J. Environ. Res. Public Health* 13 (11). doi: 10.3390/IJERPH13111088

Rizzatti, G., Lopetuso, L. R., Gibiino, G., Binda, C., and Gasbarrini, A. (2017). Proteobacteria: A common factor in human diseases. *BioMed. Res. Int.* 2017. doi: 10.1155/2017/9351507

Rojas, A., Wang, W., Glover, A., Manji, Z., Fu, Y., and Dingledine, R. (2018). Beneficial outcome of urethane treatment following status epilepticus in a rat organophosphorus toxicity model. *eNeuro* 5 (2). doi: 10.1523/ENEURO.0070-18.2018

Roman, P., Cardona, D., Sempere, L., and Carvajal, F. (2019). Microbiota and organophosphates. *NeuroToxicology* 75, 200–208. doi: 10.1016/J.NEURO.2019.09.013

Sampson, T. R., Debelius, J. W., Thron, T., Janssen, S., Shastri, G. G., Ilhan, Z. E., et al. (2016). Gut microbiota regulate motor deficits and neuroinflammation in a model of parkinson's disease. *Cell* 167 (6), 1469. doi: 10.1016/J.CELL.2016.11.018

Sharma, S., Carlson, S., Gregory-Flores, A., Hinojo-Perez, A., Olson, A., and Thippeswamy, T. (2018). Role of the fyn-PKCδ signaling in SE-induced neuroinflammation and epileptogenesis in experimental models of temporal lobe epilepsy. *Neurobiol. Dis.* 110, 102–121. doi: 10.1016/j.nbd.2017.11.008

Sharma, S., Carlson, S., Puttachary, S., Sarkar, S., Showman, L., Putra, M., et al. (2021). Mechanisms of disease-modifying effect of saracatinib (AZD0530), a Src/Fyn tyrosine kinase inhibitor, in the rat kainate model of temporal lobe epilepsy. *Neurobiol. Dis.* 156, 105410. doi: 10.1016/j.nbd.2021.105410

Shin, N. R., Whon, T. W., and Bae, J. W. (2015). Proteobacteria: microbial signature of dysbiosis in gut microbiota. *Trends Biotechnol.* 33 (9), 496–503. doi: 10.1016/J.TIBTECH.2015.06.011

Smith, L. M., Zhu, R., and Strittmatter, S. M. (2018). Disease-modifying benefit of fyn blockade persists after washout in mouse alzheimer's model. *Neuropharmacology* 130, 54–61. doi: 10.1016/j.neuropharm.2017.11.042

Stojanov, S., Berlec, A., and Štrukelj, B. (2020). 'The influence of probiotics on the Firmicutes/Bacteroidetes ratio in the treatment of obesity and inflammatory bowel disease'. *Microorganisms* 8 (11), 1715. doi: 10.3390/MICROORGANISMS8111715

Su, T., Liu, R., Lee, A., Long, Y., Du, L., Lai, S., et al. (2018). Altered intestinal microbiota with increased abundance of prevotella is associated with high risk of diarrhea-predominant irritable bowel syndrome. *Gastroenterol. Res. Pract.* 2018. doi: 10.1155/2018/6961783

Thomas, F., Hehemann, J. H., Rebuffet, E., Czjzek, M., and Michel, G. (2011). Environmental and gut bacteroidetes: The food connection. *Front. Microbiol.* 2, 93. doi: 10.3389/FMICB.2011.00093/BIBTEX

Tucker, J. B. (1996). Chemical/biological terrorism: Coping with a new threat. *Politics Life Sci.* 15 (2), 167–183. doi: 10.1017/S073093840002270X

Utembe, W., and Kamng'ona, A. W. (2021). Gut microbiota-mediated pesticide toxicity in humans: Methodological issues and challenges in the risk assessment of pesticides. *Chemosphere* 271, 129817. doi: 10.1016/J.CHEMOSPHERE.2021.129817

Vinithakumari, A. A., Padhi, P., Hernandez, B., Lin, S. J.-H., Dunkerson-Kurzhumov, A., Showman, L., et al. (2022). Clostridioides difficile infection dysregulates brain dopamine metabolism. *Microbiol. Spectr.* 10 (2). doi: 10.1128/SPECTRUM.00073-22/ASSET/2FCE37ED-FF7B-44FE-824A-A8BE59B0EF29/ASSETS/IMAGES/MEDIUM/SPECTRUM.00073-22-F005.GIF

Willis, A. D. (2019). Rarefaction, alpha diversity, and statistics. *Front. Microbiol.* 10, 2407. doi: 10.3389/FMICB.2019.02407/BIBTEX

Wu, X., Kuruba, R., and Reddy, D. S. (2018). Midazolam-resistant seizures and brain injury after acute intoxication of diisopropylfluorophosphate, an organophosphate pesticide and surrogate for nerve agents. *J. Pharmacol. Exp. Ther.* 367 (2), 302–321. doi: 10.1124/jpet.117.247106

Yanagisawa, N., Morita, H., and Nakajima, T. (2006). Sarin experiences in Japan: acute toxicity and long-term effects. *J. Neurol. Sci.* 249 (1), 76–85. doi: 10.1016/j.jns.2006.06.007

Yang, J., Li, Y., Wen, Z., Liu, W., Meng, L., and Huang, H. (2021). Oscillospira - a candidate for the next-generation probiotics. *Gut Microbes* 13 (1). doi: 10.1080/19490976.2021.1987783

Zafar, H., and Saier, M. H. (2021). Gut bacteroides species in health and disease. *Gut Microbes* 13 (1), 1–20. doi: 10.1080/19490976.2020.1848158

Zhao, Y., Zhang, Y., Wang, G., Han, R., and Xie, X. (2016). Effects of chlorpyrifos on the gut microbiome and urine metabolome in mouse (Mus musculus). *Chemosphere* 153 (287-93). doi: 10.1016/j.chemosphere.2016.03.055

frontiers | Frontiers in Public Health

TYPE Systematic Review
PUBLISHED 01 December 2022
DOI 10.3389/fpubh.2022.989496

OPEN ACCESS

EDITED BY
Fumito Maruyama,
Hiroshima University, Japan

REVIEWED BY
Yukiko Koizumi,
American Dental Association, United States
Emma Montella,
University of Naples Federico II, Italy
Cristoforo Pomara,
University of Catania, Italy

*CORRESPONDENCE
Pamela Tozzo
pamela.tozzo@unipd.it

SPECIALTY SECTION
This article was submitted to Infectious Diseases: Epidemiology and Prevention, a section of the journal Frontiers in Public Health

RECEIVED 08 July 2022
ACCEPTED 08 November 2022
PUBLISHED 01 December 2022

CITATION
Tozzo P, Delicati A and Caenazzo L (2022) Human microbiome and microbiota identification for preventing and controlling healthcare-associated infections: A systematic review.
Front. Public Health 10:989496.
doi: 10.3389/fpubh.2022.989496

Human microbiome and microbiota identification for preventing and controlling healthcare-associated infections: A systematic review

Pamela Tozzo[1]*, Arianna Delicati[1,2] and Luciana Caenazzo[1]

[1]Legal Medicine Unit, Laboratory of Forensic Genetics, Department of Cardiac, Thoracic, Vascular Sciences and Public Health, University of Padova, Padova, Italy, [2]Department of Pharmaceutical and Pharmacological Sciences, University of Padova, Padova, Italy

Objective: This systematic review describes the role of the human microbiome and microbiota in healthcare-associated infections (HAIs). Studies on the microbiota of patients, healthcare environment (HE), medical equipment, or healthcare workers (HCW) and how it could be transmitted among the different subjects will be described in order to define alarming risk factors for HAIs spreading and to identify strategies for HAIs control or prevention.

Methods: This review was performed in adherence to the Preferred Reporting Items for Systematic Reviews and Meta-Analyses (PRISMA) guidelines. After retrieval in databases, identification, and screening of available records, 36 published studies were considered eligible and included in the review.

Results: A multifaceted approach is required and the analyses of the many factors related to human microbiota, which can influence HAIs onset, could be of paramount importance in their prevention and control. In this review, we will focus mainly on the localization, transmission, and prevention of ESKAPE (*Enterococcus faecium*, *Staphylococcus aureus*, *Klebsiella pneumoniae*, *Acinetobacter baumannii*, *Pseudomonas aeruginosa*, and *Enterobacter species*) bacteria and Clostridium difficile which are the most common pathogens causing HAIs.

Conclusions: Healthcare workers' microbiota, patient's microbiota, environmental and medical equipment microbiota, ecosystem characteristics, ways of transmission, cleaning strategies, and the microbial resistome should be taken into account for future studies on more effective preventive and therapeutic strategies against HAIs.

KEYWORDS

human microbiome, human microbiota, healthcare-associated infections (HAI), prevention, infections control measures, risk factors, hospitalization, systematic review

Introduction

Healthcare-Associated Infections (HAIs) Are one of the major threats to hospitalized patients and a major public health burden. HAIs are nosocomial-acquired infections that are not present or incubating in the patient on their hospitalization but they should manifest at least 48 h after admission to the hospital (1–3). HAIs are considered those infections acquired in any healthcare facilities such as hospitals, nursing homes, ambulatory, rehabilitation centers, and any other facilities, both public or private, which provide healthcare or diagnostic service to individuals (4). HAIs have become one of the major challenges for the healthcare services of western countries due to an aging society and the increased level of immunocompromised patients in healthcare facilities, in particular for those in intensive care units (ICUs) (1, 5–8). HAIs incidence increase with prolonged hospitalization and with the utilization of invasive life-prolonging procedures including venous and arterial catheterizations, tracheal intubation, urinary catheterization, invasive intracranial pressure monitoring, and placement of sterile site drainage catheters (1, 5, 6, 9). Moreover, HAIs represent one of the most frequent complications of hospitalization worldwide, with an annual incidence ranging approximately from 5 to 15% of all hospitalized inpatients. Consequently, increasing attention has been given to HAIs by government health institutions (for instance the European Centre for Disease Prevention and Control and the Centre for Disease Control) which have implemented specific surveillance programs to collect data and have issued regulations for the mandatory reporting of such infections. In Europe, every year, more than 4 million people developed HAIs, with 16 million (6%) additional hospital days and ∼37.000 deaths. In Italy, specifically, between 450 and 700 thousand people are affected by HAIs every year. According to a 2013 national prevalence study, the prevalence of patients with at least one HAI is 6,3% (1, 10–15).

Given the clinical impact and the costs associated with HAIs, current research in this field is aimed to develop protocols for HAIs prevention or management and among the different possible solutions the first suggested was a more accurate hygiene protocol (1, 2, 15). Everything started in 1846, with Ignaz Semmelweis and his contributions in terms of hand washing, so much so that since then hand hygiene has been proposed multiple times as an important solution to control the spread of HAIs (10, 16). Nevertheless, proper hands washing is observed in <40% of cases–even in units with critically ill patients–due to poor bath-room placement, lack of time, forgetfulness or rejection of the usual recommendations, or negligence (17–19). Therefore, since HAIs arise from complex systems influenced by many factors, it is needed a more pluralistic approach for proper infection control, which cannot be limited to hand washing but should involve a multidisciplinary team including hospital doctors, infection control nurses, microbiologists, architects, and engineers with expertise in building design and facilities management.

Among the factors which influence the development of HAIs, there are the biological characteristics of the infectious agents involved as well as the susceptibility of the host to both exogenous and endogenous microorganisms (5, 20, 21). The human body harbors trillions of microbes that form a diverse ecosystem including bacteria, viruses, fungi, and protozoa; in particular, collectively they are named "human microbiota" and their genomes are referred to as the "human microbiome" (22–26). Previous studies had argued that, within the human body, microbial cells outnumber human cells 10-fold (27, 28), but recent research has demonstrated that the microbial cells are abundant as the human ones, with a more realistic ratio of about 1.3 between the former and the latter (29). The human microbiome plays an essential role in health, lipid metabolism, colonization resistance to transient organisms, and immune response (30–32) and can be influenced by different factors such as body location (33, 34), diet (35), sex (36, 37), ethnicity (38), and age (38, 39). In addition, the microbial community can also be shaped by habits (40), relationships (41, 42), disease state (43, 44), and environment (42, 45). With the latter a bidirectional influence exists; indeed, on the one hand, the environment can influence the microbiota of people who live there, on the other hand, humans release their bacteria into the surrounding environment, changing its microbial composition (27). Moreover, the Human Microbiome Project and other studies on the human microbiome have revealed a wide diversity in composition and abundance of the microbiome within an individual (alpha diversity) with differences that appear consistent between individuals (beta diversity) (33, 34, 46). In terms of human microbiome complexity, the increased number of studies on the human microbiome and the huge contribution to defining the role of the microbiome in health and diseases allowed us to highlight the direct/indirect mechanisms of action with which the microbiota act to confer protection against pathogens (7). Once pathogens entered the organism, in addition to the protection conferred by the microbiota, antimicrobial therapies could be useful were it not for the increased number of antimicrobial-resistant (AMR) microorganisms (47, 48). Nowadays, despite gram-negative bacteria remain still being associated with HAIs, gram-positive bacteria (such as *Enterococci* and *Staphylococcus epidermidis*) have become most frequently associated with HAIs in the context of both surgical site or bloodstream infection (1, 48). However, despite all these changes and the identification of the high number of possible factors (such as host genetics, age, nutrition, and environment) which can influence the human microbiota and its role in health and disease, it is poorly understood what "healthy microbiota" really means (24, 46). Therefore, this systematic review aims to analyze in detail how variations in the microbiome can be associated with HAIs. In particular, studies on the microbiota of patients, healthcare

environment (HE), medical equipment, or healthcare workers (HCW) and how it could be transmitted among the different subjects will be analyzed in order to define alarming factors for HAIs spreading and to identify strategies for HAIs control or prevention.

Methods

Research parameters

This systematic review was performed in adherence to the Preferred Reporting Items for Systematic Reviews and Meta-Analyses (PRISMA) guidelines (49). A systematic literature review regarding HAIs, the related microbiota, and methods for HAIs control and prevention was conducted using public electronic databases (PubMed and Scopus).

The works were selected according to the query: ((((“Healthcare-associated infection”) OR (“Healthcare-associated infections”)) AND (microbiome)) OR (((“nosocomial infection”) OR (“nosocomial infections”)) AND (microbiome))) AND ((control) OR (prevention)). One of the reviewers (A.D.) carried out the initial search of the papers and the consensus of research supervisors (L.C. and P.T.) was required.

Inclusion and exclusion criteria

Inclusion criteria were as follows: (1) English language; (2) Date of publication, i.e., articles published from 2000 to 2022; (3) Availability of both abstract and full text; and 4. only articles dealing with the role of the microbiome in the prevention of HAIs in healthcare facilities settings.

Papers have been excluded applying the following exclusion criteria: (A) systemic reviews or any other works (for instance chapter of a book) which is not experimental or which did not analyse the relationship among HAIs and the microbiota of different sources such as HCW, patients, HE or healthcare instrumentation (HI – medical equipment); (B) articles which are focussed on fungi or virus and not on bacteria; (C) articles which explained how HAIs are treated highlighting the emergence of new drugs; (D) articles which considered HAIs without an overview of the microbiota correlated; (E) articles which analyzed the microbiota of patients but in infections or other diseases which are not HAIs or; (F) articles which included content not relevant to the aim of the review.

Research workflow

A total of 272 works were identified through database searching. An English language filter was applied to start the screening process and narrow the search to 256 works. Duplicates (91 works) were removed manually. Then, the process continued through the screening of titles and abstracts which was followed by the evaluation of the full text of those works not excluded on the basis of the latter.

A total of 165 works were thus examined on the basis of title and abstract. A total of 62 articles were further evaluated by full-text examination to exclude irrelevant content based on the previous criteria (A-F). After a full-text reading of the selected papers, 36 were considered eligible and included in the review. Results management was performed with the use of Microsoft Office software such as Excel and Word. Zotero software was used to edit and organize the bibliography. The PRISMA flow chart in Figure 1 summarizes the workflow of the screening and selection process described above.

Results

This systemic review analyses in detail different studies, which deal with the association between microbiota and HAIs focusing on different types of microbiota, such as that of HCWs, patients, or HE, in order to define alarming factors for HAIs spreading and to identify strategies for HAI control or prevention. Over the years, new technologies such as next-generation sequencing (NGS) technologies have emerged, allowing a deeper and more precise understanding of microbiome in different contexts, providing specific knowledge toward new guidelines for combating HAIs and thus promoting and improving citizens’ health. In this sense, a multifaceted approach is required and the analyses of the many factors, which can influence HAIs onset, could be a good starting point. In this review, we will focus mainly on the localization, transmission, and prevention of “ESKAPE” bacteria (*Enterococcus* spp, *Staphylococcus aureus*, *Klebsiella* spp, *Acinetobacter* spp, *Pseudomonas aeruginosa,* and *Enterobacteriaceae*) and Clostridium difficile, which are the most common pathogens causing HAIs, despite sometimes we will present a wider microbiota landscape (Figure 2). In order to provide the reader with a better understanding, we grouped the selected studies on the basis of the relationship of HAIs with seven categories: (a) HCWs microbiota and HAIs; (b) patients microbiota and HAIs; (c) HE microbiota and HAIs; (d) medical equipment microbiota and HAIs; (e) environmental factors, ecosystem, and HAIs; (f) study of transmission/cleaning and HAIs; and (g) resistome and HAIs. A summary of the results of the studies analyzed in this review is shown in Supplementary Table 1.

Healthcare workers’ microbiota and HAIs

Transmission of infection during healthcare assistance requires three elements: the source of infecting microorganisms, a susceptible host, and a means of transmission from the

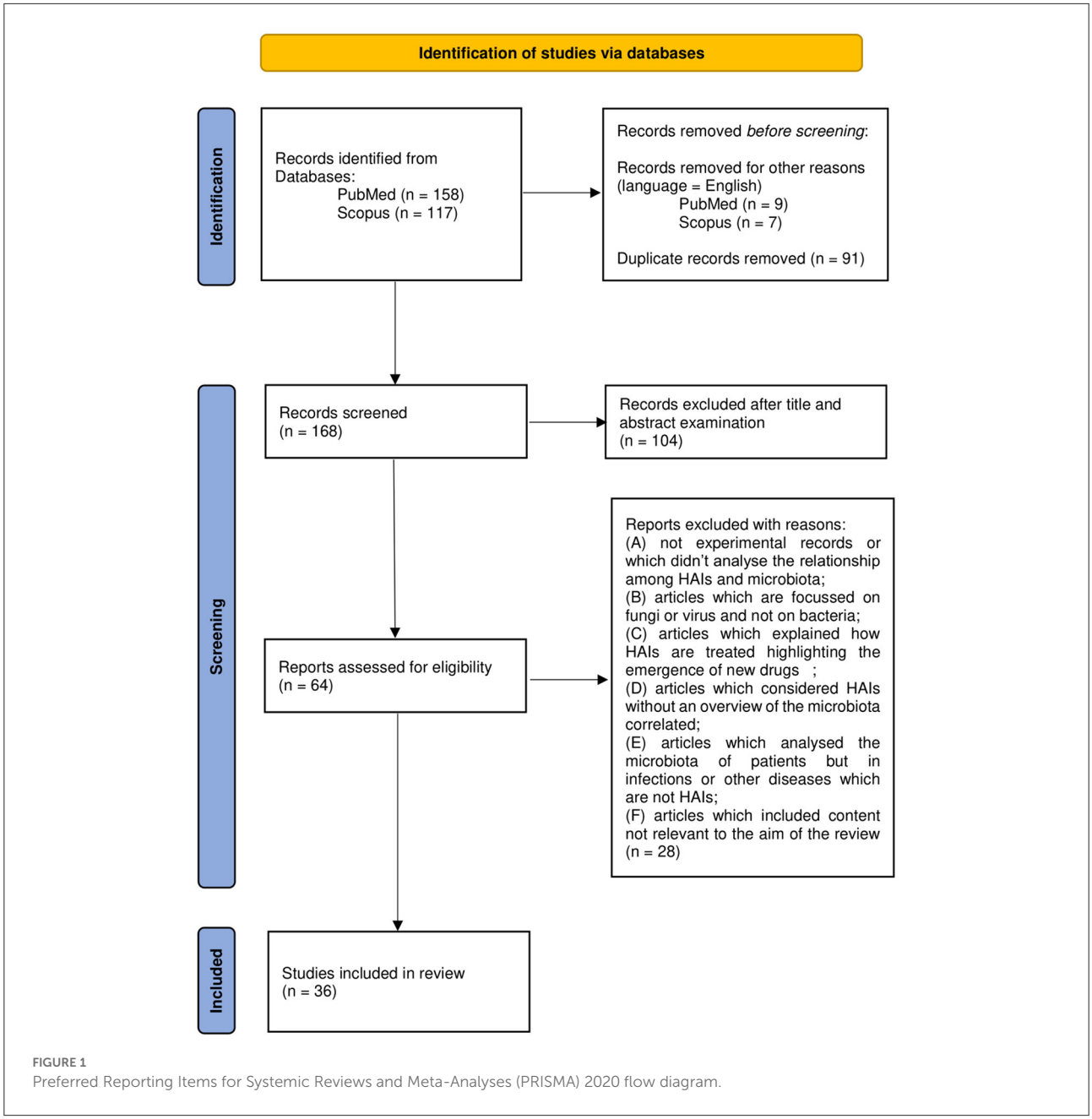

FIGURE 1
Preferred Reporting Items for Systemic Reviews and Meta-Analyses (PRISMA) 2020 flow diagram.

microorganism to the host. Infection can be endogenous when the source is represented by pathogens present within the body, but more frequently exogenous. In this case, the infection is transmitted from the outside through medical equipment or devices, the environment, healthcare personnel, or contaminated drugs (Figure 3).

There are many shreds of evidence that HCWs are one of the main risk factors involved in the large-scale dissemination of HAI-related bacteria; therefore, several studies have analyzed their implications in this context. Sereira et al. carried out the "Healthcare-associated Infections Microbiome Project," a surveillance program of 6-month targeting, among others, HCWs, collecting 216 samples from their hands, mobile phones, and protective clothing. Through their culture-dependent and culture-independent analyses, despite the high abundance of total bacteria in the protective clothing, they observed a similar distribution of the ESKAPE bacteria investigated on the different sources identifying these sites as possible hot spots for HAI-related bacteria transmission (50). As we have previously pointed out, in addition to ESKAPE bacteria, Clostridium difficile is another important HAI-related bacteria. Shoaei et al. specifically have performed phenotypic characterization coupled with molecular typing of Clostridium difficile isolates in burned patients with diarrhea, as well as their environmental context. In

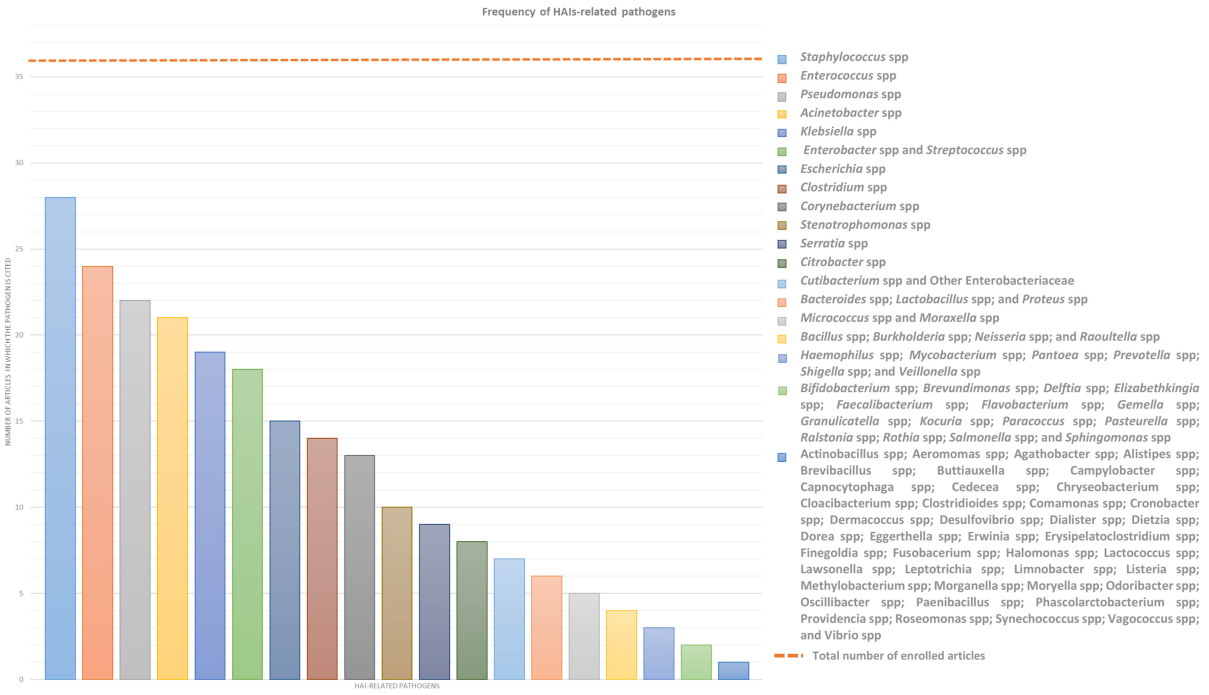

FIGURE 2
Frequency of HAIs-related pathogens. In the graph are represented the number of article out of the 36 enrolled which treated each specific pathogen to better highlight which of them result most prevalent. ESKAPE bacteria, namely *Enterococcus* spp, *Staphylococcus* spp, *Klebsiella* spp, *Acinetobacter* spp, *Pseudomonas* spp, and Enterobacteriaceae such as *Enterobacter* spp and *Escherichia* spp, in addition to *Streptococcus* spp and *Clostridium* spp resulted the most infective pathogens which should be controlled to prevent HAIs.

particular, from the point of view of HCWs-related Clostridium difficile analyses, they collected 29 swabs from HCWs dominant hands which showed positive results for Clostridium difficile colonization in 8 samples, one of which resulted colonized by a toxigenic Clostridium difficile strain (51). A similar result was highlighted by Segal et al. They identified in an anaesthesiologist the source of contamination of post-operative infections of seven ICU patients, detecting in both patients and the anaesthesiologist the same bacteria. This result was achieved using 16S rRNA amplicon metagenomics sequencing rather than the most common cultural methods. Moreover, they observed also a correlation between the time of surgery and the severity of infection, suggesting that the number of contacts between the patient and any contaminated member of the medical team may increase the possibility for the patient to acquire that particular pathogen (52).

Since HAIs are considered as those infections acquired in any healthcare facilities, which provide healthcare or diagnostic service to individuals, and not only those acquired in hospitals, all the employers of these facilities should be considered, in this context, as HCWs. On this base, Pérez-Fernández et al. performed a descriptive observational study on 19 physiotherapy and rehabilitation centers in order to discover potential microbiological risk factors for HAIs onset. They performed sampling from the hands of physiotherapists without previously informing them to prevent influencing their behavior (hand washing in particular). The majority of the detected microorganisms were gram-positive bacteria, in accordance with the usual microbiota of the human body, suggesting the necessity of reinforcing hand washing or even combining hand washing with the use of gloves to reduce the transmission of these bacteria among different patients (53).

Cruz-López et al., in addition to studying the role of HCWs as a source of external human contamination for HAIs in-patient, have gone over identifying also the huge contribution that can be attributed to the patients' relatives. They performed sampling from 35 nurses and 8 patients' relatives. In particular, stool samples or rectal swabs and swabs of different anatomical sites as well as hands swabs were collected from the HCWs only once during the first seven days of the study, and from the patients' relatives at admission, on day 3 and then every 5 days until hospital discharge. They observed that, among the different microorganisms, coagulase-negative staphylococci represented the most frequent species recovered both in HCWs and in patients' relatives. *Staphylococcus aureus* and Raoultella ornithinolytica were recovered primarily from nurses. However, they identified a wider spectrum of microorganisms that could be present in both HCWs and patients' relatives, identifying them as possible asymptomatic carriers and pathogens reservoirs that

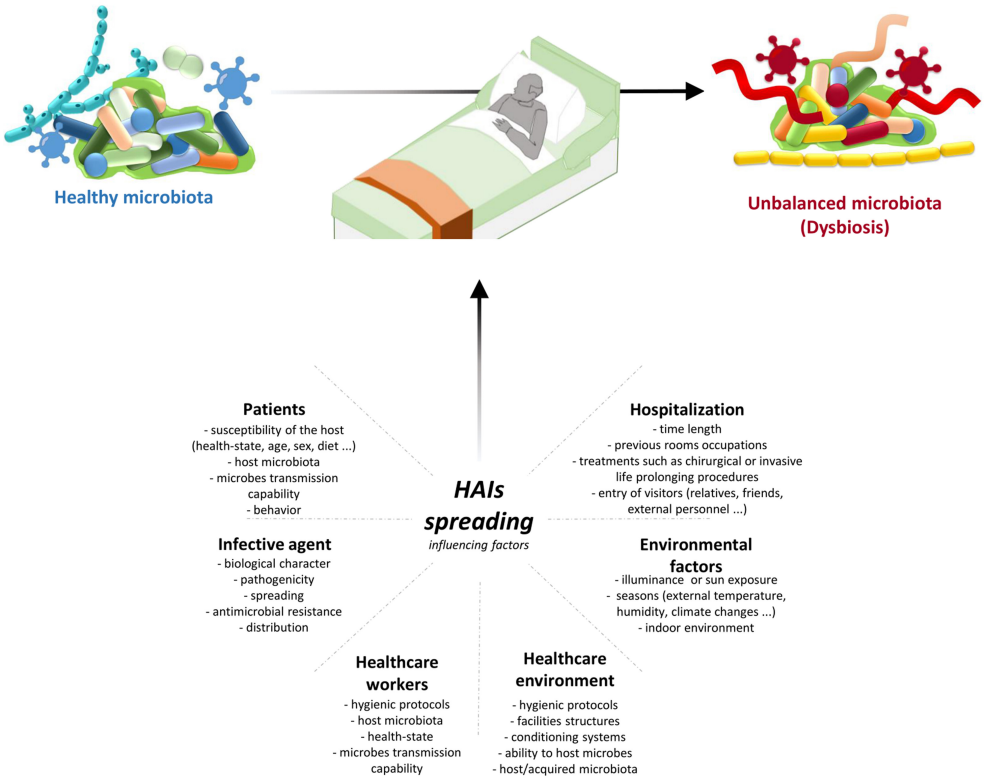

FIGURE 3
HAIs spreading influencing factors. HAIs are mainly due to the microbiota transition from an healthy state to dysbiosis. This alterations are caused by different factors: hospitalization conditions and reason for admission; both external and internal environmental factors; HE hygienic condition and HE ability to host/acquire microbes; ability to transmit microbes by the HCWs, their healthy condition, and their propensity to follow hygienic procedures; infective agent itself; and patients healthy state and their behaviour. Therefore it is important a multifaceted approach to manage all these factors and thus HAIs spreading. HAIs, healthcare-associated infections; HCWs, healthcare-workers; HE, healthcare-environment.

can facilitate the dissemination of the pathogens in the hospital setting and that, hence, should undergo strict regulation to prevent HAIs dissemination (54).

Considering this evidence, HCWs and patients' relatives/caregivers must be considered one of the main sources of pathogen spreading in different types of healthcare facilities. More than half of HAIs are preventable, especially those associated with certain behaviors, through the planning of dedicated programs to prevent and control the transmission of infections. However, it is necessary to plan and implement control programs at different levels (national, regional, local), to ensure the implementation of those measures that have proved effective in minimizing the risk of infectious complications. Although HAIs are commonly attributable to patient variables and the quality of care provided, a dedicated organizational setup has been shown to help prevent them. Therefore, ensuring correct hygiene practices of all people involved in the patient's assistance, and the use of sterile gloves and clothing should be a fundamental strategy to ensure a higher safety level for patients, especially for the immunocompromised ones.

Patients' microbiota and HAIs

Human microbiota has a central role in many biological functions therefore its variations may represent important risk factors for HAIs onset and development. In this paragraph, we are taking into account different studies that considered the patient microbiota in order to define its correlation with HAIs onset from a general point of view or focusing on either specific pathologies or pathogens. McDonald et al. worked to confirm an earlier assumption according to which critical illness would be associated with loss of health-promoting commensal microbes with a simultaneous overgrowth of pathogenic bacteria (dysbiosis), thus increasing susceptibility to HAIs, sepsis, and multi-organ failure. They collected fecal, skin, and oral samples from 115 mixed ICU patients twice: within 48 h of ICU admission and on day 10 or at ICU discharge. First of all, they observed a greater similarity among fecal and oral samples at admission, compared to those obtained at discharge, suggesting that the length of stay in an ICU is connected with endogenous microbial community disruption. Their results confirmed the correlation between

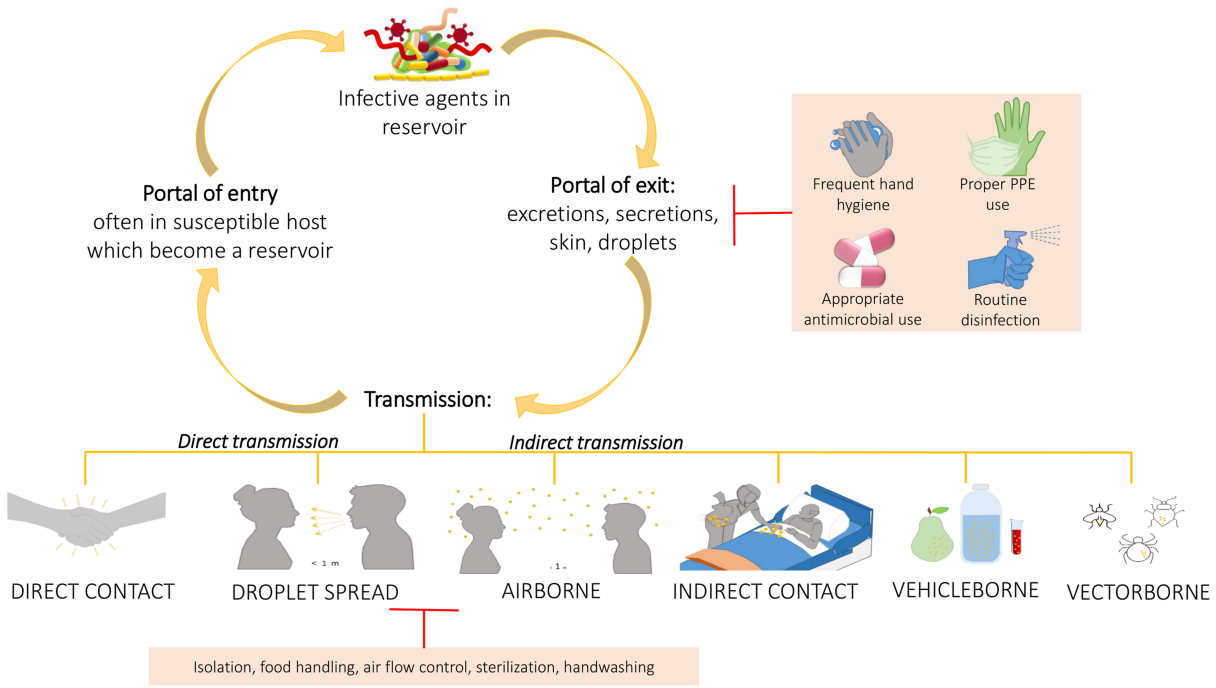

FIGURE 4
Chain of infection and some preventing strategies. A pathogen may be transmitted from a reservoir to susceptible individual through different ways. Understand the chain of infection is fundamental to HAIs prevention and control. In direct transmission, the pathogens is transferred from a reservoir to an host by direct contact such as skin-to-skin contact, or droplet spread where aerosols produced by coughing, sneezing, or even talking lead to pathogens spreading. Conversely, indirect transmission is associated to an intermediary which may be both animate (vectors) or inanimate (vehicles). Belong to this class the airborne transmission where the pathogens are included into the droplet nuclei suspended in air, this is similar to the previous but the spreading may occurs also some distance away from the source resident due to conditioner systems or air currents. In the transmission through indirect contact, different objects, such as medical devices, contaminated gloves, object in the patients' room or environment and/or medical equipment, may represent the source of contamination as well as inanimate vehicles such as food, water or other biological samples. Sometimes the vehicles are passively, other times they may aid the pathogens providing environment for growth. Similarly occurs for vectors which in general are animals such as mosquitoes, fleas, and ticks. The chain of infection may be interrupted at the "portal of exit" applying hygienic procedure such as the frequent hand hygiene, using proper personal protective equipment, performing proper routine disinfection, or using appropriately the antimicrobial to avoid strengthen antimicrobial resistance of pathogens. Sometime it is possible, instead, to break the transmission limiting the transmission itself through isolation of the infected individual, through a correct food handling, or through the application of sterilization and hygienic procedure.

critical illness and the rapid establishment of a state of dysbiosis due to the depletion of health-promoting organisms (such as Faecalibacterium which seems to have an anti-inflammatory role), and the overgrowth of known pathogens, such as *Enterobacter* and *Staphylococcus* (55). Sereira et al. in their "Healthcare-associated Infections Microbiome Project," collected 198 patients' samples through rectal, nasal, and hand swabbing. A high abundance of HAI-related pathogens were detected on all types of samples, however, the highest amount of bacteria and the greatest differences in alpha and beta-diversity was associated with the rectum samples. Moreover, during their studies, they concluded that 50% of the patients did not present any HAIs during hospitalization, 43.9% had an HAI during the hospitalization, and 6.1% was colonized by HAI-related bacteria, highlighting that a longer hospitalization seems to result in an increased HAIs incidence and, thereby, in an increased HAI-related pathogens detection, especially for bacteria like *Klebsiella pneumoniae*, *Enterobacteriaceae*, *Staphylococcus* spp, and *Acinetobacter baumannii* (50). Always through samples collected from different patients' body sites, Cruz-López et al. examined the colonization process and the possible ways of transmission of HAI-related pathogens, since patient colonization has been suggested as a risk factor in HAI development. They collected stool samples or rectal swabs and swabs from different anatomical sites in 11 in-hospital patients, at admission, on day 3, and every 5 days until the patient left the unit. Of these patients, 8 developed 1-3 HAIs for a total of 12 diagnosed HAIs. Since the main causative agents were identified in *Acinetobacter baumanii* and *Klebsiella pneumoniae*, the majority of HAIs (50%) were ventilator-associated pneumonia (VAP). Moreover, this study confirms the previous one, according to which the risk for HAIs-related pathogens acquisition increases with the time of hospitalization since on the 1st day of hospitalization only 50% of causative agents were recovered from patients' swabs (54).

Zakharkina et al. performed a study focused on the dynamics of the respiratory microbiome during mechanical ventilation in the ICU and its association with VAP. They collected a total of 111 samples of tracheal aspirates from 35 patients which have been divided into 4 groups: 11 patients with VAP (group 1), 9 patients without VAP but with colonized airways (group 2), 9 patients without VAP and without colonized airways (group 3), and 6 patients who developed pneumonia within 48 h after intubation (group 4). From a microbiological point of view, pathogens like *Acinetobacter*, *Pseudomonas*, and *Staphylococcus* were identified in patients with confirmed VAP and the duration of mechanical ventilation resulted to be associated with a decrease in microbial diversity in 83% of patients. More in detail, differences in alpha diversity were detected between group 1 and group 3 but not between groups 1 and 2. However, in group 1 patients showed a more profound dysbiosis than in group 2. Moreover, despite 27 patients receiving treatment with antibiotics at some point during their hospitalization, in this case, an association between antibiotic therapy and microbiological variations was not observed (56). Another study addressing microbial variation in mechanical ventilated ICU patients is that of Lamarche et al.; they conducted an observational study collecting samples from 34 mechanically ventilated ICU patients and from 25 healthy adults. In particular, for critically ill patients, they carried out the sampling during the 1st week of hospitalization, collecting 29 endotracheal aspirates, 26 gastric aspirates, and 10 feces specimens; whereas, for healthy adults they collected 7 bronchoalveolar lavages samples, 7 nasopharyngeal swabs, 7 oropharyngeal swabs, and 21 feces specimens. As described above, microbial dysbiosis occurred in critically ill patients, moreover, in this case, less pronounced differences in biogeographical composition, resulting in a lack of specificity between anatomical sites, were observed. Comparing ICU patients and healthy adults' operational taxonomic units (OTUs), significant differences in their abundance were shown with a strong decrease in the amount of the "health-promoting" microorganisms, in particular *Faecalibacterium* and *Neisseria*. Also, this study reiterated that in ICU patients, besides the depletion of different OTUs, there is an increase of one or few pathogenic OTUs (such as *Enterococcus*, *Pseudomonas*, and *Staphylococcus genera*), suggesting the microbial collapse in ICU patients toward a few dominant taxa which are usually isolated in HAIs and whose number is proportional to illness severity and mortality (22). More recently, Lu et al. focused their attention on patients with severe pneumonia, analyzing their skin microbiota composition and diversity in comparison with that of a healthy control group. They enrolled 30 mechanical ventilated ICU patients and 30 healthy staff members and collected from both groups skin surface samples and then, only from the patients, blood, endotracheal aspirates, and bronchoalveolar lavage fluid samples. From skin surface samples 14292 OTUs were identified, allowing identification of 590 genera. *Staphylococcus*, *Acinetobacter*, *Corynebacterium*, *Stenotrophomonas*, *Enterococcus*, *Brevibacillus*, and *Halomonas* were most abundant in the patient group, while in the healthy control group *Bacteroides*, *Phenylobacterium*, *Prevotella*, and *Streptococcus* were prevailing. However, as previously observed, patients showed also a decrease in diversity both within each sample (alpha diversity) and between samples (beta diversity). Finally, they showed an interaction between skin bacteria and respiratory microorganisms characterizing also in the other samples the same HAI-related pathogens, thereby suggesting the importance of skin microbiota along with pulmonary and gut microbiotas in the pathogenesis of severe pneumonia in ICU patients (57).

Another observational study is that performed by Mu et al. on three groups of patients (34 septic patients, 33 non-septic ICU patients, and 10 healthy adults) and 312 fecal samples. Despite the focus of their study on the gut microbiota, also in this case a significant decrease in microbiota abundance and diversity, flanked by an increase in AMR pathogens, was highlighted. Moreover, they found an association between opportunistic pathogens intestinal colonization and secondary infection development, observing a secondary infection in 23 septic patients out of 34, 14 of which resulted to be caused by *Klebsiella pneumoniae*, thus suggesting the central role of this pathogen in HAIs. Actually, *Klebsiella pneumoniae* was not the only opportunistic pathogen showing a higher abundance in both septic and non-septic ICU patient than in healthy adults; indeed, also Enterococcus strains were detected. In this study, the amount of other health-promoting bacteria, such as Faecalibacterium, was significantly lower in both septic and non-septic ICU patient than in healthy control (58).

Considering the focus on gut microbiota, in their study Lu et al. explored early intestinal colonization in very low birth weight infants (VLBWI) and how it is influenced by dominant bacteria and other factors. They collected a total of 300 anal swabs from 81 VLBWI at different times after birth until the 21st day of hospitalization. Their results showed that 188 samples out of 300 had dominant bacteria, the top five were both gram-negative bacteria (*Klebsiella pneumoniae*, *Escherichia coli*, and *Serratia marcescens*) and gram-positive bacteria (*Enterococcus faecalis* and *Enterococcus faecium*). However, the gram-negative bacteria resulted to be the main colonizers in VLBWI with a colonization rate that increased over time. In particular, HAIs due to both *Klebsiella pneumoniae* and *Serratia marcescens* proved to be significantly associated with intestinal colonization rather than those caused by *Escherichia coli* or *Enterobacter cloacae*. Finally, among different non-infectious factors considered in this, including gender, mode of delivery, gestational age, birth weight, feeding mode, and mechanical ventilation, only the latter was shown to be a factor affecting bacterial colonization in VLBWI, which was probably influenced also by the use of antibiotics to treat these patients (59). Also, Maamar et al. faced gut

microbiota colonization but they mainly focused on a broad-spectrum cefotazime-resistant (CTX-R) Enterobacteriaceae to determine their prevalence in patients and their colonization rate during hospitalization. They enrolled 63 patients collecting different rectal swabs at admission and on a weekly basis until pathogen positive detection or hospital discharge. Firstly, at admission, 13 samples resulted to be positive for CTX-R *Enterobacteriaceae* indicating a prevalence of 20.63%. The following sampling was realized for only 35 patients, 15 of them acquired the pathogens during hospitalization, resulting in a CTX-R Enterobacteriaceae acquisition rate of 42.85%. In particular, CTX-R *Klebsiella pneumoniae*, *Escherichia coli*, and *Enterobacter cloacae* were the most frequently detected microorganisms, confirming their pathogenic role. Eventually, also Maamar et al. identified antibiotic treatment as a risk factor for pathogens acquisition (60). Since the gut microbiota of an individual can shape the local environmental surfaces, Freedberg et al. collected 304 samples from ICU patients at the time of ICU admission, 80 of which were defined as eligible to be compared with ICU rooms' microbiota. In addition to these evaluations, Enterococcaceae resulted to be overrepresented in all samples and vancomycin-resistant Enterococcus (VRE) was identified specifically in 28% of the eligible patients (61).

Ke et al. turned their attention to another important HAIs-related pathogen, Clostridium difficile. They recruited 243 participants which have been divided into four groups: 112 patients with Clostridium difficile infection (CDI), 40 asymptomatic carriers, 44 non-CDI patients with diarrhea, and 47 control patients. These authors analyzed not only gut microbial composition but also a broad panel of innate and adaptative immunological markers, suggesting that all these data taken together may allow to better distinguish patients with CDI from other groups of patients. This new association may be a new marker-derived signature to detect CDI and design early and more effective therapeutic interventions. In addition, they compared the overall microbial community structure of the four groups of patients identifying CDI ones as those with the lower alpha diversity and the higher beta diversity. Consistently with previous studies, these findings suggested a depletion of some taxa, and a significantly less stable microbiome profile characterizing CDI patients. Despite this, several driven taxa, like *Klebsiella*, *Streptococcus*, *Desulfovibrio*, and *Veillonella*, were identified as the main players in driving changes in microbial correlation networks between CDI patients and other groups and many other genera showed specific variations (62). Considering the role of Clostridium difficile, Shoaei et al. evaluated the dominant bacteria structure in burned patients with and without CDI. They collected fecal samples from 23 CDI patients, 46 burned patients without CDI, and 46 healthy control adults for a total of 189 samples, and 51 skin surface samples from burned patients. Fifty-one fecal samples showed Clostridium difficile positive results with culture methods, of which 23 had toxigenic character whereas, for the second group of samples, 14 showed positivity to Clostridium difficile culture but only two of them produced results showing colonization by toxigenic Clostridium difficile strains. More generally, they demonstrated that the gut microbiota of CDI group was characterized by an overgrowth of facultative anaerobic bacteria such as Enterococcus spp and *Escherichia coli* and a reduction of beneficial bacteria such as Bacteroidetes compared to other groups. Moreover, they identified that the increase in *Akkermansia muciniphila* and the decrease in *Faecalibacterium prausnitzii* may be considered predictive microbial markers for developing nosocomial diarrhea, defining a poor CDI prognosis in burned patients (51).

Ogura et al. enrolled 29 patients to characterize Staphylococcus spp on skin healed from a pressure injury. The patients were divided into two groups since 7 of them suffered from recurrent pressure injury (RPI) within 6 weeks after healing and the other 22 did not. The results showed a significantly higher abundance of *Staphylococcus* spp in RPI-healed sites than in non-RPI-healed sites suggesting its implication in RPI. From a genomic point of view, they demonstrated the dominance of *Staphylococcus caprae* and *Staphylococcus aureus* over *Staphylococcus epidermidis*, whose presence showed extremely low results in all skin sites. Moreover, despite *Staphylococcus aureus* seeming to appear in an earlier RPI onset, it was detected alone in only two of the seven RPI patients in comparison to *Staphylococcus caprae*, which was observed alone four times (63).

Given all these studies and their similarities, it is clear how patient microbial diversity may be considered as a biomarker of prognostic value for HAIs and a starting point to define targeted therapies to correct dysbiosis and health-promoting bacteria depletion, restoring a healthy microbiome and thus improving patient outcome.

Healthcare environment microbiota and HAIs

Safety and hygiene of HE significantly contribute to the onset of HAIs, indeed different studies identified microbial contamination of the HE as an important source of pathogens transmission resulting in HAIs spreading. The monitoring of HE surfaces may be conducted through either the most common culture-dependent methods or culture-independent ones, which, in general, result to be faster, more effective and sensitive, and able to detect also uncultivable bacteria with the only fault being unable to distinguish viable from dead bacteria, leading to an overestimation of the contamination. Comar et al. performed one study of HE contamination using NGS technologies in comparison with conventional microbiological and molecular PCR methods, in order to define more precisely

the environmental microbial composition. They collected HE samples 7 h after cleaning by contact plates for microbiological analyses and sterile swabs both for molecular ones and for NGS analyses. After sampling, 216 contact plates and 108 sterile swabs were harvested to perform microbiological, molecular, and NGS analyses, respectively. In microbiological analyses, Staphylococcus showed a microbial prevalence of 81% of the total collected samples, Enterococcus spp of 13%, Candida spp of 7.9%, Acinetobacter spp of 7.4%, Clostridium difficile of 4.2%, *Pseudomonas aeruginosa* of 0.9% and Klebsiella spp of 0.5%, whereas Aspergillus was never detected. Molecular analyses allowed the identification of the searched pathogens in more samples compared to the previous method. In particular, among the others, Staphylococcus was detected in 99% of the samples, Enterococcus spp in ∼80%, Klebsiella pneumonia, and Enterobacter in 78%, often in association with *Escherichia coli* which was identified in 49% of the samples, *Acinetobacter baumannii* in 24%, *Pseudomonas aeruginosa* in 76%, and Clostridium difficile in 19%. NGS analyses allowed obtaining the following level of microbial prevalence for the most frequent pathogens: 94.5% for Cutibacterium spp, 92.6% for Staphylococcus spp, 82.4% for Streptococcus spp, 75% for Corynebacterium spp and Pseudomonas spp, 70.4% for Paracoccus spp, 65.7% for Acinetobacter spp, and 59.3% for Rothia spp. Considering all the results achieved, NGS appeared to be the only technique able to identify both searched and non-searched bacteria, with a high degree of sensitivity compared to the other two techniques, since NGS is a powerful tool for monitoring contaminating bacteria even at low concentrations (13). Another study that exploits NGS potential, rather than cultural methods, is that of Ribeiro et al., where deep-DNA-sequencing analyses were used to explore and compare the bacterial communities structures of different ICUs and neonatal intensive care units (NICUs). For this purpose, 158 samples were collected resulting in identification of 2051 OTUs for NICU and 1586 for ICU, resulting in higher diversity in the microbial composition of NICU compared to ICU, probably due to the higher transit of visitors in the former. At the genus level, sequences of 138 and 160 genera were included for ICU and NICU, respectively, among which 11 specific genera were identified as biomarkers for NICU and 6 for ICU. The HAI-related genera, which were considered biomarkers for the NICU environment by Ribeiro et al., were several facultative or obligate anaerobes, most of which, despite normal hosts of healthy adults, may be pathogenic for neonates. Instead, the main HAI-related pathogens in ICU were Pseudomonas. Collectively, these results enable to differentiate ICU and NICU environments, suggesting the central role of HCW and patients in environmental contamination since the majority of the detected pathogens are common in human microbiota (64).

Moreover, Li et al. conducted monitoring of the microbial community of ICUs. They collected 214 samples from different sites of two ICUs within a 1-year period and, then, they compared the microbial composition detected with public databases to figure out the sources of ICUs contaminations. They identified the main sources of ICUs contamination in building-related bacteria and, to a lesser extent, in human skin-related bacteria. Anyway, in addition to Proteobacteria and Firmicutes, which represent the main phyla of these two ICUs, this study showed a huge HAI-related bacteria composition characterized by Acinetobacter, Staphylococcus, Enterococcus, and Klebsiella strains (15). Again in the ICUs context, Costa et al. analyzed biofilm and ESKAPE bacteria contaminations of high-touched surfaces. Fifty-seven surfaces were selected and the samples were analyzed with four different methodologies (culture, molecular analyses, NGS, and microscopy). ICUs surfaces resulted to be contaminated by many pathogens which were identified mostly through molecular analyses rather than cultural ones, indeed from the culture-negative samples, 76.7% were shown to have live bacteria suggesting the presence of a high number of non-culturable bacteria such as those found in biofilm. Moreover, biofilms were detected in all the analyzed samples through microscopy techniques. Eventually, NGS analyses revealed a large microbial diversity with more than 830 OTUs and 170 genera, among which ESKAPE bacteria were detected in 51.8% of the NGS samples. In particular, among these HAI-related bacteria, Acinetobacter baumanii was detected in six culture-positive and five culture-negative samples, *Staphylococcus aureus* in three culture-positive and one culture-negative, Enterobacter spp in two culture-negative, and *Pseudomonas aeruginosa* in one culture-negative sample (65).

Sereira et al. during their "Healthcare-associated Infections Microbiome Project" targeted also HE in order to identify contamination hotspots, searching for specific bacteria in 666 high-touched surfaces samples. Collectively they showed that the microbial community in HE was mainly composed of *Proteobacteria* and *Firmicutes phyla*, where *Enterobacteriaceae*, *Pseudomonas*, *Acinetobacter baumanii*, and *Escherichia coli* belonged to the first phylum and Staphylococcus to the second one. Concerning hotspot sites, HCW resting rooms resulted as the most contaminated, with a high amount of both total bacteria and HAI-related bacteria. Moreover, higher diversity was shown in the unit's bathrooms as well as in bed equipment and equipment shared between hospital units (50).

Differently from Ribeiro et al. who concluded that ICUs and NICUs environment are characterized by different microbial compositions, Sereira et al. affirmed that these differences disappear over time due to the microbial community dynamicity, especially when a larger sampling size is adopted for the analyses. However, in accordance with Ribeiro et al., and Sereira et al. suggested that microbial communities which colonized HE can be influenced by patients, HCW, and the severity of illness of inpatients (50, 64). Another study, which identified in HE microbiota a possible transmission route of HAI-related pathogens, is that of Cruz-López et al. which collected environmental samples from surfaces near the patient's

bed at admission, at day 3, and every 5 days until the patient's discharge. Coagulase-negative staphylococci were the most detected species also in environmental samples; however, other HAI-related bacteria were identified, such as Acinetobacter baumanii, *Klebsiella pneumoniae*, *Enterobacter cloacae*, and Enterococcus spp. HAI causative agents were recovered both before and after infection development suggesting a mutual exchange of bacteria between patients and the environment (54).

Kelly et al. studied how HE contamination may be related to the environmental position of patients and wastewater sites. They considered 51 hospital rooms at the time of patients' admission with an eligible HAI-related pathogen and then they performed a longitudinal sampling at different times in three different sites at variable distances from the patient's bed (near to the patient, intermediate distance, and far from the patient but in the proximity of wastewater sites) resulting in 408 samples. They related the probability of HAI-pathogens detection to the distance from the patient and wastewater site evidencing that the detection of gram-negative HAI-related pathogens (such as *Acinetobacter* spp or *Pseudomonas* spp) increased toward the wastewater site, while the opposite occurred for the detection of gram-positive HAI-related pathogens (such as Clostridium difficile) which increased closer to the patient. The relation between pathogens and the distance from the patient may be helpful to evinced possible hotspots of bacterial contamination (66).

Gudakova et al. analyzed microbial contamination specifically on touch surfaces of waiting rooms in pediatric outpatient facilities, to evaluate any differences between sick-child waiting rooms and well-child waiting rooms and possible hotspot sites of contamination. They collected samples from 3 pediatric offices in one or two sampling days. Taken together, their results revealed no significant differences between the two types of waiting rooms, both characterized by a high variation in microbial burden on samples collected from the same surface type. However, they highlighted that the sites with the highest microbial contamination were seats, children's seats, and children's books. Seats hosted the highest levels of *Staphylococci*, whereas children's books showed the highest level of both *Staphylococci* and gram-negative enteric bacteria. Moreover, they noted that the level of seat contamination was higher in sick-child waiting rooms in contrast to the level of children's books contamination, the results of which were higher in well-child waiting rooms. A probable explanation of these results may be connected with the different behavior of the children in the waiting rooms which is influenced by their health state (67).

A particular consideration is that also ambulances can be categorized within HE. In this context, Sheahan et al. developed a rapid, portable, inexpensive, and easy-to-use approach to metagenomics analyses to characterize ambulances microbiota. Their system allowed them to identify, on the samples collected from different ambulances at different times, six different phyla (*Spirochaetes*, *Fusobacteria*, *Bacteroidetes*, *Actinobacteria*, *Firmicutes*, and *Proteobacteria*) for a total of 68 genera, some of which contain HAI-related pathogens, such as Clostridium spp or Staphylococcus spp. In addition, other identified genera are: Campylobacter, which is a bacteria responsible for some gastroenteritis; Shigella which is associated with shigellosis disease; and Listeria, which may lead to fatal bacterial illness. Finally, by analyzing different surface samples from three different ambulances they were able to detect probable contamination hotspots, which should require fine monitoring and cleaning procedures. Overall, their approach provided a functional and rapid platform for microbial detection and monitoring in ambulances for specific pathogens, evidencing their higher prevalence on finger monitors which enter in direct contact with patients, followed by door handles which experience direct contact with the HCW, and by soft kits which are in contact with the environment (68).

Other healthcare facilities analyzed in order to discover environmental contaminations were physiotherapy and rehabilitation centers. Pérez-Fernández et al. collected four environmental samples from each of the 19 healthcare facilities under study, in particular, three samples were taken from the treatment table (head, intermediate, and caudal section) whereas the fourth sample was of the ambient air. They observed a high value of coagulase-negative staphylococci and gram-negative non-Enterobacteriaceae bacteria but lower level of *Staphylococcus aureus* on samples collected from tables of treatment without any relevant differences among the different tables' sections. On the contrary, *Staphylococcus epidermidis*, *Micrococcus* spp, and *Bacillus* spp were the only microorganisms identified in air samples. Their results suggested greater involvement of environmental surfaces rather than the ambient air in pathogen transmission since the former was shown to host opportunistic pathogens (53).

In addition to HCW and patient microbiota analyses, Shoaei et al. performed characterization of environment microbiota in rooms of burned patients after Clostridium difficile diagnosis. Of 21 bed sheets collected samples, three resulted colonized by non-toxigenic Clostridium difficile strains, therefore also in this case a correlation between environmental contamination and HAIs, such as CDI, was highlighted (51). Considering environmental contamination and VRE colonization, Freedberg et al. tried to define if there might be worse ICU rooms. Twenty-four ICU rooms were sampled at five different time points. Pseufomonaceae characterized the microbial community detected on environmental surfaces. Moreover, comparative studies to assess microbial variation across neighboring ICU rooms were performed. The rooms' microbiota slowly diverged from baseline and it appeared similar to that of neighboring rooms; however, the speed of this divergence seemed to be associated with the patients' turnover. Moreover, analyzing VRE-colonization, the authors confirmed environment-patient

interactions, indeed when they showed a different VRE status in a time of 3/9 days both become VRE-positive (61).

Taken together all these studies allowed defining the central role of HE microbiota in the transmission of different HAI-related pathogens, most of which are not common environmental bacteria but rather are human-related bacteria released in the environment by the individuals who spend time in that environment.

Medical equipment microbiota and HAIs

Another important cause of HAIs has been recognized in the contamination of medical devices by pathogenic microorganisms in healthcare settings. Therefore, to reduce the burden of HAIs, accurate studies to characterize the microbiota of medical devices and to identify the main sources that lead to their contamination may be other important interventions to enhance the effectiveness of infection prevention and control practices. Therefore, different scholars performed studies to this end. Among them, Shoaei et al. were the only ones that, analyzing 19 samples from medical devices in hospital rooms of burned patients affected by Clostridium difficile, and did not find any positive contamination from Clostridium difficile (51). Opposite results were obtained by Pérez-Fernández et al. in their observational study on 19 physiotherapy and rehabilitation centers, in which the level of contamination on instruments and equipment used for patient therapies administration was investigated. They detected a greater presence of Enterobacteriaceae as well as *Staphylococcus epidermidis* in different devices. In addition to these bacteria, Pérez-Fernández et al. identified other important pathogens, such as *Staphylococcus aureus*, Acinetobacter spp, and *Escherichia coli* on the sponge electrode. In this study, sponge electrodes represented the instrumental samples with higher and more varied contamination, up to more than 20 different bacterial species, probably as the consequence of inadequate cleaning (53).

In addition to previous studies, Cruz-López et al. examined the colonization process and the possible transmission routes of HAI causative agents through the sampling of medical devices, such as mechanical ventilation tubes, central venous catheters, and urinary catheters. They collected samples from medical devices near to patients at different times, on day 1 of admission, day 3, and every 5 days until the patient's discharge. The same HAI pathogens identified in patients were also identified on medical devices and in particular mechanical ventilation tubes were the most colonized medical devices in those patients that developed VAP between day 1 and day 3 (54).

In their study, Mahjoub et al. worked analyzing the instrumentations of ophthalmology clinics to identify potential sources of pathogenic spread. The collection of the 33 samples was performed at 6 am before any patients or staff members entered the clinics and after the cleaning of the night before. More than half samples yielded bacterial growth, without significant differences among the clinics. Different pathogens were detected, first of all, *Staphylococcus epidermidis*, associated with post-intraocular surgical infection; followed by *Staphylococcus capitis*, implicated in surface infection such as purulent conjunctivitis; Micrococcus luteus, able to form biofilms implicated in prosthetic valve endocarditis; Corynebacterium species, causing granulomatous mastitis, and, moreover, Cutibacterium acnes, which is well-established as a cause of post-operative chronic endophthalmitis. Therefore, these findings defined medical devices as possible vectors for HAIs spreading indicating a need for increased disinfection of these instrumentations (69). Eventually, Swanson et al. performed a little different study with the aim to identify the main sources that lead to medical device contamination in addition to the characterization of the contamination itself. They used SourceTracker, a DNA sequence-based analytical tool, to identify the sources of contamination of nebulizer devices using the samples' microbiome as a biomarker. They performed source identification to look for four potential sources of microbial contamination: human gut microbiota, human oral microbiota, human skin microbiota, and hospital indoor environment microbiota. The latter was identified as the primary source of microbial contamination in nebulizers, contributing to ∼41.3% of microbiomes with a variation ranging from 20.2% to 64.8%. On the contrary, the microbiota from human sources accounted only for ∼10% of nebulizer microbiomes, with a higher prevalence referable to the human skin microbiota, followed, by human oral microbiota and human gut microbiota. However, their classification lacking some microbial sources since ∼50% of the compounds were not classified as belonging to one of the 4 groups (70).

Based on all these studies, medical devices can represent a possible way for pathogen transmission and HAIs to spread mainly due to wrong cleaning procedures, therefore infection control practices should be developed and implemented to mitigate microbial contamination of medical devices whatever the source.

Environmental factors, ecosystem, and HAIs

At present, different factors can influence HAIs. From an environmental point of view, it is possible to go beyond the HE, analyzing different environmental factors which characterize our ecosystems, such as humidity, temperature, illuminance, season, and climate changes. The following studies focused on one or more of these factors, contributing to identifying their roles in spreading HAIs, in order to develop control procedures to manage and limit the risk to human

health. One of the first studies was that of Ramos et al., which characterized the indoor environmental variations in which microbial samples were taken for the "Hospital Microbiome Project." This project was designed to investigate microbial community and environmental factors inside 10 patients' rooms and two nearby nurse stations for a period of 1 year in a newly established hospital. Both surface-bound and airborne microbes were influenced by different environmental factors (temperature, relative humidity, and humidity ratio) in their growth or survival responses. Moreover, these Authors observed variation due to light conditions, in particular, because a high degree of sunlight illumination may inhibit bacterial growth or have bactericidal powers. They also observed further correlations with the entrance of the new occupancy and activity explained in the rooms, which may represent the main cause of contamination from human-related microbial communities (71). As well as the previous study, also Freedberg et al. highlighted, in their conclusions, that the microbial community in a healthcare setting may be altered by multiple environmental factors, such as seasonal shifts, solar exposure, and temperature (61). Another study focused on temporal variation is that of Schwab et al. which evaluated the implications of seasonal variations specifically on nosocomial bloodstream infections (BSIs). They performed a retrospective cohort study based on 2 databases (one for HAIs monitoring and one with aggregated monthly climate data) collecting information on about 1196 ICUs located in 779 hospitals and in 728 different postal codes in Germany. Collectively they analyzed more than 6.5 million ICU patients and more than 19000 BSIs in a 15-year period. Through their studies, Schwab et al. were able to determine that the incidence of BSIs was correlated with temperature and vapor pressure, and inversely with relative humidity. Related to temperature the incidence of BSI was 17% higher in months with temperature $\geq$20°C compared to months with temperature <5°C. In particular, a strong correlation was observed when the mean monthly temperature of the month prior to the BSI occurrence was considered rather than the temperature of the month of occurrence. More in detail, the gram-negative bacteria were those with the most prominent effect despite the majority of bacteria increased with rising temperatures. *Enterococci* showed no seasonality while Staphylococcus pneumoniae reached a peak in wintertime. These conclusions agreed with previous studies which claimed that gram-negative BSI was most frequently in warmer months; gram-positive BSIs were inconsistent except for *Staphylococcus pneumoniae* BSIs which resulted most frequently in months with the lowest temperatures (72). A similar retrospective observational study, but on another type of HAIs, was that performed by Aghdassi et al., which included more than 2 million procedures resulting in ~32,000 surgical site infections (SSIs) from 1455 surgical departments. They matched the date of the procedures with the meteorological conditions for the month in which the procedure was performed. In accordance with the previous study also SSIs resulted most frequently in the months with temperature $\geq$20°C rather than in those with temperature <5°C with a higher correlation for those SSIs due to gram-negative bacteria. This was particularly prominent for Acinetobacter spp and Enterobacter spp for which was shown that a rise of only 1°C led to an increase in SSIs incidence of 6% and 4%, respectively. Among gram-positive bacteria, *Staphylococcus aureus* showed a stronger association with warmer temperatures. However, despite one could think that a stronger correlation should be related to human skin bacteria (such as the latter), a higher correlation between temperature and pathogens was observed for those microorganisms abundant in the human gut (such as *Acinetobacter* spp, *Enterobacter* spp, *Pseudomonas aeruginosa*, *Enterococcus* spp, and *Escherichia coli*) thereby emphasizing the importance of human gut microbiome also in HAIs pathogenesis (73). More recently, Li et al. demonstrated a significant difference in the microbial composition in healthcare settings on a seasonal time scale. However, despite some HAI-related bacteria such as *Acinetobacter*, *Pseudomonas*, *Enterococcus*, *Staphylococcus*, and *Escherichia* existing throughout the year, they observed their increase in some periods of the year, for instance, Acinetobacter was highly abundant in June and December, whereas Pseudomonas in March, April, and May (15).

In addition, Sereira et al. showed also a specific correlation between months and bacteria amount. In particular, they noted a higher median amount of HAI-related pathogens in May and September, in some sampling sites, due to an increase in *Escherichia coli* and an outbreak of Acinetobacter baumannii, respectively (50). Wu et al. characterized bacterial dynamics among the seasons collecting 10 hospital ambient air particulate matter (PM2.5) samples in summer and 9 in winter. Differently from Proteobacteria, which remain consistent through the entire sampling period, they showed a decrease of 12% in Actinobacteria phylum from summer to winter, and an increase of Firmicutes phyla which passed from 22 to 40%. More generally, the microbiota results detected were less diverse in winter by one order of magnitude overall (74).

All these studies, taken together, indicate that meteorological factors impact microbiological composition and thus may influence the occurrence of different HAIs. Therefore, based on these considerations should be developed proper protocols to control HAI-related pathogens adjusted by months.

Studies of transmission/cleaning and HAIs

Scientific evidence shows that the application of appropriate cleaning procedures together with campaigns to raise awareness for hand hygiene may lead to reduce microbial contamination and HAIs spreading. Indeed, different scholars, such as

Pérez-Fernández et al., concluded that the accumulation and proliferation of HAI-related pathogens might be due to the absence of adequate cleaning and maintenance procedures. In particular, they stated the importance of disinfection not only for HCW, but also for the entire HE including all instruments, equipment, and anything else that has come into contact with the patient (53).

We started considering three articles that tested bacterial transmission alone or in association with cleaning procedures. Del Campo et al. enrolled 30 healthy volunteers (20 women and 10 men) to perform a four-sequential steps protocol of finger-to-finger contact in the same person artificially infected with a precise bacterial inoculum. After the experimental procedure, the volunteers were grouped into three categories, based on their propensity to finger-to-finger bacteria transmission: women were classified in the medium category, whereas the men were divided into the poor or high categories. Analyzing specifically five different HAIs-related bacteria, they defined that gram-positive bacteria such as *Enterococcus faecium* and *Staphylococcus aureus* were characterized by a higher transmission efficiency in comparison to gram-negative bacteria. In particular, despite *Escherichia coli* results showing it to be a ubiquitous bacteria, it was characterized by a low transmission efficiency. Moreover, they performed a second experiment to test the inter-individual transmission chain exploring the finger-to-finger bacterial transmission with all possible combinations of individuals belonging to the three classes; from this test, they detected a reproducible transmission pattern whose efficiency was strictly dependent on the position of the poor transmitter, who cut off the transmission chain (75).

Weber et al. simulated the transmission of ESKAPE pathogens and Clostridium difficile under varying contact scenarios. They performed experiments for both direct (skin-to-skin) and indirect (skin-to-formite-to-skin) transmission by inoculating synthetic skin surrogates with a background skin microbiota or with both background skin microbiota and pathogens, simulating the transmission both before and after cleaning procedures. They observed a higher direct transfer, with smaller differences at low inoculum, compared to those at higher inoculum, for Acinetobacter baumannii, Enterobacter aerogenes, Klebsiella pneumonia, Pseudomonas aeruginosa, *Staphylococcus aureus*, and *Enterococcus faecium*, whereas no significant differences for Clostridium difficile and *Enterobacter cloacae* were observed. In comparison to direct transfer, indirect transfer gave significantly lower transmission rates, except for *Staphylococcus aureus*. Moreover, when decontamination was also investigated, greater differences were observable in the indirect transmission rather than in direct transmission, with a reduction in the transfer of some HAI-related bacteria (76).

Herruzo-Cabrera et al. compared the effect of classic handwashing on native and acquired microbiota with different alcohol solutions. They performed an "*in vitro*" test to evaluate the microbicide effect of the disinfectants on pig skin carrier models, an "*in vivo*" test on healthy volunteers comparing the hands microbiota collected before or after the cleaning, and a similar "field assay" but on HCW in a hospital ICU. Overall, they observed a high reduction of acquired and native hand microbiota (in particular for *Staphylococcus aureus* and gram-negative bacteria) for hands treated with different alcohol solutions. Conversely, only small variations were observed both in native and acquired microbiota after the common handwashing procedures. Therefore, the use of alcohol solution with some detergents or emollients can be more efficient to reduce HAIs, controlling the bacterial-hands spreading (19). Similarly, Wiemken and Ericsson studied the impact of one chlorhexidine gluconate (CHG) application on skin microbiota. They enrolled five healthy adults to analyze their skin microbiota before and after multiple time points after the CHG bathing. No significant evidence were detected in either the short or long term after single CHG use, probably due to the wide broad-spectrum activity which led to an equal reduction of different taxa without eliminating any of them. This suggests the long-period stability of skin microbiota even after a single application of CHG (77).

Differently, Ribeiro et al. analyzed the limits of cleaning procedures in ICU collecting environmental samples both before and after cleaning. Some bacteria decreased after cleaning: indeed, whereas 117 genera were detected before cleaning, only 94 were detected after it. Moreover, despite an overall decrease in diversity associated with a decrease of some genera (HAI-related genera included), some bacteria (such as *Bacillus*, *Staphylococcus*, and *Acinetobacter*) resulted to be still relatively abundant and sometimes increased. These results highlighted the limitations of the cleaning procedures, since the increase of specific genera, some of which are HAI-related (64). Also, Perry-Dow et al. focused their efforts to characterize the microbial communities of disinfected environmental surfaces. Using NGS, they analyzed two different composite samples collected from 94 rooms post-routine or terminal cleaning with bleach, quaternary ammonium compound (QAC), or a combination of the two. Among the most abundant OTUs detected, gram-negative bacteria (including enteric bacteria such as Enterobacteriaceae) resulted most abundant in QAC-cleaned rooms, whereas gram-positive bacteria (including skin microbiota bacteria such as Corynebacteriaceae) in bleach-cleaned rooms. Instead, a relative lower abundance in Enterobacteriaceae and Moraxellaceae OTUs was associated with rooms cleaned with both QAC and bleach. All these data, taken together, suggested the importance of disinfection to reduce HAIs-related pathogens' surface persistence due to the different impacts of each disinfectant on the different bacteria (78). Additionally, Sheahan et al. concluded that, after cleaning, some bacteria may persist in the environment, further suggesting the different effects of disinfection based on bacteria sensitivity. Moreover, they highlighted that, since it

is not possible to ensure a sterile workplace evermore, careful monitoring may aid to develop proper cleaning procedures based on the type of contamination (68).

Differently, Valeriani et al. performed their study on dental mirrors through two different experiments: in the first one, dental mirrors were contaminated by two different salivary solutions, and then six different sanitation procedures were applied; in the second dental mirrors used in care settings were sampled at different steps of the sanitation procedures. Overall, only the dental mirrors which underwent a complete sanitation procedure resulted negative for bacteria, whereas those contaminated or partially sanitized resulted to be positive. This suggested that the analyses of residual traces of a biological fluid microflora DNA might be an important monitoring system of correct sanitation. However, a negative result was mainly associated with culture analyses rather than molecular ones, indeed some negative culture-based microbiological samples resulted in positive to real-time PCR (14).

As we have seen, different studies demonstrated that HAI-related bacteria may persist on environmental surfaces also after cleaning procedures. Caselli et al. proposed new cleaning methods based on addition of healthy-probiotics to hospital surfaces to fight against pathogenic species. Cleaning was performed with Probiotic Cleaning Hygiene System (PCHS) by using detergents containing spores of *Bacillus subtilis*, *Bacillus pumilus*, and *Bacillus megaterium*. Surface samples were collected before the treatment and on a monthly base for the following 4 months. They monitored different HAI-related pathogens (among the others, *Staphylococcus* spp, *Acinetobacter*, *Pseudomonas* spp, and *Clostridium* spp) for which a strong decrease after the PCHS treatment was observed. The only exception was the Enterobacteriaceae group, which continued to be scarcely represented over time. Their decrease was evident 1 month after the PCHS treatment and was maintained constant. Probably the microbial decrease may be attributed to PCHS-Bacillus which, reaching 70% of the total microbiota already in 1 month, replaced most of the microbial species originally present on the surfaces, including the pathogenic ones (79). Similarly, Soffritti et al. applied the PCHS to confirm its previously shown ability to decrease the level of pathogens, also in pediatric hospital units. In their experiment, they replaced the conventional sanitation procedure with PCHS treatment for 2 months collecting and characterizing the microbiota with both culture and molecular tests, before and after the PCHS treatment. As in the previous study, they highlighted a microbial contamination reduction, with a simultaneous increase of Bacillus species, which replace the pathogen ones inhibiting their growth. In particular, before PCHS introduction, a high burden of HAI-related pathogens, such as Staphylococcus spp, Pseudomonas spp, Clostridium difficile, and Enterococcus spp and a very low amount of Bacillus spp, were detected. However, after 2 weeks significant changes were observed: Baciullus spp increased, representing 69.9% of all the microbial community, whereas other bacteria diminished. They also highlighted a microbial contamination reduction, with a simultaneous increase of Bacillus species which replace the pathogen ones inhibiting their growth (80). Both these last studies taken together suggest the greater potential of Bacillus-based cleaning procedures compared to the most common procedure used for sanitation, which are usually based on surface sterilization leading to increase resistance and pathogenic bacteria (79, 80).

Based on all these studies, it is important to develop more and more robust cleaning procedures to help management of HAIs, since the use of common cleaning procedures, such as those based on chemicals compounds, may not only let some bacteria on the surfaces (HAI-related ones included) but do not prevent recontamination phenomena, leading to the selection of resistant strains. This was sustained also by Costa et al. who showed also the incorporation of these resistant bacteria in biofilms whose persistence seemed to be not so influenced by the cleaning procedure (65). Given the improper cleaning procedure, the prior presence of patient-carriers of HAI-related bacteria increases the possibility to acquire those same bacteria by the patients who will be subsequently admitted in the same rooms. This further suggests the need to improve environmental hygiene by using a wider spectrum of cleaning or adding beneficial microbes that compete with the pathogenic ones, replacing them (Figure 4). In addition, performing intermedia cleaning during patients' hospitalization rather than only terminal cleanings as proposed by Freedberg et al. (61), or implementing cleaning procedures for those elements for which are not envisaged or, moreover, using instrumentation/structures/elements done with materials easier to clean as sustained by Gudokova et al. (67) may be further aids to HAIs-bacteria management.

Resistome and HAIs

Cleaning procedures have a starring role in pathogens transmission because either the wrong procedures or the use of chemical disinfectants may cause problems in controlling pathogen contamination, not only in terms of recontamination but also in terms of resistant strains selection. Therefore, identifying the main resistome profiles may give the bases for developing new strategies against resistant pathogens. In Maamar et al., 35 CTX-R Enterobacteriaceae strains were isolated in 28 patients. These isolates were screened for extended-spectrum beta-lactamases (ESBL)-phenotype by double-disk synergy test (DDST) with different antibiotics (ceftazidime, cefatoxime, and amoxicillin-clavulanic acid) disks. Only one isolate was classified as an AmpC producer due to its negative ESBL phenotype with resistance to amoxicillin-clavulanic acid and to cefoxitin, the 34 remaining were classified as ESBL producers. Among them, three resulted with both phenotypes AmpC and ESBL. More in detail, a careful

antimicrobial susceptibility test was performed, and all the isolates results were resistant to chloramphenicol, 32 resistant to nalidixin acid, 31 to ciprofloxacin, 29 to three different types of antibiotics (tobramycin, trimethoprim-sulfamethoxazole, and tetracyclin), 27 to gentamicin, 24 to cefoxitin, 22 to ertapenem, and 19 to imipenem. The different strains were analyzed and different resistance genes resulted in transferable by conjugation or co-transferred together. Therefore, most of the CTX-R Enterobacteriaceae strains resulted to be multidrug-resistant (MDR) bacteria, characterized by multiple resistance determinants which cause serious complications for patients limiting the therapeutic options for HAI treatment (60). Cruz-López et al. tested the antimicrobial susceptibility of the different 12 HAI causative agents identified during their study. Eleven of them were MDR bacteria and Acinetobacter baumanii showed resistance to ciprofloxacin, ceftazidime, meropenem, tetracycline, trimethoprimsulfamethoxazole whereas two of three studied *Klebsiella pneumoniae* isolates were carbapenemase producers but all results denoted ESBL producers as well as Raoultella ornithinolytica. Moreover, whereas coagulase-negative staphylococci isolates were resistant to oxacillin and *Staphylococcus hominis* to linezolid, *Enterobacter cloacae* was the only susceptible to all tested antimicrobial agents (54).

Comar et al. analyzed the resistome of the contaminating population through PCR to provide means for the control of HAI transmission. The detected and quantified 84 AMR genes such as those for methicillin, macrolides, beta-lactams (including carbapenems and erythromycin) highlighted the presence of strains resistant to these classes of antibiotics in the analyzed samples. These results allowed them to design specific interventions to fight AMR spreading, especially based on the amount and type of contamination (13). AMR spreading was investigated by Sereira et al. who defined AMR as widely distributed in patients, HE and HCW identified different hotspots of contamination (such as bed equipment, bed bathrooms, and HCW resting areas). In these sites, *Acinetobacter baumanii*, *Klebsiella pneumoniae*, *Enterobacter cloacae*, and *Escherichia coli* were identified as the most frequent AMR bacteria. AMR profiles supported these results with the detection of beta-lactamase genes, MDR, extended-spectrum cephalosporin resistance, and carbopenem resistance (50).

Caselli et al. did not limit their study to the resistome profile of a specific microbial community but also studied also its remodeling over time, analyzing the total microbial DNA extracted from the samples detecting and quantifying simultaneously 84 different AMR genes. In the beginning, several resistance genes (against beta-lactams, macrolides, quinolones, and methicillin) were detected in the samples. One month after the PCHS application, these genes decreased. These data were further confirmed through subsequent samplings, with the sole exception of the macrolides resistance gene which resulted in increases every time. This is easily explainable because this resistance gene has been constitutively identified in PCHS Bacillus species, which increase over time after PCHS application and do not acquire other new resistance over time (79). As stated above, a similar study was performed by Soffritti et al. They analyzed the entire resistome both before and after PCHS application in a children's hospital looking for 84 AMR genes. They provided evidence of resistance against macrolides, erythromycin, streptomycin/spectinomycin, erythromycin, beta-lactams, tetracyclin, fluoroquinolones, and methicillin before PCHS application decreasing by an up to 2 logs after the probiotic-based sanitation (80). Thus, confirming what was previously highlighted by Caselli et al. (79).

Whereas, the two previous studies were aimed at characterizing the resistome of the entire microbial community or, at most, those of Bacillus species, Shoaei et al. focused their studies on the AMR of Clostridium difficile isolates with different antibiotics showing their susceptibility for vancomycin and metronidazole and their resistance for moxifloxacin and clindamycin (51).

Wu et al. shifted their attention to the inhalable antibiotic resistome, spreading in healthcare settings through airborne fine PM2.5. In this type of sample, compared to urban ambient air PM2.5, the number of antibiotic resistance genes (ARGs) were nearly doubled, with the prevalence of potential pathogens bacteria of human origin such as Staphylococcus spp and Corynebacterium spp, most of which are MDR bacteria. Among the others, the major resistome components encoded by ARGs were those to aminoglycoside, macrolide-lincosamide-streptogramin, tetracycline, and beta-lactam, whereas the minor ones were bacitracin, rifamycin, sulphonamide (glyco)peptide, and fluoroquinolone. However, collectively, the hospital-specific resistome was significantly associated with the dynamic variation of the bacterial community structure, and the presence of ARG-carrying bacteria in hospital airborne PM2.5 resulted influenced by the HAI spreading (74).

Overall, based on these studies, it is evident how MDR or even pan-drug resistant bacteria cause an increasing number of HAIs, thereby AMRs are becoming a worldwide-relevant problem. Therefore, the understanding of bacteria resistome is of fundamental importance to define new therapeutic strategies to fight against HAIs.

Discussion

In recent years, a strong focus has been placed on the prevention and control of these infections due to a constantly growing epidemiological trend with strong repercussions on the health of the patients, as well as on the psychological and financial aspects which translate into a prolongation of the length of hospitalization, long-term disability, increased mortality, and spread of antibiotic resistance. The spread of nosocomial infections and multi-resistant microorganisms

represent a global health and development threat, especially in the context of HAIs. This is particularly dangerous in healthcare settings due to the diffused and wrong utilization of antimicrobials, which exercise a huge selective pressure on microbes making them stronger and thus therapies ineffective against infections (11, 13). Moreover, for a long time, cleaning was considered mostly an aesthetic requirement rather than an important safety protocol for managing HAIs, however, potential pathogens are not necessarily associated with evident dirt. Indeed, microorganisms survive for a long time on surfaces and specific cleaning procedures can lead to an increase in the number of pathogenic strains over the benign ones, rather than complete surface sterilization. Therefore, sometimes a treatment that increases the number of healthy microorganisms rather than an incomplete surface cleaning, which increases the number of resistant microorganisms, could be a better solution (11, 20). The increase of AMR microorganisms did lead to a change in the causative pathogens responsible for HAIs. Until the beginning of the 80's years, HAIs were mainly due to gram-negative bacteria (such as *Escherichia coli* and Klebsiella pneumonia). One of the challenges still open for the protection of public health is to investigate and identify the variables that influence the risk of HAIs and implement corrective actions to improve the care process, thus reducing the percentage of infected patients (81). Great progress has been made in recent years in the knowledge of the composition (microbiota) and gene expression (microbiome) of the microbial component associated with various body parts (intestinal, respiratory, skin, vaginal, oral, etc.). The advent and continuous development of "meta-omics" and computational technologies is providing revolutionary tools for the study of the microbiota and microbiome, highlighting many aspects inherent to its modulation and the multiple interactions with the 'external environment (exposome), with nutrition (foodoma) and with pathogens (infectoma), in the context of the genetic variability of the host. Unfortunately, the use of different platforms and original methods developed in-house, as well as the diffusion of structures operating in the sector outside of adequate validation, represents a serious obstacle to the consolidation and large-scale expansion of the results, while promising, so far obtained.

Future challenges in the microbiome and healthcare-related infection control should cover the following objectives:

- To facilitate the clinical application of knowledge in the microbiota by defining typical profiles associated with single individuals, age groups, and groups of pathologies for the characterization of aerobiosis and dysbiotic states of the microbiota in pediatric, adult, and elderly ages and that are related to the development of healthcare-related infections;
- To favor the standardization of diagnostic protocols based on omics technologies (e.g., standardization of sample collection and treatment, optimization of omics procedures and bioinformatic pipelines for interpreting big data), also defining the characteristics of specialists in "microbiology of the microbiota," able to provide pre-clinical and clinical tools, working closely with other specialists in public health and infectious disease, for the prevention and treatment of healthcare-related infections;
- To define the role of probiotics in improving the balance of the microbiota and their possible effectiveness in maintaining/restoring health and preventing/treating healthcare-related infections, also describing the current state of regulatory aspects and formulating indications for their revision, where deemed useful;
- To contribute to the transferability of the results obtained from research to clinical practice, ensuring safety, application homogeneity, and correspondence to suitably standardized and state-of-the-art procedures;
- To encourage the use in clinical practice of the new diagnostic applications of the microbiota through continuous dialogue with the health governance who are responsible for allowing the use and apply new available technologies.

Data availability statement

The original contributions presented in the study are included in the article/Supplementary material, further inquiries can be directed to the corresponding author/s.

Author contributions

PT: conceptualization, methodology, and writing–review and editing. AD: investigation and writing–original draft preparation. LC: supervision and writing–review and editing. All authors have read and approved the final version of the manuscript.

Funding

This study is part of a Ph.D. project funded by the Italian Ministry of University and Research, NOP Research and Innovation 2014-2020 on innovation and green topics, Ministerial Decree No. 1061 of 10 August 2021.

Conflict of interest

The authors declare that the research was conducted in the absence of any commercial or financial relationships

that could be construed as a potential conflict of interest.

Publisher's note

All claims expressed in this article are solely those of the authors and do not necessarily represent those of their affiliated organizations, or those of the publisher, the editors and the reviewers. Any product that may be evaluated in this article, or claim that may be made by its manufacturer, is not guaranteed or endorsed by the publisher.

Supplementary material

The Supplementary Material for this article can be found online at: https://www.frontiersin.org/articles/10.3389/fpubh.2022.989496/full#supplementary-material

References

1. Kollef MH, Torres A, Shorr AF, Martin-Loeches I, Micek ST. Nosocomial infection. *Criti Care Med.* (2021) 49:169–87. doi: 10.1097/CCM.0000000000004783

2. Monegro AF, Muppidi V, Regunath H. *Hospital Acquired Infections*. Treasure Island, FL: StatPearls Publishing (2022).

3. Blot S, Ruppé E, Harbarth S, Asehnoune K, Poulakou G, Luyt CE, et al. Healthcare-associated infections in adult intensive care unit patients: Changes in epidemiology, diagnosis, prevention and contributions of new technologies. *Intensive Crit Care Nurs.* (2022) 70:103227. doi: 10.1016/j.iccn.2022.103227

4. Tabatabaei SM, Behmanesh Pour F, Osmani S. Epidemiology of hospital-acquired infections and related anti-microbial resistance patterns in a tertiary-care teaching hospital in Zahedan, Southeast Iran. *Int J Infect.* (2015) 2:e29079. doi: 10.17795/iji-29079

5. Friedrich AW. Control of hospital acquired infections and antimicrobial resistance in Europe: the way to go. *Wien Med Wochenschr.* (2019) 169:25–30. doi: 10.1007/s10354-018-0676-5

6. Quainoo S, Coolen JPM, van Hijum SAFT, Huynen MA, Melchers WJG, van Schaik W, et al. Whole-genome sequencing of bacterial pathogens: the future of nosocomial outbreak analysis. *Clin Microbiol Rev.* (2017) 30:1015–63. doi: 10.1128/CMR.00016-17

7. Kim S, Covington A, Pamer EG. The intestinal microbiota: Antibiotics, colonization resistance, and enteric pathogens. *Immunol Rev.* (2017) 279:90–105. doi: 10.1111/imr.12563

8. Montella E, Ferraro A, Sperlì G, Triassi M, Santini S, Improta G. Predictive analysis of healthcare-associated blood stream infections in the neonatal intensive care unit using artificial intelligence: A single center study. *Int J Environ Res Public Health.* (2022) 19:2498. doi: 10.3390/ijerph19052498

9. Dabar G, Harmouche C, Salameh P, Jaber BL, Jamaleddine G, Waked M, et al. Community- and healthcare-associated infections in critically ill patients: a multicenter cohort study. *Int J Infect Dis.* (2015) 37:80–5. doi: 10.1016/j.ijid.2015.05.024

10. World Health Organization, WHO Patient Safety. *WHO Guidelines on Hand Hygiene in Health Care.* (2009).

11. D'Accolti M, Soffritti I, Mazzacane S, Caselli E. Fighting AMR in the healthcare environment: Microbiome-based sanitation approaches and monitoring tools. *IJMS.* (2019) 20:1535. doi: 10.3390/ijms20071535

12. World Health Organization. *Report on the Burden of Endemic Health Care-Associated Infection Worldwide*. Geneva: World Health Organization (2011).

13. Comar M, D'Accolti M, Cason C, Soffritti I, Campisciano G, Lanzoni L, et al. Introduction of NGS in environmental surveillance for healthcare-associated infection control. *Microorganisms.* (2019) 7:708. doi: 10.3390/microorganisms7120708

14. Valeriani F, Protano C, Gianfranceschi G, Cozza P, Campanella V, Liguori G, et al. Infection control in healthcare settings: perspectives for mfDNA analysis in monitoring sanitation procedures. *BMC Infect Dis.* (2016) 16:394. doi: 10.1186/s12879-016-1714-9

15. Li K, Zhu Q, Jiang F, Li H, Liu J, Yu T, et al. Monitoring microbial communities in intensive care units over one year in China. *Sci Total Environ.* (2022) 811:152353. doi: 10.1016/j.scitotenv.2021.152353

16. Loudon I. Semmelweis and his thesis. *J R Soc Med.* (2005) 98:555. doi: 10.1177/014107680509801220

17. Erasmus V, Daha TJ, Brug H, Richardus JH, Behrendt MD, Vos MC, et al. Systematic review of studies on compliance with hand hygiene guidelines in hospital care. *Infect Control Hospital Epidemiol.* (2010) 31:283–94. doi: 10.1086/650451

18. Voss A, Widmer AF. No time for handwashing!? Hand washing versus alcoholic rub: can we afford 100% compliance? *Infect Control Hosp Epidemiol.* (1997) 18:205–8. doi: 10.1086/647590

19. Herruzo-Cabrera R, Garcia-Caballero J. A new alcohol solution (N-duopropenide) for hygienic (or routine) hand disinfection is more useful than classic handwashing: *in vitro* and *in vivo* studies in burn and other intensive care units. *Burns.* (2001) 27:747–52. doi: 10.1016/S0305-4179(01)00013-4

20. Beggs C, Knibbs LD, Johnson GR, Morawska L. Environmental contamination and hospital-acquired infection: Factors that are easily overlooked. *Indoor Air.* (2015) 25:462–74. doi: 10.1111/ina.12170

21. Mirande C, Bizine I, Giannetti A, Picot N, van Belkum A. Epidemiological aspects of healthcare-associated infections and microbial genomics. *Eur J Clin Microbiol Infect Dis.* (2018) 37:823–31. doi: 10.1007/s10096-017-3170-x

22. Lamarche D, Johnstone J, Zytaruk N, Clarke F, Hand L, Loukov D, et al. Microbial dysbiosis and mortality during mechanical ventilation: A prospective observational study. *Respir Res.* (2018) 19:245. doi: 10.1186/s12931-018-0950-5

23. Slattery J, Macfabe DF, Frye RE. The significance of the enteric microbiome on the development of childhood disease: A review of prebiotic and probiotic therapies in disorders of childhood. *Clin Med Insights Pediatr.* (2016) 10:CMPed.S38338. doi: 10.4137/CMPed.S38338

24. Kates AE, Tischendorf JS, Schweizer M, Herwaldt L, Samore M, Dukes KC, et al. Research agenda for microbiome based research for multidrug-resistant organism prevention in the veterans health administration system. *Infect Control Hosp Epidemiol.* (2018) 39:202–9. doi: 10.1017/ice.2017.311

25. Ursell LK, Metcalf JL, Parfrey LW, Knight R. Defining the human microbiome. *Nutr Rev.* (2012) 70 Suppl 1:S38–44. doi: 10.1111/j.1753-4887.2012.00493.x

26. Shafquat A, Joice R, Simmons SL, Huttenhower C. Functional and phylogenetic assembly of microbial communities in the human microbiome. *Trends Microbiol.* (2014) 22:261–6. doi: 10.1016/j.tim.2014.01.011

27. Tozzo P, D'Angiolella G, Brun P, Castagliuolo I, Gino S, Caenazzo L. Skin microbiome analysis for forensic human identification: what do we know so far? *Microorganisms.* (2020) 8:873. doi: 10.3390/microorganisms8060873

28. Savage DC. Microbial ecology of the gastrointestinal tract. *Annu Rev Microbiol.* (1977) 31:107–33. doi: 10.1146/annurev.mi.31.100177.000543

29. Sender R, Fuchs S, Milo R. Are we really vastly outnumbered? Revisiting the ratio of bacterial to host cells in humans. *Cell.* (2016) 164:337–40. doi: 10.1016/j.cell.2016.01.013

30. Schmedes SE, Woerner AE, Budowle B. Forensic human identification using skin microbiomes. *Appl Environ Microbiol.* (2017) 83:e01672–17. doi: 10.1128/AEM.01672-17

31. Oh J, Byrd AL, Park M, NISC Comparative Sequencing Program, Kong HH, Segre JA. Temporal stability of the human skin microbiome. *Cell.* (2016) 165:854–66. doi: 10.1016/j.cell.2016.04.008

32. Belkaid Y, Segre JA. Dialogue between skin microbiota and immunity. *Science.* (2014) 346:954–9. doi: 10.1126/science.1260144

33. Costello EK, Lauber CL, Hamady M, Fierer N, Gordon JI, Knight R. Bacterial community variation in human body habitats across space and time. *Science.* (2009) 326:1694–7. doi: 10.1126/science.1177486

34. Schommer NN, Gallo RL. Structure and function of the human skin microbiome. *Trends Microbiol.* (2013) 21:660–8. doi: 10.1016/j.tim.2013.10.001

35. De Filippo C, Cavalieri D, Di Paola M, Ramazzotti M, Poullet JB, Massart S, et al. Impact of diet in shaping gut microbiota revealed by a comparative study in children from Europe and rural Africa. *Proc Natl Acad Sci USA.* (2010) 107:14691–6. doi: 10.1073/pnas.1005963107

36. Marples RR. Sex, constancy, and skin bacteria. *Arch Dermatol Res.* (1982) 272:317–20. doi: 10.1007/BF00509062

37. Fierer N, Hamady M, Lauber CL, Knight R. The influence of sex, handedness, and washing on the diversity of hand surface bacteria. *Proc Natl Acad Sci USA.* (2008) 105:17994–9. doi: 10.1073/pnas.0807920105

38. Yatsunenko T, Rey FE, Manary MJ, Trehan I, Dominguez-Bello MG, Contreras M, et al. Human gut microbiome viewed across age and geography. *Nature.* (2012) 486:222–7. doi: 10.1038/nature11053

39. Somerville DA. The normal flora of the skin in different age groups. *Br J Dermatol.* (1969) 81:248–58. doi: 10.1111/j.1365-2133.1969.tb13976.x

40. Camelo-Castillo AJ, Mira A, Pico A, Nibali L, Henderson B, Donos N, et al. Subgingival microbiota in health compared to periodontitis and the influence of smoking. *Front Microbiol.* (2015) 6:119. doi: 10.3389/fmicb.2015.00119

41. Williams DW, Gibson G. Classification of individuals and the potential to detect sexual contact using the microbiome of the pubic region. *Forensic Sci Int Genet.* (2019) 41:177–87. doi: 10.1016/j.fsigen.2019.05.004

42. Ross AA, Doxey AC, Neufeld JD. The skin microbiome of cohabiting couples. Sharpton T, editor. *mSystems.* (2017) 2:e00043–17. doi: 10.1128/mSystems.00043-17

43. Oh J, Freeman AF, Park M, Sokolic R, Candotti F, Holland SM, et al. The altered landscape of the human skin microbiome in patients with primary immunodeficiencies. *Genome Res.* (2013) 23:2103–14. doi: 10.1101/gr.159467.113

44. Dicksved J, Halfvarson J, Rosenquist M, Järnerot G, Tysk C, Apajalahti J, et al. Molecular analysis of the gut microbiota of identical twins with Crohn's disease. *ISME J.* (2008) 2:716–27. doi: 10.1038/ismej.2008.37

45. Fujiyoshi S, Tanaka D, Maruyama F. Transmission of airborne bacteria across built environments and its measurement standards: A review. *Front Microbiol.* (2017) 8:2336. doi: 10.3389/fmicb.2017.02336

46. The Human Microbiome Project Consortium, Huttenhower C, Gevers D, Knight R, Abubucker S, Badger JH, et al. Structure, function and diversity of the healthy human microbiome. *Nature.* (2012) 486:207–14. doi: 10.1038/nature11234

47. Haque M, Sartelli M, McKimm J, Abu Bakar MB. Health care-associated infections - an overview. *IDR.* (2018) 11:2321–33. doi: 10.2147/IDR.S177247

48. Weinstein RA, Gaynes R, Edwards JR, National Nosocomial Infections Surveillance System. Overview of nosocomial infections caused by gram-negative bacilli. *Clin Infect Dis.* (2005) 41:848–54. doi: 10.1086/432803

49. Page MJ, McKenzie JE, Bossuyt PM, Boutron I, Hoffmann TC, Mulrow CD, et al. The PRISMA 2020 statement: an updated guideline for reporting systematic reviews. *BMJ.* (2021) 372:n71. doi: 10.1136/bmj.n71

50. Sereia AFR, Christoff AP, Cruz GNF, da Cunha PA, da Cruz GCK, Tartari DC, et al. Healthcare-associated infections-related bacteriome and antimicrobial resistance profiling: assessing contamination hotspots in a developing country public hospital. *Front Microbiol.* (2021) 12:711471. doi: 10.3389/fmicb.2021.711471

51. Shoaei P, Shojaei H, Siadat SD, Moshiri A, Vakili B, Yadegari S, et al. Gut microbiota in burned patients with Clostridioides difficile infection. *Burns.* (2021) 2021:S0305417921003454. doi: 10.1016/j.burns.2021.11.023

52. Segal E, Bar Yosef S, Axel A, Keller N, Shlaeffer F, Amir A, et al. Outbreak of sepsis following surgery: utilizing 16S RNA sequencing to detect the source of infection. *Cureus.* (2022) 14:e22487. doi: 10.7759/cureus.22487

53. Pérez-Fernández T, Llinares-Pinel F, Troya-Franco M, Fernández-Rosa L. Analysis of the microbiota of the physiotherapist's environment. *Arch Phys Med Rehabilit.* (2020) 101:1789–95. doi: 10.1016/j.apmr.2020.06.006

54. Cruz-López F, Villarreal-Treviño L, Morfin-Otero R, Martínez-Meléndez A, Camacho-Ortiz A, Rodríguez-Noriega E, et al. Dynamics of colonization in patients with health care-associated infections at step-down care units from a tertiary care hospital in Mexico. *Am J Infect Control.* (2020) 48:1329–35. doi: 10.1016/j.ajic.2020.04.016

55. McDonald D, Ackermann G, Khailova L, Baird C, Heyland D, Kozar R, et al. Extreme dysbiosis of the microbiome in critical illness. Green Tringe S, editor. *mSphere.* (2016) 1:e00199–16. doi: 10.1128/mSphere.00199-16

56. Zakharkina T, Martin-Loeches I, Matamoros S, Povoa P, Torres A, Kastelijn JB, et al. The dynamics of the pulmonary microbiome during mechanical ventilation in the intensive care unit and the association with occurrence of pneumonia. *Thorax.* (2017) 72:803–10. doi: 10.1136/thoraxjnl-2016-209158

57. Lu S, Zhang W, Li X, Xian J, Hu Y, Zhou Y. Skin bacterial richness and diversity in intensive care unit patients with severe pneumonia. *Int J Infect Dis.* (2022) 121:75–84. doi: 10.1016/j.ijid.2022.05.006

58. Mu S, Xiang H, Wang Y, Wei W, Long X, Han Y, et al. The pathogens of secondary infection in septic patients share a similar genotype to those that predominate in the gut. *Crit Care.* (2022) 26:68. doi: 10.1186/s13054-022-03943-z

59. Lu Y, Cai X, Zheng Y, Lyv Q, Wu J. Dominant bacteria and influencing factors of early intestinal colonization in very low birth weight infants: A prospective cohort study. *J Clin Lab Analy.* (2022) 36:e24290. doi: 10.1002/jcla.24290

60. Maamar E, Ferjani S, Jendoubi A, Hammami S, Hamzaoui Z, Mayonnove-Coulange L, et al. High prevalence of gut microbiota colonization with broad-spectrum cephalosporin resistant enterobacteriaceae in a tunisian intensive care unit. *Front Microbiol.* (2016) 7:e01859. doi: 10.3389/fmicb.2016.01859

61. Freedberg DE, Richardson M, Nattakom M, Cheung J, Lynch E, Zachariah P, et al. Are there bad ICU rooms? Temporal relationship between patient and ICU room microbiome, and influence on vancomycin-resistant enterococcus colonization. Young VB. editor. *mSphere.* (2022) 7:e01007–21. doi: 10.1128/msphere.01007-21

62. Ke S, Pollock NR, Wang XW, Chen X, Daugherty K, Lin Q, et al. Integrating gut microbiome and host immune markers to understand the pathogenesis of Clostridioides difficile infection. *Gut Microbes.* (2021) 13:1935186. doi: 10.1080/19490976.2021.1935186

63. Ogura K, Furuya H, Takahashi N, Shibata K, Endo M, Watanabe S, et al. Interspecies regulation between *Staphylococcus caprae* and *Staphylococcus aureus* colonized on healed skin after injury. *Front Microbiol.* (2022) 13:818398. doi: 10.3389/fmicb.2022.818398

64. Ribeiro LF, Lopes EM, Kishi LT, Ribeiro LFC, Menegueti MG, Gaspar GG, et al. Microbial community profiling in intensive care units expose limitations in current sanitary standards. *Front Public Health.* (2019) 7:240. doi: 10.3389/fpubh.2019.00240

65. Costa DM, Johani K, Melo DS, Lopes LKO, Lopes Lima LKO, Tipple AFV, et al. Biofilm contamination of high-touched surfaces in intensive care units: epidemiology and potential impacts. *Lett Appl Microbiol.* (2019) 68:269–76. doi: 10.1111/lam.13127

66. Kelly BJ, Bekele S, Loughrey S, Huang E, Tolomeo P, David MZ, et al. Healthcare microenvironments define multidrug-resistant organism persistence. *Infect Control Hosp Epidemiol.* (2021) 2021:1–7. doi: 10.1017/ice.2021.323

67. Gudakova I, Kim J, Meredith JF, Webb G. Microbial contamination on touch surfaces in sick- and well-child waiting rooms in pediatric outpatient facilities. *Pediat Infect Dis J.* (2017) 36:e303–6. doi: 10.1097/INF.0000000000001759

68. Sheahan T, Hakstol R, Kailasam S, Glaister GD, Hudson AJ, Wieden HJ. Rapid metagenomics analysis of EMS vehicles for monitoring pathogen load using nanopore DNA sequencing. Moreno-Hagelsieb G, editor. *PLoS ONE.* (2019) 14:e0219961. doi: 10.1371/journal.pone.0219961

69. Mahjoub H, Zhang SX, Wang J, Memon W, Mostafa H, Breazzano MP. Characterizing the microbiota of instrumentation in ophthalmology clinics during and beyond the COVID-19 pandemic. *Graefes Arch Clin Exp Ophthalmol.* (2022) doi: 10.1007/s00417-022-05639-0

70. Swanson CS, Dhand R, Cao L, Ferris J, Elder CS, He Q. Microbiome-based source identification of microbial contamination in nebulizers used by inpatients. *J Hospital Infect.* (2022) 122:157–61. doi: 10.1016/j.jhin.2022.01.008

71. Ramos T, Dedesko S, Siegel JA, Gilbert JA, Stephens B. Spatial and temporal variations in indoor environmental conditions, human occupancy, and operational characteristics in a new hospital building. Morais PV. editor. *PLoS ONE.* (2015) 10:e0118207. doi: 10.1371/journal.pone.0118207

72. Schwab F, Gastmeier P, Hoffmann P, Meyer E. Summer, sun and sepsis—The influence of outside temperature on nosocomial bloodstream infections: A cohort study and review of the literature. Leekha S, editor. *PLoS ONE.* (2020) 15:e0234656. doi: 10.1371/journal.pone.0234656

73. Aghdassi SJS, Gastmeier P, Hoffmann P, Schwab F. Increase in surgical site infections caused by gram-negative bacteria in warmer temperatures: Results from a retrospective observational study. *Infect Control Hosp Epidemiol.* (2021) 42:417–24. doi: 10.1017/ice.2020.463

74. Wu D, Jin L, Xie J, Liu H, Zhao J, Ye D, et al. Inhalable antibiotic resistomes emitted from hospitals: metagenomic insights into bacterial

hosts, clinical relevance, and environmental risks. *Microbiome.* (2022) 10:19. doi: 10.1186/s40168-021-01197-5

75. Del Campo R, Martínez-García L, Sánchez-Díaz AM, Baquero F. Biology of hand-to-hand bacterial transmission. *Microbiol Spectr.* (2019) 7:e2016. doi: 10.1128/microbiolspec.MTBP-0011-2016

76. Weber KL, LeSassier DS, Kappell AD, Schulte KQ, Westfall N, Albright NC, et al. Simulating transmission of ESKAPE pathogens plus C. difficile in relevant clinical scenarios. *BMC Infect Dis.* (2020) 20:411. doi: 10.1186/s12879-020-05121-4

77. Wiemken TL, Ericsson AC. Chlorhexidine gluconate does not result in epidermal microbiota dysbiosis in healthy adults. *Am J Infect Control.* (2021) 49:769–74. doi: 10.1016/j.ajic.2020.11.021

78. Perry-Dow KA, de Man TJB, Halpin AL, Shams AM, Rose LJ, Noble-Wang JA. The effect of disinfectants on the microbial community on environmental healthcare surfaces using next generation sequencing. *Am J Infect Control.* (2022) 50:54–60. doi: 10.1016/j.ajic.2021.08.027

79. Caselli E, D'Accolti M, Vandini A, Lanzoni L, Camerada MT, Coccagna M, et al. Impact of a probiotic-based cleaning intervention on the microbiota ecosystem of the hospital surfaces: Focus on the resistome remodulation. Chang YF, editor. *PLoS ONE.* (2016) 11:e0148857. doi: 10.1371/journal.pone.0148857

80. Soffritti I, D'Accolti M, Cason C, Lanzoni L, Bisi M, Volta A, et al. Introduction of probiotic-based sanitation in the emergency ward of a children's hospital during the COVID-19 pandemic. *Infect Drug Resist.* (2022) 15:1399–410. doi: 10.2147/IDR.S356740

81. Montella E, Di Cicco MV, Ferraro A, Centobelli P, Raiola E, Triassi M, et al. The application of Lean Six Sigma methodology to reduce the risk of healthcare-associated infections in surgery departments. *J Eval Clin Pract.* (2017) 23:530–9. doi: 10.1111/jep.12662

frontiers | Frontiers in Immunology

TYPE Review
PUBLISHED 30 January 2023
DOI 10.3389/fimmu.2023.1091165

OPEN ACCESS

EDITED BY
Matija Rijavec,
University Clinic of Pulmonary and Allergic Diseases Golnik, Slovenia

REVIEWED BY
Soraya Mezouar,
Aix-Marseille University, France
Zhifeng Fang,
Shihezi University, China

*CORRESPONDENCE
Zhongping Gu
gu-zhong-ping@163.com
Tao Jiang
jiangtaochest@163.com
Wenchen Wang
18392187970@163.com

†These authors contributed equally to this work

SPECIALTY SECTION
This article was submitted to Microbial Immunology, a section of the journal Frontiers in Immunology

RECEIVED 06 November 2022
ACCEPTED 16 January 2023
PUBLISHED 30 January 2023

CITATION
Sun Y, Wen M, Liu Y, Wang Y, Jing P, Gu Z, Jiang T and Wang W (2023) The human microbiome: A promising target for lung cancer treatment. *Front. Immunol.* 14:1091165. doi: 10.3389/fimmu.2023.1091165

The human microbiome: A promising target for lung cancer treatment

Ying Sun†, Miaomiao Wen†, Yue Liu†, Yu Wang†, Pengyu Jing, Zhongping Gu*, Tao Jiang* and Wenchen Wang*

Department of Thoracic Surgery, The Second Affiliated Hospital, Air Force Medical University, Xi'an, China

Lung cancer is the leading cause of cancer-related deaths worldwide, and insights into its underlying mechanisms as well as potential therapeutic strategies are urgently needed. The microbiome plays an important role in human health, and is also responsible for the initiation and progression of lung cancer through its induction of inflammatory responses and participation in immune regulation, as well as for its role in the generation of metabolic disorders and genotoxicity. Here, the distribution of human microflora along with its biological functions, the relationship between the microbiome and clinical characteristics, and the role of the microbiome in clinical treatment of lung cancer were comprehensively reviewed. This review provides a basis for the current understanding of lung cancer mechanisms with a focus on the microbiome, and contributes to future decisions on treatment management.

KEYWORDS

microbiome, pulmonary infection, immunology, clinical application, malignant mechanism, lung cancer

1 Introduction

Lung cancer has the highest morbidity and mortality worldwide, with approximately 2 million new cases and 1.76 million deaths in 2021 (1, 2). In recent years, researchers have found that more than 16% of cancer cases are related to infections, and most infections are caused by microorganisms (3). The relationship between microbes and cancer has attracted considerable attention in academia. Bacteria were first discovered in tumors over a hundred years ago, and the existence of microorganisms in various tumors has been successively reported (4, 5). Healthy lungs are traditionally thought to be sterile, but recent studies have found that they also harbor microbial communities, including *Firmicutes*, *Proteobacteria*, *Bacteroidetes*, and *Actinobacteria* (6, 7). In addition, early epidemiological data have suggested that bacterial infections are common in lung cancer patients, especially as the disease progresses, and it is almost 50% to 70%. The pathogenic bacteria initially colonizing the lung might persist in patients with lung cancer as the disease progresses (8). Furthermore, the microflora residing outside the lung, such as the oral cavity, airways and gut, can also affect the occurrence and development of lung cancer, suggesting that the human microflora

may play a direct or indirect role in lung cancer onset and progression. This article reviews the role of the human microbiome in lung cancer as well as providing a basis for a potential role of the microbiome in therapeutic methods and drug discovery of lung cancer.

2 Distribution and function of human microflora

Humans coexist with and host a variety of microbes, such as bacteria, fungi, and viruses. All these microorganisms inhabiting specific areas of the human body constitute the human microbiota, which plays an important role in physiological activities such as nutrient absorption, substance metabolism, and immune regulation, and is also closely related to the occurrence of diseases such as infectious diseases, metabolic disorders, and different cancer types.

2.1 Distribution

Oral microorganisms

The oral cavity contains more than 700 species of bacteria. Oral microorganisms reside in biofilms throughout the mouth and form an ecosystem that helps to maintain a healthy microenvironment. The oral microbiota was composed of *Firmicutes*, *Bacteroidetes*, *Proteobacteria*, *Actinobacteria*, *Spirrochaetes*, and *Fusobacteria*, accounting for 94% of the total classification. The remaining phyla, such as *Saccharibacteria*, *Synergistetes*, *SR1*, *Gracilibacteria*, *Chlamydia*, *Chloroflexi*, *Tenericutes*, and *Chlorobi*, account for 6% of the taxa. The oral microbiome is impressive in its breadth and depth: one milliliter of saliva contains 1.0×10^8 microbial cells and 700 different prokaryotic taxa. Among these, it contains bacteria, fungi, viruses, archaea, and protozoa, of which approximately 54% are culturable and have been identified, 14% are culturable and not identified, and 32% are unculturable (9).

Respiratory microorganisms

When the human microbial group plan was launched in 2007, the lungs were not included among the sampled organs, in part as they were thought to be sterile (10). With the increasing development and popularity of high-throughput sequencing and sequence assembly technology, together with databases of sequenced organisms (11, 12), the identification and quantification of organisms from mixed metagenomic samples has been possible through high-throughput metagenomic sequencing, a convenient, and so far the fastest strategy for the study of lung microbes (13). Respiratory microbes grow rapidly in early life of the host and are influenced by the environment, age, and immune status of the host (14). Indeed, it has been proven that birth, the first postnatal hour, and the first 3 to 4 months of exposure to the living environment are important stages for a stable development of respiratory flora (15).

In healthy lungs, two phyla are mainly present, *Bacteroidetes* and *Firmicutes*, which constitute the pulmonary microbiota, whereas *Prevotella* and *Veillonella* spp. are dominant (16–18). Compared to the upper respiratory tract, the microbiota of the lung mucosa is phylogenetically diverse. In addition, the lower respiratory system is mainly composed of *Pseudomonas*, *Streptococcus*, *Fusobacterium*, *Megacoccus* and *Sphingosphingomonas* (18, 19). Some studies have shown that the lungs are susceptible to oropharyngeal bacterial colonies (16, 17, 20). For example, Bassis et al. compared the microbial composition in the oral and nasal cavities, lungs, and stomach of healthy adults and found that the microbial communities in gastric juices and alveolar lavage fluid (BAL) were mainly derived from the inhalation and colonization of oropharyngeal flora (21).

Gut microorganisms

The gut provides a convenient habitat for all kinds of microorganisms, with comprise an estimated total of 1.0×10^{13} - 1.0×10^{14}. The human gut microbiota is composed of at least 1000 - 1200 species of bacteria, mainly *Firmicutes*, *Bacteroidetes*, *Proteobacteria*, *Actinobacteria*, *Fusobacteria*, *Verrucomicrobia*, and others. Among these, *Firmicutes* (64%) and *Bacteroidetes* (28%) were the main components in most individuals. *Actinobacteria*, *Proteobacteria*, and *Verrucomicrobia* were minor components. The human gut microbiome is extremely large and scientists have not been able to determine the number of gut microbes that people may carry. It has been estimated that a 70 kg adult (3.0×10^{13} cells) carries approximately 3.8×10^{13} bacteria (0.2 kg) (22, 23).

The composition of the human gut microbiota varies among populations, and the difference in individual composition is mainly reflected in the proportion of bacteria of each phylum. The diversity of species of gut microbiota in humans increases with time, mostly during the first three years (approximately 100 species in the first few weeks of life, 700 between six months and three years of age, and 1,000 in adulthood). Agedness is another stage at which the gut microbiota changes dramatically. At this stage, the number of facultative bacteria increases, the ratio of *Bacteroidetes* to *Firmicutes* increases, and that of *Bifidobacterium* decreases. Claesson et al. reported that, compared with young people, the differences in gut microbiota composition especially in *Ruminococcaceae* family (comprised of *Ruminococcus*, *Sporobacter*, and *Faecalibacterium* species), among individuals was significantly higher in the elderly, and the *Bifidobacterium* proportions, the *Clostridium* cluster IV, as well as the species diversity within each individual was significantly reduced, which is likely related to diet, health status, and immune system decay (24, 25).

Other microorganisms

Several decades ago, concentrations of intestinal bile acid were found to be much higher in breast cyst fluid than in serum in women with fibrocystic breast disease (26–28). Although the mechanisms for maintaining high bile concentrations within breast cysts remain to be studied, these studies suggest that breast tissue, like other parts of the body, is composed of an unique microbiome. Bacteria can also be detected in breast milk, possibly because microbes can travel from the surface of the skin into ducts and breast tissue. The most common genera in milk are *Staphylococcus*, *Streptococcus*, *Lactobacillus*, *Pseudomonas*, *Bifidobacterium*, *Corynebacterium*, *Enterococcus*, *Acinetobacter*, *Rothia*, *Cutibacterium*, *Veillonella* and *Bacteroides* (29). Urbaniak et al. studied the differences in microbial

communities in 81 pairs of patients with and without breast cancer, and found that *Proteobacteria* composition was different between them, together with regional divergence (30).

The stomach has generally been considered to have fewer symbiotic bacteria because of its highly acidic environment and high protein hydrolase content (31, 32). However, recent studies have shown that a wide variety of bacteria can be found in the human stomach. *Firmicutes* and *Proteobacteria* are the major phyla, and *Streptococcus* and *Prevotella* are the major species in the stomach of individuals without *Helicobacter pylori* (HB) (33, 34) (Figure 1). Infection with HB can disturb the microbial community in the stomach (35).

In normal prostate, estimations concerning the microorganism number and composition are difficult since access to non-diseased prostate tissue is restricted. However, a number of previous studies have characterized the microbial composition in prostate cancer and normal surgically resected specimens, and found that no bacteria were present in normal prostate tissue (36–38). On the contrary, one study detected a positive result for bacteria in tissue specimens of benign prostatic hyperplasia (BPH) (39). However, it cannot be discarded that the positive result may owe to contamination (40). In addition, normal prostatic fluid may prevent microbial growth because of its highly antibacterial properties. Microbial invasion occurs only in the prostate upon prostatitis or other pathological occurrences (41).

2.2 Influence of microbiome on human development and physiological function

The microbiome plays an important role in human development and physiology. In this context, changes in the oral microbiome may cause oral and systemic diseases (42) and an imbalance in the respiratory microbiome may affect the occurrence of lung diseases (43). The gut microbiome accounts for a relatively high proportion of the human body, and its functions have been fully studied, including nutrient metabolism and immune regulation. The following sections focus on the role of oral, respiratory, and intestinal microbiota in human development and physiological function (Figure 1).

2.2.1 Oral microbiome

The human oral microecosystem contains a large diversity of microorganisms, including bacteria, fungi, viruses, mycoplasma and protozoa. Of these, bacteria (about 700 species) make up the majority of the healthy oral microbiome and are mainly composed of six phyla, including Firmicutes, Actinobacteria, Proteobacteria, Fusobacteria, Bacteroides and Spirochaetas (44). In addition to bacteria, about 100 fungi also make up an important part of the oral microbiome, of which *Candida* is the most common. In the oral microecosystem, microbes such as bacteria and fungi attach to the surface of teeth and form a biofilm called plaque with the surrounding extracellular matrix in order to protect themselves from fluctuations in the oral environment and external drug stimuli and evade host defense mechanisms (45).

The balance of oral microecosystem not only contributes to the maintenance of oral health, but also has a potential impact on the overall health. Microorganisms in oral microecosystems achieve dynamic balance between each other and the host through complex interspecific interactions such as symbiosis, competition and confrontation (46). This paper summarizes the physiological function of normal microbial flora in oral cavity.

2.2.1.1 Maintaining the microecology in the mouth

The normal microflora in oral cavity can maintain the microecological balance well. When pathogenic bacteria such as *P. seudomonas aeruginosa* invade, the oral flora inhibits their growth in

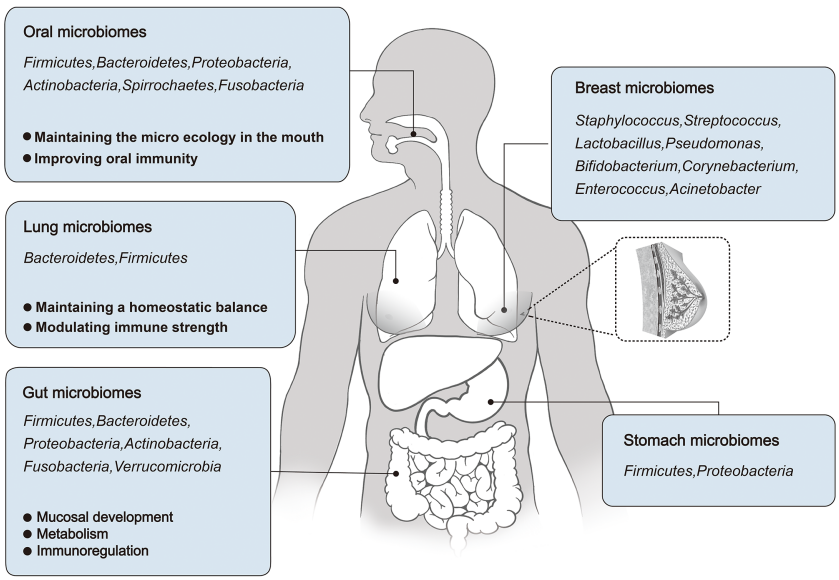

FIGURE 1
An overview of the microbial distribution in human body, and the roles of Oral, Lung, and Gut microbiomes in human development and physiological function.

saliva by producing lactic acid (47). Therefore, the normal oral flora plays an important role in preventing the invasion of pathogenic bacteria. However, disturbances in oral microecology such as oral flora imbalance or reduction of oral symbiotic bacteria provide opportunities for the invasion and colonization of respiratory pathogens such as *Staphylococcus aureus*, *Pseudococcus aeruginosa*, *Enterococcus faecalis* and *Acinetobacter* (48–51).

2.2.1.2 Improving oral immunity

Natural aging, hypoplasia of parotid and submandibular glands, and medications (antihypertensive drugs, anticholinergics) can alter saliva composition or affect saliva secretion or flow rate, leading to dry mouth and poor oral hygiene (52). This may lead to the transfer of normal oral flora to communities containing more pathogens (53).

2.2.2 Respiratory microbiome

The respiratory tract is a complex organ system whose main function is the exchange of oxygen and carbon dioxide. It is divided into the upper respiratory tract, which includes the nasal passages, pharynx, larynx, and lower respiratory tract, which includes the conducting airways (trachea and bronchi), small airways (bronchioles), and respiratory areas (alveoli). Because the respiratory tract is connected to the outside world, a large number of airborne microorganisms and particles, including viruses, bacteria and fungi, continue to migrate or be removed from the respiratory tract. The bacterial burden of the upper respiratory tract is about 100-10000 times than that of the lower respiratory tract, and the nasal cavity is dominated by *Propionibacterium*, *Corynebacterium*, *Staphylococcus* and *Moraxella*. *Prevotella*, *Vermicelli*, *Streptococcus*, *Haemophilus*, *Fusobacterium*, *Neisseria* and *Corynebacterium* were predominant in oral cavity (54, 55). *Prevotella*, *Vermicelli*, and *Streptococcus* colonize in the lower respiratory tract, and these microbial compositions differ from those observed in the oral and nasal cavities (56). As mentioned earlier, the gut microbiome of young children stabilizes at about 3 years of age, similar to that of adults, and this pattern of community maturation is reproduced in the upper respiratory tract microbiome (14, 57, 58). The following is a comprehensive summary of the physiological function of respiratory microorganisms in human body.

2.2.2.1 Maintaining a homeostatic balance

The respiratory tract is the main site of continuous contact with exogenous microorganisms. Airway epithelium acts as a sensor for the presence of microorganisms, and its epithelial cells are in constant contact with the environment. This interaction is a key factor in maintaining stable homeostasis. The environmental conditions necessary for microbial growth in the respiratory tract (such as PH, temperature, nutrition, oxygen tension, and activation of inflammatory cells in the host) are heterogeneous, so considerable regional variation can be observed in a single healthy lung (59).

2.2.2.2 Modulating immune strength

In health conditions, the microbiome can also regulate immune strength. Symbiotic fungi have been shown to influence the immune system and regulate the bacterial community, thus contributing to the recovery of bacterial flora after antibiotic treatment (60, 61).

2.2.3 Gut microbiome

2.2.3.1 Mucosal development

Gut microorganisms can affect intestinal mucosal development and homeostasis. Comparative studies of conventional and germ-free animals have shown that the gut microbiota is essential for the formation and functional realization of the intestinal mucosal immune system during infancy (62). A poor development of villous capillaries in the infancy of sterile mice and a consequential still dysplasia in adulthood confirmed that the gut microbiota contributes to the formation of the intestinal immune ultrastructure (63). The gut microbiome also contributes to the development of intestinal intraepithelial lymphocytes (IILs). Compared with conventionally grown animals, the production of intestinal mucosal-associated lymphoid tissue and antibodies was strongly reduced, and the original center, cell lamina propria, and cell lymphoid follicles of the mesenteric lymph node were significantly decreased in germ-free animals. Meanwhile, gut microbiota plays an important immunomodulatory role in intestinal mucosal homeostasis, with direct consequences in human health (64, 65).

2.2.3.2 Metabolic

Gut microbiota improves nutrient metabolism. The gut is an important site of digestion and absorption in the human body. Here, gut microbiota can contribute in foor digestion and decomposition, also could promote intestinal peristalsis and inhibit the proliferation of pathogenic bacteria. Gut microbiota can also provide various substrates, enzymes, and energy necessary for human metabolism, and participate in metabolic processes. Among them, *Firmicutes*, *Bacteroidetes*, and some anaerobic microorganisms can decompose complex carbohydrates in the gut to produce short-chain fatty acids (SCFAs), such as acetic acid, propionic acid, and butyric acid (65–68). SCFAs are not only the energy source of gut microorganisms themselves and the intestinal epithelial cells of the host, participating in adipogenesis and gluconeogenesis, but can also regulate the intestinal immunity of the host, reducing the pH of the colonic environment and inhibiting harmful bacterial growth and colonic inflammation (69).

Most pathogens cannot compete with the resident microbiome for carbohydrate food sources and are therefore effectively excluded from the gut under normal circumstances. Thus, disruption of the gut ecosystem appears to play an important role in the establishment of pathogenic bacteria. For example, antibiotic treatment disrupts the cross-feeding network between mucinous and non-mucinous degradants and allows for pathogenic bacteria such as *Salmonella typhimurium* and *Clostridioides difficile* (70).

Besides playing a role in carbohydrate metabolism, gut microorganisms also participate in bile acid metabolism, tryptophan metabolism and other processes. Bile acids are produced in the liver and metabolized by enzymes produced by gut bacteria and are essential for maintaining a healthy gut microbiome, balancing lipid and carbohydrate metabolism, as well as innate

immunity. The ability of intestinal flora to convert intestinal bile acid organisms into their unbound forms is critical to gastrointestinal .metabolic homeostasis, and these unbound bile acids activate bile acid signaling receptors (71, 72). The main bacterial genera involved in bile acid metabolism are *Bacteroides*, *Clostridium*, *Lactobacillus*, *bifidobacterium* and *listeria* (73, 74). Clinical patients with hepatoenteric diseases often present with intestinal ecological disorders characterized by reduced microbial diversity and a reduced abundance of firmicutes, leading to lower levels of intestinal secondary bile acids and higher levels of conjugated bile acids (75–77). Therefore, bile acid metabolism and intestinal flora interact, and when this balance is disrupted, a variety of clinical disease phenotypes can result.

Tryptophan metabolism is another important function of intestinal microorganisms to promote nutrient metabolism. As a nutrient enhancer, tryptophan plays a crucial role in the balance between intestinal immune tolerance and intestinal flora maintenance. Tryptophan is absorbed in the small intestine, but when it reaches the colon it can be broken down by gut bacteria such as *Clostridium sporogenes*, *Escherichia coli* and *Lactobacillus* to produce various indole derivatives that play an important role in key aspects of bacterial ecological balance (78–80).

2.2.3.3 Immune regulation

Gut microorganisms regulate the human immune system through immune cells and their metabolites. Recent studies have shown that gut microorganisms can over-activate CD8+T cells, which can promote chronic inflammation and T-cell failure (81, 82). Signals from gut microbes also provide appropriate conditions for dendritic cell generation (83). Gut microorganisms can also participate in immune regulation through metabolites, which further guide or influence immune cells. For example, lactic acid and pyruvate, metabolites derived from gut microorganisms, can promote immune responses by inducing G-protein coupled receptor (GPR)-31 to mediate the production of intestinal C-X3-C Motif Chemokine Receptor (CX3CR)-1-positive dendritic cells (84). Furthermore, *Odoribacter splanchnicus* and *Bilophila* genus were negatively correlated with tumor necrosis factor (TNF)-α production following lipopolysaccharide (LPS) and *C. albicans* stimulation. *Barnesiella* was negatively associated with LPS-and *B. fragilis*-induced interferon (IFN)-γ production. This included common gut commensals, such as *Dorea longicatena* and *Dorea formicigenerans*, where higher species abundance was associated with higher IFN-γ levels in response to *C. albicans* hyphae. Both species of *Dorea* can metabolize sialic acids, which are usually found at the end of mucins; and the release of these acids is associated with mucin degradation, and may increase gut permeability. Both *Streptococcus parasanguinis* and *Streptococcus australis* were associated with IFN-γ production whereas other species, such as *Streptococcus mitis/oralis/pneumoniae*, were associated with IL-1β production. Also the correlation of *Bifidobacterium pseudocatenulatum* and IFN-γ was positive. In contrast, the correlation of *Bifidobacterium adolescentis* and TNF-α was negatively. In addition, *P. distasonis* was negatively associated with TNF-α and IL-1β after stimulation with *C. albicans* hyphae (85–88).

3 Relationship between microbiome and clinical features of lung cancer

3.1 Pathological types

The microbiota may be specifically related to the pathological types of lung cancer tissues (Details in Table 1). Based on histological features, lung cancer can be divided into small cell lung cancer (SCLC) and non-small cell lung cancer (NSCLC), which can be further divided into adenocarcinoma (AC), squamous cell carcinoma (SCC), and large cell carcinoma (LCC). *Klebsiella*, *Acidovorax*, *Polarmonas, and Rhodoferax* have found to be more frequent in SCLC (89). This was later confirmed by Greathouse et al. (90). *Xylobacter*, *Eufluobacter*, and *Clostridium* were also positively correlated with SCLC occurrence. However, *Prevotella* and *Pseudobutyrivibrio ruminis* may be negatively correlated with SCLC (91).

The microbiome can be also used as a biomarker for NSCLC screening. Five bacterial genera showed abnormal abundance in the sputum of patients with NSCLC compared to that of controls (92). Also, contents of *Prevotella*, *Lactobacillus*, *Rikenellaceae*, *Treptococcus*, *Enterobacteriaceae*, *Oscillospira*, and *Bacteroides plebeius* were significantly higher in the feces of patients with NSCLC than in healthy controls (93). However, *Leptum*, *Faecalibacterium prausnitzii*, *Ruminococcus*, and *Clostridia* contents were found decreased in patients with NSCLC (94).

Furthermore, there were differences between the microbiomes of patients with SCC and AC. *Acidovorax* is enriched in SCC with TP53 mutations, but not in AC (90). Significant changes were observed in *Capnocytophaga*, *Selenomonas*, *Veillonella*, and *Neisseria* in SCC and AC saliva samples, whereas the microbiome of patients with SCC seemed to be more diverse than that of those with AC. Therefore, *Acidovorax* and *Veillonella* can be used as sputum biomarkers for SCC diagnosis (92) (95). SCC is specifically associated with *Enterobacteriaceae* microorganisms (96) (97). Levels of *Capnocytophaga* and *Rothia* were also higher in SCC than in AC. However, increases in *Capnocytophaga*, *Selenomonas*, *Veillonella*, and *Neisseria* were associated with AC (95). *Capnocytophaga* can be used as a diagnostic biomarker for AC sputum with 72% sensitivity and 85% specificity (92). In addition, Yu et al. observed an increased abundance of *Thermus* sp. and a decrease in the abundance of *Ralstonia* sp. In AC (98), whereas Greathouse et al. confirmed that *Pseudomonas* is specifically present in AC (89). In addition, John Cunningham (JC) virus was observed in tumor tissues and metastatic lymph nodes of patients with AC, suggesting that this virus may be involved in the occurrence of AC (99). Last, Huang et al. found that the number of *Veillonella*, *Megacoccus*, *Actinomyces* and *Arthrobacter* was significantly higher in AC than in SCC.

3.2 Progression and prognosis

The microbiome features are closely associated with the progression of lung cancer (Table 1). In this line, Guo et al. found that *Legionella* was more abundant in patients with metastatic lung cancer (98). Also, *Phascolarctobacterium* has been found to be enriched in patients with clinical benefit and has been related to an

TABLE 1 Relationship between microbiome and clinical features of lung cancer.

Clinical features		Related bacteria	Potential biological functions	References
Clinical Features	SCLC	*Klebsiella, Acidovorax, Polarmonas, Rhodoferax*	More common in SCLC	(56)(57)
		Xylobacter, Eufluobacter, Clostridium	Be associated with the occurrence of SCLC	(58)
	NSCLC	Five genera of bacteria	Early sputum detection markers	(59)
		Prevotella, Lactobacillus, Rikenellaceae, Treptococcus, Enterobacteriacea, Oscillospira, Bacteroides plebeius	Fecal markers	(60)
		Leptum, Faecalibacterium prausnitzii, Ruminococcus, Clostridia	Dysregulation of butyrate metabolism	(61)
	SCC	*Acidovorax*	Enriched in squamous cell carcinoma with TP53 mutation	(57)
		Acidovorax, Veillonella	Sputum biomarkers in SCC	(59)(62)
		Microorganisms of the family Enterobacteriaceae	Be related with SCC	(63)
	AC	*Capnocytophaga, Selenomonas, Veillonella, Neisseria*	Biomarkers of sputum diagnostic	(59)(62)
		Thermus	High phylogenetic diversity	(65)
		Pseudomonas	Specific microorganisms present in adenocarcinoma	(56)
Progression and prognosis of lung cancer	Progression	*Legionella*	With higher abundance in lung cancer patients with metastasis	(65)
		Phascolarctobacterium, Dialister	*Phascolarctobacterium* was enriched in patients with clinical benefit, *Dialister* is more common in patients with progressive disease	(67)
		Streptococcus,	There are differences between patients with metastatic and non-metastatic NSCLC	(68)
		Veillonella, Rothia		
	Prognosis	*Koribacteraceae*	Associated with increased RFS and DFS in lung cancer patients	(70)
		Bacteroidaceae, Lachnospiraceae, Ruminococcaceae	Associated with reduced RFS or DFS	

extension of progression-free survival (PFS), whereas *Dialister* is more common in patients with progressive disease, and its higher abundance is related to reduction of progression-free and overall survival (OS) (100).

Huang et al. (101) sequenced 33 cases of broncholavage fluid (14 cases of squamous cell carcinoma and 19 cases of adenocarcinoma) and 52 cases of sputum samples (15 cases of squamous cell carcinoma and 37 cases of adenocarcinoma). The results showed that the number of *Veillonell*, *Megasphaera*, *Actinomyces* and *Arthrobacter* in lung adenocarcinoma without metastasis was significantly higher than that in lung squamous cell carcinoma without metastasis. The contents of *Capnocytophaga* and *Rothia* in metastatic lung adenocarcinoma were significantly lower than those in metastatic lung squamous cell carcinoma. *Streptococcus* content was significantly lower in lung adenocarcinoma with metastasis than in lung adenocarcinoma without metastasis. The contents of *Veillonella* and *Rothia* in lung squamous cell carcinoma with metastasis were significantly higher than those in lung squamous cell carcinoma without metastasis. Jungnickel et al. (102) found that the number and volume of metastatic cancer nodules in the lung of mice exposed to *Haemophilus parainfluenzae* increased significantly. It is speculated that *Haemophilus parainfluenzae* may promote the upregulation of TLR2 or TLR4, induce the high expression of cytokine IL-17C, aggravate the inflammatory response of neutrophils and thus play a role in promoting cancer. In basic experiments (102, 103), it was found that *Hemophilus parainfluenzae* in the lung and the imbalance of lung flora promoted the metastasis of mouse cancer cells to the lung, indicating that lung flora was involved in the metastasis of lung cancer. Besides, the lung and gut microbiota may affect the prognosis of patients with lung cancer (104). The potential relationship between the lung microbiome and prognosis of lung cancer has been first demonstrated by Peters. Specifically, the abundance of *Koribacteraceae* in lung tissue is associated with an increase in relapse-free survival (RFS) and disease-free survival (DFS) in patients with lung cancer. On the contrary, the abundance of *Bacteroidaceae*, *Lachnospiraceae*, and *Ruminococcaceae* was correlated with a decrease in RFS or DFS of lung cancer (105). These further indicated that the dynamic changes of some microflora might be related to the progression of lung cancer.

4 Microbiome and biological function of lung cancer

The human microbiome significantly affects the occurrence and development of lung cancer by regulating tumor cells and the microenvironment (106–108).

4.1 Tumor cells

Proliferation, invasion, and metastasis are the core biological characteristics of tumor cells (109). The human microbiome can directly or indirectly affect lung cancer cell proliferation, invasion, metastasis, genomic instability, and mutations (Figure 2A).

Enrichment of lower airway microbiota and oral symbiotic bacteria frequently occurs in lung cancer, and these bacteria can trigger the host transcriptome associated with carcinogenesis. Compared with healthy people, extracellular signal-regulated kinase (ERK)- and phosphoinositide 3-kinase (PI3K)-signaling pathways of the lower airway transcriptome in patients with lung cancer are significantly upregulated, which is related to the enrichment of *Streptococcus*, *Prevotella*, and *Veillonella* oral groups in lower airways (110). Recent studies further found that tiny *Vibrio* is the most abundant microbe that drives the upregulation of interleukin (IL)-17, PI3K, mitogen-activated protein kinase (MAPK), and ERK pathways in the airway transcriptomes of patients with lung cancer and is associated with poor prognosis (111). In human lung cancer, not only is the pulmonary microflora changed, but the local adaptive immune gamma-delta (γδ)-T cells are also activated and directly promote the proliferation of tumor cells through effector molecules such as IL-22 and amphiregulin (103). In addition to the lung microbiota, other bacteria such as HP and its produced urease may also play an important role in lung mucosal proliferation and carcinogenesis. Recently, HP urease was found to enter the lung through gastroesophageal reflux and provide an antigenic trigger for pulmonary granuloma, which leads to subsequent lung mucosal proliferation and carcinogenesis (112).

Changes in the microbiota of patients with lung cancer may contribute to advancing disease progression. The "transition" of microorganisms to *Firmicutes* in the lower lobe of the lung may be a sign of increased pathogenicity and is associated with poorer prognosis (113). Such low airway microbiota is more common in stage IIIB - IV lung cancer with lymph node metastasis (111). In addition, the gut microbiota plays an important role in the invasion and metastasis of lung cancer. Toll-like receptors (TLRs) on the membrane surface of intestinal epithelial cells are pathogen-related recognition receptors that bind different microbial ligands, such as LPS, viral double-stranded RNA, and parasites and fungi-derived toxins (114). These enter the lungs and activate the adaptive immunity through TLRs, leading to T-cell differentiation and macrophage and dendritic cell activation. For example, TLR4 stimulation by heat-inactivated *Escherichia coli* increase the adhesion, migration and metastatic diffusion of NSCLC cells *in vivo*, mainly through p38 MAPK and ERK1/2 signaling pathways (115).

Microorganisms and their metabolites may produce tumorigenic effects by directly affecting epithelial cells or oncogenes (116). Pulmonary PAH-degrading bacteria, such as *Massilia* and *Acidovorax*, are more prevalent in smokers with lung cancer and TP53 mutations. The enrichment of these bacteria is combined with the trend of DNA recombination and repair pathway disorders, suggesting that contact of lung symbiotic microorganisms with tobacco may lead to mutations in host genes (117). An imbalance in the composition of microbial flora produces various toxins that lead to genotoxicity, promote the generation of free radicals, and cause DNA damage, thereby leading to a cycle arrest and apoptosis of cells without DNA repair systems (112). In addition, other microorganisms and their metabolites, such as HP, intestinal deoxycholic acid and shicholic acid, can cause DNA damage and increase the gene mutation load, thus inducing lung cancer (112, 118).

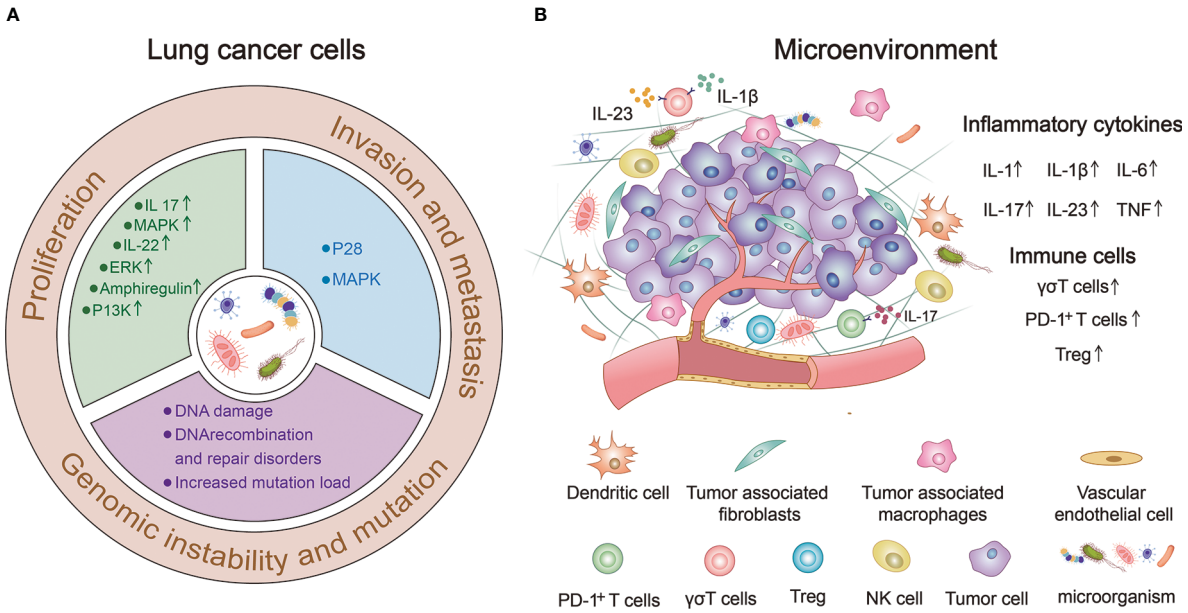

FIGURE 2
The human microbiome can significantly influence the occurrence and progression of lung cancer. **(A)** Human microbiota can directly or indirectly affect the proliferation, invasion, metastasis, genomic instability and mutation of lung cancer cells. **(B)** Human microorganisms participate in the composition of lung cancer microenvironment (TME) and regulate the occurrence and development of lung cancer by up-regulating the expression of immune cells and inflammatory factors.

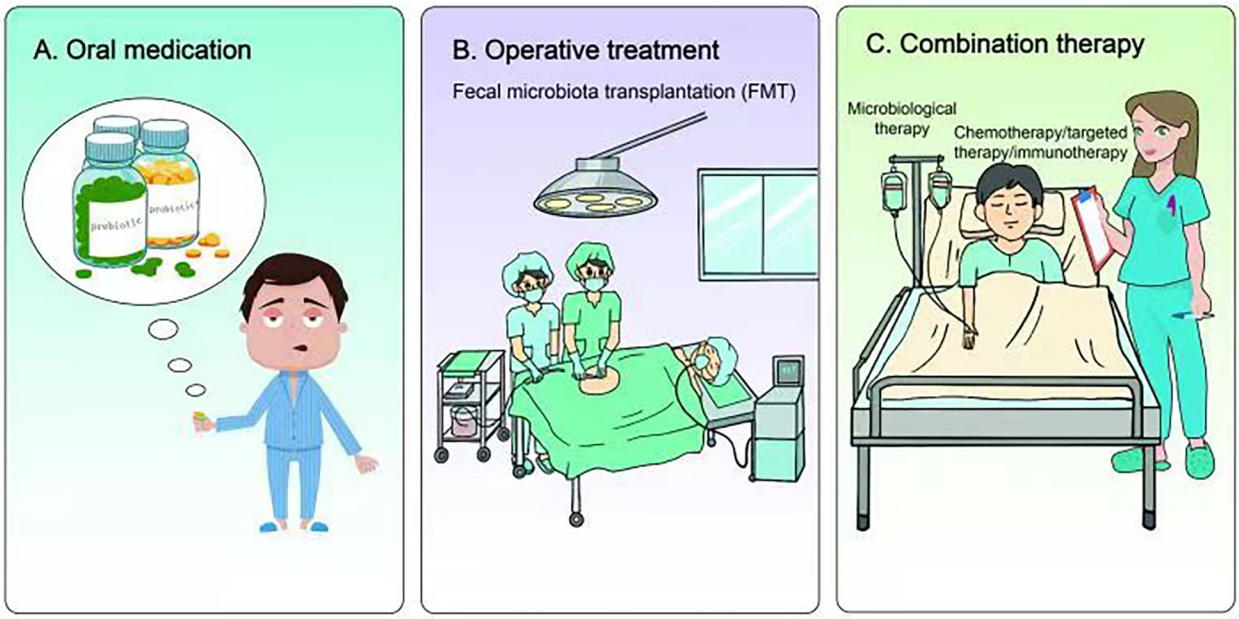

FIGURE 3
Research and application of microbiome in lung cancer treatment. **(A)** Nutritional intervention with prebiotics and probiotics can not only restore the homeostasis of internal organs or lower airway, but also reduce microbial-induced inflammation, genotoxicity and cell proliferation, thus improving the treatment of lung cancer. **(B)** Fecal microbiota transplantation (FMT) can also restore host homeostasis and reduce microbial-induced inflammation. Preclinical studies have shown that FMT therapy may have certain advantages in combating immunotherapy resistance in lung cancer. **(C)** Chemotherapy, targeted therapy or immunotherapy combined with microbial therapy can improve the clinical treatment effect of lung cancer patients.

4.2 Tumor microenvironment

The tumor microenvironment (TME) is an environment composed of various physical and chemical factors surrounding tumor cells, including neighbor tumor cells, immune cells, stromal cells, extracellular matrix, and a variety of soluble molecules, and is an important aspect of the tumor. TME plays an important role in the occurrence and development of tumors (119). Figure 2B provides a good summary of the microbial involvement in the composition of lung TME and the mechanism of regulating the occurrence and development of lung cancer (120–122).

In a mouse model of KRAS-TP53 co-mutation (KP) lung cancer, airway microbiosis disorder caused by Tiny Vibrio led to the recruitment of Th17 cells, increased IL-17 production, increased PD-1+T cell-expression, and recruitment of neutrophils, which resulted in a reduced survival and increased the burden of lung tumors (111). Gut microbiota can also activate B cells, T cells, and other immune cells, which inflate the lungs through hemato-vascular or lymphatic pathways and activate the immune response to affect lung inflammation (114, 123–125). It has been reported that an imbalance in intestinal flora may regulate the TLR4/NF-KB signaling pathway of the lung immune system by modulating the intestinal barrier, activating pulmonary oxidative stress, and mediating the response to lung injury (126). Intestinal symbiotic bacteria and their metabolites, short-chain fatty acids (SCFAs), such as propionic acid and butyric acid in patients with NSCLC directly stimulate intestinal-epithelial cells to regulate the release of T-regulatory (Treg) cells (127). Treg cells can inhibit airway inflammation by stimulating SCFAs, suggesting that immune cells play an important role in microbial-mediated inflammation (125). In addition, HP produces some relevant adaptive immune effects on T cells, in addition to inducing extensive innate immune signal transduction effects in the lungs (128, 129).

Studies have shown correlations between lung cancer cell growth and unbalances in the airway microbial community. This locally dysregulated microbiome stimulates the production of IL-1β and IL-23 in myeloid cells, which in turn induce the proliferation and adaptive activation of lung-resident Vγ6+Vδ1+γδT-immune cells. Activated γδT cells produce IL-17, which promotes neutrophil infiltration and inflammation in the TME (103, 108). The theory of IL-17-mediated inflammatory pathway has also been confirmed in other studies and animal models (130, 131). Therefore, IL-17 produced by adaptive immune γδT cells plays a role in mediating the inflammatory pathways. In addition, increasing evidence suggests that HP contributes to inducing lung tumors. HP-derived LPS induces the production of pro-inflammatory factors, including IL-1, IL-6, and TNF. This inflammation can develop into chronic bronchitis which can be often accompanied by lung cancer (132).

5 Research and application of microbiome in the treatment of lung cancer

Currently, the application of microbiomal knowledge to clinical research is a matter of extensive research. From the perspective of nutritional intervention, prebiotics and probiotics play indispensable roles. They can not only restore homeostasis of visceral organs or lower airways but also reduce microbial-induced inflammation, genotoxicity,

and cell proliferation (133, 134) (Figure 3). Lee et al. found that *Bifidobacterium* was abundant in the intestinal tract of patients with NSCLC who responded to clinical treatment. Further, when a commercial *Bifidobacterium* strain was used to treat mice tumors with the same genotype the tumor load could be reduced by inducing the host immune response and cooperating with immunotherapeutic or chemotherapeutic drugs (135). Yusuke Tomita et al. used 588 strains of *Clostridium butyricum* (MIYAIRI 588 strain) to ameliorate symptoms associated with ecological disturbance caused by antibiotics (ATBs), suggesting that probiotic Clostridium butyricum therapy (CBT) has a positive effect on improving immune checkpoint blockade (ICB) in patients with cancer (136). On the other hand, oral administration of *Lactobacillus acidophilus* enhanced the antitumor effect of cisplatin, reduced tumor size, and improved the survival rate of mice (137). Therefore, prebiotics and probiotics can improve lung cancer treatment.

In addition to nutritional intervention of prebiotics and probiotics, fecal microbiota transplantation (FMT) also restored host homeostasis and reduced microbial-induced inflammation (138, 139) (Figure 3). Although there is currently a lack of clinical application of FMT in lung cancer or other tumor types, previous preclinical studies have found that FMT could reverse the response to immunotherapy of drug-resistant patients by increasing the recruitment of CCR9+CXCR3+CD4+ T lymphocytes into tumor lesions in mice. These results indicate that FMT may have some advantages in battling resistance to lung cancer immunotherapy.

A number of studies have found that the gut microbiome of patients with lung cancer who respond to clinical treatment is significantly different from that of patients who do not respond, indicating that some favorable/unfavorable microorganisms are enriched in responders and non-responders respectively, thus implying a potentially predictive value for lung cancer clinical treatment (140–142) (Figure 3). Concerning chemotherapy, patients with advanced lung cancer treated with *Enterococcus* and *Human Bariniella* combined with immunochemotherapy showed longer PFS (143). In terms of targeted therapy, the role and therapeutic effects of the microbiota are very optimistic according to preclinical studies (144). In a mouse lung cancer model, *Bacteroides ovatus* and *Bacteroides xylanisolvens* were positively correlated with the treatment results. Oral or intragastric administration of these responsive bacteria could significantly improve the efficacy of Erlotinib and induce CXCL9 and IFN-γ expression (144). In immunotherapy, combined microbial therapy can improve the response to and effect of immune checkpoint inhibitors (ICIs). A recent study explored the role of gut microbes in the effectiveness of immunotherapy (145). The intestinal microbial community can affect the immune regulation mechanism by regulating T cell differentiation and significantly improve the therapeutic effect of ICI (140, 146–149). Mice using stool samples from patients who responded positively to immunotherapy, whereas mice using stool samples from patients who did not respond did not. A retrospective study reported that *Clostridium butyricum* treatment (CBT) before or after ICI treatment significantly extended patients' progression-free survival (PFS)non-progressive survival and overall survival (OS) (136). Improved survival in these patients can be attributed to more efficient immunomodulatory effects.

6 Future perspectives

The microbiome characteristics have significant effects in tumor development, however, how the microbiome responds to lung cancer, in particular, how lung cancer cells and TME shape the local microbial community of the lungs, is unknown. However, it has been shown that in colorectal cancer (CRC), loss of surface barrier function can cause tumor inflammation induced by symbiotic bacteria. In particular, the breakdown of tight connections between colon tumor cells allows bacterial degradation products such as LPS, to enter the tumor stroma, causing bone marrow-derived cells to be recruited to the TME. Therefore, understanding the interaction between the human microbiome and lung cancer cells, and identifying the cellular and molecular mediators involved in this interaction are relevant issues to be explored in order to find future potential targets for lung cancer treatment.

In addition, when considering the influence of microbiome on the efficacy of chemotherapy, targeted therapy, and immunotherapy for lung cancer, it is necessary to distinguish between the specific roles of the local lung microbiome, the distal gut microbiome, and oral bacteria in tumor growth and related immune responses (111). It is possible that selectively targeting one of these compartments may lead to different effects on lung cancer progression and treatment, thus providing new strategies for lung cancer treatments in the future.

Author contributions

Both authors contributed equally to the writing of the review.

Funding

This study was funded by the National Natural Science Foundation of China (82002421), Young Talent Program of Tangdu Hospital, Health Research Fund of Shaanxi Province (2021B004) and Discipline Innovation Development Plan Project of Tangdu Hospital (2021LCYJ005).

Conflict of interest

The authors declare that the research was conducted in the absence of any commercial or financial relationships that could be construed as a potential conflict of interest.

Publisher's note

References

1. Thai AA, Solomon BJ, Sequist LV, Gainor JF, Heist RS. Lung cancer. *Lancet (Lond Engl)* (2021) 398(10299):535–54. doi: 10.1016/s0140-6736(21)00312-3

2. Rock CL, Thomson CA, Sullivan KR, Howe CL, Kushi LH, Caan BJ, et al. American Cancer society nutrition and physical activity guideline for cancer survivors. *CA: Cancer J Clin* (2022) 72(3):230–62. doi: 10.3322/caac.21719

3. de Martel C, Ferlay J, Franceschi S, Vignat J, Bray F, Forman D, et al. Global burden of cancers attributable to infections in 2008: A review and synthetic analysis. *Lancet Oncol* (2012) 13(6):607–15. doi: 10.1016/s1470-2045(12)70137-7

4. Banerjee S, Tian T, Wei Z, Shih N, Feldman MD, Peck KN, et al. Distinct microbial signatures associated with different breast cancer types. *Front Microbiol* (2018) 9:951. doi: 10.3389/fmicb.2018.00951

5. Poore GD, Kopylova E, Zhu Q, Carpenter C, Fraraccio S, Wandro S, et al. Microbiome analyses of blood and tissues suggest cancer diagnostic approach. *Nature* (2020) 579(7800):567–74. doi: 10.1038/s41586-020-2095-1

6. Charlson ES, Bittinger K, Haas AR, Fitzgerald AS, Frank I, Yadav A, et al. Topographical continuity of bacterial populations in the healthy human respiratory tract. *Am J Respir Crit Care Med* (2011) 184(8):957–63. doi: 10.1164/rccm.201104-0655OC

7. Apostolou P, Tsantsaridou A, Papasotiriou I, Toloudi M, Chatziioannou M, Giamouzis G. Bacterial and fungal microflora in surgically removed lung cancer samples. *J Cardiothoracic Surg* (2011) 6:137. doi: 10.1186/1749-8090-6-137

8. Akinosoglou KS, Karkoulias K, Marangos M. Infectious complications in patients with lung cancer. *Eur Rev Med Pharmacol Sci* (2013) 17(1):8–18. PMID: 23329518

9. Caselli E, Fabbri C, D'Accolti M, Soffritti I, Bassi C, Mazzacane S, et al. Defining the oral microbiome by whole-genome sequencing and resistome analysis: The complexity of the healthy picture. *BMC Microbiol* (2020) 20(1):120. doi: 10.1186/s12866-020-01801-y

10. Turnbaugh PJ, Ley RE, Hamady M, Fraser-Liggett CM, Knight R, Gordon JI. The human microbiome project. *Nature* (2007) 449(7164):804–10. doi: 10.1038/nature06244

11. Wood DE, Salzberg SL. Kraken: Ultrafast metagenomic sequence classification using exact alignments. *Genome Biol* (2014) 15(3):R46. doi: 10.1186/gb-2014-15-3-r46

12. Petersen TN, Lukjancenko O, Thomsen MCF, Maddalena Sperotto M, Lund O, Møller Aarestrup F, et al. Mgmapper: Reference based mapping and taxonomy annotation of metagenomics sequence reads. *PloS One* (2017) 12(5):e0176469. doi: 10.1371/journal.pone.0176469

13. Wooley JC, Ye Y. Metagenomics: Facts and artifacts, and computational challenges*. *J Comput Sci Technol* (2009) 25(1):71–81. doi: 10.1007/s11390-010-9306-4

14. Teo SM, Mok D, Pham K, Kusel M, Serralha M, Troy N, et al. The infant nasopharyngeal microbiome impacts severity of lower respiratory infection and risk of asthma development. *Cell Host Microbe* (2015) 17(5):704–15. doi: 10.1016/j.chom.2015.03.008

15. Stiemsma LT, Turvey SE. Asthma and the microbiome: Defining the critical window in early life. *Allergy Asthma Clin Immunol* (2017) 13:3. doi: 10.1186/s13223-016-0173-6

16. Morris A, Beck JM, Schloss PD, Campbell TB, Crothers K, Curtis JL, et al. Comparison of the respiratory microbiome in healthy nonsmokers and smokers. *Am J Respir Crit Care Med* (2013) 187(10):1067–75. doi: 10.1164/rccm.201210-1913OC

17. Segal LN, Alekseyenko AV, Clemente JC, Kulkarni R, Wu B, Gao Z, et al. Enrichment of lung microbiome with supraglottic taxa is associated with increased pulmonary inflammation. *Microbiome* (2013) 1(1):19. doi: 10.1186/2049-2618-1-19

18. Hilty M, Burke C, Pedro H, Cardenas P, Bush A, Bossley C, et al. Disordered microbial communities in asthmatic airways. *PloS One* (2010) 5(1):e8578. doi: 10.1371/journal.pone.0008578

19. Beck JM, Young VB, Huffnagle GB. The microbiome of the lung. *Trans Res* (2012) 160(4):258–66. doi: 10.1016/j.trsl.2012.02.005

20. Dickson RP, Erb-Downward JR, Freeman CM, McCloskey L, Beck JM, Huffnagle GB, et al. Spatial variation in the healthy human lung microbiome and the adapted island model of lung biogeography. *Ann Am Thorac Soc* (2015) 12(6):821–30. doi: 10.1513/AnnalsATS.201501-029OC

21. Bassis CM, Erb-Downward JR, Dickson RP, Freeman CM, Schmidt TM, Young VB, et al. Analysis of the upper respiratory tract microbiotas as the source of the lung and gastric microbiotas in healthy individuals. *mBio* (2015) 6(2):e00037. doi: 10.1128/mBio.00037-15

22. Sender R, Fuchs S, Milo R. Are we really vastly outnumbered? revisiting the ratio of bacterial to host cells in humans. *Cell* (2016) 164(3):337–40. doi: 10.1016/j.cell.2016.01.013

23. Sender R, Fuchs S, Milo R. Revised estimates for the number of human and bacteria cells in the body. *PloS Biol* (2016) 14(8):e1002533. doi: 10.1371/journal.pbio.1002533

24. Claesson MJ, Cusack S, O'Sullivan O, Greene-Diniz R, de Weerd H, Flannery E, et al. Composition, variability, and temporal stability of the intestinal microbiota of the elderly. *Proc Natl Acad Sci USA* (2011) 108 Suppl 1(Suppl 1):4586–91. doi: 10.1073/pnas.1000097107

25. Claesson MJ, Jeffery IB, Conde S, Power SE, O'Connor EM, Cusack S, et al. Gut microbiota composition correlates with diet and health in the elderly. *Nature* (2012) 488 (7410):178–84. doi: 10.1038/nature11319

26. Raju U, Levitz M, Javitt NB. Bile acids in human breast cyst fluid: The identification of lithocholic acid. *J Clin Endocrinol Metab* (1990) 70(4):1030–4. doi: 10.1210/jcem-70-4-1030

27. Javitt NB, Budai K, Miller DG, Cahan AC, Raju U, Levitz M. Breast-gut connection: Origin of chenodeoxycholic acid in breast cyst fluid. *Lancet (Lond Engl)* (1994) 343(8898):633–5. doi: 10.1016/s0140-6736(94)92635-2

28. Swales KE, Korbonits M, Carpenter R, Walsh DT, Warner TD, Bishop-Bailey D. The farnesoid X receptor is expressed in breast cancer and regulates apoptosis and aromatase expression. *Cancer Res* (2006) 66(20):10120–6. doi: 10.1158/0008-5472.can-06-2399

29. Zimmermann P, Curtis N. Breast milk microbiota: A review of the factors that influence composition. *J infection* (2020) 81(1):17–47. doi: 10.1016/j.jinf.2020.01.023

30. Urbaniak C, Cummins J, Brackstone M, Macklaim JM, Gloor GB, Baban CK, et al. Microbiota of human breast tissue. *Appl Environ Microbiol* (2014) 80(10):3007–14. doi: 10.1128/aem.00242-14

31. Yang I, Nell S, Suerbaum S. Survival in hostile territory: The microbiota of the stomach. *FEMS Microbiol Rev* (2013) 37(5):736–61. doi: 10.1111/1574-6976.12027

32. Wu WM, Yang YS, Peng LH. Microbiota in the stomach: New insights. *J Digestive Dis* (2014) 15(2):54–61. doi: 10.1111/1751-2980.12116

33. Bik EM, Eckburg PB, Gill SR, Nelson KE, Purdom EA, Francois F, et al. Molecular analysis of the bacterial microbiota in the human stomach. *Proc Natl Acad Sci USA* (2006) 103(3):732–7. doi: 10.1073/pnas.0506655103

34. Li XX, Wong GL, To KF, Wong VW, Lai LH, Chow DK, et al. Bacterial microbiota profiling in gastritis without helicobacter pylori infection or non-steroidal anti-inflammatory drug use. *PloS One* (2009) 4(11):e7985. doi: 10.1371/journal.pone.0007985

35. Mailhe M, Ricaboni D, Vitton V, Gonzalez JM, Bachar D, Dubourg G, et al. Repertoire of the gut microbiota from stomach to colon using culturomics and next-generation sequencing. *BMC Microbiol* (2018) 18(1):157. doi: 10.1186/s12866-018-1304-7

36. Fassi Fehri L, Mak TN, Laube B, Brinkmann V, Ogilvie LA, Mollenkopf H, et al. Prevalence of propionibacterium acnes in diseased prostates and its inflammatory and transforming activity on prostate epithelial cells. *Int J Med Microbiol IJMM* (2011) 301 (1):69–78. doi: 10.1016/j.ijmm.2010.08.014

37. Sfanos KS, Sauvageot J, Fedor HL, Dick JD, De Marzo AM, Isaacs WB. A molecular analysis of prokaryotic and viral DNA sequences in prostate tissue from patients with prostate cancer indicates the presence of multiple and diverse microorganisms. *Prostate* (2008) 68(3):306–20. doi: 10.1002/pros.20680

38. Cohen RJ, Shannon BA, McNeal JE, Shannon T, Garrett KL. Propionibacterium acnes associated with inflammation in radical prostatectomy specimens: A possible link to cancer evolution? *J Urol* (2005) 173(6):1969–74. doi: 10.1097/01.ju.0000158161.15277.78

39. Hochreiter WW, Duncan JL, Schaeffer AJ. Evaluation of the bacterial flora of the prostate using a 16s rrna gene based polymerase chain reaction. *J Urol* (2000) 163(1):127–30.

40. Salter SJ, Cox MJ, Turek EM, Calus ST, Cookson WO, Moffatt MF, et al. Reagent and laboratory contamination can critically impact sequence-based microbiome analyses. *BMC Biol* (2014) 12:87. doi: 10.1186/s12915-014-0087-z

41. Fair WR, Parrish RF. Antibacterial substances in prostatic fluid. *Prog Clin Biol Res* (1981) 75a:247–64. PMID: 7041133

42. Mager DL, Ximenez-Fyvie LA, Haffajee AD, Socransky SS. Distribution of selected bacterial species on intraoral surfaces. *J Clin Periodontology* (2003) 30(7):644–54. doi: 10.1034/j.1600-051x.2003.00376.x

43. Venkataraman A, Bassis CM, Beck JM, Young VB, Curtis JL, Huffnagle GB, et al. Application of a neutral community model to assess structuring of the human lung microbiome. *mBio* (2015) 6(1):e02284–14. doi: 10.1128/mBio.02284-14

44. Verma D, Garg PK, Dubey AK. Insights into the human oral microbiome. *Arch Microbiol* (2018) 200(4):525–40. doi: 10.1007/s00203-018-1505-3

45. Jhajharia K, Parolia A, Shetty KV, Mehta LK. Biofilm in endodontics: A review. *J Int Soc Prev Community Dentistry* (2015) 5(1):1–12. doi: 10.4103/2231-0762.151956

46. Hasan NA, Young BA, Minard-Smith AT, Saeed K, Li H, Heizer EM, et al. Microbial community profiling of human saliva using shotgun metagenomic sequencing. *PloS One* (2014) 9(5):e97699. doi: 10.1371/journal.pone.0097699

47. He X, Hu W, He J, Guo L, Lux R, Shi W. Community-based interference against integration of pseudomonas aeruginosa into human salivary microbial biofilm. *Mol Oral Microbiol* (2011) 26(6):337–52. doi: 10.1111/j.2041-1014.2011.00622.x

48. Baena-Monroy T, Moreno-Maldonado V, Franco-Martínez F, Aldape-Barrios B, Quindós G, Sánchez-Vargas LO. Candida albicans, staphylococcus aureus and streptococcus mutans colonization in patients wearing dental prosthesis. *Medicina oral patologia Oral y cirugia bucal* (2005) 10 Suppl1:E27–39. PMID: 15800465

49. Passariello C, Puttini M, Iebba V, Pera P, Gigola P. Influence of oral conditions on colonization by highly toxigenic staphylococcus aureus strains. *Oral Dis* (2012) 18 (4):402–9. doi: 10.1111/j.1601-0825.2011.01889.x

50. Colombo AV, Barbosa GM, Higashi D, di Micheli G, Rodrigues PH, Simionato MRL. Quantitative detection of staphylococcus aureus, enterococcus faecalis and pseudomonas aeruginosa in human oral epithelial cells from subjects with periodontitis and periodontal health. *J Med Microbiol* (2013) 62(Pt 10):1592–600. doi: 10.1099/jmm.0.055830-0

51. Souto R, Silva-Boghossian CM, Colombo AP. Prevalence of pseudomonas aeruginosa and acinetobacter spp. In: *Subgingival biofilm and saliva of subjects with chronic periodontal infection. Brazilian journal of microbiology*, vol. 45. (2014). p. 495–501. doi: 10.1590/s1517-83822014000200017

52. Mathews SA, Kurien BT, Scofield RH. Oral manifestations of sjögren's syndrome. *J Dental Res* (2008) 87(4):308–18. doi: 10.1177/154405910808700411

53. Scannapieco FA. Role of oral bacteria in respiratory infection. *J periodontology* (1999) 70(7):793–802. doi: 10.1902/jop.1999.70.7.793

54. Koch CD, Gladwin MT, Freeman BA, Lundberg JO, Weitzberg E, Morris A. Enterosalivary nitrate metabolism and the microbiome: Intersection of microbial metabolism, nitric oxide and diet in cardiac and pulmonary vascular health. *Free Radical Biol Med* (2017) 105:48–67. doi: 10.1016/j.freeradbiomed.2016.12.015

55. Huffnagle GB, Dickson RP, Lukacs NW. The respiratory tract microbiome and lung inflammation: A two-way Street. *Mucosal Immunol* (2017) 10(2):299–306. doi: 10.1038/mi.2016.108

56. Salisbury ML, Han MK, Dickson RP, Molyneaux PL. Microbiome in interstitial lung disease: From pathogenesis to treatment target. *Curr Opin pulmonary Med* (2017) 23 (5):404–10. doi: 10.1097/mcp.0000000000000399

57. Yatsunenko T, Rey FE, Manary MJ, Trehan I, Dominguez-Bello MG, Contreras M, et al. Human gut microbiome viewed across age and geography. *Nature* (2012) 486 (7402):222–7. doi: 10.1038/nature11053

58. Biesbroek G, Tsivtsivadze E, Sanders EA, Montijn R, Veenhoven RH, Keijser BJ, et al. Early respiratory microbiota composition determines bacterial succession patterns and respiratory health in children. *Am J Respir Crit Care Med* (2014) 190(11):1283–92. doi: 10.1164/rccm.201407-1240OC

59. O'Dwyer DN, Dickson RP, Moore BB. The lung microbiome, immunity, and the pathogenesis of chronic lung disease. *J Immunol (Baltimore Md 1950)* (2016) 196 (12):4839–47. doi: 10.4049/jimmunol.1600279

60. Erb Downward JR, Falkowski NR, Mason KL, Muraglia R, Huffnagle GB. Modulation of post-antibiotic bacterial community reassembly and host response by candida albicans. *Sci Rep* (2013) 3:2191. doi: 10.1038/srep02191

61. Marsland BJ, Gollwitzer ES. Host-microorganism interactions in lung diseases. *Nat Rev Immunol* (2014) 14(12):827–35. doi: 10.1038/nri3769

62. Allam-Ndoul B, Castonguay-Paradis S, Veilleux A. Gut microbiota and intestinal trans-epithelial permeability. *Int J Mol Sci* (2020) 21(17):6402. doi: 10.3390/ijms21176402

63. Weiss GA, Hennet T. Mechanisms and consequences of intestinal dysbiosis. *Cell Mol Life Sci CMLS* (2017) 74(16):2959–77. doi: 10.1007/s00018-017-2509-x

64. Tytgat HLP, Nobrega FL, van der Oost J, de Vos WM. Bowel biofilms: Tipping points between a healthy and compromised gut? *Trends Microbiol* (2019) 27(1):17–25. doi: 10.1016/j.tim.2018.08.009

65. Tan S, Li D, Zhu X. Cancer immunotherapy: Pros, cons and beyond. *Biomedicine pharmacotherapy = Biomedecine pharmacotherapie* (2020) 124:109821. doi: 10.1016/j.biopha.2020.109821

66. Louis P, Flint HJ. Formation of propionate and butyrate by the human colonic microbiota. *Environ Microbiol* (2017) 19(1):29–41. doi: 10.1111/1462-2920.13589

67. Lin L, Zhang J. Role of intestinal microbiota and metabolites on gut homeostasis and human diseases. *BMC Immunol* (2017) 18(1):2. doi: 10.1186/s12865-016-0187-3

68. Thursby E, Juge N. Introduction to the human gut microbiota. *Biochem J* (2017) 474(11):1823–36. doi: 10.1042/bcj20160510

69. Perry RJ, Peng L, Barry NA, Cline GW, Zhang D, Cardone RL, et al. Acetate mediates a microbiome-Brain-β-Cell axis to promote metabolic syndrome. *Nature* (2016) 534(7606):213–7. doi: 10.1038/nature18309

70. Ng KM, Ferreyra JA, Higginbottom SK, Lynch JB, Kashyap PC, Gopinath S, et al. Microbiota-liberated host sugars facilitate post-antibiotic expansion of enteric pathogens. *Nature* (2013) 502(7469):96–9. doi: 10.1038/nature12503

71. Thomas C, Pellicciari R, Pruzanski M, Auwerx J, Schoonjans K. Targeting bile-acid signalling for metabolic diseases. *Nat Rev Drug Discov* (2008) 7(8):678–93. doi: 10.1038/nrd2619

72. Zollner G, Wagner M, Trauner M. Nuclear receptors as drug targets in cholestasis and drug-induced hepatotoxicity. *Pharmacol Ther* (2010) 126(3):228–43. doi: 10.1016/j.pharmthera.2010.03.005

73. Chiang JY. Bile acids: Regulation of synthesis. *J Lipid Res* (2009) 50(10):1955–66. doi: 10.1194/jlr.R900010-JLR200

74. Gérard P. Metabolism of cholesterol and bile acids by the gut microbiota. *Pathog (Basel Switzerland)* (2013) 3(1):14–24. doi: 10.3390/pathogens3010014

75. Frank DN, St Amand AL, Feldman RA, Boedeker EC, Harpaz N, Pace NR. Molecular-phylogenetic characterization of microbial community imbalances in human inflammatory bowel diseases. *Proc Natl Acad Sci United States America* (2007) 104 (34):13780–5. doi: 10.1073/pnas.0706625104

76. Sokol H, Seksik P, Furet JP, Firmesse O, Nion-Larmurier I, Beaugerie L, et al. Low counts of faecalibacterium prausnitzii in colitis microbiota. *Inflammatory Bowel Dis* (2009) 15(8):1183–9. doi: 10.1002/ibd.20903

77. Swidsinski A, Loening-Baucke V, Vaneechoutte M, Doerffel Y. Active crohn's disease and ulcerative colitis can be specifically diagnosed and monitored based on the biostructure of the fecal flora. *Inflammatory Bowel Dis* (2008) 14(2):147–61. doi: 10.1002/ibd.20330

78. Lee JH, Lee J. Indole as an intercellular signal in microbial communities. *FEMS Microbiol Rev* (2010) 34(4):426–44. doi: 10.1111/j.1574-6976.2009.00204.x

79. Williams BB, Van Benschoten AH, Cimermancic P, Donia MS, Zimmermann M, Taketani M, et al. Discovery and characterization of gut microbiota decarboxylases that can produce the neurotransmitter tryptamine. *Cell Host Microbe* (2014) 16(4):495–503. doi: 10.1016/j.chom.2014.09.001

80. Hubbard TD, Murray IA, Perdew GH. Indole and tryptophan metabolism: Endogenous and dietary routes to ah receptor activation. *Drug Metab disposition: Biol fate chemicals* (2015) 43(10):1522–35. doi: 10.1124/dmd.115.064246

81. Yu AI, Zhao L, Eaton KA, Ho S, Chen J, Poe S, et al. Gut microbiota modulate Cd8 t cell responses to influence colitis-associated tumorigenesis. *Cell Rep* (2020) 31 (1):107471. doi: 10.1016/j.celrep.2020.03.035

82. Zou Z, Tao T, Li H, Zhu X. Mtor signaling pathway and mtor inhibitors in cancer: Progress and challenges. *Cell bioscience* (2020) 10:31. doi: 10.1186/s13578-020-00396-1

83. Ganal SC, Sanos SL, Kallfass C, Oberle K, Johner C, Kirschning C, et al. Priming of natural killer cells by nonmucosal mononuclear phagocytes requires instructive signals from commensal microbiota. *Immunity* (2012) 37(1):171–86. doi: 10.1016/j.immuni.2012.05.020

84. Morita N, Umemoto E, Fujita S, Hayashi A, Kikuta J, Kimura I, et al. Gpr31-dependent dendrite protrusion of intestinal Cx3cr1(+) cells by bacterial metabolites. *Nature* (2019) 566(7742):110–4. doi: 10.1038/s41586-019-0884-1

85. Crost EH, Tailford LE, Le Gall G, Fons M, Henrissat B, Juge N. Utilisation of mucin glycans by the human gut symbiont ruminococcus gnavus is strain-dependent. *PloS One* (2013) 8(10):e76341. doi: 10.1371/journal.pone.0076341

86. López P, González-Rodríguez I, Gueimonde M, Margolles A, Suárez A. Immune response to bifidobacterium bifidum strains support Treg/Th17 plasticity. *PloS One* (2011) 6(9):e24776. doi: 10.1371/journal.pone.0024776

87. Ménard O, Butel MJ, Gaboriau-Routhiau V, Waligora-Dupriet AJ. Gnotobiotic mouse immune response induced by bifidobacterium sp. *Strains Isolated Infants. Appl Environ Microbiol* (2008) 74(3):660–6. doi: 10.1128/aem.01261-07

88. Schirmer M, Smeekens SP, Vlamakis H, Jaeger M, Oosting M, Franzosa EA, et al. Linking the human gut microbiome to inflammatory cytokine production capacity. *Cell* (2016) 167(4):1125–36.e8. doi: 10.1016/j.cell.2016.10.020

89. Erb-Downward JR, Thompson DL, Han MK, Freeman CM, McCloskey L, Schmidt LA, et al. Analysis of the lung microbiome in the "Healthy" smoker and in copd. *PloS One* (2011) 6(2):e16384. doi: 10.1371/journal.pone.0016384

90. Greathouse KL, White JR, Vargas AJ, Bliskovsky VV, Beck JA, von Muhlinen N, et al. Interaction between the microbiome and Tp53 in human lung cancer. *Genome Biol* (2018) 19(1):123. doi: 10.1186/s13059-018-1501-6

91. Zhang L, Zhan H, Xu W, Yan S, Ng SC. The role of gut mycobiome in health and diseases. *Ther Adv Gastroenterol* (2021) 14:17562848211047130. doi: 10.1177/17562848211047130

92. Leng Q, Holden VK, Deepak J, Todd NW, Jiang F. Microbiota biomarkers for lung cancer. *Diagnostics (Basel Switzerland)* (2021) 11(3):407. doi: 10.3390/diagnostics11030407

93. Botticelli A, Vernocchi P, Marini F, Quagliariello A, Cerbelli B, Reddel S, et al. Gut metabolomics profiling of non-small cell lung cancer (Nsclc) patients under immunotherapy treatment. *J Trans Med* (2020) 18(1):49. doi: 10.1186/s12967-020-02231-0

94. Gui Q, Li H, Wang A, Zhao X, Tan Z, Chen L, et al. The association between gut butyrate-producing bacteria and non-Small-Cell lung cancer. *J Clin Lab Anal* (2020) 34 (8):e23318. doi: 10.1002/jcla.23318

95. Yan X, Yang M, Liu J, Gao R, Hu J, Li J, et al. Discovery and validation of potential bacterial biomarkers for lung cancer. *Am J Cancer Res* (2015) 5(10):3111–22. PMID: 26693063

96. Gomes S, Cavadas B, Ferreira JC, Marques PI, Monteiro C, Sucena M, et al. Profiling of lung microbiota discloses differences in adenocarcinoma and squamous cell carcinoma. *Sci Rep* (2019) 9(1):12838. doi: 10.1038/s41598-019-49195-w

97. Greathouse KL, White JR, Vargas AJ, Bliskovsky VV, Beck JA, von Muhlinen N, et al. Author correction: Interaction between the microbiome and Tp53 in human lung cancer. *Genome Biol* (2020) 21(1):41. doi: 10.1186/s13059-020-01961-0

98. Yu G, Gail MH, Consonni D, Carugno M, Humphrys M, Pesatori AC, et al. Characterizing human lung tissue microbiota and its relationship to epidemiological and clinical features. *Genome Biol* (2016) 17(1):163. doi: 10.1186/s13059-016-1021-1

99. Han AJ, Xiong M, Zong YS. Association of Epstein-Barr virus with lymphoepithelioma-like carcinoma of the lung in southern China. *Am J Clin Pathol* (2000) 114(2):220–6. doi: 10.1309/148k-nd54-6njx-na61

100. Zhang F, Ferrero M, Dong N, D'Auria G, Reyes-Prieto M, Herreros-Pomares A, et al. Analysis of the gut microbiota: An emerging source of biomarkers for immune checkpoint blockade therapy in non-small cell lung cancer. *Cancers* (2021) 13(11):2514. doi: 10.3390/cancers13112514

101. Huang D, Su X, Yuan M, Zhang S, He J, Deng Q, et al. The characterization of lung microbiome in lung cancer patients with different clinicopathology. *Am J Cancer Res* (2019) 9(9):2047–63. PMID: 31598405

102. Jungnickel C, Schmidt LH, Bittigkoffer L, Wolf L, Wolf A, Ritzmann F, et al. Il-17c mediates the recruitment of tumor-associated neutrophils and lung tumor growth. *Oncogene* (2017) 36(29):4182–90. doi: 10.1038/onc.2017.28

103. Le Noci V, Guglielmetti S, Arioli S, Camisaschi C, Bianchi F, Sommariva M, et al. Modulation of pulmonary microbiota by antibiotic or probiotic aerosol therapy: A strategy to promote immunosurveillance against lung metastases. *Cell Rep* (2018) 24 (13):3528–38. doi: 10.1016/j.celrep.2018.08.090

104. Dickson RP, Schultz MJ, van der Poll T, Schouten LR, Falkowski NR, Luth JE, et al. Lung microbiota predict clinical outcomes in critically ill patients. *Am J Respir Crit Care Med* (2020) 201(5):555–63. doi: 10.1164/rccm.201907-1487OC

105. Peters BA, Hayes RB, Goparaju C, Reid C, Pass HI, Ahn J. The microbiome in lung cancer tissue and recurrence-free survival. *Cancer Epidemiol Biomarkers Prev* (2019) 28(4):731–40. doi: 10.1158/1055-9965.epi-18-0966

106. Segal LN, Clemente JC, Tsay JC, Koralov SB, Keller BC, Wu BG, et al. Enrichment of the lung microbiome with oral taxa is associated with lung inflammation of a Th17 phenotype. *Nat Microbiol* (2016) 1:16031. doi: 10.1038/nmicrobiol.2016.31

107. Palucka AK, Coussens LM. The basis of oncoimmunology. *Cell* (2016) 164 (6):1233–47. doi: 10.1016/j.cell.2016.01.049

108. Jin C, Lagoudas GK, Zhao C, Bullman S, Bhutkar A, Hu B, et al. Commensal microbiota promote lung cancer development *Via* Γδ T cells. *Cell* (2019) 176(5):998–1013.e16. doi: 10.1016/j.cell.2018.12.040

109. Hanahan D, Weinberg RA. Hallmarks of cancer: The next generation. *Cell* (2011) 144(5):646–74. doi: 10.1016/j.cell.2011.02.013

110. Tsay JJ, Wu BG, Badri MH, Clemente JC, Shen N, Meyn P, et al. Airway microbiota is associated with upregulation of the Pi3k pathway in lung cancer. *Am J Respir Crit Care Med* (2018) 198(9):1188–98. doi: 10.1164/rccm.201710-2118OC

111. Tsay JJ, Wu BG, Sulaiman I, Gershner K, Schluger R, Li Y, et al. Lower airway dysbiosis affects lung cancer progression. *Cancer Discov* (2021) 11(2):293–307. doi: 10.1158/2159-8290.cd-20-0263

112. Alhinai EA, Walton GE, Commane DM. The role of the gut microbiota in colorectal cancer causation. *Int J Mol Sci* (2019) 20(21):5295. doi: 10.3390/ijms20215295

113. Bingula R, Filaire E, Molnar I, Delmas E, Berthon JY, Vasson MP, et al. Characterisation of microbiota in saliva, bronchoalveolar lavage fluid, non-malignant, peritumoural and tumour tissue in non-small cell lung cancer patients: A cross-sectional clinical trial. *Respir Res* (2020) 21(1):129. doi: 10.1186/s12931-020-01392-2

114. Samuelson DR, Welsh DA, Shellito JE. Regulation of lung immunity and host defense by the intestinal microbiota. *Front Microbiol* (2015) 6:1085. doi: 10.3389/fmicb.2015.01085

115. Chow SC, Gowing SD, Cools-Lartigue JJ, Chen CB, Berube J, Yoon HW, et al. Gram negative bacteria increase non-small cell lung cancer metastasis *Via* toll-like receptor 4 activation and mitogen-activated protein kinase phosphorylation. *Int J Cancer* (2015) 136(6):1341–50. doi: 10.1002/ijc.29111

116. Ramírez-Labrada AG, Isla D, Artal A, Arias M, Rezusta A, Pardo J, et al. The influence of lung microbiota on lung carcinogenesis, immunity, and immunotherapy. *Trends Cancer* (2020) 6(2):86–97. doi: 10.1016/j.trecan.2019.12.007

117. Dong H, Tan Q, Xu Y, Zhu Y, Yao Y, Wang Y, et al. Convergent alteration of lung tissue microbiota and tumor cells in lung cancer. *iScience* (2022) 25(1):103638. doi: 10.1016/j.isci.2021.103638

118. Louis P, Hold GL, Flint HJ. The gut microbiota, bacterial metabolites and colorectal cancer. *Nat Rev Microbiol* (2014) 12(10):661–72. doi: 10.1038/nrmicro3344

119. Chen Q, Liu G, Liu S, Su H, Wang Y, Li J, et al. Remodeling the tumor microenvironment with emerging nanotherapeutics. *Trends Pharmacol Sci* (2018) 39 (1):59–74. doi: 10.1016/j.tips.2017.10.009

120. Laroumagne S, Lepage B, Hermant C, Plat G, Phelippeau M, Bigay-Game L, et al. Bronchial colonisation in patients with lung cancer: A prospective study. *Eur Respir J* (2013) 42(1):220–9. doi: 10.1183/09031936.00062212

121. Liu HX, Tao LL, Zhang J, Zhu YG, Zheng Y, Liu D, et al. Difference of lower airway microbiome in bilateral protected specimen brush between lung cancer patients with unilateral lobar masses and control subjects. *Int J Cancer* (2018) 142(4):769–78. doi: 10.1002/ijc.31098

122. Mao Q, Jiang F, Yin R, Wang J, Xia W, Dong G, et al. Interplay between the lung microbiome and lung cancer. *Cancer Lett* (2018) 415:40–8. doi: 10.1016/j.canlet.2017.11.036

123. Bingula R, Filaire M, Radosevic-Robin N, Bey M, Berthon JY, Bernalier-Donadille A, et al. Desired turbulence? gut-lung axis, immunity, and lung cancer. *J Oncol* (2017) 2017:5035371. doi: 10.1155/2017/5035371

124. Budden KF, Gellatly SL, Wood DL, Cooper MA, Morrison M, Hugenholtz P, et al. Emerging pathogenic links between microbiota and the gut-lung axis. *Nat Rev Microbiol* (2017) 15(1):55–63. doi: 10.1038/nrmicro.2016.142

125. Schuijt TJ, Lankelma JM, Scicluna BP, de Sousa e Melo F, Roelofs JJ, de Boer JD, et al. The gut microbiota plays a protective role in the host defence against pneumococcal pneumonia. *Gut* (2016) 65(4):575–83. doi: 10.1136/gutjnl-2015-309728

126. Tang J, Xu L, Zeng Y, Gong F. Effect of gut microbiota on lps-induced acute lung injury by regulating the Tlr4/Nf-kb signaling pathway. *Int Immunopharmacol* (2021) 91:107272. doi: 10.1016/j.intimp.2020.107272

127. Bingula R, Filaire M, Radosevic-Robin N, Berthon JY, Bernalier-Donadille A, Vasson MP, et al. Characterisation of gut, lung, and upper airways microbiota in patients with non-small cell lung carcinoma: Study protocol for case-control observational trial. *Medicine* (2018) 97(50):e13676. doi: 10.1097/md.0000000000013676

128. Altobelli A, Bauer M, Velez K, Cover TL, Müller A. Helicobacter pylori vaca targets myeloid cells in the gastric lamina propria to promote peripherally induced regulatory T-cell differentiation and persistent infection. *mBio* (2019) 10(2):e00261–19. doi: 10.1128/mBio.00261-19

129. van Wijck Y, John-Schuster G, van Schadewijk A, van den Oever RL, Obieglo K, Hiemstra PS, et al. Extract of helicobacter pylori ameliorates parameters of airway inflammation and goblet cell hyperplasia following repeated allergen exposure. *Int Arch Allergy Immunol* (2019) 180(1):1–9. doi: 10.1159/000500598

130. Zitvogel L, Kroemer G. Lower airway dysbiosis exacerbates lung cancer. *Cancer Discovery* (2021) 11(2):224–6. doi: 10.1158/2159-8290.cd-20-1641

131. Yadava K, Pattaroni C, Sichelstiel AK, Trompette A, Gollwitzer ES, Salami O, et al. Microbiota promotes chronic pulmonary inflammation by enhancing il-17a and autoantibodies. *Am J Respir Crit Care Med* (2016) 193(9):975–87. doi: 10.1164/rccm.201504-0779OC

132. Kanbay M, Kanbay A, Boyacioglu S. Helicobacter pylori infection as a possible risk factor for respiratory system disease: A review of the literature. *Respir Med* (2007) 101 (2):203–9. doi: 10.1016/j.rmed.2006.04.022

133. Schwabe RF, Jobin C. The microbiome and cancer. *Nat Rev Cancer* (2013) 13 (11):800–12. doi: 10.1038/nrc3610

134. Zmora N, Zeevi D, Korem T, Segal E, Elinav E. Taking it personally: Personalized utilization of the human microbiome in health and disease. *Cell Host Microbe* (2016) 19 (1):12–20. doi: 10.1016/j.chom.2015.12.016

135. Lee SH, Cho SY, Yoon Y, Park C, Sohn J, Jeong JJ, et al. Bifidobacterium bifidum strains synergize with immune checkpoint inhibitors to reduce tumour burden in mice. *Nat Microbiol* (2021) 6(3):277–88. doi: 10.1038/s41564-020-00831-6

136. Tomita Y, Ikeda T, Sakata S, Saruwatari K, Sato R, Iyama S, et al. Association of probiotic clostridium butyricum therapy with survival and response to immune checkpoint blockade in patients with lung cancer. *Cancer Immunol Res* (2020) 8 (10):1236–42. doi: 10.1158/2326-6066.cir-20-0051

137. Gui QF, Lu HF, Zhang CX, Xu ZR, Yang YH. Well-balanced commensal microbiota contributes to anti-cancer response in a lung cancer mouse model. *Genet Mol Res GMR* (2015) 14(2):5642–51. doi: 10.4238/2015.May.25.16

138. Paramsothy S, Kamm MA, Kaakoush NO, Walsh AJ, van den Bogaerde J, Samuel D, et al. Multidonor intensive faecal microbiota transplantation for active ulcerative colitis: A randomised placebo-controlled trial. *Lancet (Lond Engl)* (2017) 389 (10075):1218–28. doi: 10.1016/s0140-6736(17)30182-4

139. Ford AC. Stool as a treatment for ibs: More questions than answers? *Lancet Gastroenterol Hepatol* (2018) 3(1):2–3. doi: 10.1016/s2468-1253(17)30337-0

140. Routy B, Le Chatelier E, Derosa L, Duong CPM, Alou MT, Daillère R, et al. Gut microbiome influences efficacy of pd-1-Based immunotherapy against epithelial tumors. *Sci (New York NY)* (2018) 359(6371):91–7. doi: 10.1126/science.aan3706

141. Song P, Yang D, Wang H, Cui X, Si X, Zhang X, et al. Relationship between intestinal flora structure and metabolite analysis and immunotherapy efficacy in Chinese nsclc patients. *Thorac Cancer* (2020) 11(6):1621–32. doi: 10.1111/1759-7714.13442

142. Zhang C, Wang J, Sun Z, Cao Y, Mu Z, Ji X. Commensal microbiota contributes to predicting the response to immune checkpoint inhibitors in non-Small-Cell lung cancer patients. *Cancer Sci* (2021) 112(8):3005–17. doi: 10.1111/cas.14979

143. Daillère R, Vétizou M, Waldschmitt N, Yamazaki T, Isnard C, Poirier-Colame V, et al. Enterococcus hirae and barnesiella intestinihominis facilitate cyclophosphamide-induced therapeutic immunomodulatory effects. *Immunity* (2016) 45(4):931–43. doi: 10.1016/j.immuni.2016.09.009

144. Heshiki Y, Vazquez-Uribe R, Li J, Ni Y, Quainoo S, Imamovic L, et al. Predictable modulation of cancer treatment outcomes by the gut microbiota. *Microbiome* (2020) 8 (1):28. doi: 10.1186/s40168-020-00811-2

145. Tartour E, Zitvogel L. Lung cancer: Potential targets for immunotherapy. *Lancet Respir Med* (2013) 1(7):551–63. doi: 10.1016/s2213-2600(13)70159-0

146. Gopalakrishnan V, Spencer CN, Nezi L, Reuben A, Andrews MC, Karpinets TV, et al. Gut microbiome modulates response to anti-Pd-1 immunotherapy in melanoma patients. *Sci (New York NY)* (2018) 359(6371):97–103. doi: 10.1126/science.aan4236

147. Sivan A, Corrales L, Hubert N, Williams JB, Aquino-Michaels K, Earley ZM, et al. Commensal bifidobacterium promotes antitumor immunity and facilitates anti-Pd-L1 efficacy. *Sci (New York NY)* (2015) 350(6264):1084–9. doi: 10.1126/science.aac4255

148. Iida N, Dzutsev A, Stewart CA, Smith L, Bouladoux N, Weingarten RA, et al. Commensal bacteria control cancer response to therapy by modulating the tumor microenvironment. *Sci (New York NY)* (2013) 342(6161):967–70. doi: 10.1126/science.1240527

149. Viaud S, Saccheri F, Mignot G, Yamazaki T, Daillère R, Hannani D, et al. The intestinal microbiota modulates the anticancer immune effects of cyclophosphamide. *Sci (New York NY)* (2013) 342(6161):971–6. doi: 10.1126/science.1240537

frontiers | Frontiers in Microbiomes

TYPE Original Research
PUBLISHED 14 February 2023
DOI 10.3389/frmbi.2022.1097124

OPEN ACCESS

EDITED BY
Mina Rho,
Hanyang University, Republic of Korea

REVIEWED BY
Eugeni Belda,
Institut de Recherche pour le Development (IRD), France
Tasha M. Santiago-Rodriguez,
Diversigen, United States

*CORRESPONDENCE
Arbel D. Tadmor
arbel.tadmor@tron-mainz.de
Gita Mahmoudabadi
gitam@stanford.edu
Rob Phillips
phillips@pboc.caltech.edu

†These authors have contributed equally to this work

SPECIALTY SECTION
This article was submitted to Omics Approaches, a section of the journal Frontiers in Microbiomes

RECEIVED 13 November 2022
ACCEPTED 16 December 2022
PUBLISHED 14 February 2023

CITATION
Tadmor AD, Mahmoudabadi G, Foley HB and Phillips R (2023) Identification and spatio-temporal tracking of ubiquitous phage families in the human microbiome. *Front. Microbiomes* 1:1097124. doi: 10.3389/frmbi.2022.1097124

Identification and spatio-temporal tracking of ubiquitous phage families in the human microbiome

Arbel D. Tadmor[1,2*†], Gita Mahmoudabadi[3,4*†], Helen B. Foley[5,6] and Rob Phillips[7,8*]

[1]TRON - Translational Oncology at the University Medical Center of the Johannes Gutenberg University Mainz, Mainz, Germany, [2]Department of Biochemistry and Molecular Biophysics, California Institute of Technology, Pasadena, CA, United States, [3]Department of Bioengineering, California Institute of Technology, Pasadena, CA, United States, [4]Department of Bioengineering, Stanford University, Stanford, CA, United States, [5]Department of Preventive Medicine, USC Keck School of Medicine, Los Angeles, CA, United States, [6]Department of Applied Physics, California Institute of Technology, Pasadena, CA, United States, [7]Department of Physics, California Institute of Technology, Pasadena, CA, United States, [8]Division of Biology and Biological Engineering, California Institute of Technology, Pasadena, CA, United States

Viruses are a major component of the human microbiome, yet their diversity, lifestyles, spatiotemporal dynamics, and functional impact are not well understood. Elucidating the ecology of human associated phages may have a major impact on human health due to the potential ability of phages to modulate the abundance and phenotype of commensal bacteria. Analyzing 690 Human Microbiome Project metagenomes from 103 subjects sampled across up to 18 habitats, we found that despite the great interpersonal diversity observed among human viromes, humans harbor distinct phage families characterized by their shared conserved hallmark genes known as large terminase subunit (TerL) genes. Phylogenetic analysis of these phage families revealed that different habitats in the oral cavity and gut have unique phage community structures. Over a ~7-month timescale most of these phage families persisted in the oral cavity and gut, however, presence in certain oral habitats appeared to be transitory, possibly due to host migration within the oral cavity. Interestingly, certain phage families were found to be highly correlated with pathogenic, carriage and disease-related isolates, and may potentially serve as novel biomarkers for disease. Our findings shed new light on the core human virome and offer a metagenomic-independent way to probe the core virome using widely shared conserved phage markers.

KEYWORDS

core human virome, human phage markers, phageome, human microbiome, oral virome, metagenome clustering, metagenomic clustering by reference library, MCRL

Introduction

Bacteriophages are a major component of the human microbiome, with saliva, for example, containing 10^8 virus-like particles per milliliter (Pride et al., 2012), and stool containing up to 10^9 virus-like particles per gram (Reyes et al., 2012). Viruses are also frequently encountered as prophages, with an estimated ~60% of sequenced bacterial genomes predicted to encode at least one integrated phage genetic element (Casjens, 2003; Edwards and Rohwer, 2005). The degree to which these pervasive phage genetic elements modulate the abundance and phenotype of commensal microbiota and impact human health is currently unknown. Phages, for example, have been shown to promote pathogenicity in bacteria, confer antibiotic resistance to hosts, and transduce genes that alter host fitness (Waldor and Mekalanos, 1996; Brüssow et al., 2004; Willner et al., 2011; Pride et al., 2012; Quirós et al., 2014; Navarro and Muniesa, 2017). Furthermore, commensal phages have been correlated with various medical conditions such as type I diabetes, chronic infection, and inflammatory bowel disease (Zhao et al., 2017; Łusiak-Szelachowska et al., 2017; Secor et al., 2017). Phages may therefore potentially have a significant impact on human health.

Despite the abundance of phages in human microbial habitats and their postulated impact on human health, we have a very limited understanding of phage ecology in the human body, in particular the identity of their hosts, their lifestyles, their spatial distribution, their temporal dynamics, and their potential role in mediating disease. Applying standard metagenomic approaches to address such questions is challenging in part because of the staggering genomic diversity that is a hallmark of viruses (Paez-Espino et al., 2016a) and the fundamental plasticity of viral genomes, making it difficult to target and precisely track in space and time specific phage families. Indeed, with few exceptions (Stern et al., 2012; Manrique et al., 2016), previous metagenomic studies have largely focused on the heterogeneity of human viromes (Reyes et al., 2010; Minot et al., 2011; Pride et al., 2012; Reyes et al., 2012; Moreno-Gallego et al., 2019; Shkoporov et al., 2019; Gregory et al., 2020; Zuo et al., 2020; Garmaeva et al., 2021). Conversely, traditional methods that are based on targeting universally conserved genes such as the small subunit ribosomal RNA (SSU rRNA) gene for mapping microbial diversity are not applicable to phages because there is no analogous universally conserved gene in viruses (Rohwer and Edwards, 2002; Edwards and Rohwer, 2005).

In this study we aimed to combine the benefits of metagenomic and targeted sequencing approaches to discover phage families that may be widely present in the human virome. We were motivated by the hypothesis that - in analogy to the SSU rRNA marker - there would be core phage families (whether lytic or lysogenic) that could be represented and identified by conserved marker sequences. If we could find such markers, then in analogy to phylogenetic profiling of SSU rRNA markers, we could use phylogenetic analysis to explore intra-family sequence diversity and track such members across different body habitats, different subjects, and different time points. In this context, we use the term "family" to informally denote phages that have a high degree of sequence similarity across a shared marker gene, and within each family, we use the term "sublineage" to denote members that are more phylogenetically similar based on their shared marker gene. As such, in our framework, we do not necessarily expect that members of the same phage family share homology or similarity across their entire genomes.

We chose to focus our search for phage markers on the large terminase (TerL) subunit, one of the most powerful molecular machines in nature (Sun et al., 2008), a component of the DNA packaging and cleaving mechanism present in numerous double stranded DNA (dsDNA) phages (Rao and Feiss, 2008) and considered to be an important signature of dsDNA phage genomes (Casjens, 2003). Typically, TerL genes of different phages exhibit little overall sequence similarity (Eppler et al., 1991; Chai et al., 1992; Moore and Prevelige, 2002; Rao and Feiss, 2008) and contain only a handful of conserved functional amino acid residues (Rao and Feiss, 2008). However, we previously found that in the case of termites, the hindgut microbiomes of numerous termite species from different parts of the globe shared a certain TerL gene family that was conserved across most amino acid residues enabling us to construct a universal phage marker for this family of phages in termites (Tadmor et al., 2011). Therefore, while the TerL gene in and of itself is not universally conserved and therefore cannot serve as a general purpose universal marker for phages, our finding raised the possibility that other TerL gene families may exist in other species that are conserved and widely shared across members of those species, including humans. Adopting this marker-based approach to the human virome, we were indeed able to identify a set of unrelated TerL-based phage families that are ubiquitously shared across humans. Within each family, phylogenetic analysis enabled us to map with high resolution sublineages across different subjects, body habitats and time points (for an overview of our methodology see Figure S1).

Materials and methods

Sample collection

Samples from nine orally healthy adults were kindly donated to us by Bik et al. who had collected these samples through a collaboration with a dentist and in accordance to the Stanford IRB protocols (Bik et al., 2010). For each subject, oral biofilm samples were collected from six oral sites using sterile curettes. These oral sites include the tongue ventral, tongue dorsum, buccal mucosa, sub-gingiva, supra-gingiva, and the hard palate. Upon collection, the samples were deposited in PBS buffer. For

the viral fraction experiments, additional tongue dorsum samples were collected from a tenth subject that refrained from brushing their teeth or tongue for a minimum of 8 hours prior to sample collection to allow for a substantial buildup of plaque on the tongue dorsum. The samples were collected wearing gloves with a tongue scraper and deposited into a sterile collection tube. Exclusion criteria included: antibiotic use in the preceding three months, active cavities, or gum disease. Sample collection and processing protocols were approved by Caltech Institutional Review Board (IRB protocol 14-0430) and Institutional Biosafety Committee (IBC protocol 13-198).

Datasets analyzed

All metagenomes and viromes analyzed in this study were assembled by the original authors providing those datasets. Apart from the selection pressure analysis, which was performed on nucleotide sequences, analysis was performed on amino acid alignments. The following datasets and databases were analyzed in our study:

(1) The Mira dataset (Belda-Ferre et al., 2012) comprising six metagenomes corresponding to supragingival dental plaque collected from six patients in Spain and divided into three categories based on the number of caries per individual: two individuals who never developed caries in their lives (metagenomes M_{HA}, M_{HB}), two individuals who had been regularly treated for caries in the past and had a low number of active caries (1 and 4) at the time of sampling of sampling (metagenomes M_{PCA}, M_{PCB}), and two individuals who had a high number of active caries (8 and 15) and poor oral hygiene (metagenomes M_{AA}, M_{AB}). In all cases, plaque material from all teeth surfaces was pooled avoiding active cavities if present, and for each of the above six conditions a single metagenome was generated. The mean and median length of contigs in these metagenomes were 336 ± 167 nt (s.d.) and 409 nt, respectively. The mean genome size was 87.7 Mbases. Assembled translated metagenomes can be found on MG-RAST (Glass et al., 2010) with the following IDs: 4447192.3, 4447102.3, 4447103.3, 4447101.3, 4447943.3, 4447903.3.

(2) The Xie dataset (Xie et al., 2010) comprising a metagenome of supragingival and subgingival plaque collected and pooled from eight teeth of a caries-free and periodontally healthy individual from the United States. The mean and median length of contigs in this metagenome were 372 ± 126 nt s.d. and 411 nt, respectively. The genome size was 29.5 Mbases. The assembled translated metagenome can be found on MG-RAST with the ID 4446622.3.

(3) The HMP dataset (Methé et al., 2012) comprising contributions from 103 healthy individuals sampled from up to 15 body habitats, including: attached/keratinized gingiva, buccal mucosa, hard palate, palatine tonsils, saliva, subgingival plaque, supragingival plaque, throat, tongue dorsum, stool, anterior nares, posterior fornix, mid vagina, vaginal introitus, and the retroauricular crease. All subjects were subjugated to rigorous inclusion criteria to control for their health (Aagaard et al., 2013). 748 assembled metagenomes generated in Phase I of the HMP study were subjected to internal quality control assessment based on HMP study guidelines (Methé et al., 2012), remaining with 690 metagenomes that were used in the current analysis (Table S8). Metadata from the HMP cohort such as the Medical Record Number (MRN), collection site, visit number, and the replicate number were extracted as previously described (Markowitz et al., 2012). The mean and median length of contigs in HMP metagenomes passing HMP quality control were 582 ± 124 nt (s.d.) and 561 nt, respectively, and for oral metagenomes 529 ± 57 nt (s.d.) and 534 nt, respectively. The HMP metagenomes are available through the IMG/M database.

(4) The Pride dataset (Pride et al., 2012) comprising of viromes extracted from saliva samples of five subjects sampled at day 1, day 30 and day 60 or 90. Subjects were healthy and had not taken antibiotics for at least one year prior to donating samples. All subjects had good oral health based on rigorous inclusion criteria (Pride et al., 2012). The mean and median length of contigs in these metagenome were 328 ± 44 nt (s.d.) and 349 nt, respectively. Assembled translated metagenomes can be found on MG-RAST with the following IDs: 4445735.3, 4446121.3, 4445731.3, 4445728.3, 4446126.3, 4446075.3, 4445734.3, 4445729.3, 4446125.3, 4446124.3, 4445730.3, 4446122.3, 4446120.3, 4445737.3, and 4445736.3.

(5) The MetagenomesOnline (MgOl) portal (Wommack et al., 2012) hosted on the VIROME platform comprising 270 metagenomic libraries, including a large number of viromes. Environmental viromes in Figure 1H were selected to match the following filtering criteria: Genesis=natural, Environmental package=all excluding host-associated viromes, and considering only viromes of DNA viruses, resulting in 109 viromes. The mean and median length of contigs in these viromes were 377 ± 70 nt (s.d.) and 362 nt (range 319 – 1362 nt), respectively.

(6) The Human Oral Microbiome Database (HOMD) dataset (Chen et al., 2010) comprising genomes of oral bacteria sequenced either as part of the HOMD project or as part of other sequencing projects, including the HMP study.

(7) NCBI's non-redundant (nr) protein database, comprising all non-redundant GenBank CDS translations, the protein data bank (PDB), SwissProt, the Protein Information Resource (PIR) database and the Protein Research Foundation (PRF) database, excluding environmental samples from WGS projects.

(8) The IMG/M database (Chen et al., 2018) comprising at the time of analysis 16338 bacterial and archaeal isolates, 475 viral isolates, and 1335 environmental metagenomes. Environmental metagenomes in Figure 1G were selected as follows: for each environmental 'family' class a maximum of 50 metagenomes were randomly selected, limiting metagenomes to 5 GB due to the downloading limitation of the IMG platform, resulting in 448 metagenomes. Of these, we retained only metagenomes with constructed protein databases and excluded metatranscriptomes. In order for our comparison between HMP oral metagenomes and environmental metagenomes to be unbiased, we further controlled for the average contig length and the total genome size. To control for the average contig length we selected only environmental metagenomes whose average contig length exceeded the minimal contig length of assembled HMP metagenomes (300 bp) (Methé et al., 2012). To control for the genome size, we excluded environmental metagenomes whose genome size was below the minimal genome size of HMP oral metagenomes. Applying these selection criteria resulted in 233 environmental metagenomes analyzed in Figure 1G.

(9) The IMG/VR database (Paez-Espino et al., 2016b) (IMG_VR_2018-07-01_4) comprising at the time of analysis viral contigs from 3663 metagenomes available on IMG satisfying the constraint "Ecosystem phylum =Environmental".

(10) NCBI's env_nr database containing nearly 10 million proteins sequences from whole genome sequencing (WGS) metagenomic projects.

DNA extraction

DNA extraction was performed on each sample using the MoBio PowerBiofilm® DNA Isolation Kit, which uses a DNA extraction and purification protocol optimized for biofilms. It combines the benefits of a chemical lysis treatment with the physical forces applied during a bead-beating process. Disposable lab coats and face masks were worn at all times.

Degenerate primer design

Degenerate primers for the TerL markers were designed based on sequences obtained from the HMP dataset, the Xie dataset, the Mira dataset and HOMD as follows: candidate 3' positions for primers were chosen when possible at positions achieving a bit score of at least 3.5 when RPS-BLASTing the amino acid sequence of the given TerL marker against the Conserved Domains Database (CDD) (Marchler-Bauer et al., 2016). Primers were then selected in regions spanned by all datasets, requiring that the percent identity of the majority consensus amino acid residue, when equally weighted across all datasets, was at least 90% while limiting the degeneracy of each primer to 64 fold. Primer sequences were then designed using the CODEHOP algorithm (Rose et al., 1998), with the core region maximally degenerate based on the genetic code, and the consensus clamp region chosen to match the codon bias present in the alignments. Primer nucleotide sequences were optimized to have a GC clamp at the 3' end, minimize homodimers, heterodimers and hairpins, and have a melting temperature of 60°C. Degenerate primer sequences and targeted conserved amino acid motifs are provided in Table S3.

PCR preparation

PCR reactions using the degenerate primers described above were performed in a laminar flowhood. Each PCR reaction contained 10.5 µL of RT-PCR Grade Water (Ambion®), 1 µL of extracted DNA at 1 ng/µL, a premix containing AccuStart™ Taq DNA polymerase, dNTPs, and $MgCl_2$, and 0.5 µL of reverse and 0.5 µL of forward primers (at 50 ng/µL). A higher than recommended concentration was used since the primes are 32-64 fold degenerate. For MiSeq sequencing, primers were barcoded using error-detecting barcodes (appended onto the forward primer sequence) and synthesized by IDT (Hamady et al., 2008). For each extraction protocol, we performed three negative controls that instead of biofilm sample contained RT-PCR Grade Water (Ambion®), free of any DNAase and RNAse. These three extraction controls along with five no template controls were used during each PCR session to ensure there is no contamination being introduced during either process. Disposable lab coats and face masks were worn at all times. After each session all surfaces were cleaned with DNA AWAY™ and 95% ethanol. The flowhood interior surfaces and the equipment inside were exposed to UV for one hour at the end of each session. The following PCR thermocycling protocol was used in accordance to PerfeCTa qPCR SuperMix recommendations: 1) 10-minute activation of AccuStart™ Taq DNA polymerase at 95°C, 2) 10 seconds of DNA denaturation at 95°C, 3) 20 seconds of annealing at 60°C, 4) 30 seconds of extension at 72°C, 40 cycles repeating steps 2 to 4, followed by 5 minutes of final extension at 72°C.

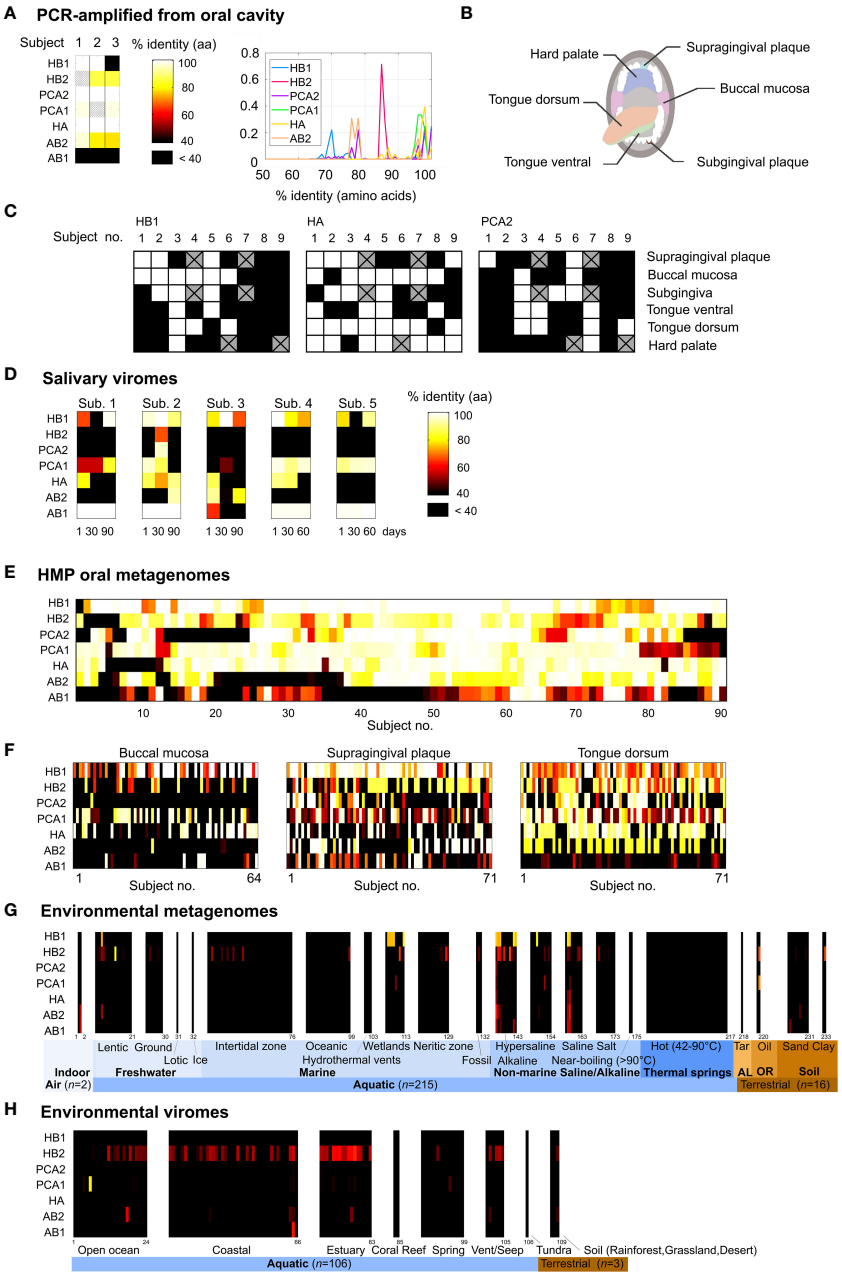

FIGURE 1
Prevalence of the TerL phage families in the human oral cavity and in natural environments. **(A)** Percent identity between the TerL markers and PCR-amplified TerL sequences obtained from the tongue dorsum, subgingival plaque and supragingival plaque of three orally healthy subjects (unless otherwise stated, percent identities in this study were calculated based on amino acid alignments). The heat map indicates the maximum percent identity across all PCR-amplified sequences. Striped cells indicate that the expected PCR band was present but sequencing failed. **(B)** Oral habitats analyzed by targeted sequencing. **(C)** Percent identity between the TerL markers and PCR-amplified TerL sequences across the oral habitats indicated in (B). Crossed out cells correspond to samples that were unavailable for testing. **(D)** Presence of the TerL phage families in salivary viromes obtained from five periodontally healthy subjects over a 60- to 90-day period (Pride et al., 2012). Heat map applies to panels d-h and shows the maximum percent identity across all BLAST alignments exceeding a predetermined optimal alignment length threshold (Supporting Text S4). **(E)** Prevalence of the TerL phage families across 90 subjects based on 382 HMP oral metagenomes regardless of collection site, visit number, or replicate. **(F)** Prevalence of the TerL phage families across 206 HMP oral metagenomes corresponding to three oral habitats, taking into account one metagenome per subject. **(G)** Prevalence of the TerL phage families across 233 metagenomes from natural environments. AL, asphalt lakes; OR, oil reservoir. **(H)** Prevalence of the TerL phage families across 109 viromes of DNA viruses from natural environments.

Gel electrophoresis and PCR cleanup

2% agarose in TAE buffer was used to cast the gels. 5 µL of PCR reaction was mixed with 1 µL of 6X loading dye and set to run for 30 min at 100V. PCR products were purified using the QIAquick PCR Purification Kit from QIAGEN in accordance to their manual.

Sequencing and sequence analysis

Double-stranded DNA concentration in PCR-purified products was measured and standardized using the Qubit instrument. Sequences amplified for the AB2, HB2 and PCA1 markers were sent for Sanger sequencing following the IDT standard protocol. Sequences amplified for the HB1, HA and PCA2 markers were sent for MiSeq sequencing. Because each sample for MiSeq sequencing was barcoded during the PCR reaction, the samples were mixed into one vial and sent to GENEWIZ, Inc for library preparation and Illumina MiSeq sequencing (2 × 300bp Paired-End sequencing). *join_paired_ends.py* script from the Quantitative Insights Into Microbial Ecology (QIIME) package (Caporaso et al., 2010) was used to join paired-end reads. We then performed several quality control steps to eliminate any sequences that arose due to sequencing error. Paired reads that had any mismatches across their overlapping bases were eliminated. The overlap between the paired reads constituted the entire length of the sequence. Using an in-house script developed for this project, *seqQualityFilters.py*, we then eliminated sequences with any bases with Phred scores of 29 or below (excluded from this step were the first and last two bases which are generally associated with low Phred scores for all sequences). Using the same in-house script (i) sequences were assigned to their respective TerL markers based on their primer sequences; (ii) sequences with incorrect barcode lengths or incorrect primer sequences were eliminated; (iii) the primer and barcode sequences were removed and the barcode sequences were written to a separate file for a later step; (iv) sequences with incorrect lengths were removed. *split_libraries_fastq.py* from QIIME was used to demultiplex the reads based on their barcode sequence, while further eliminating reads with any errors in their barcodes. MiSeq sequences analyzed in Figure 1A and Table S5 were clustered using QIIME's *pick_otus.py* script, based on their sequence similarity into operational taxonomic units (OTUs) (Edgar, 2010) using an OTU cutoff of 95% for HA and PCA2, and 98% for HB1.

Viral fraction protocol

To test if oral phages carrying close homologs of HB1 are lytic we tested the bacterial and viral fractions derived from an oral sample for the presence of the HB1 marker. Saliva samples were defrosted from storage at -20°C. Samples and an extraction control were vortexed for 2 minutes at half-speed, followed by centrifugation at 8000g for 10 minutes. The supernatant was removed to a fresh tube and the pellet was resuspended in sterile filtered PBS. Supernatant and pellet were re-centrifuged (8000g, 5 minutes). 200µL of the original supernatant (putative viral fraction, VF) were filtered through a PBS-rinsed 0.2µm 13mm tuffryn filter. Original pellet (putative bacterial fraction, BF) was rinsed and resuspended 200µL PBS. BF and VF, as well as extraction controls, were extracted according to standard protocol with PowerBiofilm DNA Isolation Kit (MoBio). TerL markers HB1 and HA were amplified as described above. Markers were amplified from 1 µL template using 0.8 µL of 10 micromolar forward and reverse primers, with PerfeCTa MasterMix. Marker HB1 was also amplified using 2 µL of template and 0.8 µL of 100µM primers. PCR products were assayed for presence or absence on 2% agarose gel (Figure S7). Six replicates of the same VF extract were amplified to test for low-copy templates in the viral fraction.

Identifying shared TerL markers in the human oral cavity

Identifying viral gene families in the Mira metagenomes

To identify TerL markers core to the human oral cavity we focused our analysis on the six plaque metagenomes from the Mira dataset reflecting human subjects with varying degrees of oral hygiene. We applied to each of these metagenomes a clustering algorithm called Metagenomic Clustering by Reference Library (MCRL) that was developed by the current authors (Tadmor and Phillips, 2022). Briefly, MCRL uses a reference library containing a set of reference sequences (in this case the viral RefSeq database v48 (Pruitt et al., 2007) containing ~97,000 viral genes) to initially identify and retain all reference sequences that have putative homologs in the given input metagenome. MCRL then proceeds to apply an iterative greedy clustering algorithm to the list of retained reference sequences and, upon convergence, reports the subset of reference sequences that are homologous to minimally overlapping sets of contigs in the metagenome. Thus, the final output of MCRL is the list of reference sequences with putative homologs in the input metagenome that have minimally overlapping "signatures" in the metagenome. A "signature" of a reference sequence in a metagenome is the list of contigs in the metagenome yielding an E value below 0.001 when BLASTing the amino acid sequence of reference sequence against the translated metagenome. Reference sequences reported by MCRL therefore reflect potential different and unrelated gene families present in the metagenome.

To maximize detection sensitivity, we applied MCRL using its default parameters and a "stringent overlap" condition wherein two reference sequences are determined to overlap if their signatures overlap by more than 50% regardless of the reference sequence. In terms of sensitivity, we have previously shown that when using a stringent overlap condition MCRL achieves a sensitivity of at least 95% for detecting TerL gene families that exhibit up to 30% divergence compared to the viral RefSeq database, and overall has better sensitivity compared to conventional metagenomic clustering methods (Tadmor and Phillips, 2022). A detailed discussion of MCRL's default parameters, robustness to changes in parameters or presence of noise, and a benchmark comparing MCRL to standard metagenomic clustering methods in terms of sensitivity and accuracy is provided in (Tadmor and Phillips, 2022). When applying MCRL to each of the six Mira metagenomes, analyzing in total 1.75×10^6 translated contigs, MCRL reported in total 7411 viral RefSeq genes (as depicted in Figure S2A).

Screening for shared TerL sequences

To enrich for TerL candidates with significant putative homologs in the metagenomes and to remove spurious solutions, we retained from the list of 7411 viral RefSeq genes reported by MCRL a total of 76 reference genes encoding TerL genes (based on the RefSeq annotation provided by MCRL) that have a signature size of 5 or higher and that share at least 10% identical amino acid residues when aligned against their representative contig (the representative contig of a reference sequence is the contig yielding the lowest E value when BLASTing that reference sequence against the metagenome).

To enrich for closely related TerL lineages that are potentially shared across humans we BLASTed the amino acid sequence of the representative contig corresponding to each of the 76 homologous TerL RefSeq genes identified by MCRL in the Mira dataset against the translated oral metagenome from the Xie study - an oral metagenome of a healthy individual from a different continent participating in an independent study – and retained only candidates that yielded at least 75% identity at the amino acid level. A 75% identity threshold was empirically motivated based on our previous experimental results in the termite hindgut system (Tadmor et al., 2011) where we found that the universally shared TerL lineage in this ecosystem exhibited 81.1% ± 7.8 identity at the amino acid level across different termite species. Indeed, this threshold was justified in retrospect given that the diversity of HMP metagenomic sequences closely related to the markers was captured using a 70% identity threshold at the amino acid level, as shown in Figure S9 and discussed in Supporting Text S8. This final filtering step left us with 11 TerL gene fragments (Table S2). We then BLASTed all 11 TerL gene fragments against each other at the protein level and removed redundant sequences, leaving us with seven non-homologous independent candidates for shared TerL markers (Table S3).

Obtaining full-length TerL markers

Since the metagenomes used to obtain the TerL marker candidates have relatively short contigs (with a mean contig length of 336 nt), the seven candidate TerL markers identified in the Mira dataset span only a fragment of the TerL gene length, which spans on average 1650 nt. To obtain shared TerL markers that span the entire length of a TerL gene we collected and aligned for each of the seven TerL candidate markers closely related amino acid sequences from the Xie, Mira, HOMD and the HMP datasets yielding at least 70% identity at the amino acid level. For each of the seven alignments we then selected the sequence that maximized the average percent identity across all other sequences (applying equal weights to each database), penalizing shorter sequences by setting the alignment score in positions containing gaps to 0. In this manner, we identified for each of the seven TerL candidates a closely related sequence spanning the entire length of the TerL gene. Contigs carrying the full-length TerL genes are listed in Table S3 and annotation for these contigs is provided in Figure S5.

BLAST alignments

All BLAST analyses were performed locally using blastp v2.2.22+ with default settings on amino acid alignments. Alignment thresholds are discussed in Supporting Text S4 and S8.

Collection of TerL marker homologs present in bacterial and phage isolates

To exhaustively identify all close homologs of the TerL markers in bacterial and phage isolates, each of the seven TerL markers were BLASTed against all available genomes on the IMG platform, NCBI's non-redundant (nr) protein database, and the HOMD database. For our phylogenetic analysis we included all TerL sequences that yielded at least 70% identity at the amino acid level across at least 90% of the TerL marker length, remaining with approximately 2300 hits (Table S10).

Determining health-related status of isolates

Each isolate harboring a close homolog of a TerL marker was assigned a "health-related status" to reflect its pathogenicity or potential association with disease. The decision regarding the health-related status was determined as follows: when information about the pathogenicity of the isolate or details about the bacterium's isolation were provided in IMG annotation or in annotation from another public database this

information was used to determine the health-related status of the isolate. When public annotation was not available or not sufficiently detailed, original publications describing the isolation of the bacterium were sought. When the information provided in the original publication was not sufficiently detailed, the original authors were consulted. Based on the above information, the health-related status isolates was assigned to one of the following categories: "P"=the bacterial isolate/strain was designated as a pathogen by the author and/or the bacterium was isolated from a sick individual with a diagnosed disease or from a diseased organ, a diseased body site, a sterile body site, or a diseased animal. Sterile body sites include, for example, blood, cerebral spinal fluid, lymph nodes, peritoneal fluid, synovial fluid, and internal organs. "C"=the bacterial isolate was designated as a carriage strain by the author. "H"=the bacterial isolate/strain is not considered to be pathogenic by the author and/or was isolated from a healthy subject, healthy tissue or a healthy animal. When the required information was insufficient or unavailable to determine the health-related status of the isolate, the health-related status was designated "n.a.". In case of phage isolates, the health-related status pertains to the bacterium strain from which the phage was induced. The health-related status for all isolates is provided in Table S10 along with appropriate references.

Phylogenetic analysis

Phylogenetic analysis was performed on translated TerL sequences obtained from all 690 HMP metagenomes passing HMP quality control criteria as well as all bacterial and phage isolates harboring close homologs of the markers listed in Table S10, taking one representative per OTU as described below (OTU assignment for all isolates is provided in Table S10). Phylogenetic analysis was performed based on sequence alignments spanning at least 400 amino acids and yielding at least 70% identity at the amino acid level compared to the TerL markers, resulting in alignments spanning on average 69.2% of the TerL gene length (range: 62.7% to 88.9%). In the case of human bacterial isolates, one representative strain was selected per species per body region and per given health-related status, using a 3% OTU threshold at the amino acid level with alignments spanning at least 98% of the TerL marker length. For non-human bacterial isolates, one representative strain per species was selected. Translated nucleotide sequences were then aligned with MUSCLE (Edgar, 2004) in MEGA (Tamura et al., 2013). The optimal amino acid substitution model was estimated with ProtTest3.4 (Darriba et al., 2011) using the AIC criterion allowing for 48 model combinations permitted in SplitsTree4 (Huson and Bryant, 2006) with +G and +I options (amino acid frequencies are hard-coded in SplitsTree4). Models tested include: WAG (Whelan and Goldman, 2001), JTT (Jones et al., 1992), mtREV (Adachi and Hasegawa, 1996), mtMam (Cao et al., 1998), Dayhoff (Dayhoff and Schwartz, 1978), CpREV (Adachi et al., 2000). Optimal model-averaged parameters using Akaike weights were estimated with ProtTest3.4 for the shape parameter of the gamma distribution (α), and the proportion of invariant sites (Pinv). Neighbor-Net networks were estimated with SplitsTree4 (Huson and Bryant, 2006) based on amino acid sequence alignments using maximum likelihood distances estimated with optimal model-averaged parameters.

Selection pressure analysis

Selection pressure analysis was performed using codeml codon models included in the PAML package (Yang, 2007). Sequence alignments were generated using Geneious global alignment with free end gaps with default gap open and gap extension penalties, using an identity cost matrix (Kearse et al., 2012). Phylogenetic trees were created using SeaView GTR model with default parameters (Gouy et al., 2009). We tested NSsite models with different number of site classes: M0 (one site class with constant ω, where $\omega = dN/dS$), M1a (two site classes: $\omega=1$, $\omega<1$) and M2a (three site classes: $\omega=1$, $\omega<1$, $\omega>1$). The CodonFreq parameter was set to F3x4. Models M0 and M1a were compared against each other as were M1a and M2a. The models were compared using the likelihood ratio test and the statistical significance of the outcome was determined based on the chi-squared distribution (Yang, 2007).

Results and discussion

Hunting for shared phage families in the human oral virome

The habitat we chose to begin our search for ubiquitous phage families in humans was the oral cavity due to its rich microbial diversity (Huttenhower et al., 2012), presence of many unique niches that can be explored, and its relevance to human health as a gateway to the human body (Li et al., 2000). The most straightforward way to find a TerL marker core to the human oral virome would be to perform a joint phylogenetic analysis of all TerL sequences across multiple oral metagenomes obtained from different individuals. Such an approach, however, is impractical due to the highly divergent nature of TerL sequences, the relatively short lengths of contigs, and limitations of metagenomic annotation (Supporting Text S1). To circumvent these challenges we devised a method based on a combination of clustering and filtering steps. To this end, we applied a novel metagenomic clustering method that we developed that uses a reference library of annotated viral sequences to extract putative unrelated viral gene families from a metagenome

(Tadmor and Phillips, 2022) (see Materials and Methods). This approach enabled us to examine the putative viral gene families present in six metagenomes of supragingival dental plaque samples obtained from six individuals from Spain with varying degrees of oral hygiene (Belda-Ferre et al., 2012), referred to as the Mira dataset (see Figure S2A and the Materials and Methods section for a summary of our search strategy). Analzying in total nearly two million contigs, our search algorithm identified an average of 1236 viral gene families per metagenome (Table S1), of which 76 encoded TerL genes (Table S2). Since our goal was to establish whether the majority of healthy humans share certain conserved phage markers, we narrowed the list of TerL candidates to those that were conserved across the majority of the TerL gene in at least two human subjects from two independent studies from different parts of the world. The second study we selected, which we refer to as the Xie dataset, was obtained from the oral cavity a healthy individual from the United States (Xie et al., 2010). This final screening step left us with seven non-homologous TerL gene fragments labeled *H*A, *H*B1, *H*B2, *PC*A2, *PC*A1, *A*B1, *A*B2, with the prefix corresponding to the oral health of the subject in which the marker discovered, indicating good (*H*), mediocre (*PC*), or poor (*A*) oral hygiene (Figure S2). Such a labeling scheme enabled us to correlate marker prevalence with oral hygiene (see below). Lastly, each TerL gene fragment was swapped with a closely related homologous full-length TerL sequence, using the Human Oral Microbiome Database (HOMD) (Chen et al., 2010) and the Human Microbiome Project (HMP) dataset (Methé et al., 2012) to expand our sequence search space to include full length sequences (see Material and Methods for objective search strategy). The HMP dataset was excluded from the step of identifying shared phage markers in order to avoid introduction of biases in subsequent analyses of this dataset.

Our full-length phage markers corresponded to HK97-associated COG4626/pfam03354 Terminase_1 (HA, HB1, HB2, PCA2, AB1), and SPP1-associated COG1783/pfam04466 Terminase_3 (PCA1), with AB2 not corresponding to any known pfam/COG (Table S3). These results were consistent with phylogenetic analysis of the TerL markers in the broader context of TerL genes observed in nature (Figure S4). The seven full-length TerL marker genes we obtained represent unrelated lineages since any pair of TerL markers exhibited little or no sequence similarity at the amino acid level (Table S4), as is typically the case for TerL genes. Going back to the Mira study, we BLASTed the full-length TerL markers against the six oral metagenomes and found that apart from PCA2, all markers achieved alignments exceeding 70% identity at the amino acid level in 3 to 5 of the six subjects, confirming the shared presence of these markers in this small cohort (Figure S2B).

Experimental validation of phage families derived bioinformatically from metagenomic datasets

To confirm that our bioinformatically-derived TerL-based phage families can also be verified experimentally we tested for the presence of TerL markers in oral samples collected from orally healthy subjects using targeted sequencing. Using amino acid alignments from multiple public datasets we designed degenerate primers (Rose et al., 1998) targeting conserved amino acid motifs (Table S3, Figure S3). Sequencing the resulting PCR products, we were indeed able to experimentally identify the presence of all but one (AB1) of the phage families in at least two of the three tested individuals (Figure 1A, Table S5). Using the same targeted sequencing approach we then tested for the presence of three of the phage families (HB1, HA, and PCA2) across six oral habitats collected from nine additional subjects (Figure 1B). We found all three phage families in this cohort were robustly present in the oral cavity (Figure 1C). In a companion paper we discuss in greater depth TerL sequence diversity obtained by targeted sequencing, including HB1 sequences obtained from 61 individuals across three continents (Mahmoudabadi et al., 2019).

Evidence for the functionality of sequences retrieved by the phage markers

Although whole community metagenomes provide a snapshot into both lytic and lysogenic phage families, it has the drawback that it does not provide direct evidence that the sequences we recover are part of functional phages. However, several indirect lines of evidence suggest that the shared TerL lineages we identified encode functional genes associated with genuine phage elements. First, we confirmed that the original contigs encoding the TerL markers harbored larger phage-like elements (Figure S5), and that close homologs of most of the markers can be found in extended prophage-like elements (Figure S6, Supporting Text S2), helping to rule out non-genuine phage elements such as gene transfer agents (GTAs) and bacteriocins (Supporting Text S3). Second, we confirmed that sequences retrieved using the markers or primers were under substantial negative selection (Table S6), lacked premature stop codons or frameshift mutations and functional signatures typical of TerL genes were strictly conserved in these sequences (see Figure S3 for alignments and Table S7 for a summary of conserved functional signatures). Finally, we showed that the markers can be detected in virus-like particles (VLPs) using a fourth metagenomic dataset comprising 15 salivary viromes obtained from five periodontally healthy human subjects (Pride et al., 2012) (Figure 1D). In the case of

HB1, we further experimentally verified these results by showing that this marker could be detected by PCR amplification in virus-like particles extracted from a tenth oral sample from our own cohort of oral samples (Figure S7A). Taken together, the evidence above suggests that, overall, TerL sequences retrieved using our markers encode functional genes that have either been active in recent evolutionary history and/or are part of a population of functional phages, and thus we speculate are not degenerating pseudogenes experiencing random drift (Supporting Text S3).

Prevalence of the phage markers in the HMP oral metagenomes

We next explored the prevalence of these phage families within the HMP oral cohort, which comprises 90 subjects sampled from up to eight oral sites spanning in total 382 metagenomes (Table S8). We found that remarkably virtually all 90 subjects were positive for the HB1 phage family with at least 70% identity, and 76% of subjects were positive for the HB1 phage family with at least 95% identity (see Figures 1E, 2A, for alignment criteria see Supporting Text S4). Likewise, more than 85% of subjects were positive for the HA and PCA1 phage families with at least 70% identity at the amino acid level, and 72% and 63% of subjects were positive for the HA and PCA1 phage families, respectively, with at least 95% identity (Figure 2A). In addition, nearly all subjects were positive for any pair combination of HB1, HB2, HA and PCA1 (Figure 2B), however, presence of any specific pair of phage families was only weakly correlated (absolute Spearman's rank correlation ≤0.24), consistent with these markers representing independent TerL phage families. Since all subjects participating in the HMP study were orally healthy, perhaps expectedly, we found that markers obtained from metagenomes of orally healthy subjects in the Mira dataset (HB1, HB2, HA) were more prevalent than markers obtained from metagenomes of subjects with oral health problems (Supporting Text S5). Given the high prevalence of TerL phage families in the HMP, Mira, and Xie oral metagenomes, the salivary VLP metagenomes, and our own oral cohort interrogated by targeted sequencing suggests that these TerL phage families are ubiquitous in humans and contribute to a widely shared human virome. In Supporting Text S2 we summarize the requirements we propose a ubiquitous viral marker should satisfy.

Prevalence of the phage families in natural environments

To check whether the TerL phage families that we identified are in fact specific to the human virome or also prevalent in natural environments, we compared the prevalence of the TerL phage families across three oral habitats (206 metagenomes) with their prevalence across 233 environmental metagenomes from the IMG/M database (Chen et al., 2018) collected from over 70 unique sites across 13 countries, selected to have comparable genome sizes (number of assembled coding contigs) and contig lengths to HMP oral metagenomes (Table S9). Our comparison indicates that members of the TerL phage families were mostly prevalent in human oral metagenomes and relatively sparse in environmental metagenomes, with most markers, except for HB1 and to a lesser extent HB2, displaying relatively remote homologs in a small subset of environmental metagenomes (Figures 1F, G). In Supporting Text S6 we show that members of the HB1 and HB2 phage families appearing in environmental samples are phylogenetically distinct from their respective human-associated counterparts. To rule out potential sampling bias, we repeated this analysis in 3663 environmental metagenomes from the IMG/VR database spanning 35 distinct ecosystems (listed in Table S9), comprising in total nearly 20 million viral contigs (Paez-Espino et al., 2016b). Indeed, this analysis revealed a similar pattern of prevalence, as shown in Figure S8. An analysis of 109 environmental viromes (metagenomes of VLPs) deposited in the VIROME portal (Wommack et al., 2012) also revealed similar patterns (Table S9 and Figure 1H). In addition, we confirmed that the env_nr database did not contain more divergent homologs when using PSI-BLAST, and ruled out potential biases related to contig length, genome size, community complexity, read depth, method of assembly and sequencing technology (Supporting Text S7). Lastly, we performed an exhaustive search for TerL phage families in bacterial and viral genomes deposited in the IMG/M and non-redundant (nr) protein databases (Pruitt et al., 2007). Consistent with our analyses of whole community and VLP metagenomes, we found that except for six genomes originating from environmental bacteria that were positive for HB1, and two genomes positive for HB2 isolated from sewage and industrial environments, all remaining ~2300 genomes were obtained from bacteria isolated from human, animal, or insect (HB1) hosts (Table S10). These results agree with our previous finding and show that aside from HB1 and to a lesser extent HB2, the shared TerL phage families were quite specific to the viromes of humans and animals.

Distribution of the phage families across the human body

To elucidate the spatial distribution of the TerL phage families across the human body we mapped the presence of members of these families across seven body sites collected from 94 healthy individuals spanning 379 HMP metagenomes. Presence was determined based on a 70% identity threshold because this threshold captured the majority of phage family members (Figure S9), however, our findings did not depend on

the applied percent identity threshold, as further discussed in Supporting Text S8.

We found that most TerL phage families (HA, PCA1, PCA2, AB1, AB2) were indeed prevalent in the oral cavity and generally absent from stool, the nasal cavity, the female urogenital (UG) tract, and skin, except for a mild presence of PCA1 in skin (Figure 2C). HB1 and HB2 phage families, however, were exceptional and were found to be widespread not only in the oral cavity, but also in a considerable fraction of stool samples (Figure 2C), with up to ~90% and ~60% of subjects containing HB1 and HB2 TerL phage families in stool samples, respectively, when controlling for genome size (Supporting Text S7). To confirm the distribution of these phage families in stool samples, we tested for their presence in 14 metagenomic studies investigating stool samples obtained from heathy individuals included in the Gut Virome Database (GVD) (Gregory et al., 2020). We found the HB1 phage family in nearly all studies, including 11 viromes (metagenomes of VLPs), showing that

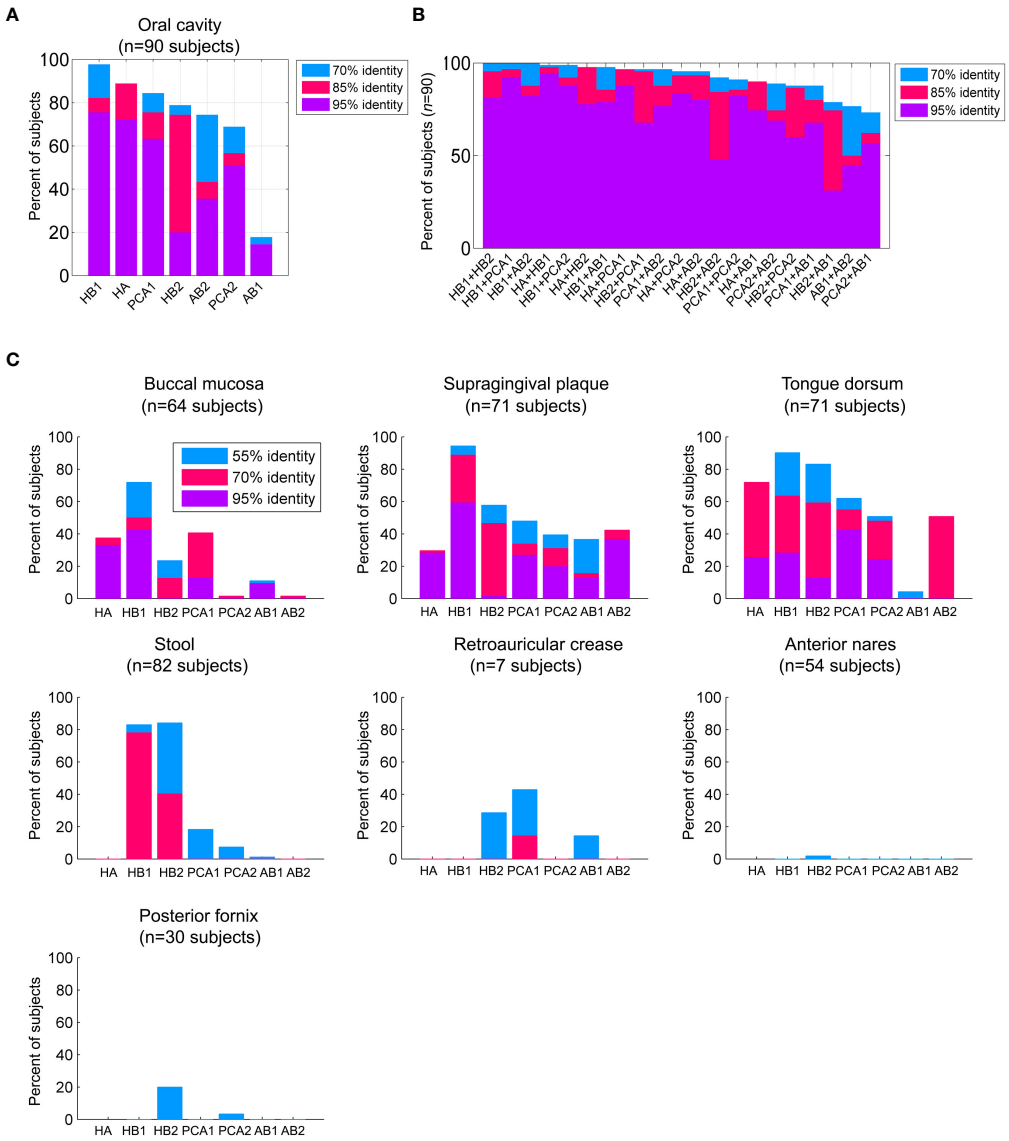

FIGURE 2
Prevalence of the TerL phage families across human habitats. **(A)** Percent of subjects that were positive for the TerL phage families in the oral cavity regardless of collection site, visit number, or replicate evaluated across 90 subjects based on 382 HMP oral metagenomes passing HMP quality control criteria. For all panels, a TerL phage family was considered present in a subject if the maximum percent identity of its TerL sequence across all BLAST alignments spanning at least 150 amino acids exceeded the indicated percent identity threshold. **(B)** Percent of subjects positive for any pair combination of TerL phage families. **(C)** Presence of TerL phage families across seven body habitats taking into account one metagenome per subject. Alignments in all panels were performed on amino acid sequences.

HB1 was present in stool samples of individuals across four continents. With few exceptions, the remaining markers were either not detected in the gut studies, or present only as remote homologs, confirming the distribution we observed in the HMP metagenomes (Table S11). HB2 phage family was present in all three whole community studies, and to a lesser extent in viromes. The remaining phage families were largely absent from the gut studies, confirming the spatial patterns of distribution we had observed in the HMP metagenomes (Table S11).

We next contrasted our findings in the HMP dataset with the presence of the markers in bacteria and phages isolated from different human body habitats. To this end we exhaustively searched the IMG, HOMD and the non-redundant (nr) protein databases for close homologs of the markers, carefully determining for each isolate its health-related status, for example, was it isolated from a healthy human subject or a human subject diagnosed with a certain disease, was the isolate designated as a human pathogen, a carriage strain, or was the isolate obtained from a non-human host (see Materials and Methods for precise criteria and Table S10 for a comprehensive list of isolates). Focusing on bacterial isolates obtained from healthy individuals, we indeed found that the HA and PCA1 phage families were present in oral and/or airway bacterial isolates from the *Streptococcus* genus, a genus known to be highly abundant in the oral cavity of healthy humans (Huttenhower et al., 2012). Likewise, AB2 was found in an oral bacterial isolate from the *Actinomyces* genus, a genus also known for its abundance in the oral cavity of healthy humans (Huttenhower et al., 2012) (phylogenetic placement of all bacterial hosts is summarized in Table S12). No oral bacterial isolates were found for PCA2, however, PCA2 was found in colon and gastric isolates, the latter suspected to be a swallowed oral bacterium caught in the act of transiting (see Table S10 for further details).

Finally, members of the HB1 and HB2 phage families were found in multiple gut bacterial isolates from the widespread Firmicutes phylum (Huttenhower et al., 2012), in agreement with our metagenomic analysis. Interestingly, however, no bacterial isolate from the oral cavity or airways, including carriage and pathogenic strains, was found to contain even distant homologs of the HB1 marker despite the overwhelming abundance of HB1 in the oral cavity of healthy humans. One possible explanation for this intriguing result could be that in healthy humans, the HB1 phage family found in the oral cavity is predominately lytic, a prediction that we were able to experimentally confirm, as we further discuss below. Despite the high prevalence of HB1 and HB2 phage families in stool samples, they were not related to the crAss-like phage family (Guerin et al., 2018), a recently identified widespread family of phages in gut viromes.

Phylogenetic analysis of TerL phage families

Thus far our attention has been focused on the prevalence of each phage family. However, within each family, members display incredible inter-and intra-subject sequence diversity (Tables S5, S13). To better characterize this sequence diversity, we wished to understand whether each phage family was comprised of a single indivisible TerL lineage, or, conversely, multiple distinct TerL sublineages, in which case we aimed to determine how different body sites were associated with different sublineages. For our marker-based phylogenetic analysis we chose to use phylogenetic networks (Bryant and Moulton, 2004; Huson and Bryant, 2006) to account for possible viral recombination events, events which cannot be represented by phylogenetic trees (Lemey et al., 2009).

A phylogenetic analysis of the HB1 TerL phage family revealed that it is comprised of three main sublineages: (i) a sublineage consisting primarily of gut metagenomic sequences and gut bacterial isolates (the "GI clade" in Figure 3A), (ii) a sublineage consisting nearly exclusively of oral metagenomic sequences and completely devoid of bacterial isolates (the "oral clade" in Figure 3A), and (iii) a sublineage consisting primarily of environmental sequences (the "Environmental clade" in Figure 3A and Supporting Text S6). The phylogenetic distinction between gut and oral sequences was supported with 98% bootstrap support by a maximum likelihood phylogenetic tree after removing potentially recombinant sequences (Figure S10). The finding that metagenomic HB1 gut-derived sequences grouped with 16 human-associated bacterial isolates from the gut is consistent with the notion that the human gut is generally dominated by phages exhibiting a lysogenic lifestyle (Reyes et al., 2010; Reyes et al., 2012; Ogilvie and Jones, 2015). In contrast, the oral HB1 clade was devoid of bacterial isolates and grouped with the lytic *Lactococcus lactis* phage 1706, further supporting our prediction that oral phages positive for the HB1 marker should be predominately lytic. To further explore this hypothesis, we filtered oral samples obtained from an orally healthy subject through a 0.2 μm pore size filter and performed multiple PCRs on the bacterial and the viral fractions. We were unable to amplify HB1 from any of the PCRs performed on the bacterial fraction, however, we were able to amplify HB1 from the majority of samples corresponding to viral fractions (Figure S7A). When the same experiment was performed on the HA marker, the opposite result was obtained: we could amplify HA from all samples originating from the bacterial fraction, yet we could not amplify HA from any of the samples originating from the viral fraction (Figure S7B). These experiments support our hypothesis that the HB1 phage family in the oral cavity is likely predominately lytic.

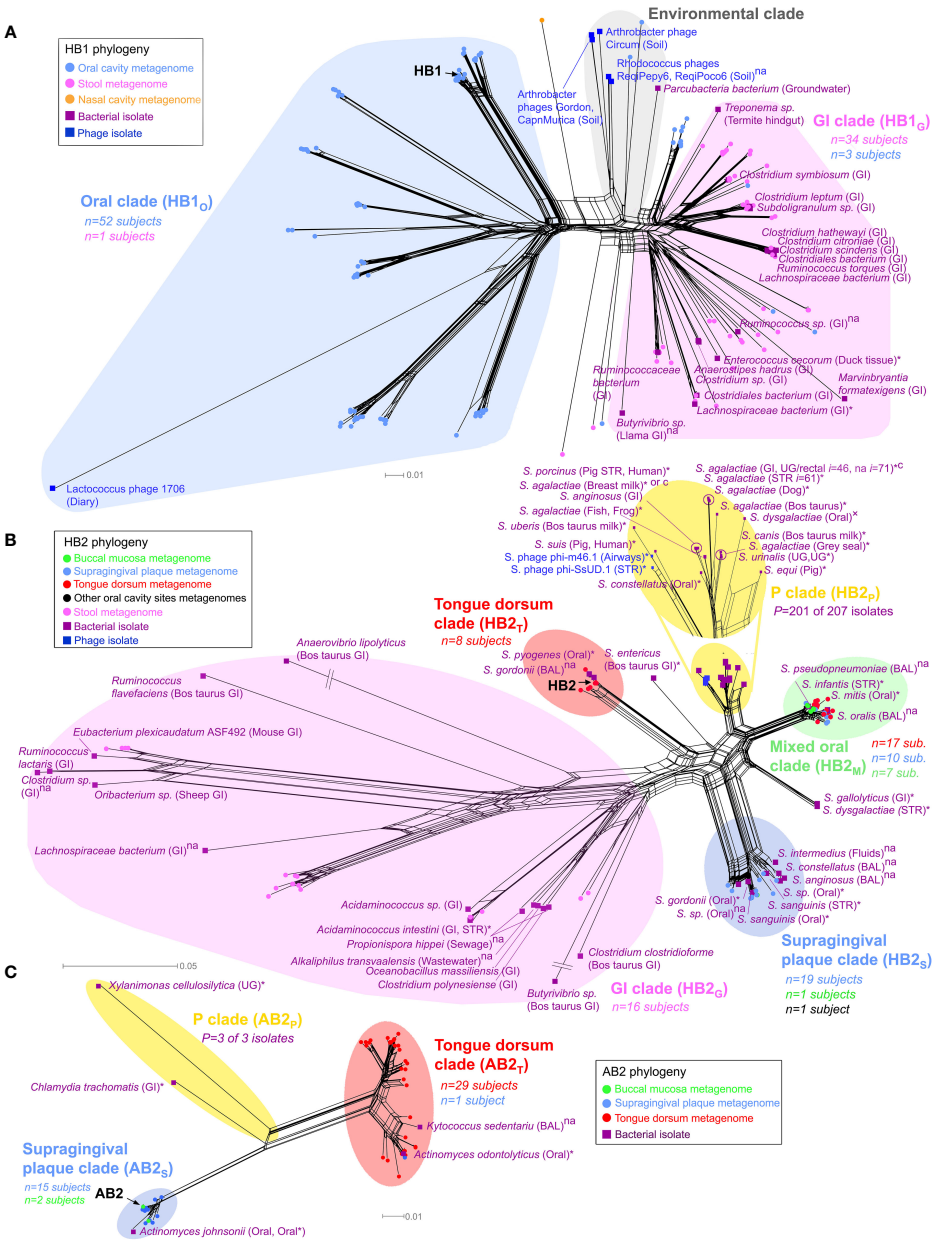

FIGURE 3
Phylogenetic analysis of TerL phage families. Neighbor-Net analysis for **(A)** HB1, **(B)** HB2 and **(C)** AB2 phage families based on 386, 341, and 350 unambiguous amino acid residues, respectively including sequences obtained from the HMP metagenomes (circular nodes) and sequenced bacterial and phage isolates (square nodes). Pathogenic bacteria, bacteria isolated from diseased body sites, sterile organs, individuals with diagnosed diseases or diseased animals are marked with an asterisk, otherwise "x" denotes suspected pathogenicity, "c" denotes a carriage strain, and "na" denotes unknown health-related status. Bacterial isolates belonging to the same species, sampled from the same body region (mouth, skin, nose, the gastrointestinal (GI) tract or the UG tract), and with the same health-related status were consolidated using a 3% OTU threshold at the amino acid level (OTU assignment for all isolates is provided in Table S10). *n* denotes the number of HMP subjects contributing sequences to a given clade color coded by the body habitat indicated in the legend, *P* denotes the total number of disease or carriage associated human bacterial isolates within a "P" clade out of all isolates in the given clade. In the "P" clade of HB2, *i* denotes the total number of human bacterial isolates represented by the given OTU (shown for $I \geq 10$). If unstated, bacterial isolates were obtained from humans. See Materials and Methods for precise inclusion criteria of sequences. Neighbor-Net networks were calculated with SplitsTree4 (Huson and Bryant, 2006). Phylogenetic analysis of HB1, HB2 and AB2 was based on 176, 139 and 57 sequences, respectively, using optimal models determined by the AIC criterion (WAG+I+G) with optimal α and Pinv parameters. BAL, bronchoalveolar lavage; STR, sterile body site.

Spatial distribution of phage family sublineages

Our phylogenetic analysis further revealed TerL sublineages that displayed remarkable specificity to certain oral habitats. For example, the oral clade of the HB1 phage family contained distinct sublineages uniquely associated with the tongue dorsum, and different sublineages that were uniquely associated with supragingival plaque (Figure S11A). The HB2 phage family followed a similar oral/gut organization as HB1 (Figure 3B), and like HB1 also displayed sublineages uniquely associated with either the tongue dorsum or supragingival plaque. Similar site-specific sublineages were found for the AB2, HA, and PCA1 phage families (Figure 3C and Figures S11B, S12A, respectively). Such exclusive associations between certain TerL phage sublineages and specific oral habitats suggests that proximal habitats within the oral cavity can comprise unique phage communities that remain localized despite constant contact between these habitats mediated by the tongue and saliva. These findings are in line with the site-specialist worldview of the oral cavity microbiome where most microbes in the mouth are found in specific oral habitats (Welch et al., 2019). However, most phage families also contained sublineages obtained from a mixture of oral habitats (denoted as "M" clades, highlighted in green in Figure 3B and Figures S11, S12), possibly an indication that the bacterial hosts of these specific phage family members colonize multiple oral habitats, a hypothesis we further explore below.

Phage family sublineages potentially associated with pathogenicity

Interestingly, most phage families contained certain clades that were not found in the HMP study. These clades, denoted as "P" clades, are highlighted in yellow in the phylogenetic networks (Figures 3B, C and Figures S11B, S12). The absence of HMP metagenomic sequences from "P" clades was statistically significant (Table S14), and confirmed by targeted sequencing in our own cohort of oral samples (see below). This observation can possibly be explained by the fact that the vast majority of human-associated bacterial isolates in "P" clades were either pathogens, were isolated from diseased body sites, were isolated from individuals with a diagnosed disease, or were carriage strains, as indicated in Table S14, whereas the subjects participating in the HMP study and in our cohort were healthy (all bacterial isolates belonging to "P" clades are highlighted in Table S10). Since "P" clades were absent in healthy individuals, "P" clades could possibly serve as specific biomarkers for detection of potential pathogens in humans. Another intriguing feature of "P" clades was the presence of bacteria isolated from animals (HP2, HA, PCA1), potentially revealing a phage signature of animal-to-human transmission. For example, the "P" clade of HB2 (Figure 3B) contains a mixture of human pathogens, carriage strains and sequences isolated from animals, including *Streptococcus suis sv.* JS14 and *Streptococcus porcinus Jelinkova* 176, two human pathogens originally isolated from pigs (Table S10).

Phylogenetic analysis of PCR-amplified sequences supports metagenomic results

To independently confirm phylogenies that were based on HMP metagenomic sequences, we also inferred phylogenies based on PCR-amplified TerL sequences together with HMP metagenomic sequences. In Supporting Text S9 we show that PCR-amplified alleles obtained from specific oral sites for HB1, HB2, HA, PCA1, PCA2 and AB2 were generally intermixed and indistinguishable from metagenomic alleles obtained from the same body sites. Our analysis also showed that none of the PCR-amplified TerL sequences mapped to "P" clades, further supporting our observation that heathy subjects did not contribute TerL alleles to "P" clades. These results show that our metagenomic-based phylogenetic inferences could be confirmed by targeted sequencing, indicating that the phylogenic patterns we observed in metagenomic datasets were not a result of sequencing or assembly artifacts.

Temporal stability of phage families

Finally, to explore the temporal dynamics of phage families we estimated their persistence across specific body habitats in subjects sampled between two consecutive visits, separated on average by 219 ± 69 (s.d.) days (Huttenhower et al., 2012). We quantified this persistence by measuring the fraction of subjects for which a phage family was detected in the first visit but was absent in the second visit, or vice versa, denoted by f_{switch} (Figure 4). We found that presence of most families (HB1, HB2, PCA1, and AB1) was stable in the oral cavity (f_{switch}=0), with HB1 and HB2 also stable in the gut ($f_{switch} \leq 0.08$). Indeed, members of a phage family that were present in both visits often had identical amino acid sequences (Figure S13), consistent with previous studies that showed that salivary and fecal viromes are genetically stable (Reyes et al., 2010; Pride et al., 2012; Minot et al., 2013; Ogilvie and Jones, 2015; Shkoporov et al., 2019). However, when considering specific oral habitats, most families exhibited considerable temporal variability, with variability highest in the buccal mucosa (f_{switch} = 0.36 ± 0.06, omitting AB1). One possible explanation for habitat variability could be host migration within the oral cavity. For example, the fact that buccal mucosa-derived sequences typically mapped to "M" clades (clades containing a mixture of sequences from different oral habitats) may indicate that the buccal mucosa contains

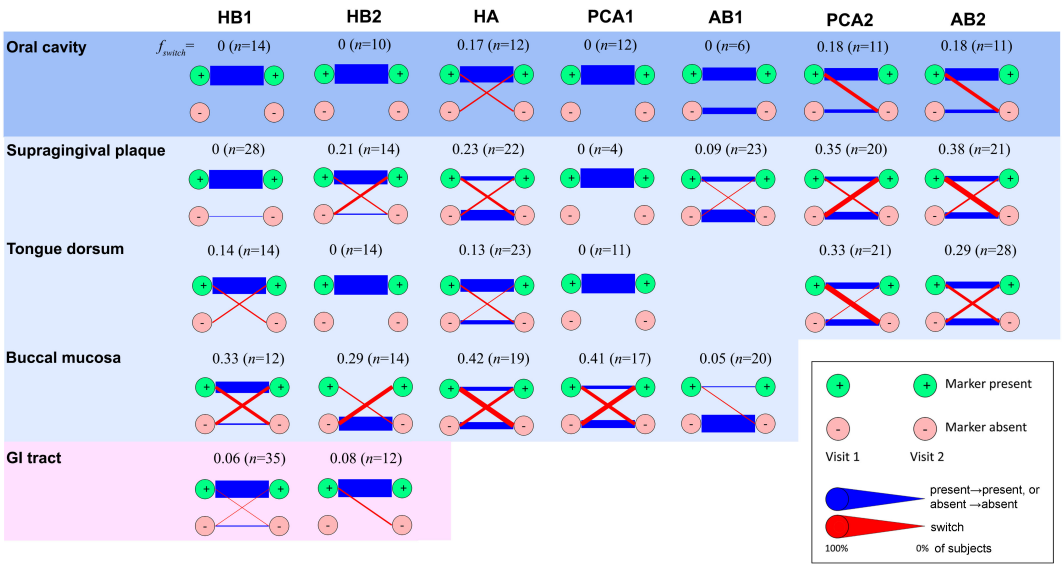

FIGURE 4
Temporal stability of phage families. Presence of a phage family was determined in two consecutive visits of the same subject considering one metagenome per habitat. In the case of the oral cavity, oral habitats were considered both separately and as a single ecosystem (top row). In the latter case, presence was required in any oral habitat, and absence was required for all oral habitats. A phage family was considered present if any alignment against the corresponding TerL marker sequence spanning at least 150 aa exceeded 70% identity at the amino acid level (see Supporting Text S4 for optimal alignment length criteria for the HMP metagenomes). Reducing the percent identity threshold to 55% did not have a significant impact on results. To minimize potential coverage bias, a marker was determined to be absent if no alignment spanning a minimum of 75 aa exceeded 40% identity, allowing us to also rule out remote homologs and homologs on short contigs. Blue lines denote unchanged state (presence in both visits or absence in both visits). Red lines denote a change (presence in visit 1 and absence in visit 2, or vice versa). Line widths are proportional to the fraction of subjects that share the same transition. *n* denotes the total number of subjects. Diagrams for habitats for which a marker was found to be always absent were omitted.

bacterial hosts that can colonize multiple oral habitats that possibly migrate between different compartments (see examples for potential host migration events in Figure S13).

Conclusions

Much like classical SSU rRNA studies, we found that by focusing our analysis on TerL markers we were able to identify certain TerL phage families that were both conserved and widely shared across the human oral microbiome. This finding is intriguing in light of the tremendous genetic diversity of viruses in nature (Edwards and Rohwer, 2005; Paez-Espino et al., 2016a), the lack of conservation of the TerL gene (Eppler et al., 1991; Chai et al., 1992; Moore and Prevelige, 2002; Rao and Feiss, 2008), and the individualized nature of human viromes established by previous studies (Reyes et al., 2010; Minot et al., 2011; Pride et al., 2012; Reyes et al., 2012; Shkoporov et al., 2019; Moreno-Gallego et al., 2019; Gregory et al., 2020; Zuo et al., 2020; Garmaeva et al., 2021). Overall, the shared TerL lineages we identified accounted for, on average, about 25% of all nonredundant TerL gene families (Table S15), adding to the growing body of evidence of the existence of widely shared members of the human virome (Stern et al., 2012; Manrique et al., 2016; Moreno-Gallego et al., 2019).

Although our marker-based approach provided a relatively narrow genomic window into the core human virome, focusing on a single gene enabled us to perform a comparative analysis of this gene across different subjects, different habitats and different time points. Furthermore, our markers, through the use of primers that we developed, enable sequence diversity analysis that is independent of metagenome sequencing. It would therefore be interesting to complement this study with single cell sequencing and genome assembly approaches, which could help shed light on the covariation between different phage families and their bacterial hosts across different body habitats. Furthermore, our analysis focused only on shared phage families within the oral cavity, however, our approach can be extended to other sites to create a comprehensive atlas of shared TerL phage families across the entire human body. More broadly, the fact that we have identified to date phage families with shared TerL lineages in both humans and termites (Tadmor et al., 2011) suggests that phage families with shared TerL lineages across species of organisms may be a common theme in the animal

kingdom. Consequently, a comprehensive catalog of ubiquitous TerL phage families could potentially be expanded to encompass other organisms, possibly serving as a useful means for classifying and cataloging recurrent viral diversity core to different organisms.

Data availability statement

Experimental sequences used in the current study are available at: https://github.com/gitamahm/human_virome.

Ethics statement

The human samples collected in this study followed Caltech Institutional Review Board IRB protocol 14-0430 and Institutional Biosafety Committee IBC protocol 13-198 with subjects providing written consent. Additional human samples analyzed in this study were provided to us by Bik et al. [The ISME journal 4, 962 (2010)] and were collected in accordance to Stanford IRB protocols.

Author contributions

AT and RP conceived the study, AT devised and performed the bioinformatic analysis as well as designed the degenerate primers for the markers, GM designed and executed experiments and performed the selection pressure analysis, HF and GM performed the experiments testing bacterial and viral fractions of oral samples, GM and AT performed data analysis related to experiments, and RP scientifically oversaw the project and advised. The paper was written by AT and critically reviewed and edited by all authors. All authors contributed to the article and approved the submitted version.

Funding

This work was supported by the NIH Director's Pioneer Award, the NIH's Eureka grant no. R01-GM098465, and the National Science Foundation Graduate Research Fellowship Program (GRFP).

Acknowledgments

We wish to thank S. R. Quake, D. A. Relman, and P. C. Blainey for their initial advice on the project and D. A. Relman for donating to us oral samples, E. M. Rubin, N. C. Kyrpides, V. M. Markowitz, T. B. K. Reddy and H. Huot-Creasy, A. Clum, and N. Ivanova for providing support with the IMG and HMP datasets, E. Allen-Vercoe, D. W. Verner-Jeffreys, C. Michel, N. J. Croucher, M. Kilian, M. J. Loessner, L. Ikryannikova, J. Izard, M. Hilty, M. Sizova, P. Glaser, M. R. Davies, O. L. Franco, M. J. Wolin, M. Gottschalk and S. Moineau for providing information regarding bacterial isolates, and D. H. Huson and D. Bryant for providing support for SplitsTree4. We further wish to thank J. Boedicker, F. Weinert, and K. Homyk for their involvement in the initial experimental verification of the markers, and A. Debnath for assisting with initial investigations. The IMG/VR sequence data were produced by the US Department of Energy Joint Genome Institute (https://www.jgi.doe.gov/) in collaboration with the user community and was authorized to use in this study.

Conflict of interest

The authors declare that the research was conducted in the absence of any commercial or financial relationships that could be construed as a potential conflict of interest.

Publisher's note

Supplementary material

The Supplementary Material for this article can be found online at: https://www.frontiersin.org/articles/10.3389/frmbi.2022.1097124/full#supplementary-material

References

Aagaard, K., Petrosino, J., Keitel, W., Watson, M., Katancik, J., Garcia, N., et al. (2013). The human microbiome project strategy for comprehensive sampling of the human microbiome and why it matters. *FASEB J.* 27, 1012–1022. doi: 10.1096/fj.12-220806

Adachi, J., and Hasegawa, M. (1996). Model of amino acid substitution in proteins encoded by mitochondrial DNA. *J. Mol. Evol.* 42, 459–468. doi: 10.1007/BF02498640

Adachi, J., Waddell, P. J., Martin, W., and Hasegawa, M. (2000). Plastid genome phylogeny and a model of amino acid substitution for proteins encoded by chloroplast DNA. *J. Mol. Evol.* 50, 348–358. doi: 10.1007/s002399910038

Belda-Ferre, P., Alcaraz, L. D., Cabrera-Rubio, R., Romero, H., Simón-Soro, A., Pignatelli, M., et al. (2012). The oral metagenome in health and disease. *ISME J.* 6, 46–56. doi: 10.1038/ismej.2011.85

Bik, E. M., Long, C. D., Armitage, G. C., Loomer, P., Emerson, J., Mongodin, E. F., et al. (2010). Bacterial diversity in the oral cavity of 10 healthy individuals. *ISME J.* 4, 962. doi: 10.1038/ismej.2010.30

Brüssow, H., Canchaya, C., and Hardt, W.-D. (2004). Phages and the evolution of bacterial pathogens: From genomic rearrangements to lysogenic conversion. *Microbiol. Mol. Biol. Rev.* 68, 560–602. doi: 10.1128/MMBR.68.3.560-602.2004

Bryant, D., and Moulton, V. (2004). Neighbor-net: An agglomerative method for the construction of phylogenetic networks. *Mol. Biol. Evol.* 21, 255. doi: 10.1093/molbev/msh018

Cao, Y., Janke, A., Waddell, P. J., Westerman, M., Takenaka, O., Murata, S., et al. (1998). Conflict among individual mitochondrial proteins in resolving the phylogeny of eutherian orders. *J. Mol. Evol.* 47, 307–322. doi: 10.1007/PL00006389

Caporaso, J. G., Kuczynski, J., Stombaugh, J., Bittinger, K., Bushman, F. D., Costello, E. K., et al. (2010). QIIME allows analysis of high-throughput community sequencing data. *Nat. Methods* 7, 335. doi: 10.1038/nmeth.f.303

Casjens, S. (2003). Prophages and bacterial genomics: What have we learned so far? *Mol. Microbiol.* 49, 277–300. doi: 10.1046/j.1365-2958.2003.03580.x

Chai, S., Bravo, A., Lüder, G., Nedlin, A., Trautner, T., Alonso, J., et al. (1992). Molecular analysis of the bacillus subtilis bacteriophage SPP 1 region encompassing genes 1 to 6: The products of gene 1 and gene 2 are required for pac cleavage. *J. Mol. Biol.* 224, 87–102. doi: 10.1016/0022-2836(92)90578-8

Chen, T., Yu, W.-H., Izard, J., Baranova, O. V., Lakshmanan, A., Dewhirst, F. E., et al. (2010). The human oral microbiome database: A web accessible resource for investigating oral microbe taxonomic and genomic information. *Database: J. Biol. Database Curation* 2010, baq013. doi: 10.1093/database/baq013

Chen, I.-M. A., Gulyaeva, A., Sinha, T., Shkoporov, A. N., Clooney, A. G., Stockdale, S. R., et al. (2018). IMG/M v. 5.0: An integrated data management and comparative analysis system for microbial genomes and microbiomes. *Nucleic Acids Res.* 47, D666–D677. doi: 10.1093/nar/gky901

Darriba, D., Taboada, G. L., Doallo, R., and Posada, D. (2011). ProtTest 3: Fast selection of best-fit models of protein evolution. *Bioinformatics* 27, 1164–1165. doi: 10.1093/bioinformatics/btr088

Dayhoff, M. O., and Schwartz, R. M. (1978). *In atlas of protein sequence and structure* (Washington DC: Citeseer), 5(3), 345–352.

Edgar, R. (2004). MUSCLE: A multiple sequence alignment method with reduced time and space complexity. *BMC Bioinf.* 5, 113. doi: 10.1186/1471-2105-5-113

Edgar, R. C. (2010). Search and clustering orders of magnitude faster than BLAST. *Bioinformatics* 26, 2460–2461. doi: 10.1093/bioinformatics/btq461

Edwards, R., and Rohwer, F. (2005). Viral metagenomics. *Nat. Rev. Microbiol.* 3, 504–510. doi: 10.1038/nrmicro1163

Eppler, K., Wyckoff, E., Goates, J., Parr, R., and Casjens, S. (1991). Nucleotide sequence of the bacteriophage P22 genes required for DNA packaging. *Virology* 183, 519–538. doi: 10.1016/0042-6822(91)90981-G

Garmaeva, S., Gulyaeva, A., Sinha, T., Shkoporov, A. N., Clooney, A. G., Stockdale, S. R., et al. (2021). Stability of the human gut virome and effect of gluten-free diet. *Cell Rep.* 35, 109132. doi: 10.1016/j.celrep.2021.109132

Glass, E. M., Wilkening, J., Wilke, A., Antonopoulos, D., and Meyer, F. (2010). Using the metagenomics RAST server (MG-RAST) for analyzing shotgun metagenomes. *Cold Spring Harbor Protoc.* 2010, prot5368. doi: 10.1101/pdb.prot5368

Gouy, M., Guindon, S., and Gascuel, O. (2009). SeaView version 4: A multiplatform graphical user interface for sequence alignment and phylogenetic tree building. *Mol. Biol. Evol.* 27 (2), 221–224. doi: 10.1093/molbev/msp259

Gregory, A. C., Zablocki, O., Zayed, A. A., Howell, A., Bolduc, B., Sullivan, M. B., et al. (2020). The gut virome database reveals age-dependent patterns of virome diversity in the human gut. *Cell Host Microbe* 28, 724–740. e728. doi: 10.1016/j.chom.2020.08.003

Guerin, E., Shkoporov, A., Stockdale, S. R., Clooney, A. G., Ryan, F.J., Sutton, T. D., et al. (2018). Biology and taxonomy of crAss-like bacteriophages, the most abundant virus in the human gut. *Cell Host Microbe* 24, 653–664. e656. doi: 10.1016/j.chom.2018.10.002

Hamady, M., Walker, J. J., Harris, J. K., Gold, N. J., and Knight, R. (2008). Error-correcting barcoded primers for pyrosequencing hundreds of samples in multiplex. *Nat. Methods* 5, 235. doi: 10.1038/nmeth.1184

Huson, D., and Bryant, D. (2006). Application of phylogenetic networks in evolutionary studies. *Mol. Biol. Evol.* 23, 254. doi: 10.1093/molbev/msj030

Huttenhower, C., Gevers, D., Knight, R., Abubucker, S., Badger, J. H., Chinwalla, A. T., et al. (2012). Structure, function and diversity of the healthy human microbiome. *Nature* 486, 207. doi: 10.1038/nature11234

Jones, D., Taylor, W., and Thornton, J. (1992) 8, 275–282.

Kearse, M., Moir, R., Wilson, A., Stones-Havas, S., Cheung, M., Sturrock, S., et al. (2012). Geneious basic: An integrated and extendable desktop software platform for the organization and analysis of sequence data. *Bioinformatics* 28, 1647–1649. doi: 10.1093/bioinformatics/bts199

Lemey, P., Salemi, M., and Vandamme, A. M. (2009). *The phylogenetic handbook: A practical approach to phylogenetic analysis and hypothesis testing* (Cambridge: Cambridge University Press).

Li, X., Kolltveit, K. M., Tronstad, L., and Olsen, I. (2000). Systemic diseases caused by oral infection. *Clin. Microbiol. Rev.* 13, 547–558. doi: 10.1128/CMR.13.4.547

Łusiak-Szelachowska, M., Weber-Dąbrowska, B., Jończyk-Matysiak, E., Wojciechowska, R., and Górski, A. (2017). Bacteriophages in the gastrointestinal tract and their implications. *Gut Pathog.* 9, 44. doi: 10.1186/s13099-017-0196-7

Mahmoudabadi, G., Homyk, K., Foley, H., Catching, A., Mahmoudabadi, A., Cheung, A., et al. (2019). Human phageprints: A high-resolution exploration of oral phages reveals globally-distributed phage families with individual-specific and temporally-stable community compositions. *BioRxiv*. doi: 10.1101/516864

Manrique, P., Bolduc, B., Walk, S. T., Oost der van, J., Vos, W. M., and Young, M. J. (2016). Healthy human gut phageome. *Proc. Natl. Acad. Sci.* 113, 10400–10405. doi: 10.1073/pnas.1601060113

Marchler-Bauer, A., Bo, Y., Han, L., He, J., Lanczycki, C. J., Lu, S., et al. (2016). CDD/SPARCLE: Functional classification of proteins *via* subfamily domain architectures. *Nucleic Acids Res.* 45, D200–D203. doi: 10.1093/nar/gkw1129

Markowitz, V. M., Chen, I., Chu, K., Szeto, E., Palaniappan, K., Jacob, B., et al. (2012). IMG/M-HMP: A metagenome comparative analysis system for the human microbiome project. *PloS One* 7, 1–7. doi: 10.1371/journal.pone.0040151

Methé, B. A., Nelson, K. E., Pop, M., Creasy, H. H., Giglio, M. G., Huttenhower, C., et al. (2012). A framework for human microbiome research. *Nature* 486, 215–221. doi: 10.1038/nature11209

Minot, S., Sinha, R., Chen, J., Li, H. S., Keilbaugh, A., Wu, G.D., et al. (2011). The human gut virome: Inter-individual variation and dynamic response to diet. *Genome Res.* 21, 1616–1625. doi: 10.1101/gr.122705.111

Minot, S., Bryson, A., Chehoud, C., Wu, G. D., Lewis, J. D., Bushman, F. D., et al. (2013). Rapid evolution of the human gut virome. *Proc. Natl. Acad. Sci.* 110, 12450–12455. doi: 10.1073/pnas.1300833110

Moore, S. D., and Prevelige, P. E.Jr. (2002). DNA Packaging: A new class of molecular motors. *Curr. Biol.* 12, R96–R98. doi: 10.1016/S0960-9822(02)00670-X

Moreno-Gallego, J. L., Chou, S.-P., Rienzi Di, S. C., Goodrich, J. K., Spector, T. D., Bell, J. T., et al. (2019). Virome diversity correlates with intestinal microbiome diversity in adult monozygotic twins. *Cell Host Microbe* 25, 261–272. e265. doi: 10.1016/j.chom.2019.01.019

Navarro, F., and Muniesa, M. (2017). Phages in the human body. *Front. Microbiol.* 8, 566. doi: 10.3389/fmicb.2017.00566

Ogilvie, L. A., and Jones, B. V. (2015). The human gut virome: A multifaceted majority. *Front. Microbiol.* 6, 918. doi: 10.3389/fmicb.2015.00918

Paez-Espino, D., Chen, I.-M. A., Palaniappan, K., Ratner, A., Chu, K., Szeto, E., et al. (2016a). Uncovering earth's virome. *Nature* 536, 425. doi: 10.1038/nature19094

Paez-Espino, D., Pavlopoulos, G. A., Thomas, A. D., Huntemann, M., and Mikhailova, N. (2016b). IMG/VR: A database of cultured and uncultured DNA viruses and retroviruses. *Nucleic Acids Res.* 45 (D1), gkw1030. doi: 10.1093/nar/gkw1030

Pride, D. T., Salzman, J., Haynes, M., Rohwer, F., Davis-Long, C., White, R. A., et al. (2012). Evidence of a robust resident bacteriophage population revealed through analysis of the human salivary virome. *ISME J.* 6, 915–926. doi: 10.1038/ismej.2011.169

Pruitt, K. D., Tatusova, T., and Maglott, D. R. (2007). NCBI reference sequences (RefSeq): A curated non-redundant sequence database of genomes, transcripts and proteins. *Nucleic Acids Res.* 35, D61–D65. doi: 10.1093/nar/gkl842

Quirós, P., Colomer-Lluch, M., Martínez-Castillo, A., Miró, E., Argente, M., Jofre, J., et al. (2014). Antibiotic resistance genes in the bacteriophage DNA fraction of human fecal samples. *Antimicrob. Agents Chemother.* 58, 606–609. doi: 10.1128/AAC.01684-13

Rao, V. B., and Feiss, M. (2008). The bacteriophage DNA packaging motor. *Annu. Rev. Genet.* 42, 647–681. doi: 10.1146/annurev.genet.42.110807.091545

Reyes, A., Haynes, M., Hanson, N., Angly, F., Heath, A., Rohwer, F., et al. (2010). Viruses in the faecal microbiota of monozygotic twins and their mothers. *Nature* 466, 334–338. doi: 10.1038/nature09199

Reyes, A., Semenkovich, N. P., Whiteson, K., Rohwer, F., and Gordon, J. I. (2012). Going viral: Next-generation sequencing applied to phage populations in the human gut. *Nat. Rev. Microbiol.* 10, 607–617. doi: 10.1038/nrmicro2853

Rohwer, F., and Edwards, R. (2002). The phage proteomic tree: a genome-based taxonomy for phage. *J. Bacteriol* 184, 4529–4535. doi: 10.1128/JB.184.16.4529-4535.2002

Rose, T., Schultz, E., Henikoff, J., Pietrokovski, S., McCallum, C., and Henikoff, S. (1998). Consensus-degenerate hybrid oligonucleotide primers for amplification of distantly related sequences. *Nucleic Acids Res.* 26, 1628. doi: 10.1093/nar/26.7.1628

Secor, P. R., Michaels, L. A., Smigiel, K. S., Rohani, M. G., Jennings, L. K., Hisert, K. B., et al. (2017). Filamentous bacteriophage produced by pseudomonas aeruginosa alters the inflammatory response and promotes noninvasive infection in vivo. *Infection Immun.* 85, e00648–e00616. doi: 10.1128/IAI.00648-16

Shkoporov, A. N., Clooney, A. G., Sutton, T. D., Ryan, F. J., Daly, K. M., Nolan, J. A., et al. (2019). The human gut virome is highly diverse, stable, and individual specific. *Cell Host Microbe* 26, 527–541. e525. doi: 10.1016/j.chom.2019.09.009

Stern, A., Mick, E., Tirosh, I., Sagy, O., and Sorek, R. (2012). CRISPR targeting reveals a reservoir of common phages associated with the human gut microbiome. *Genome Res.* 22, 1985–1994. doi: 10.1101/gr.138297.112

Sun, S., Kondabagil, K., Draper, B., Alam, T., Bowman, V., Zhang, Z., et al. (2008). The structure of the phage T4 DNA packaging motor suggests a mechanism dependent on electrostatic forces. *Cell* 135, 1251–1262. doi: 10.1016/j.cell.2008.11.015

Tadmor, A. D., Ottesen, E. A., Leadbetter, J. R., and Phillips, R. (2011). Probing individual environmental bacteria for viruses by using microfluidic digital PCR. *Science* 333, 58–62. doi: 10.1126/science.1200758

Tadmor, A. D., and Phillips, R. (2022). MCRL: Using a reference library to compress a metagenome into a non-redundant list of sequences, considering viruses as a case study. *Bioinformatics* 38, 631–647. doi: 10.1093/bioinformatics/btab703

Tamura, K., Stecher, G., Peterson, D., Filipski, A., and Kumar, S. (2013). MEGA6: Molecular evolutionary genetics analysis version 6.0. *Mol. Biol. Evol.* 30, 2725–2729. doi: 10.1093/molbev/mst197

Waldor, M. K., and Mekalanos, J. J. (1996). Lysogenic conversion by a filamentous phage encoding cholera toxin. *Science* 272, 1910–1914. doi: 10.1126/science.272.5270.1910

Welch, J. L. M., Dewhirst, F. E., and Borisy, G. G. (2019). Biogeography of the oral microbiome: The site-specialist hypothesis. *Annu. Rev. Microbiol.* 73, 335-358. doi: 10.1146/annurev-micro-090817-062503

Whelan, S., and Goldman, N. (2001). A general empirical model of protein evolution derived from multiple protein families using a maximum-likelihood approach. *Mol. Biol. Evol.* 18, 691–699. doi: 10.1093/oxfordjournals.molbev.a003851

Willner, D., Furlan, M., Schmieder, R., Grasis, J. A., Pride, D. T., Relman, D. A., et al. (2011). Metagenomic detection of phage-encoded platelet-binding factors in the human oral cavity. *Proc. Natl. Acad. Sci.* 108, 4547–4553. doi: 10.1073/pnas.1000089107

Wommack, K. E., Bhavsar, J., Polson, S. W., Chen, J., Dumas, M., Srinivasiah, S., et al. (2012). VIROME: A standard operating procedure for analysis of viral metagenome sequences. *Standards genomic Sci.* 6, 421. doi: 10.4056/sigs.2945050

Xie, G., Chain, P., Lo, C. C., Liu, K. L., Gans, J., Merritt, J., et al. (2010). Community and gene composition of a human dental plaque microbiota obtained by metagenomic sequencing. *Mol. Oral. Microbiol.* 25, 391–405. doi: 10.1111/j.2041-1014.2010.00587.x

Yang, Z. (2007). PAML 4: Phylogenetic analysis by maximum likelihood. *Mol. Biol. Evol.* 24, 1586–1591. doi: 10.1093/molbev/msm088

Zhao, G., Vatanen, T., Droit, L., Park, A., Kostic, A. D., Poon, T. W., et al. (2017). Intestinal virome changes precede autoimmunity in type I diabetes-susceptible children. *Proc. Natl. Acad. Sci.* 114, E6166–E6175. doi: 10.1073/pnas.1706359114

Zuo, T., Sun, Y., Wan, Y., Yeoh, Y. K., Zhang, F., Cheung, C. P., et al. (2020). Human-Gut-DNA virome variations across geography, ethnicity, and urbanization. *Cell Host Microbe* 28, 741–751. e744. doi: 10.1016/j.chom.2020.08.005

Frontiers in Public Health

Explores and addresses today's fast-moving healthcare challenges

One of the most cited journals in its field, which promotes discussion around inter-sectoral public health challenges spanning health promotion to climate change, transportation, environmental change and even species diversity.

Discover the latest Research Topics

See more →

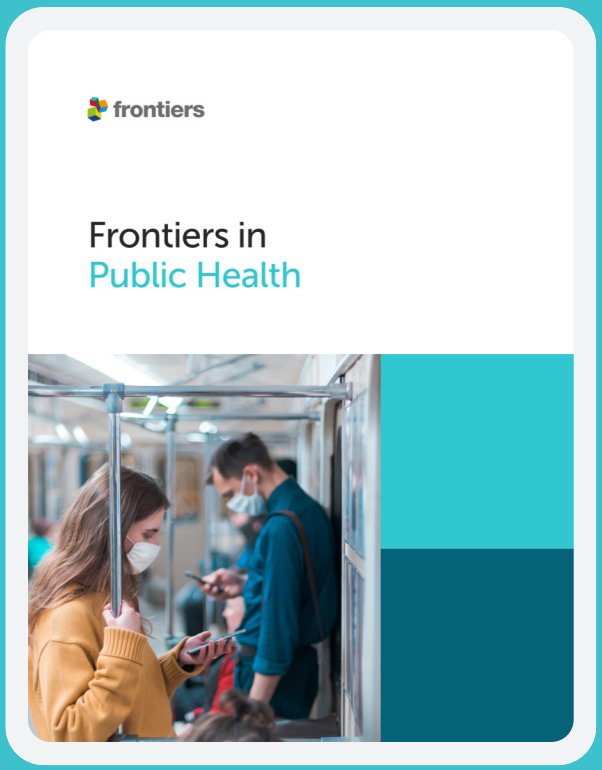

Frontiers

Avenue du Tribunal-Fédéral 34
1005 Lausanne, Switzerland
frontiersin.org

Contact us

+41 (0)21 510 17 00
frontiersin.org/about/contact